S Saleem

PhD

2012

PROTEOMIC PROFILING OF PRO AND ACTIVE MATRIX METALLOPROTEINASES USING TANDEM MASS SPECTROMETRY

S SALEEM

PhD

2012

Proteomic Profiling of Pro and Active Matrix Metalloproteinases using Tandem Mass Spectrometry

Optimization of Affinity Chromatography and nHPLC-MALDI-MS/MS for Proteomic discrimination of Matrix Metalloproteinases in pre-clinical Cancer Model

SAIRA SALEEM

submitted for the degree of Doctor of Philosophy

Institute of Cancer Therapeutics

University of Bradford

2012

Acknowledgements

I would like to express my sincere gratitude to my supervisors Dr Chris W. Sutton and Dr Jason H Gill for their guidance and illustrious advices during the course of this research work. I am especially thankful to Dr Chris W. Sutton for his careful review of my thesis and his valuable comments on my work. A heartfelt thanks to my colleagues at Institute of Cancer Therapeutics for their assistance with this research work and friendly discussions. I am thankful to Shaukat Khanam Memorial Cancer Hospital and Research Centre, Pakistan and University of Bradford for funding this work.

All my friends deserve my special thanks for bringing joy into my life outside the laboratory. I would like to express deep gratitude to Dr. Natasha Nabi Anwar for her selfless help and encouragement. I am extremely thankful to Alison Darnbrough for being there for every help I needed. My deepest thanks goes to my family for their unfailing love and support through it all.

Abstract

Matrix metalloproteinases (MMPs) network with other biological molecules to maintain the extracellular matrix (ECM) in normal physiology and perform different roles. Understanding and assigning specific role to each of 24 members of these endoproteinases is impeded because of lack of specific and efficient detection methods in biological samples. Moreover, MMP-based anti-cancer drug development has also been challenged because, currently, there is no robust methodology to distinguish the inactive pro-enzymes, active enzymes or those complexed with endogenous inhibitors in biological specimens. The objective of this project is to develop a chemical proteomics strategy based on Matrix assisted laser desorption ionization tandem mass spectrometry (MALDI-MS/MS) to help identify and discriminate the various MMP forms. Firstly, a triazine dye-based ligand immobilized on chromatography beads was utilized to assess whether it binds to recombinant human MMPs (rhMMPs). The results highlighted that the ligand interacts with latent forms of MMPs in agreement with the literature. Secondly, the potential of the ligand was assessed using MALDI-MS/MS based methodology in *in vitro* cancer models. Cell line culture supernatants were used in amounts to emulate the availability of tumour biopsies in clinical settings. The MS/MS spectral peaks specific to MMPs (MMP-2 and MMP-14), and two endogenous inhibitors TIMP-1 and TIMP-2 were found in affinity chromatography eluates of cell culture supernatants with higher Mascot scores for the latter. While western blot detected MMP-2 in cell extracts, MALDI-MS/MS did not detect MMPs because of amounts below the limit of detection (LOD) of the instrument. Although the ligand was found to be interacting with MMPs and detergent-free salt elution buffers improved MALDI analysis, recovery of MMPs from biological samples was sub-optimal. The dye ligand was observed to bind other enzymes and despite various strategies to reduce non-specific binding of proteins or enable selective elution did not improve MMP enrichment. Further work using methodology described in this study is required after scaling up the MMP amounts in biological specimen and to resolve the issue of non-specific binding of proteins to the ligand by understanding its structure.

Contents

Acknowledgements I

Abstract II

Contents III

Abbreviations IX

List of Figures XIII

List of Tables XVII

List of Appendices XIX

1 Introduction 1

1.1 Definition of Cancer 1

1.2 Hallmarks of Cancer 1

1.2.1 Limitless Replicative Potential 2

1.2.2 Self Sufficiency and Insensitivity to Antigrowth Signal 2

1.2.3 Evasion of Apoptosis 3

1.2.4 Angiogenesis 4

1.2.5 Cancer Invasion and Metastasis 5

1.3 Matrix Metalloproteinases (MMPs) 7

1.4 MMPs in Normal Physiology and Degradative Diseases 8

1.5 Role of MMPs in Cancer 9

1.6 Regulation of MMPs 12

1.6.1 Transcriptional and Translational Regulation 12

1.6.2 Post-Translational Regulation 12

1.6.3 Regulation by Protease Inhibitors and other Factors 15

1.7 MMP Structure 16

1.7.1 Pro-peptide Domain 16

1.7.2 Catalytic Domain 17
1.7.3 Fibronectin Type II Domains 18
1.7.4 The Linker Region 18
1.7.5 Hemopexin Domain 19
1.8 Purification of MMPs 19
1.8.1 Conventional MMP Purification Methods 22
1.8.2 Synthetic Inhibitors-Based Methods 23
1.8.3 Activity Based Probes for Proteomic Profiling (ABPP) 23
1.8.4 Affinity Chromatography 24
1.9 Mass Spectrometry 33
1.9.1 MALDI-Mass Spectrometry 35
1.9.2 MALDI-MS-TOF 36
1.10 Proteomics 39
1.10.1 Chemical Proteomics 40
1.10.2 Separation Techniques 41
1.10.3 Proteomics Approaches 43
1.11 Aims and Objectives 44
2 Materials and Methods 47
2.1 Reagents & Chemicals 47
2.2 Immobilization of OliveH-7G on Chromatography Beads: H-7G-Sepharose and H-7G-Sephadex 47
2.3 Cell Culture 48
2.3.1 Cell Counting 48
2.3.2 Tumour Cell Line Growth Kinetics 48
2.3.3 Collection of Culture Supernatant 49
2.3.4 Harvesting of Cells 49
2.4 Affinity Chromatography of Recombinant, Secreted and Cellular MMPs 51
2.4.1 Salt Elution 51
2.5 Protein Concentration: NAP-5 Columns and Dialysis Method 52
2.6 Bradford Assay for Quantification of Total Proteins 54

2.7 ELISA for Quantification of MMP-2 54

2.8 SDS-Polyacrylamide Gel Electrophoresis (SDS-PAGE) 56

2.8.1 Coomassie Brilliant Blue Staining 56

2.8.2 Silver Staining 57

2.8.3 Western Blotting for MMP-2 57

2.9 Trypsin Digestion 58

2.9.1 Proteomics: In-Solution Trypsin Digestion 58

2.9.2 Proteomics: On-Bead Trypsin Digestion 59

2.10 Desalting of Digested Protein 59

2.10.1 Desalting by Isolute C18 Cartridges 59

2.10.2 Desalt with Zip tips 60

2.10.3 Desalt with Pierce Columns 60

2.11 Manual MALDI-MS of Peptides 61

2.11.1 Instrumentation 61

2.11.2 Matrix Solution Preparation 61

2.11.3 Mass Spectrum Acquisition 61

2.12 nHPLC coupled to MALDI-MS/MS for Protein Identification (LC-MS/MS) 62

2.12.1 Reverse phase nHPLC Fractionation of Modified Peptides 62

2.12.2 nHPLC Gradient Conditions 62

2.12.3 Fraction Collection 63

2.12.4 Mass Spectrum Acquisition 64

2.12.5 WARP-LC and Database searching 64

3 Procion Olive H-7G Dye Characteristics 67

3.1 Introduction 67

3.1.1 Aims 69

3.2 Materials and Methods 69

3.2.1 Spectrophotometery 69

3.2.2 MALDI-MS of Olive H-7G 70

3.2.3 nHPLC of Olive H-7G (Analytical Runs) 70

3.3 Results 71
3.3.1 Spectrophotometery of Olive H-7G 71
3.3.2 Olive H-7G Molecular Mass Confirmation by MALDI-MS 72
3.3.3 nHPLC Profiles of Olive H-7G 74
3.4 Discussion 75
4 Characterization of Recombinant Human MMPs (rhMMPs) by MALDI-MS 77
4.1 Introduction 77
4.1.1 Aims 77
4.2 Materials and Methods 81
4.2.1 MALDI-MS of Intact Proteins 81
4.2.2 Theoretical Digests for MMPs (SequenceEditor Software) 82
4.2.3 MALDI-MS of Trypsin Digests 83
4.2.4 Manual MALDI-MS/MS of rhMMP Peptides 84
4.2.5 Interaction between rhMMP-14/rhMMP-2 and Olive H-7G 84
4.2.6 Interaction between rhMMP Mixture and Olive H-7G 84
4.3 Results 85
4.3.1 Molecular Mass of Intact rhMMPs by MALDI-MS 85
4.3.2 Mass Spectra for Controls in Trypsin Digestion 86
4.3.3 Peptide Mass Fingerprints (PMF) of rhMMPs 87
4.3.4 MS/MS Ion Search for Peptide Fragment of rhMMPs 92
4.3.5 Elastase and Lysine-N for complete Digestion of rhMMPs 106
4.3.6 Interaction between rhMMP-2/rhMMP-14 and Olive H-7G 106
4.3.7 Interaction between Mixture of 11 rhMMPs and Olive H-7G 107
4.4 Discussion 108
5 Dye Ligand Chromatography of rhMMPs 114
5.1 Introduction 114
5.1.1 Aims 114
5.2 Materials and Methods 115
5.2.1 Synthesis of H-7G-Sepharose Beads 115

5.2.2 Synthesis of Olive H-7G-Magnetic Beads (H-7G-MB) 115
5.2.3 H-7G-Sepharose Capture of rhMMP Mixture 116
5.2.4 H-7G-MB Capture of rhMMP Mixture 118
5.2.5 Preparation of rhMMPs Peptides (In-solution) 121
5.2.6 Preparation of rhMMPs Peptides (On-bead) 121
5.2.7 Removal of Detergent from Peptide Solution 122
5.2.8 Reverse phase nHPLC coupled to MALDI-MS/MS 122
5.2.9 Enrichment of rhMMP-2 122
5.2.10 Quantification of rhMMP-2 in Chromatographic Fractions 123
5.3 Results 123
5.3.1 MALDI-MS of Mixture of 4 rhMMPs (H-7G-Sepharose Captured) 123
5.3.2 MALDI-MS of Mixture of 9 rhMMPs (H-7G-Sepharose Captured) 126
5.3.3 MALDI-MS of Mixture of 11 rhMMPs (H-7G-MB Captured) 127
5.3.4 LC-MS/MS of rhMMP Peptides 129
5.3.5 rhMMP Recovery from H-7G-Sepharose 134
5.4 Discussion 135

6 Purification of Secreted and Cellular MMPs from Pre-clinical Cancer Model and Proteomic Mass Spectrometry 140

6.1 Introduction 140
6.1.1 Aims 143
6.2 Materials and Methods 144
6.2.1 Preparation of Foetal Calf Serum (FCS) for LC-MS/MS 144
6.2.2 Preparation of Culture Supernatants (Serum+ and Serum-free) 145
6.2.3 Specific variations in Olive H-7G Chromatography applied for Culture Supernatants 145
6.2.4 Protein Extraction from Cells 147
6.2.5 Olive H-7G Chromatography of Cell Extracts 148
6.3 Results 148
6.3.1 *In vitro* Models 148
6.3.2 LC-MS/MS of Foetal Calf Serum (FCS) 148

6.3.3 HT1080 and HT29- S+CS vs. SFCS 149
6.3.4 Olive H-7G Chromatography- HT1080 S+CS vs. SFCS (Salt Elution) 158
6.3.5 H-7G Chromatography of HT1080 SFCS (EDTA Elution) 168
6.3.6 H-7G Chromatography of HT1080 SFCS (Salt + EDTA Elution) 170
6.3.7 H-7G Chromatography of HT1080 SF Cell Extract 172
6.3.8 Olive H-7G Chromatography of HT29 SFCS (Salt Elution) 176
6.4 Discussion 177
7 Strategies to remove Non-specific binding and Enhance MMP Enrichment 183
7.1 Introduction 183
7.1.1 Aims 184
7.2 Materials and Methods 185
7.2.1 Pre-clearing Dermal Papilla Culture Supernatant using Sepahrose (Non-Cancer source of MMPs) 185
7.2.2 ADP/GDP use in HT1080 SFCS 186
7.2.3 Low Porosity Beads (Sephadex) 186
7.3 Results 187
7.3.1 LC-MS/MS of Dermal Papilla Culture Supernatant Fractions 187
7.3.2 ADP/GDP use in HT1080 SFCS 189
7.3.3 LC-MS/MS for H-7G-Sephadex Fractions 190
7.4 Discussion 193
8 Conclusions 196
Future Work 205
References 206
Appendices 221

Abbreviations

ABPP:	Activity based protein profiling
ADAMS:	A disintegrin and metalloproteinase
ADP:	Adenosine diphosphate
ALS:	Amyolateral sclerosis
AP-1:	Activator protein 1
APMA:	4-amino phenyl mercurial acetate
ATP:	Adenosine triphosphate
ATSDR:	Agency for toxic substance and disease registry
BSA:	Bovine serum albumin
BRC:	Background reducing concentrate
C127:	A murine mammary tumour-derived cell lin
$CaCl_2$:	Calcium chloride
CaR-1:	Human rectal carcinoma cell line
CCR-1:	Chemokine receptor 1
CD95:	Cluster of differentiation 95
cDNA :	Complimentary deoxyribonucleic acid
CHCA:	α-cyano-4-hydroxycinnamic acid
CHO:	Chinese hamster ovary cell line
CH_3CN:	Acetonitrile
CID:	Collision induced dissociation
CO_2:	Carbon dioxide
CXCL-12:	Chemokine ligand-12
Da:	Dalton
DBC:	Development buffer concentrate
DEAE:	Diethylaminoethyl
dH_2O:	Distilled water
DIGE:	Differential in-gel electrophoresis
DMSO:	Dimethyl sulfoxide
DNA:	Deoxyribonucleic acid
DTT:	1, 4-Dithiothreitol
EBI:	European bioinformatics institute
ECE:	Endothelin converting enzyme
ECL:	Enhanced chemiluminescence
ECM:	Extracellular matrix

EDTA: Ethylenediaminetetraacetic acid

EGFR: Epidermal growth factor receptor

ESI: Electrospray ionization

ETS-1/2: E twenty-six family of transcription factors

FAB: Fast atom bombardment

FD: Field desorption

FCS: Foetal calf serum

FGF: Fibroblast growth factor

FN II: Fibronectin type 2

FT: Flow-through

GATA-1: Guanidine-adenosine-tyrosine-adenosine sequence binding transcription factor 1

GDP: Guanosine diphosphate

Gly: Glycine

GTP: Guanosine triphosphate

H_2O_2: Hydrogen peroxide

H_2SO_4: Sulphuric acid

H_3PO_4: Phosphoric acid

HAP: High abundance proteins

HBSS: Hank's balanced salt solution

HCl: Hydrochloric acid

HER-2: Human epithelial receptor 2

$HgCl_2$: Mercuric chloride

HPLC: High pressure liquid chromatography

Hsp-α: Heat shock protein alpha

HxBP-rh: Hydroxamate benzophenone-rhodamine

IAC: Iodoacetamide

ICT: Institute of Cancer Therapeutics

ICAT: Isotope-coded affinity tag

IDC: Image developer concentrate

IL-1β: Interleukin-1 beta

IGFBP-3: Insulin-like growth factor binding protein-3

IGFBP-5: Insulin-like growth factor binding protein-5

IMAC: Immobilized metal ion affinity chromatography

IRBP: Interphotoreceptor retinoid-binding protein

iTRAQ: Isobaric tag for relative and absolute quantification

KCl:	Potassium chloride
kDa:	Kilodalton
LAP:	Low abundance proteins
LC:	Liquid chromatography
LOD:	Limit of detection
m/z:	Mass-to-charge ratio
MALDI-MS:	Matrix assisted laser desorption ionization mass spectrometry
MCP-1:	Monocyte chemotactic protein-1
mg:	Milligram
mL:	Milliliter
mM:	Millimolar
$MgCl_{2:}$	Magnesium chloride
MMP:	Matrix metalloproteinase
MS:	Mass spectrometry
MS/MS:	Tandem mass spectrometry
mRNA:	Messenger ribonucleic acid
MWCO:	Molecular weight cut off
MDD:	Mean minimum detectable dose
N:	Normal (concentration unit)
NaCl:	Sodium chloride
NaOH:	Sodium hydroxide
Na_2CO_3:	Sodium carbonate
Na_3N:	Sodium azide
Na_3PO_4:	Sodium phosphate
NH_4HCO_3:	Ammonium bicarbonate
NAD:	Nicotinamide adenine dinucleotide
NADP:	Nicotinamide adenine dinucleotide phosphate
NaSCN:	Sodium thiocyanide
NCBI:	National centre for biotechnology information
nL:	Nanolitre
nm:	nanometre
NMR:	Nuclear magnetic resonance
NSCLC:	Non-small cell lung carcinoma
OA:	Osteoarthritis
OSC-2:	Oesophageal squamous cell carcinomas

p53:	protein 53kDa
PAGE:	Polyacrylamide gel electrophoresis
PBS:	Phosphate buffered saline
Phe:	Phenylalanine
pI:	Isoelectric point
PI-3 kinase:	Phosphoinositide 3 kinase family
PMSF:	Phenylmethanesulfonylfluoride
Ppm:	Parts per million
PVDF:	Polyvinylidene fluoride
PKB:	Protein kinase B
RA:	Rheumatoid arthritis
RANTES:	Regulated upon activation, normal T-cell expressed and secreted
Rpm:	revolutions per minute
RPMI-1640:	Rosewell Park Memorial Institute-1640
rhMMPs:	Recombinant forms of human pro-MMPs
S+CS:	Serum-containing culture supernatant
SA:	Sinapinic acid
SC:	Sensitizing concentrate
SDS:	Sodium dodecyl sulphate
SFCS:	Serum-free culture supernatant
SILAC:	Stable isotope labeling by amino acids in cell culture
SIMS:	Secondary ion mass spectrometry
SM:	Starting material
SRC:	Silver reagent concentrate
TBS:	Tris buffered saline
TFA:	Trifluoroacetic acid
TGF-β1:	Transforming growth factor
Thr:	Threonine
TIMP:	Tissue inhibitor of metalloproteinase
TMB:	Tetramethylbenzidine
TNF-α:	Tumour necrosis factor alpha
TOF:	Time of flight
tPA:	Tissue plasminogen activator
VEGF:	Vascular endothelial growth factor
Zn^{2+}:	Zinc ion

List of Figures

Figure 1.1 Acquired capabilities for the development of cancer cells. 5

Figure 1.2 MMP discovery timeline in chronological order. 11

Figure 1.3 Conversion from latent to active MMP. 14

Figure 1.4 The 3D diagram of human pro-MMP-2 and TIMP-2 complex. 21

Figure 1.5 Principle of affinity chromatography. 26

Figure 1.6 Conventional MMP purification methods. 32

Figure 1.7 Schematic diagram of LIFT TOF/TOF MS. 38

Figure 1.8 Challenges for MMP enrichment. 46

Figure 2.1 Workflow for enrichment of MMPs from cell lines. 50

Figure 2.2 Flowchart for affinity chromatography. 53

Figure 2.3 Standard curve for BSA standards. 55

Figure 2.4 Standard curve for ELISA standards. 56

Figure 2.5 LC-MS/MS workflow. 65

Figure 2.6 LC-MS/MS workflow supported by WARP-LC. 66

Figure 3.1 Structure of Procion Olive H-7G. 68

Figure 3.2 Coupling of triazinyl dyes to the matrix bearing hydroxyl groups. 69

Figure 3.3 Photometric scanning (200-1000nm) of Olive H-7G to measure absorption λ (n=5). 72

Figure 3.4 MALDI mass spectrum of CHCA matrix (spectral range 700-4000). 73

Figure 3.5 MALDI mass spectra of Olive H-7G (spectral range 700-4000). 73

Figure 3.6 HPLC profile of 80nM Olive H-7G (n=3). 74

Figure 4.1 Applications of MALDI-MS in proteomics. 78

Figure 4.2 MALDI mass spectra for intact rhMMP-3, rhMMP-7, rhMMP-10 and rhMMP-14. 86

Figure 4.3 Mass spectra for Myo, Try and Myo + Try controls. 87

Figure 4.4 A. MS PMF of rhMMP-1 annotated tryptic peptides, B. Mass data for peptides in daltons, C. Sequence coverage, ID peptides in red, active site green and arrow heads pointing start of various regions. 94

Figure 4.5 A. MS PMF of rhMMP-2 annotated tryptic peptides, B. Mass data for peptides in daltons, C. Sequence coverage, ID peptides in red, active site green and arrow heads pointing start of various regions. 95

Figure 4.6 A. MS PMF of rhMMP-3 annotated tryptic peptides, B. Mass data for peptides in daltons, C. Sequence coverage, ID peptides in red, active site green and arrow heads pointing start of various regions. 96

Figure 4.7 A. MS PMF of rhMMP-7 annotated tryptic peptides, B. Mass data for peptides in daltons, C. Sequence coverage, ID peptides in red, active site green and arrow heads pointing start of various regions. 97

Figure 4.8 A. MS PMF of rhMMP-8 annotated tryptic peptides, B. Mass data for peptides in daltons, C. Sequence coverage, ID peptides in red, active site green and arrow heads pointing start of various regions. 98

Figure 4.9 A. MS PMF of rhMMP-9 annotated tryptic peptides, B. Mass data of peptides.. 99

Figure 4.10 MMP-9 Sequence coverage, ID peptides in red, active site green and arrow heads pointing start of various regions. 100

Figure 4.11 A. MS PMF of rhMMP-10 annotated tryptic peptides, B. Mass data for peptides in Daltons. 101

Figure 4.12 Sequence coverage for MMP-10, ID peptides in red, active site green and arrow heads pointing start of various regions. 102

Figure 4.13 A. MS PMF of rhMMP-13 annotated tryptic peptides, B. Mass data for peptides in daltons, C. Sequence coverage, ID peptides in red, active site green and arrow heads pointing start of various regions. 103

Figure 4.14 A. MS PMF of rhMMP-14 annotated tryptic peptides, B. Mass data for peptides in daltons, C. Sequence coverage, ID peptides in red, active site green and arrow heads pointing start of various regions. 104

Figure 4.15 Peptide fragments of rhMMP-1, rhMMP-2, rhMMP-3, rhMMP-7, rhMMP-8, rhMMP-9, rhMMP-13 and rhMMP-14. 105

Figure 4.16 Mass Spectra of Olive H-7G and H-7G-MMP-2 complex. 107

Figure 4.17 Mass spectra of Olive H-7G-MMP complex. 108

Figure 5.1 Reaction between H-7G-Sepharose beads and mixture of (A) 4 rhMMPs, (B) 9 rhMMPs. 118

Figure 5.2 Experimental design for magnetic beads. 119

Figure 5.3 Reaction between magnetic beads and mixture of 11 rhMMPs. 121

Figure 5.4 MALDI mass spectra for H-7G-Sepharose, H-7G-Sepharose FT and mixture of 4 rhMMPs. 125

Figure 5.5 MALDI mass spectra for H-7G-Sepharose, H-7G-Sepharose FT and mixture of 9 rhMMPs (n=3). 126

Figure 5.6 MALDI mass spectra of MB, MB-MMP, H-7G-MB-MMP and mixture of 11 rhMMPs. 128

Figure 5.7 nHPLC profiles for mixture of 9 rhMMPs, H-7G-Sepharose, sepharose and corresponding FT. 130

Figure 6.1 Tumour cell line growth curves. 151

Figure 6.2 Gene expression of MMPs in cell lines. Rreproduced courtesy of Jenifer Atkinson, (Atkinson, Pennington et al. 2007). 155

Figure 6.3 MALDI mass spectra of HT1080 S+CS and SFCS. 157

Figure 6.4 MALDI mass spectra of HT1080 cell lysates (SFCS). 157

Figure 6.5 SDS-PAGE to show capture of proteins by H-7G-Sepharose chromatography beads. 162

Figure 6.6 Staining of S+CS and SFCS H-7G-Sepharose chromatography fractions to show recovery of proteins. 162

Figure 6.7 Immuno-blotting to show MMP-2 capture by H-7G-Sepharose chromatography beads (after elution) from HT1080 S+CS and SFCS. 163

Figure 6.8 Immuno-blotting of HT1080 culture cupernatants and Olive H-7G chromatography fractions. 163

Figure 6.9 MALDI mass spectra of HT1080 eluate showing detergent peaks. 164

Figure 6.10 Protein expression of HT1080 cell extracts (Method I) and H-7G-Sepharose chromatography fractions. 175

Figure 7.1 Affinity chromatography of dermal papilla culture supernatant before and after sepharose pre-clearing. 186

Figure 7.2 Trypsin digestion for H-7G-Sephadex chromatography fractions. 187

Figure 7.3 HPLC profiles and LC-MS/MS results for sepharose pre-clearing experiment (n=1). 188

Figure 7.4 Protein expression of HT1080 SFCS and chromatography fractions after removal of ADP/GDP binding proteins. 189

Figure 8.1 Screening rhMMPs for Olive H-7G in present study. 200

List of Tables

Table 3.1 HPLC gradient parameters for analytical runs of Olive H-7G. 71

Table 4.1 MMP characteristics. 79

Table 4.2 Concentration of intact rhMMPs for molecular mass determination..... 82

Table 4.3 Protein to dye ratios for reaction..... 84

Table 4.4 MMP theoretical and molecular masses by MALDI-MS. 85

Table 5.1 Final concentration of rhMMPs in mixtures. 117

Table 5.2 Final concentration in mixture of 11 rhMMPs. 120

Table 5.3 Theoretical and experimental digest peaks for 4 rhMMP mixture, H-7G-Sepharose and sepharose. 125

Table 5.4 LC-MS/MS results. 131

Table 5.5 Sequence coverage of MMPs to discriminate 'Pro' and 'Active' forms. 132

Table 5.6 MMP recovery from H-7G-Sepharose based on ELISA. 134

Table 6.1 Trypsin digestion for EDTA eluates. 146

Table 6.2 MMP-2 production by HT1080 and HT29 culture supernatants. 156

Table 6.3 MMP-2 production by HT1080 cell lysates..... 156

Table 6.4 Protein amounts in HT1080 SFCS and H-7G-Sepharose chromatography fractions (Detergent-free elution buffers). 159

Table 6.5 MMP-2 amounts in HT1080 SFCS to show yield in H-7G-Sepharose chromatography. 160

Table 6.6 Sequence of signature peptides in MMP-2, MMP-14, TIMP-1 and TIMP-2 detected in HT1080 SFCS eluates from 0.3 and 2M NaCl containing buffers..... 166

Table 6.7 Protein (BA) and MMP-2 amounts (ELISA) in EDTA eluates (10mM, 100mM) and LC-MS/MS results. 168

Table 6.8 Proteins eluted in 10mM and 100mM EDTA. 169

Table 6.9 TIMP-1 and TIMP-2 Mascot scores in Salt + EDTA eluates. 170

Table 6.10 Proteins eluted in Salt + EDTA elution buffers. 171

Table 6.11 Protein (BA) and MMP-2 (ELISA) amounts in HT1080 cells Salt Extract and H-7G-Sepharose chromatography fractions..... 173

Table 6.12 Protein (BA) and MMP-2 (ELISA) amounts in HT1080 cells DMSO Extract and H-7G-Sepharose chromatography fractions. 173

Table 6.13 Protein (BA) and MMP-2 (ELISA) amounts in HT1080 cells Urea Extract and H-7G-Sepharose chromatography fractions..... 173

Table 6.14 Protein (BA) and MMP-2 (ELISA) amounts in cell lysates (Method II) and Olive H-7G chromatography fractions and LC-MS/MS results. 176

Table 7.1 LC-MS/MS of HT1080 SFCS chromatography fractions after ADP/GDP suppression of proteins. 190

Table 7.2 Proteins binding non-specifically to H-7G-Sephadex (No elution)..... 190

Table 7.3 Proteins eluted from H-7G-Sephadex using 0.3M and 5M NaCl buffers..... 191

Table 7.4 Proteins in eluates of H-7G-Sephadex. 192

List of Appendices

Appendix 1 Buffer compositions. 221

Appendix 2 Cell lines origin. 222

Appendix 3 Horse heart myoglobin theoretical digests. 223

Appendix 4 MMP theoretical digests. 224

Appendix 5 Experimental *m/z* of rhMMPs including signature peptides. 233

Appendix 6 Mass peaks of Brij-35. 235

Appendix 7 FCS LC-MS/MS results. 236

Appendix 8 BSA peptide sequences. 237

Appendix 9 LC-MS/MS (HT1080 SFCS E2a). 239

Appendix 10 Publication. 240

CHAPTER 1

INTRODUCTION

1 Introduction

1.1 Definition of Cancer

Cancer is a broad and complex family of diseases that remains one of the most frequent causes of death worldwide (Varmus, 2006). Although cancer has multiple causes and exhibits a wide range of genetic, physiological and histological features, an acceptable clinical definition states that cancer is a set of diseases characterized by up-regulated cell growth leading to invasion of surrounding tissues and metastasis to different parts of the body (Kinzler and Vogelstein, 1996). Cancer research over the last few decades has defined cancer to be a disease involving dynamic changes in the genome. The discoveries of mutations that produce oncogenes with dominant gain of function and tumour suppressor genes with recessive loss of function in animal models have set the foundation of cancer research. Several lines of investigation suggest that tumourigenesis is a multi-step process where alterations at genetic level drive the progressive transformation of normal human cells into highly malignant derivatives. These genetic alterations can be as subtle as point mutations and as substantial as changes in chromosome compliment (Kinzler and Vogelstein, 1996). Cancer cells have defects in regulatory circuits that govern normal cell proliferation and homeostasis.

1.2 Hallmarks of Cancer

Cancer arises from the stepwise accumulation of several genetic alterations in a cell over time, resulting in uncontrolled growth, the formation of a tumour and the ability of cells from that tumour to metastasize (Fearon and Vogelstein, 1990). The uncontrolled cell growth observed in cancers is complex and is thought to result from the deregulation of a number of features under exquisite control in healthy cells. It has been suggested that the successful breaching of anticancer defense mechanisms in each cell is achieved by acquiring novel capabilities caused by changes in molecular,

biochemical and cellular traits regulating their proliferation, differentiation and death (Hanahan and Weinberg, 2000). Hanahan and Weinberg proposed that six essential alterations in cell physiology collectively dictate malignant growth namely self-sufficiency in growth signals, insensitivity to antigrowth signals, evasion of programmed cell death (apoptosis), limitless replicative potential, sustained angiogenesis and tissue invasion and metastasis (Figure 1.1).

1.2.1 Limitless Replicative Potential

Mammalian cells carry an intrinsic program that limits the replicative potential of a cell and the number of divisions it may undergo. Healthy cells stop dividing (senescence) once a maximum number of cell doubling has been reached. In cancer cells, this senescence mechanism is de-regulated resulting in an override of replicative control. This replicative process is deregulated via telomeres which are specialized lengths of chromosome ends (Hanahan and Weinberg, 2000). As a cell divides, these telomeres shorten until eventually chromosomes become unprotected, signaling the senescent switch. A major mechanism for overcoming this switch is the up-regulation of an enzyme called telomerase which is able to renew the length of telomeres resulting in a limitless replication (Blackburn, 2005).

1.2.2 Self Sufficiency and Insensitivity to Antigrowth Signal

Normal cells in culture require specific mitogenic factors and matrices in order to proliferate; this is in contrast to cancer cells which have shown a greatly reduced dependency on exogenous growth stimulation. Growth signaling autonomy by activation of dominant oncogenes is a feature of tumour cells which liberates it from homeostatic mechanisms in tissues (Hanahan and Weinberg, 2000). The over-expression of receptors HER-2/neu has been reported in mammary carcinomas which enables the cancer cells to respond to ambient levels of signals which otherwise will not illicit a cellular response (Yarden and Ullrich, 1988). The genetically damaged cancer cells are supported by surrounding stromal cells such as inflammatory cells which have been reported to promote growth at the site of neoplasia

(Hudson et al., 1999). In order to keep dividing to establish the tumour, cancer cells devise ways to avoid terminal differentiation. In addition to self-sufficiency in growth signals, cancer cells have developed a number of modifications to become insensitive to growth inhibitory signals. The tumour cells become insensitive to antigrowth signals via disrupting various mechanisms controlling cell division. Fynan reported that disruption of retinoblastoma protein signal circuitry switches the quiescent cells to dividing cells (Fynan and Reiss, 1993). One of the strategies followed by tumour cells is to shift the balance from myc-mad complex to myc-max complex formation, the latter being the anti-differentiation signal which promotes growth (Foley and Eisenman, 1999). It too must be disrupted in order for a clone of cells to expand to a size that constitute a macroscopic tumour. It has been found that a cell achieves limitless replicative potential by escaping senescence, multiplying for additional generations to enter crisis state and without limit, the trait termed as immortalization (Wright et al., 1989).

1.2.3 Evasion of Apoptosis

In healthy cells, inappropriate proliferation is controlled by the tightly regulated process of apoptosis, a precisely choreographed series of steps in which cell membranes are disrupted, cytoskeletons are broken down, chromosomes are degraded and the nucleus is fragmented (Hanahan and Weinberg, 2000). All types of cancer cells alter expression of survival and death signal receptors on their cell surface to escape programmed cell death (Hanahan and Weinberg, 2000). In the event of abnormality such as DNA damage, oncogene activation or insufficient survival signals, cell death is stimulated (Evan and Littlewood, 1998). Tumour cells grow rapidly by decreasing the expression of p53 protein which, as part of the defense system of cell, loses its function (Symonds et al., 1994). Resistance to apoptosis is acquired by impairing the apoptotic signaling circuitry. It was found that lung cancer cells develop non-signaling CD95 (Fas) receptors which do not bind Fas death signals hence cells continue to divide and grow into a tumour (Pitti et al., 1998). The cell survival signaling pathway PI-3

kinase-AKT/PKB is activated in most parts of human tumours (Hanahan and Weinberg, 2000).

1.2.4 Angiogenesis

Angiogenesis is an invasive process in which new vessels emerge from existing endothelial vessels as opposed to vasculogenesis in which vessels differentiate from stem cells (Stetler-Stevenson, 1999). Circulatory system develops by both vasculogenesis and angiogenesis during embryonic life. However, in the adults, with the single exception of the reproductive cycle in females, angiogenesis is initiated only in response to a pathologic condition, such as inflammation, rheumatoid arthritis, hypoxia and cancer. The rapid growth of tumours results in their requirement of their own blood supply and it is known that tumours do not grow beyond 1-2mm unless there is a supply of oxygen and nutrients (Carmeliet and Jain, 2000). Angiogenesis is a dynamic process, controlled by a large number of pro- including vascular endothelial growth factor (VEGF) and fibroblast growth factor (FGF) and anti-angiogenic factors (including thrombospondin-1 and endostatin) (Bergers and Benjamin, 2003). In order to maintain a sufficient blood supply carrying nutrients for rapidly dividing cells in tumour, it develops more and more blood vessels (Folkman, 1997). Various studies at transcriptional level have confirmed the down-regulation of antiangiogenic factors during tumour growth such as thrombospondin-1 which in turn is regulated by p53 tumour suppressor gene (Dameron et al., 1994). An up-regulation of angiogenic inducers such as VEGF further supports the idea that tumour promotes neo-vascularisation (Volpert et al., 1997).

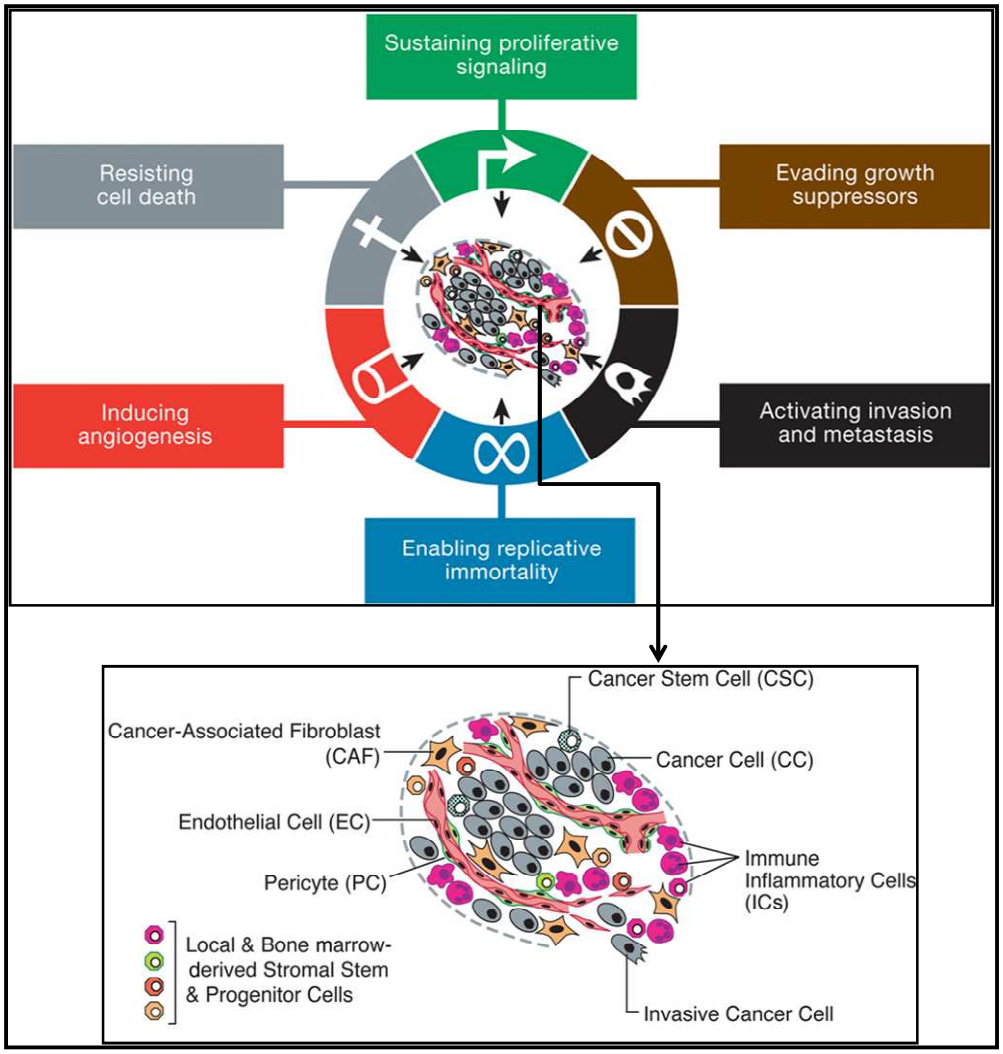

Figure 1.1 Acquired capabilities for the development of cancer cells. Taken from (Hanahan and Weinberg, 2011).

1.2.5 Cancer Invasion and Metastasis

Metastasis describes both the process of cancer spread, and the resultant secondary cancer, the actual metastatic lesion. Since most cancer patients present with localized disease that is effectively managed with multimodality therapies including surgery, radiation, and chemotherapy, the development of metastasis at distant secondary organs must involve the dissemination of metastatic cells before patients present with a primary tumour. Based on the work of several groups, it is believed that the process of metastasis involves tumour cells leaving the primary tumour through well-regulated lyses of surrounding stroma. These cells must pass through the tumour basement membrane and then through or between endothelial cells in order to enter the

circulation. While in the circulation, tumour cells must resist the process of anoikis (programmed cell death associated with loss of cellular contact), evade immune recognition, cope with the sheer physical stress of the circulatory system, and eventually arrest at a distant organ. At the distant site, the cell must exit the circulation, survive the stresses of a new and likely hostile microenvironment, proliferate, induce angiogenesis and/or co-opt existing blood vessels, and then successfully grow into a measurable metastatic lesion (Steeg and Theodorescu, 2008).

The timing, pattern and sites for the spread of cancer are in part defined by the specific cancer type. The route of spread of cancer may include blood stream (haematogenous), lymphatic vessels, or third space extension i.e., ascitic fluid dissemination as seen in ovarian cancer. The site of distant metastasis may include regional lymph nodes, or visceral organs such as lungs, liver, brain, and bone. Weiss et al. have shown that the primary site of metastases tend to occur at the first capillary bed encountered (Weiss et al., 1988). However, it is increasingly believed that the specific site of distant metastasis is not simply due to the anatomical location of the primary tumour or proximity to secondary sites, but rather, involves interactions between tumour cells and the local micro-environment at the secondary site. For many reasons, metastatic lesions are often not amenable to the surgical treatment achieved in the management of the primary tumour. Metastasis remains the overwhelming cause of approximately 90% deaths for cancer patients (Hanahan and Weinberg, 2000). The development of metastases at distant secondary organs is often so widespread that surgery is not possible. In addition, metastatic lesions themselves demonstrate increased resistance to conventional treatment modalities i.e., chemotherapy. This resistance to therapy may be acquired as a result of past treatment of the patient or may be an innate feature of cells that have successfully negotiated the metastatic process. Based on the challenges that metastatic disease presents, new treatment options are needed in order to decrease morbidity and mortality.

1.3 Matrix Metalloproteinases (MMPs)

The cancer degradome defines the complete set of protease genes or the repertoire of proteases expressed by a certain tissue during cancer (Lopez-Otin and Overall, 2002). The human degradome is composed of 569 protease and protease-related genes (Puente and Lopez-Otin, 2004; Puente et al., 2003). Human proteases can be divided into five different catalytic classes, with metalloproteinases, serine and cysteine proteases being the most abundant ones (194, 176 and 150 genes in human genome, respectively), while aspartic and threonine proteases are composed of smaller numbers (21 and 28, respectively). The family of matrix metalloproteinases (MMPs), also known as matrixins, represents a sub-group of zinc endopeptidases which mediate both normal and pathological tissue remodeling processes. The human genome has 24 matrixin genes which include a duplicated *MMP23* gene. Thus, there are 23 different MMPs (Murphy and Nagase, 2008a). In these endopeptidases, a conserved methionine forming a 'Met-turn' eight residues downstream of the Zn^{2+} binding motif HEXXHXXGXXH supports the active site cleft structure around the catalytic Zn^{2+} (Bode et al., 1993).

In 1962 Gross and Lapiere first reported vertebrate collagenolytic activity in tadpole tissues (tailfin, skin, intestine and gill) undergoing metamorphosis (Gross and Lapiere, 1962). These tissues are rapidly remodeling the ECM, hence triggering apoptosis, cell differentiation and growth (Shi et al., 1998). Since degradation of collagen is important in wound healing, tissue regeneration and diseases such as arthritis, cancer, atherosclerosis, aneurysm and tissue ulcerations, this discovery stimulated many researchers to look into human tissues. MMP-1 can degrade a broad range of substrates including types I, II, III, VII, VIII, and X collagens as well as casein, gelatin, α-1 antitrypsin, myelin basic protein, L-Selectin, pro-TNF, IL-1β, IGFBP-3, IGFBP-5, pro-MMP-2 and pro-MMP-9. A significant role of MMP-1 is the degradation of fibrillar collagens in ECM remodeling, characterized by the cleavage of the interstitial collagen triple helix into ¾, ¼ fragments. MMP-1 is expressed by fibroblasts, keratinocytes, endothelial cells, monocytes and macrophages. MMP-10 is expressed naturally in keratinocytes, T cells,

menstrual endometrium and a few tumour samples. MMP-10 degrades a broad range of substrates including gelatin, collagen types III, IV and V, fibronectin and aggrecan. MMP-10 can activate other MMPs such as MMP-1 and MMP-8. MMP-13 has been demonstrated to degrade a range of ECM proteins, including collagen types I, II, III, IV, IX, X and XIV, gelatin, aggrecan, perlecan and fibronectin. MMP-13 is distinguished from the other human collagenases by its efficient degradation of type II collagen. MMP-13 is expressed by fibroblasts, chrondrocytes and and squamous epithelial cells. Over ~40 years (1962–2001), 28 different MMP genes have been identified. The founding member of the MMP family, *Xenopus* collagenase, now thought to be collagenase 4 (MMP-18), was discovered in 1962 by J. Gross and C. M. Lapiere (Gross and Lapiere, 1962) and the last member, epilysin (MMP-28), was reported by Strongin in 2001 (Marchenko et al., 2001). With the completion of the genome project, it is clear that all members of this family have now been identified (Greenlee et al., 2007).

1.4 MMPs in Normal Physiology and Degradative Diseases

These enzymes are present in normal healthy individuals and have been shown to play an important role in processes such as wound healing, pregnancy and bone resorption. The hallmark of disease involving MMPs appears to be a stoichiometric imbalance between active MMPs and tissue inhibitor of metalloproteinases (TIMPs), leading to excessive tissue disruption and often degradation. MMPs have been implicated in the development or progression of several diseases or syndromes. The destructive mechanism of cellular damage in myocardial infarction and vascular disease is suggested to involve MMP-2, MMP-9 and MMP-14 (Deschamps et al., 2005; Hayashidani et al., 2003; Longo et al., 2002; Matsumura et al., 2005). Chase and Newby (2003) have proposed that multiple steps of MMP gene induction occur in vascular pathologies due to the progressive recruitment of different cell types and inductive factors during different phases of the disease (Chase and Newby, 2003). In rheumatoid arthritis (RA) and osteoarthritis (OA), the MMPs are known to be central to destruction at the synovial membrane (Okada et al., 1986). In particular, MMP-1 and MMP-13 are produced by

synovial fibroblasts and macrophages, and chondrocytes are rate limiting in the process of collagen degradation. Furthermore, the expression of MMPs in synovial membranes, cartilage, tendon and bone of synovial joints in both RA and OA often correlates with tissue destruction (Murphy and Nagase, 2008b; Smeets et al., 2001). MMPs such as MMP-2, MMP-3, MMP-9, MMP-10 and MMP-19 are also elevated in arthritis and, along with MMP-13 these enzymes degrade non-collagen matrix components of the joints (Cawston and Wilson, 2006). Therefore, various diagnostic and therapeutic strategies in OA and RA are focused on the involvement of MMPs in these diseases (Okada et al., 1990).

1.5 Role of MMPs in Cancer

Tumour growth is orchestrated by degradation of the ECM, release of sequestered growth factors and/or the generation of bioactive fragments (Noel et al., 2008). A number of cancer studies have correlated MMP expression and disease outcome (Egeblad and Werb, 2002). For instance, MMP-9 mobilizes VEGF from the ECM (Bergers et al., 2000) and cleaves type IV collagen to generate tumstatin, an angiogenesis inhibitor (Hamano et al., 2003). The MMPs are clearly implicated in angiogenesis. The most direct and compelling evidence for this conclusion is that MMP inhibitors, both synthetic and endogenous, inhibit angiogenic responses both *in vitro* and *in vivo* (Hiraoka et al., 1998). Moreover, recent studies provide evidence that MMP-deficient mice exhibit delayed or diminished angiogenic responses during development or in response to tumour xenografts (Itoh et al., 1998). While these studies clearly implicate functional MMP activity in the angiogenic response, there is some debate regarding the possible molecular targets that are involved and their precise role in angiogenesis. Understanding what, where, when, and how MMP activity is involved in the angiogenic phenotype has enormous implications for cancer therapy because angiogenesis is necessary for tumour growth and metastasis. Current therapeutic approaches targeting MMP activity utilize general class inhibitors that are selective, but not specific, for some MMP family members. This has resulted in moderately severe, but reversible, musculo-skeletal

complications. This experience highlights a need for a better understanding of the specific MMPs and their precise role in the angiogenic response. In this way, we can discern what MMPs to target, and when to target them, with the aim of limiting side effects and possible complications. MMPs reportedly produced by endothelial cells are MMP-1, MMP-2, MMP-9, and MT-1-MMP. Of these, MMP-2 and MT-1-MMP are the most studied for their role in angiogenesis (Hiraoka et al., 1998; Zhou et al., 2000).

The molecular mechanisms underlying the cellular events of angiogenesis have been examined utilizing a number of *in vitro* models. These have been helpful in examining the role of proteases in angiogenesis. They include growth of endothelial cells or vascular explants in amniotic membranes, fibrin clots, type I collagen, or basement membrane matrices. In these assays, endothelial cells acquire a migratory or invasive phenotype, reorganize the ECM, and in some cases recapitulate the tubular morphology of micro vessels complete with lumen formation. In many early studies, the ECM was viewed as a barrier to endothelial cell invasion. The principal role of MMP activity was to remove this barrier and allow endothelial cell migration. Recent studies challenge this notion and suggest that cell–ECM interactions profoundly influence cell behavior. These interactions not only influence MMP production but are subject to modulation and regulation by MMP activity. In this way, MMP activity can directly and indirectly mediate the angiogenic response. MMPs work in a complex cascade with other factors in tumour progression, promoting invasion, immune escape and many other events. It is possible that obtaining a detailed understanding of the potential role of MMPs in the different cell types associated with tumours may improve our understanding of this disease and aid the design of therapeutic strategies. Proteins involved in cancer cell motility and chemotactically-guided extravasation of arrested cancer cells at secondary sites are mediated by MMPs.

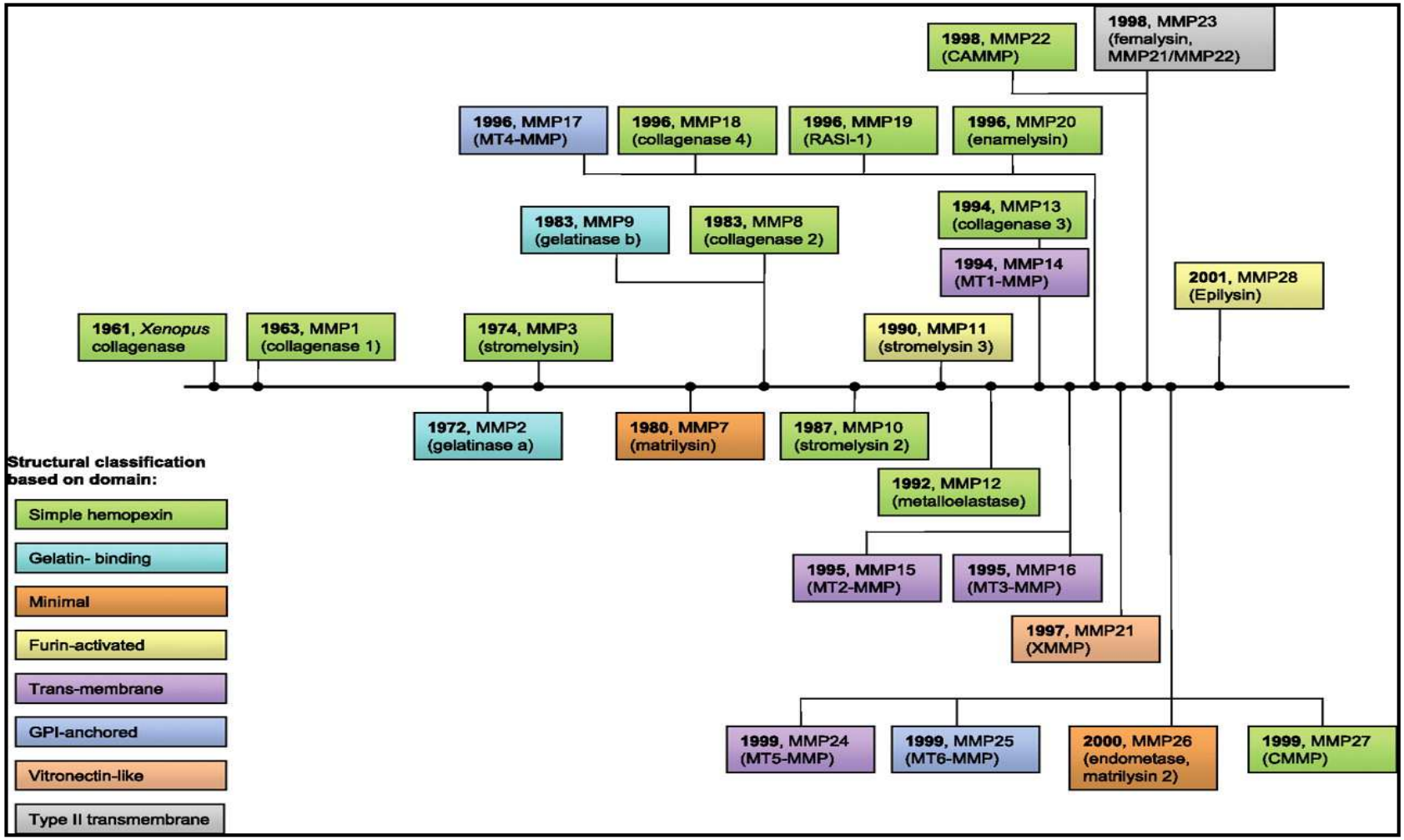

Figure 1.2 MMP discovery timeline in chronological order.

Taken from (Greenlee et al., 2007).

1.6 Regulation of MMPs

MMPs are produced in different cell types under unique conditions, and thus distinctive inductive and suppressive factors regulate their expression which has been detailed comprehensively in several studies.

1.6.1 Transcriptional and Translational Regulation

Transcription factors which can be activators and repressors tightly regulate MMPs at the gene expression level (Greenlee et al., 2007). Moreover, mRNA stability has been reported to play a role in regulation of MMP-1, MMP-2, and MMP-9. (Overall et al., 1991). GATA-1 in endothelial cells and members of the AP-1 family, c-Jun, Jun-D, c-Fos, Fos-B, and Fra-1 proteins in lung cancer cells activate the MMP-2 promoter (Choi et al., 2005; Han et al., 2003). Epidermal growth factor receptor (EGFR) activation up-regulates MMP-14 in lung fibroblasts (Kheradmand et al., 1998). Chemokines have been shown to regulate several members of the MMP family. Indirect evidence shows that activation of CCR-1, the receptor for RANTES, MCP-1, and CXCL-12, induces secretion of MMP-9 in primary human monocytes (Klier et al., 2001). Reactive oxygen species (ROS), including singlet O_2, hydroxyl radical, superoxide anion, and hydrogen peroxide can affect MMP gene expression through activation of several transcription factors. For example, H_2O_2 production by mitochondria can activate MMP-1 gene expression through activation of AP-1 and Ets-1 transcription factors (Nelson and Melendez, 2004). The role of shear mechanical stress elevates the mRNA level of MMP-1, MMP-3, and MMP-13 and the three transcription factors c-Fos, Ets-1, and Ets-2, suggesting a new mechanism for tissue degradation in rheumatic joints (Sun and Yokota, 2001).

1.6.2 Post-Translational Regulation

MMP activity is kept in check by post-translational modification (PTM) of MMPs mediated through activation of latent MMPs and compartmentalization.

1.6.2.1 Activation of MMPs

The MMPs are synthesized and secreted as pre-pro-enzymes and the signal peptide is removed during translation to generate pro-MMPs (Overall and Lopez-Otin, 2002). MMPs can be activated both proteolytically (*in vivo* and *in vitro*) by other proteases or by autolysis, and non-proteolytically by chemical agents (*in vitro*). Chemical agents such as APMA (4-aminophenylmercuric acetate), $HgCl_2$, SDS, chaotropic agents, reactive agents and even heat treatment or low pH cause activation *in vitro* (Visse and Nagase, 2003). The pro-peptides have the 'cysteine switch' motif PRCGXPD in which the cysteine residue coordinates with the catalytic Zn^{2+} in the catalytic domain, keeping the pro-MMPs inactive (Van Wart and Birkedal-Hansen, 1990). The stepwise activation proceeds as an intramolecular reaction to cleave the Cys switch-Zn^{2+} interaction and subsequent hydrolysis of exposed Zn^{+2} ions. This intermediate could be activated by removal of pro-peptide either by other activated MMPs or chemical agents (Nagase et al., 1990). For regulation of these activated enzymes to avoid destruction within a cell, TIMPs bind with intermediates before the MMP is fully activated. Intracellular activation of pro-MMP-11 by furin and its secretion as an active protease demands endogenous inhibition for regulation of its activity (Pei and Weiss, 1995). MMP-26 is unique enzyme distinguished by the presence of histidine in place of arginine in highly conserved sequence of pro-petide domain PRCGV/NPD. Arginine residue is positively charged in the physiological pH range. In contrast, histidine is only positively charged at pH values below 7. This intrinsic feature of histidine may make MMP-26 more sensitive to pH changes; affect the stability and possibly the activation mechanisms of the MMP-26 zymogen (Marchenko et al., 2001).

Several MMPs are exception to this rule. An alternatively spliced transcript of MMP-11 lacking the signal peptide and the pro-peptide domain encodes an active intracellular form, but its function is not known (Luo et al., 2002). Cell surface activation of pro-MMP-2 is mediated by MT-1-MMP and TIMP-2 facilitated by hemopexin domain of MT-1-MMP (Itoh et al., 2001). Membrane bound MMPs all have a furin-like pro-protein convertase recognition sequence RX[R/K]R at the C-terminus of the pro-peptide. Pericellular

activation of MMP-2 on the cell surface is achieved by the interaction of pro-MMP-2 to MMP-14 and TIMP-2. This complex tethers the zymogen in place and allows a second active MMP-14 to cleave the pro-domain and liberate the activated MMP2 (Strongin et al., 1995).

1.6.2.2 Localization of MMPs

MMPs can be either free in the cytosol or bound to the surface of a cell such as the compartmentalization of MMPs in inflammatory cells. For example, pro-MMP-8, pro-MMP-9, and pro-MMP-25 are packaged into granules within neutrophils to be released upon leukocyte activation (Eickelberg et al., 1999). The cell surface expression pattern of MMP-14 is one potential regulator of MMP-2 activity, since MMP-2 activation would then be dependent on co-localization with MMP-14 (Haas, 2005). MMP-9 is secreted but also has a cell surface-bound form which is expressed on neutrophils in response to pro-inflammatory mediators and can cleave gelatin, type IV collagen, elastin, and α-1 proteinase inhibitor *in vitro* (Owen et al., 2003) The cell surface activation of MMP-2 and MMP-7 suggest that localization of MMPs to the cell surface is a general means of regulating MMP activity.

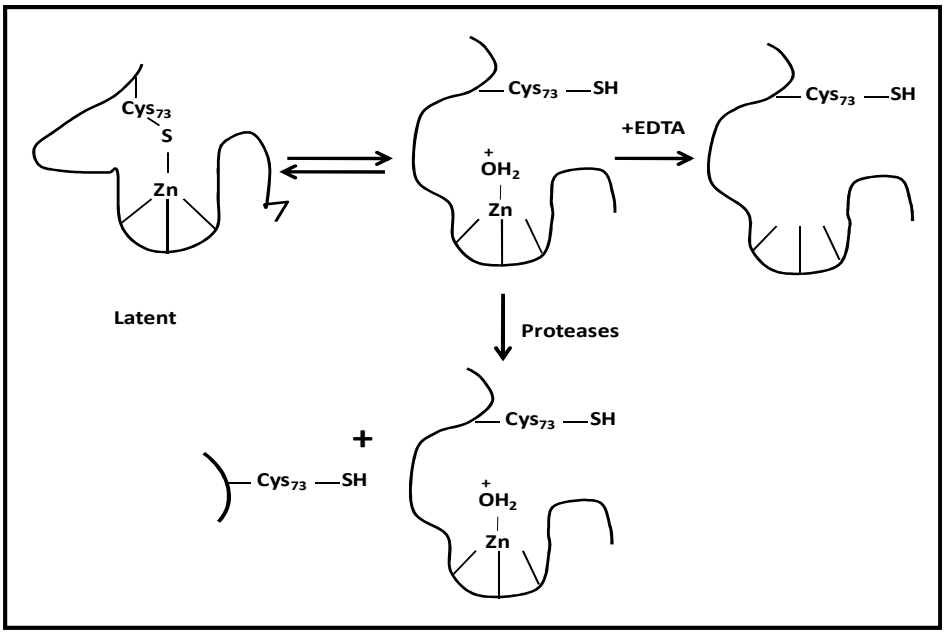

Figure 1.3 Conversion from latent to active MMP.

1.6.3 Regulation by Protease Inhibitors and other Factors

1.6.3.1 Natural Inhibitors

MMPs have several naturally occurring inhibitors (Murphy and Nagase, 2008a). To date, four members of the family have been characterized TIMP-1, TIMP-2, TIMP-3, and TIMP-4 of which TIMP-1 and TIMP-3 are glycoproteins. TIMP-2 has been shown to inhibit tumour growth, angiogenesis, invasion, and metastasis in experimental models, an observation consistent with a role of MMP activity in these processes. Studies have shown that TIMP-3 is a major regulator not only of matrix metalloproteinases but ADAMS (Wang et al., 2006) including ADAM-10 (Amour et al., 2000). Crystal structures for TIMP-1 in complex with MMP-3 have been described (Gomis-Ruth et al., 1997). TIMPs bind with their edge into the entire length of the active site cleft of MMPs when forming complexes (Gomis-Ruth et al., 1997). It has also been shown that TIMP-2 has a bi-functional effect on MMP-2 since MT-MMP-mediated pro-MMP-2 activation requires a small amount of TIMP-2 to make activation progress, whereas a greater concentration of TIMP-2 inhibits MMP-2 (Kinoshita et al., 1998). TGF-β1 increases the mRNA of both TIMP-1 and TIMP-3 in human chondrocytes and rat osteoblasts (Wang et al., 2006). TIMP-4 is a good inhibitor for all classes of MMPs without notable preference for specific MMPs (Stratmann et al., 2001).

1.6.3.2 Synthetic Inhibitors

A number of small molecules are also good inhibitors of MMPs activities (Mix et al., 2001), (Bernardo et al., 2002). There are broad-spectrum inhibitors which interfere with most MMPs and specific inhibitors working on only one or two members. Due to redundancy of MMPs, inhibition effects are not easy to predict, making synthetic inhibitors poor candidates for therapeutic use. In a clinical trial of merimastat, serious musculo-skeletal side effects in cancer patients were observed. In addition, other clinical trials were stopped due to decreased survival or no survival benefit detected. On the other hand, more promising, specific MMP inhibitors are in preliminary stages of research. A

specific inhibitor with affinity for MMP-2 and MMP-9, ONO-4817, has been shown to decrease neutrophil migration. The potential involvement of any of the 24 MMPs in both normal tissue maintenance and the destructive or reparative aspects of many diseases has produced numerous challenges when considering the potential application of MMP inhibitors as therapeutic agents. A detailed understanding of MMP expression patterns, in terms of both cellular origins and timing is essential. Furthermore, some knowledge of the precise role of an individual MMP within each context is important. This needs to be coupled with the ability to generate specific inhibitors, either targeting the active site or other interaction sites.

1.7 MMP Structure

Numerous 3D structures of MMPs have been determined both by X-ray crystallography and NMR spectroscopy (Maskos, 2005) including full-length pro-MMP-1 (Jozic et al., 2005), pro-MMP-2 (Morgunova et al., 1999), the pro-MMP-2-TIMP-2 complex (Morgunova et al., 2002), pro-MMP-3 without the linker region and the hemopexin domain (Becker et al., 1995) and pro-MMP-9 without the linker region and the hemopexin domain (Elkins et al., 2002). Figure 1.4 shows the structure of pro-MMP-2-TIMP-2 complex and individual domain structures. The overall polypeptide folds of pro-peptide domains, catalytic domains and hemopexin domains from other MMPs are essentially super-imposable. Typically MMPs consist of a pro-peptide of about 80 amino acids, a catalytic domain of about 170 amino acids, a linker peptide of variable lengths (also called the ‘hinge region’ and a hemopexin domain of about 200 amino acids. MMP-7 (matrilysin-1), MMP-26 (matrilysin-2) and MMP-23 are exceptions as they lack the linker peptide and the hemopexin domain. MMP-23 has a unique C-terminal cysteine-rich domain and an immunoglobulin-like domain immediately after the C-terminus of the catalytic domain.

1.7.1 Pro-peptide Domain

The signature of matrixins ‘cysteine switch’ motif PRCGXPD is found in the pro-peptide. The pro-peptide consists of three α-chains and connecting loops

(Figure 1.4). The cysteine switch sequence lies in the substrate binding site, but the orientation of this segment is opposite from that of a peptide substrate. The proteinase susceptible 'bait region' is located between helix-1 and helix-2, but the structure of this region has not been resolved in the case of pro-MMP-1, pro-MMP-3 and pro-MMP-9 due to its lack of rigidity for X-ray crystallography. This region of pro-MMP-2 is however stabilized by a disulphide bond. The SH group of cysteine interacts with the catalytic zinc ion. Upon activation the interaction of Cys-Zn^{2+} is disrupted, which allows a water molecule to bind to the zinc atom (Figure 1.3). The pro-peptide domains of MMPs may also play an important role in folding the pro-enzymes during synthesis.

1.7.2 Catalytic Domain

Binding of a peptide substrate to the enzyme is primarily dictated by the structure of the substrate binding site of the catalytic domain, including a hydrophobic pocket called the 'S1 pocket' located to the right of the zinc atom. This pocket varies in depth in different MMPs. It is therefore one of the determining factors of substrate specificity of MMPs. The catalytic domain consists of a 5-stranded β-pleated sheet, three α-helices and a connective loops (Figure 1.4). It contains two zinc ions; one catalytic and one structural. Usually three calcium ions are found which are thought to stabilize the structure. MT-1-MMP (MMP-14), MT-2-MMP (MMP-15), MT-3-MMP (MMP-16) and MT-5-MMP (MMP-24) have a membrane tethered loop, an additional 8 residues between β-strand II and III. This loop is critical for activation of pro-MMP-2 in the case of MT-1-MMP (English et al., 2001). Non-catalytic domains also help protein substrate recognition interaction. Binding of a substrate to the active enzyme displaces the water molecule from the zinc, and peptide bond hydrolysis is facilitated by the carboxylate group of the glutamate in the active site which draws a proton from the displaced water and allows a nucleophilic attack of the polarized water on the carbonyl carbon of the peptide bond.

1.7.3 Fibronectin Type II Domains

Fibronectin type II (FN II) domains are inserted in the loop between the fifth β-strand and the second helix of the catalytic domains of gelatinases (Figure 1.4) The FN II domains in MMP-2 and MMP-9 have a similar conformation. They consist of two anti-parallel β-sheets connected with a short α-helix and stabilized by two disulfide bonds, however, the sequence position of the FN II domains in the two gelatinases are significantly different. After super-imposing the catalytic domains of pro-MMP-2 and pro-MMP-9, FN II domain-1 and domain-3 fall roughly in the same places, but the position of domain-2 differs. Domain-2 of pro-MMP-2 has an area that interacts with the catalytic domain, but the corresponding domain of pro-MMP-9 is rotated and twisted away from the catalytic domain without making contact (Elkins et al., 2002) Domain-3 in both pro-gelatinases makes contact with the pro-peptide and with the catalytic domain (Morgunova et al., 1999) and (Elkins et al., 2002).

1.7.4 The Linker Region

Two domains, hemopexin and catalytic, are connected by the linker region. This region is considered to be flexible for MMP-9 (Rosenblum et al., 2007), but a number of prolines are found (Iyer et al., 2006; Jozic et al., 2005; Morgunova et al., 1999). This suggests that this region has structural constraint suited for specific functions. Mutation of this region in MMP-1 (Tsukada and Pourmotabbed, 2002) and MMP-8 (Knauper et al., 1997) reduced the collagenolytic activity, supporting the notion that the correct movement and arrangement between the catalytic domain and the hemopexin domain is important for this activity. Studies of MMP-9 and MMP-14 have found that the linker region can be extensively and heterogeneously N- and O-glycosylated and that these sugar chains have significant effects on the cellular biochemistry of these MMPs (Van den Steen et al., 2006; Wu et al., 2004).

1.7.5 Hemopexin Domain

The hemopexin domain has a 4-bladed β-propeller structure with a single disulfide bond between the first and the fourth blades (Figure 1.4) (Gomis-Ruth et al., 1996) The centre of the propeller generally contains one calcium ion and a chloride. The hemopexin domains are essential for collagenases to express their triple helical collagen degrading activity and for MT-1-MMP to dimerize on the cell surface. The latter event is essential for MT-1-MMP to activate pro-MMP-2 (Itoh et al., 2001) and to cleave collagen (Itoh et al., 2006). The cooperation between the catalytic and hemopexin domains is considered to be important for the expression of collagenolytic activity of collagenases (Chung et al., 2004).

1.8 Purification of MMPs

MMPs operate in concert with many other proteins such as chemokines, growth factors, substrates, hormones, cofactors, receptors and cleavage products creating a protease web. More than 35 chemokines involved in macrophage and neutrophil infiltration have been shown to be regulated by MMPs (Butler and Overall, 2009). Various proteomic approaches are being used to tease out this network to identify the roles played by each protein and their potential for therapeutic modification. MMP inhibitor-based therapy failure was a consequence of an incomplete picture of MMP biology resulting from inadequate knowledge of substrate repertoires and physiological pathways under MMP control and that individual members of the MMP family have unique functions that render broad-spectrum inhibition undesirable and even advantageous for tumourigenesis and metastasis (Butler and Overall, 2009).

A great deal of research was dedicated to understanding the MMP biology for which purification methods for MMPs are a central requirement. These studies highlighted various characteristics of MMPs which were not clear before such as site of action, redundancy, regulatory effects, diagnostic value and therapeutic potential. For instance, in proteomic screens, identification of intracellular substrates for MMPs such as Hsp-90α has changed the idea that

MMPs work only extracellularly (Butler et al., 2008). High-content screens such as LC-MALDI, isotope tag for relative absolute quantitation (iTRAQ), isotope coded affinity tag (iCAT), two dimensional polyacrylamide gel electrophoresis (2D-PAGE) and differential in-gel electrophoresis (DIGE) often lead to the identification of more than one MMP substrates within a given pathway (Butler and Overall, 2009). MMP-7 was identified as a serum biomarker for renal cell carcinoma proteomically (Sarkissian et al., 2008). The lethality of the double knock out approach for inhibiting MMP functions highlights the importance of using system-wide proteomic analysis to elucidate the network in which a protease lies in order to identify alternate up-stream or down-stream non-MMP targets that might be more easily and specifically modulated (Butler et al., 2008). A highly specific MMP-12 inhibitor belonging to phosphinic peptide library may have important therapeutic applications in diseases such as aortic abdominal aneurysm and atherosclerosis (Devel et al., 2006).

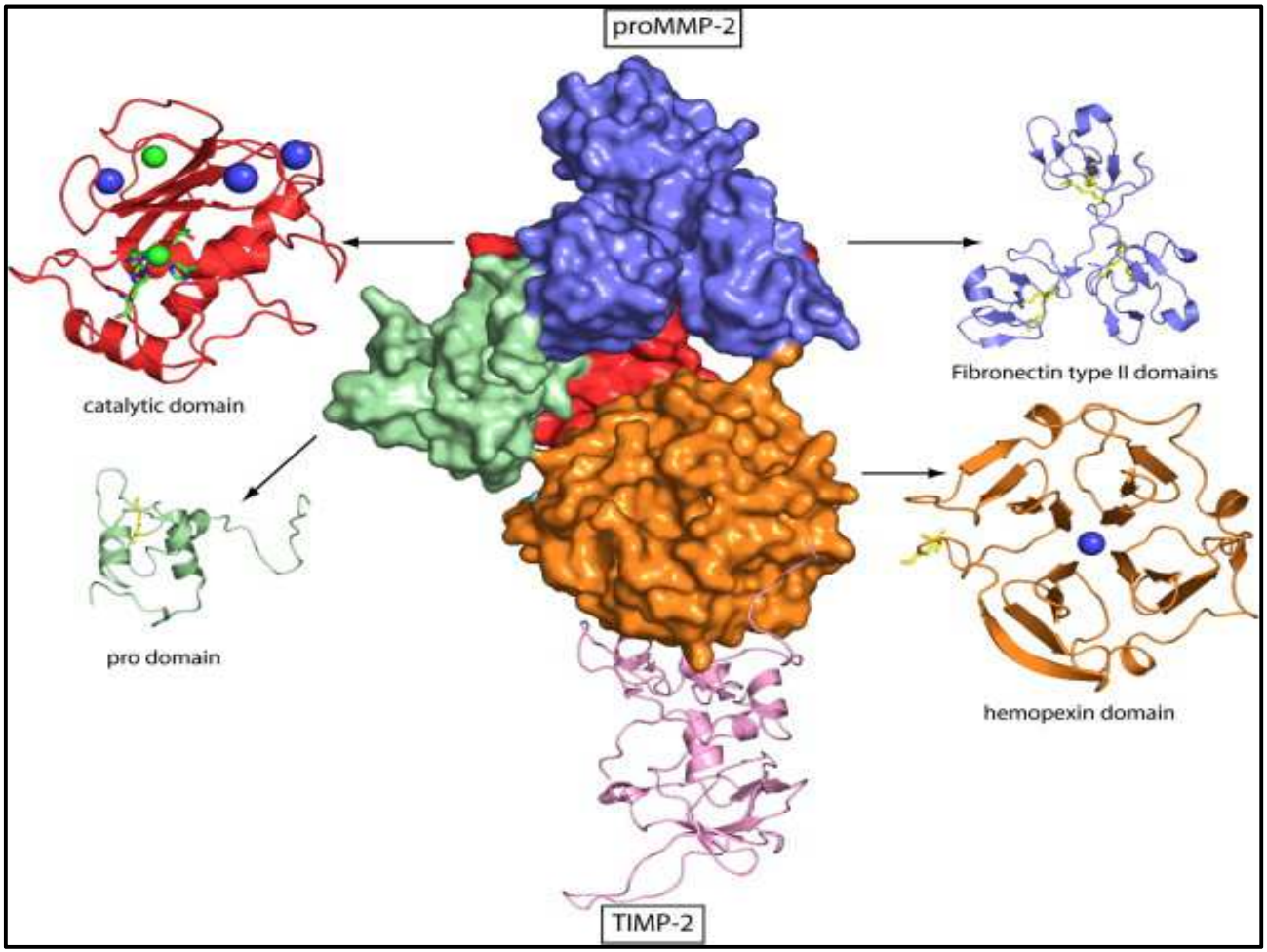

Figure 1.4 The 3D diagram of human pro-MMP-2 and TIMP-2 complex.

Taken from (Murphy and Nagase, 2008a).

The pro-domain is shown in green, catalytic domain in red, fibronectin type II domains in blue, hemopexin domain in orange, and TIMP-2 in pink. Zinc ions are green sphere, calcium ions are blue sphere and disulfide bonds in yellow. The image was prepared by Rob Visse of Imperial College London based on Brookhaven Protein Data Bank entry 1GXD.

1.8.1 Conventional MMP Purification Methods

Before the emergence of proteomics, a number of MMPs and their inhibitors were purified using multi-step conventional protein purification methods. In an attempt to isolate the two neutrophil metalloproteinases, collagenase and gelatinase, separation and further purification was done by sequential gel filtration chromatography, DEAE-cellulose, heparin-Sepharose, and Sephadex G-50 chromatography (Murphy et al., 1982). The precursor of human MMP-3 (pro-MMP-3) was purified from rheumatoid synovial fibroblasts to investigate steps of its activation by an endopeptidase and mercurial compound amino phenyl mercurial acetate (APMA). The latent form of MMP-3 was purified starting from gel filtration chromatography, elution with concanavalin A-Sepharose and removal of unbound pro-MMP-3 by passing the filtrate through anti-collagenase immuno-adsorbant column (Okada et al., 1988). The fact that gelatin shows specificity towards fibronectin, forms the basis of gelatin-Sepharose affinity chromatography and is therefore used to purifiy gelatinases (pro-MM-2 and pro-MMP-9) in combination with other chromatography methods. In an attempt to study activation and interactions with other MMPs, stromelysin-2 (MMP-10) was separated from pro-MMP-2 and pro-MMP-9 using gelatin-Sepharose columns (Nakamura et al., 1998). MMPs remain associated with Inter-photoreceptor retinoid binding protein (IRBP) by procedures commonly used for its purification, including ion exchange, concanavalin A affinity and gel filtration chromatographies. Through each step of the purification both gelatinase and caseinase (stromelysin) activities were detected by zymography with IRBP prepared from bovine interphotoreceptor matrix. However, inclusion of gelatin affinity chromatography did not totally remove the gelatinases.

Much of this activity was latent and was only revealed following fractionation or by pre-activation before zymography (Plantner and Quinn, 1997). Pro-collagenase-activator (stromelysin) was purified by DEAE-cellulose, Ultrogel AcA-44, and zinc chelate sepharose chromatographies, from the culture medium of the guinea pig carrageenin granuloma model. On SDS-PAGE, the

activator migrated as a principal band of approximately 44kDa. The molecule when tested on pro-collagenase from human lung fibroblasts in a concentration dependent manner, an enhancement of collagenase activity of trypsin-treated crude culture medium was observed. A loss of about 50% of its activity occured after heating. In addition, this activator degraded gelatin and casein (Pardo et al., 1991).

1.8.2 Synthetic Inhibitors-Based Methods

Highly potent inhibitors of MMPs have been developed by grafting a zinc-binding moiety such as a hydroxamate ($CONH\text{-}O^-$), a carboxylate (COO^-), a thiolate (S^-), or a phosphinyl (PO_2^-) to a suitable peptide sequence. One of the very effective hydroxamate based inhibitors, BB-94, has been found to show poor selectivity (Cuniasse et al., 2005). Recombinant mouse MT-5-MMP products have been purified and characterized using BB-94 Q-Sepharose column and eluted with a gradient of 0.15-1M NaCl (Wang et al., 1999). Several N-carboxyalkyl peptides were synthesized and tested as inhibitors of pig synovial MMP-1, MMP-2, and MMP-3. The most potent of the series, $CH_3CH_2CH_2(R,S)CH(COOH)\text{-}NH\text{-}Leu\text{-}Phe\text{-}Ala\text{-}NH_2$, competitively inhibited cleavage of dinitrophenyl-Pro-Leu-Gly-Leu-Trp-Ala-D-Arg-NH2 at the Gly-Leu bond by MMP-1 and MMP-2. A similar inhibitory potency was found for MMP-1 with soluble Type I collagen and MMP-3 with substance-P as substrate. The inhibitor was coupled to EAH-Sepharose 4B through a C-terminal amide. In the presence of 2M NaCl (pH 7.2), this matrix bound MMP-1, MMP-2, and MMP-3 from concentrated culture medium of pig synovial membranes. The enzymes co-eluted at pH 4.1 and subsequently were resolved by chromatography on DEAE-Sephacel and heparin-Sepharose. This procedure provided a rapid means of obtaining all three MMPs from one source in approximately 15% yield each (Stack et al., 1991).

1.8.3 Activity Based Probes for Proteomic Profiling (ABPP)

Failure of conventional proteomic methods for functional analysis and of clinical trials of MMPs due to unknown toxicity mechanisms led to the fashioning of activity based proteomic probes. The need to develop activity

based probes was stressed since post-translational changes affect function of proteins so only quantitation does not establish specific roles (Jessani and Cravatt, 2004). Since metalloproteinases are a diverse class of enzymes with some common structural features, ABPP probes have been designed which incorporate hydroxamate and a benzophenone photo cross-linking group to enhance selectivity. An ABPP HxBP-rh has been shown to bind to active and not the zymogen or inhibitor bound form of MMP-2, MMP-7 and MMP-9 added to mouse kidney proteome (Saghatelian et al., 2004).

1.8.4 Affinity Chromatography

Affinity chromatography that was first described by Cuatrecasas (Cuatrecasas and Wilchek, 1968; Cuatrecasas et al., 1968) involved reversible adsorption of a protein to a specific ligand immobilized on chromatography beads and is based on bio-specific interactions. The mixture containing protein of interest is applied to the chromatography system. The target protein binds to the ligand immobilized on solid surface which is eluted using buffers to reverse the binding (Figure 1.5). The definition of affinity chromatography can be broad. Often it includes immobilized metal ion affinity chromatography (IMAC), covalent chromatography, and biomimetic ligands (dyes). In a more narrow definition only biological functional pairs are included such as receptor/ligand, antibody/antigen, enzyme/inhibitor, hormone/receptor, nucleic acid/nucleic acid-binding protein, and lectin/glycoprotein. The use of these functional pairs often also requires production of the adsorbent (ligand) that is immobilized to the matrix. A vast array of chromatography systems currently exist and these are tailor-made for each adsorbent. In addition, pre-activated gel matrices for ligand immobilization are commercially available from several suppliers. The same suppliers also offer ready-to-use affinity matrices for a wide variety of functional pairs as gels or pre-packed columns. Combinatorial methods can also be employed to find new ligands to a vast array of different targets. Additionally, synthetic ligands can be designed using structural information of the target (Li et al., 1998).

To facilitate the purification of recombinant proteins a large number of different affinity fusion systems are available, each relying on a specific interaction to a ligand (Ford et al., 1991). Fusion system is a genetically engineered protein to contain a carboxy- or amino-terminal which forms the biochemical basis for affinity chromatography. A variety of fusion tags have been developed such as oligo-histidines for recovery by IMAC, carbohydrate binding proteins recognized by lectins and a biotin binding domain for *in vivo* biotinylation which creates affinity of a fusion protein for avidin or streptavidin. It must be stressed, however, that different applications may have demands on removal of the fusion moiety, achieved by site-specific cleavage. In addition to the specific affinity addressed to the fusion moiety, decreased protease susceptibility and increased or decreased solubility of the target protein can sometimes be achieved (Stahl and Nygren, 1997).

Affinity chromatography has several inherent advantages over the classical means of protein purification. The technique offers high selectivity and high capacity. Since the method eliminates steps the equipment e.g.; columns, cartridges etc, can be down-sized, thereby improving the process economics. Furthermore, it can preferably be used early in the capture process and the protein is concentrated during the process thus, allowing large volumes to be loaded. However, large scale affinity chromatography of proteins suffers from problems dealing with regulatory compliance.

Problems concerning ligand leakage and sensitivity towards cleaning procedures must be solved. Stromelysin has been proposed to play a major role in the pathologic degradation of diseased cartilage of OA and RA patients. A truncated, recombinant form of this enzyme, with the sequence Phe83 to Thr260 (mSL-t) was expressed and purified from *E. coli* to investigate its biochemical and biophysical properties, and to develop inhibitors for arthritis treatment. LC-ESI-MS technique was utilized for the characterization of mSL-t. The mass spectra of mSL-t showed the presence of a number of different protein components in addition to the full-length mSL-t form. The full length mSL-t was successfully separated from auto-degradation products using affinity chromatography and detected by LC-ESI-MS (Qoronfleh et al., 1997).

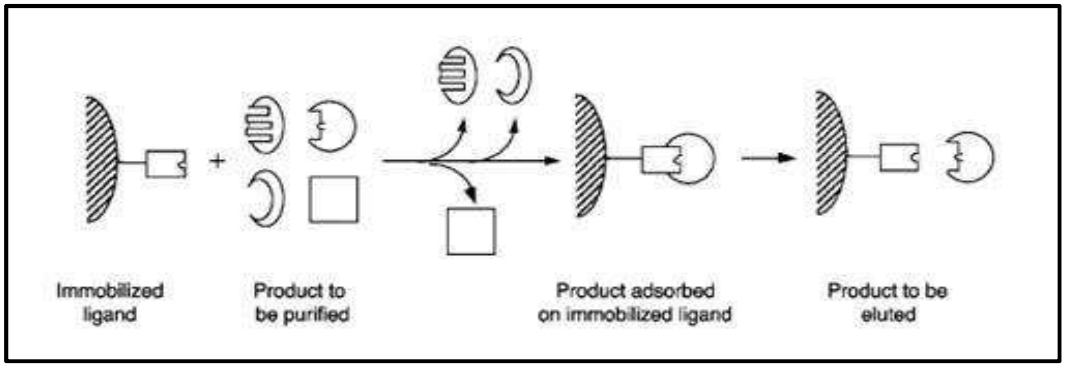

Figure 1.5 Principle of affinity chromatography.

1.8.4.1 Dye-Ligand Chromatography

A number of textile dyes, known as reactive dyes, have been used for protein purification in dye-ligand affinity systems, since they were found to bind proteins in a selective and reversible manner. Reactive dyes are colored compounds capable of forming covalent bonds with the hydroxyl groups of cellulosic fibers, with the amino, hydroxyl and mercapto groups of protein fibers and with the amino groups of polyamides (Zollinger, 1991). An experimental evidence for such bonds being formed by hydroxyl groups of cellulose was given by Zollinger's group in the early 1960's. With dyeing of a dichlorotriazine dye, evidence was found in the same group by micro-biological degradation to products containing the dye bound to a glucose unit (Zollinger, 1961). Di- and monochlorotriazine reactive dyes were the first reactive dyes for cellulosic fibers (Rattee and Stephen, 1954); they were introduced commercially in 1956 and 1957, respectively (Zollinger, 1991)

For selectivity of a dye towards its target protein there has to be a precise fit between dye structure and an acceptor site on protein surface (Madhusudan and Vijayan, 1992). Roschlau and Hess were first to immobilize covalently Cibacron Blue on Sephadex G-200 directly and to purify yeast pyruvate kinase with this affinity sorbent (Roschlau and Hess, 1972). The polycyclic anionic ligand Cibacron Blue dye affinity ligand that interacts with proteins is thought to be due to it acting as a mimic of NAD+ and NADP+, or through non-specific electrostatic, hydrophobic, and other forces. The fractionation of human plasma of 27 different plasma proteins on immobilized Cibacron Blue

F3-GA has been studied. The column was eluted using first, a low molarity buffer (30mM H_3P0_4/Na_3PO_4, then a linear salt gradient (0-1M NaCl in the buffer above) was applied. Finally, bound proteins were recovered with 0.5M NaSCN. The recovery of individual proteins ranged between 52 and >95% (Gianazza and Arnaud, 1982). Reactive dyes are all synthetic in nature, and interact mostly with the active sites of proteins by mimicking the structure of the substrates, cofactors, or binding agents for those proteins (Denizli and Piskin, 2001). A large number of proteins have been purified taking advantage of these interactions of proteins with dyes but there are relatively few proteases among them. In a study to understand the role played by stromelysin in OA, dog synovial fibroblasts were stimulated to express canine pro-stromelysin. The APMA-activatable metalloproteinase present in the culture supernatants was purified using a combination of ion-exchange and dye-ligand affinity chromatography. The purified canine stromelysin showed similar characteristics as shown by recombinant pro-MMP-3 such as both co-migrated on reducing SDS-PAGE as a doublet with apparent molecular masses of 54 and 56kDa and both inhibited by 1,10-phenanthroline or recombinant human TIMPs (Bayne et al., 1992).

Initially, dye ligands were pursued for their biomimetic function and they were readily available from major chemical companies; they were cheap, non-toxic and stable when attached to a support matrix. Synthetic ligands based on triazine chemistry have some similarities with their dye predecessors display significant stability and resistance to both chemical and biological degradation. This property also confers long-term stability and re-usability, and synthetic ligand adsorbents can be used for at least 100 cycles. These affinity adsorbents display dynamic protein-binding capacities in the range 5-40 mg/mL. The triazines are symmetrical hexameric rings of alternating carbons and nitrogens. Chlorotriazine derivatives such as atrazine were used as herbicides and Agency for Toxic Substance and Disease Registry (ATSDR) concluded that atrazine is not a likely human carcinogen. (www.atsdr.cdc.gov).

Dye ligands such as Cibacron Blue quickly found application in investigations of plasma fractionation and the recovery of albumin (Watson et al., 1978).

Procion Blue and Red triazine derivatives have been compared in the purification of α-1-proteinase inhibitor with the finding that a Procion Red Fractogel was more effective (Gunzer and Hennrich, 1984). A study by Datar et al. reports on use of lysine-agarose to the recovery of tissue plasminogen activators (tPA) expressed in *E. coli* (Datar et al., 1993).

Affinity chromatography was applied to cytokine purification, tissue necrosis factors, and tPA purification (Werner and Berthold, 1988; Zoon et al., 1979). Blue-agarose and a mimetic green adsorbant were used to purify Interferon-α (Swaminathan and Khanna, 1999). With ever increasing demands on purity, yield, and reliability, repeatability and consistency, synthetic ligand chromatography is set to assume a significant position in the bio-separations armory.

1.8.4.1.1 Immobilized Reactive Red-120 for the Purification of Proteases

Many matrix metalloproteinases have been purified either from animal or human tissues, from cultured cell lines or from eukaryotic cells expressing recombinant enzymes using Reactive Red-120 as immobilized ligand (Murphy et al., 1992). The above mentioned dye ligand bound collagenase from the crude extract from human buffy coats which was eluted by 1M NaCl. Yields ranged from 53-100% of applied collagenase depending upon the amount of contaminating haemoglobin (Mookhtiar and Van Wart, 1990). The two recombinant forms of stromelysin, with molecular weight 57kDa and 60kDa (glycosylated) (Okada et al., 1988) were purified from C127 cell culture supernatants using Procion Red-Sepharose. Both forms were heat-activated and displayed similar specific activities with respect to many different substrates. The important finding of the study was that a large part of the C-terminal portion is not necessary for enzyme activity. Natural pro-MMP-3 was purified from human gingival fibroblast culture medium (6L) initially by binding to dextran sulphate beads equilibrated with buffer (pH 8.5) containing 0.15M NaCl. All metalloproteinases bound to this matrix were eluted with column buffer containing 1M NaCl. The eluate was chromatographed on DEAE-Sepharose to bind gelatinase to this matrix, whereas collagenase and stromelysin did not. The column flow-through was

loaded directly on to heparin-Sepharose (Pharmacia) to bind collagenase. Finally the pool containing pro-MMP-3 activity was chromatographed on Procion Red-Sepharose (Pharmacia). The enzyme was eluted with a gradient of 0-1M NaCl Fractions containing pro-MMP-3 were finally chromatographed on Ultrogel AcA44, from which enzyme was eluted as a single protein and activity peak (Koklitis et al., 1991).

1.8.4.1.2 Purification of Metalloproteinases on Dyematrex Green A

Since an influential work in 1985 by J.L. Seltzer (Seltzer et al., 1985), several reports on purification of matrix metalloproteinases from diverse starting materials with Dyematrex Reactive Green A (Green A is also known as Procion Olive H-7G) have been published (Enghild et al., 1989; Imai and Okada, 2008; Lark et al., 1990; Okada et al., 1990; Okada et al., 1986). A number of MMPs have been purified using immobilized triazine dyes as part of a sequence of chromatography steps to isolate each enzyme. In a study to confirm the pro-MMP-3 mechanism activation , concanavalin A-Sepharose (bound glycosylated pro-MMP-3), DEAE-Cellulose, gelatin-Sepharose (removed pro-MMP-2), anti-human MMP-3-Sepharose, Green A Dyematrex gel and Ultrogel AcA44 were used to purify the protease from culture medium of human rheumatoid (Okada et al., 1988). pro-MMP-7 (matrilysin-1) was purified by a five-step protocol from culture medium of CaR-1 human rectal carcinoma cells using DEAE-cellulose, Green A Dyematrex gel, DEAE-cellulose, chelating Sepharose and Ultrogel AcA44 to yield a single protein band (28kDa) of pro-MMP-7 on SDS-PAGE (Imai et al., 1995). In another study pro-MMP-10 was purified from the culture media of OSC-2 cells derived from a moderately differentiated squamous cell carcinoma of the tongue (Nakamura et al., 1998) using DEAE-cellulose followed by Green A Dyematrex gel (a linear gradient of NaCl,0.15-2M, eluted pro-MMP-1, pro-MMP-2, pro-MMP-3, pro-MMP-9 and pro-MMP-10.

The gelatinases (pro-MMP-2 and 9) were subsequently purified by gelatin-Sepharose, pro-MMP-1 and pro-MMP-3 by immuno-affinity columns and the pro-MMP-10 (56kDa on SDS-PAGE) recovered in unbound fractions for further chromatography on DEAE-Cellulose and Ultrogel AcA44. Also, though

soluble C-terminus MMP-14 (MT1-MMP) has been successfully purified, there are no reports showing purification of full-length membrane-anchored pro-MMP-14 from cell membranes. However, these processes are extremely laborious and time-consuming (summarized in Figure 1.6). MMPs could be purified by immuno-purification but this would require production of specific antibodies, in significant large quantities (mg), for each MMP and prove prohibitively expensive. (Imai and Okada, 2008). Retained proteases were eluted through ionic strength increase e.g., Okada, purified MMP-3 and its pro- form (pro-MMP-3) from culture supernatant of human rheumatoid synovial fibroblasts (Okada et al., 1986). Partially purified enzyme was loaded on a Green A column equilibrated with 50mM Tris-HCl buffer, 0.15M NaCl and 5mM $CaCl_2$. The column was developed with 0.3M NaCl and 0.05% Brij-35 in the same buffer which successfully eluted pro-MMP-3 and with 2M NaCl which eluted two proteases, pro-MMP-1 and pro-MMP-2. They reported furthermore that MMP-3 activated by APMA was no longer retained when reloaded on Green A column. This underscores that immobilized dyes can be selective. Reported yields and purification factors for these MMPs were variable depending on purification starting material. For example canine pro-stromelysin from cultured synoviocytes was purified to electrophoretic purity by only a DEAE-Sepharose step followed by immobilized Green A (Bayen, 1992). Gelatin-Sepharose chromatography was used for isolation of pro-MMP-2 (72kDa) and pro-MMP-9 (92kDa) from human plasma. For further separation of MMP-2 gel filtration chromatography was followed. Stromelysin-1 was isolated from plasma by Matrex Green A affinity chromatography.

Immuno-blotting of plasma fractions with antibodies to unique peptide regions of human gelatinases differentiated the 72kDa gelatinase from the 92kDa gelatinase and identified human stromelysin as a 57kDa. TIMP-1 (28kDa) and TIMP-2 (21kDa) were also identified by immune-blotting of gelatin-Sepharose bound plasma proteins using non-crossreacting antibodies to each protein (Moutsiakis et al., 1992). Pharmacia Blue sepharose and Amicon Green sepharose were used for the purification of gelatinases from human skin, maintained in serum-free organ culture. The dialyzed and

lyophilized medium was fractionated with ammonium sulfate, and applied to Pharmacia Blue sepharose in a batch step. The 0.4NaCl eluate was then subjected to gel filtration on sephacryl S-200, followed by gradient elution from Amicon Green sepharose. The fractions with gelatinolytic activity are applied to a Bio-Rad TSK-Phenyl-5PW HPLC column and finally applied to a Pharmacia Mono-Q FPLC column and eluted with a gradient of sodium chloride. The enzyme appeared as two bands, corresponding to enzymatic activity zymograms on SDS-PAGE (Seltzer et al., 1985).

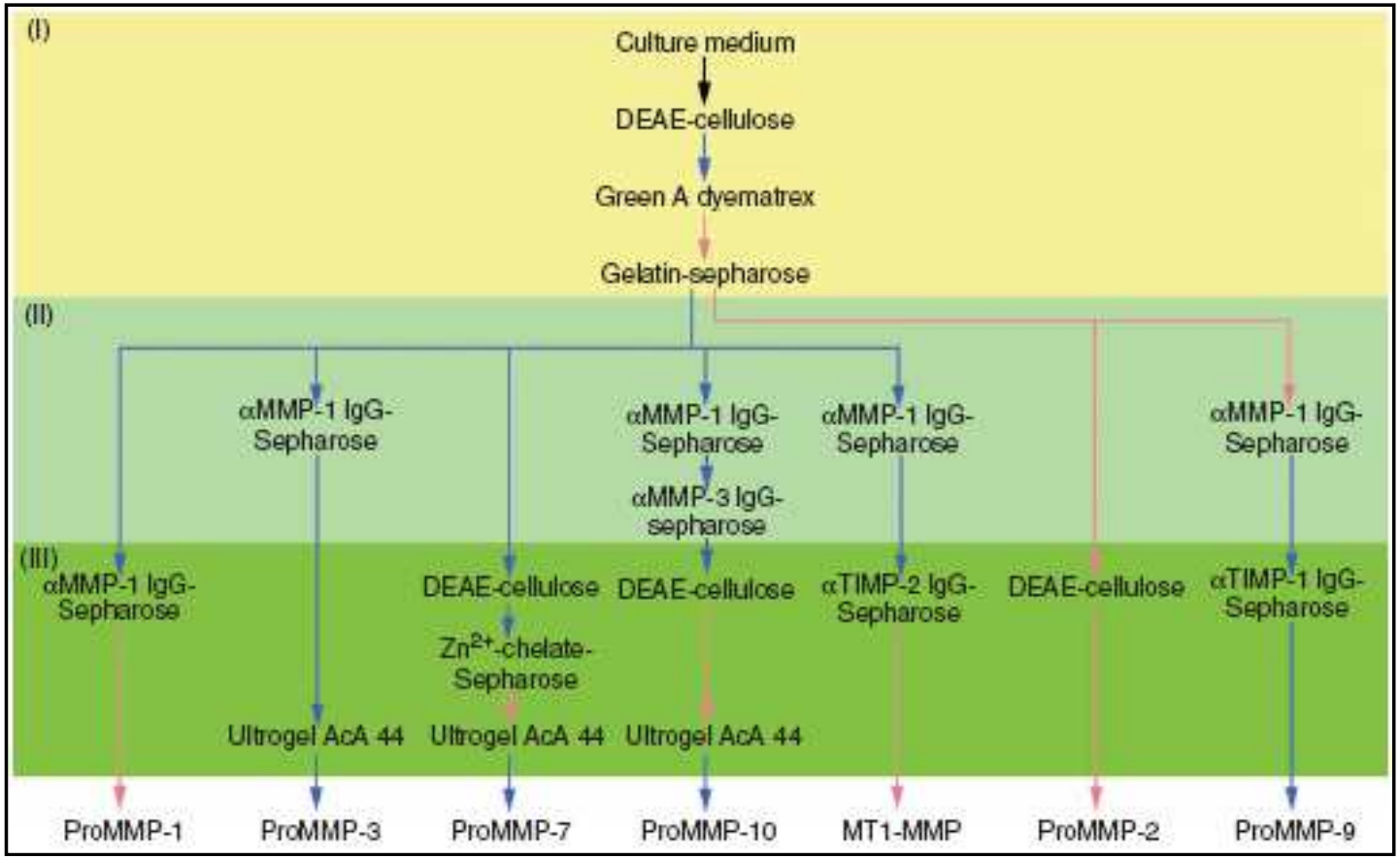

Figure 1.6 Conventional MMP purification methods.

Taken from (Imai and Okada, 2008).

Common steps: (I), Removal of non-target pro-MMPs. (II), Purify target MMPs to homogeneity. (III), Blue arrows: effluents; Red arrows: eluates.

1.9 Mass Spectrometry

A major advance that enabled examination of protein structure by MS and MS/MS was the introduction of soft ionization techniques to 'volatilize' bio-molecules, in particular electrospray ionization (ESI) and matrix assisted laser desorption/ionization (MALDI). In MALDI, samples are co-crystallized onto a sample plate with a small organic matrix compound that usually has a conjugated aromatic ring structure, and thus can absorb the wavelength of the laser (Muddiman et al., 1997). The matrix provides energy to molecules for vaporization to be ionized. Although multiply charged ions can be produced, more typically, only singly charged ions are observed in MALDI. Mass spectrometry and tandem mass spectrometry (MS/MS) experiments are major tools used in protein identification. Mass spectrometers measure the mass-to-charge (*m/z*) of analytes; for protein studies, this can include intact proteins and protein complexes (Sobott et al., 2002), fragment ions produced by gas-phase activation of protein ions (top-down sequencing) (Kelleher, 2004), peptides produced by enzymatic or chemical digestion of proteins (mass mapping) (Kleno et al., 2004), and fragment ions produced by gas-phase activation of mass-selected peptide ions (bottom-up sequencing) (Yates, 1998).

The application of mass spectrometry and MS/MS to proteomics takes advantage of the vast and growing array of genome and protein data stored in databases. The information produced by the mass spectrometer, lists of peak intensities and *m/z* values, can be compared with lists generated from 'theoretical' digestion of a protein or 'theoretical' fragmentation of a peptide. Applications to analyze smaller quantities of sample (such as biopsies) or the detection of low abundance proteins (LAP) are driving the development of more sensitive mass spectrometers, as well as high resolution separation technologies, to provide structural information on individual components in complex mixtures of proteins derived from biological samples. Protein identification by mass spectrometry requires an interplay between mass spectrometry instrumentation (how molecules are ionized, activated, and detected) and gas-phase peptide chemistry (which bonds are broken, at what

rate) and how cleavage depends on factors such as peptide/protein charge state, size, amino acid composition and sequence. Upon detection, the ion intensity vs. their *m/z* is determined by the mass spectrometer, generating the mass spectra. Selected peptides, named 'precursor ions' are subjected to collision-induced dissociation (CID) in the mass spectrometer. The *m/z* of the fragmentation products is then measured. This step is the second dimension of the mass spectrometer cycle, which produces the MS/MS spectra for each selected precursor ion. The MS/MS spectra obtained are searched against databases containing the *in-silico*-generated MS/MS spectra of each possible peptide of the selected organism's proteome. This leads to the identification of the proteins populating the analyzed sample. However, even this database-derived information is neither complete (only about 15–30% of MS/MS are identified), nor quantitative. Peptides must be able to co-crystallize efficiently with the matrix, for instance, with α-cyano-4-hydroxycinnamic acid (CHCA) matrix, the majority of the ions observed are 800–1800Da, while with sinapinic acid (SA) matrix larger ions give better signals.

Mass spectrometry is not a quantitative technique because different peptides have different ionization efficiencies, meaning that two different peptides at the same abundance will generate different signal intensities. To circumvent this, different strategies have been developed to overcome this problem and many groups have reviewed this subject extensively (Overall and Blobel, 2007; Overall and Dean, 2006; Tao and Aebersold, 2003). Most of the methods achieve relative quantification by comparing protein abundance in two or more samples. Results are expressed as fold of increased or decreased abundance. Two method classes were developed: isotopic labeling or label-free based quantification. The methods using labels rely on the inclusion of stable isotopes in the label, which has the exact same molecular structure, but different mass. Proteins and peptides can be labeled metabolically in cell culture by incorporation of isotope-containing amino acids and has been termed stable isotope labeling by amino acids in cell cultures (SILAC) (Ong et al., 2002). Alternatively, labels can be chemically incorporated after protein isolation. Good examples of such labels are the

ICAT (Gygi et al., 1999) and the iTRAQ (Ross et al., 2004). After the labeling step, peptides from the different samples are mixed and analyzed in a single MS/MS analysis. In the case of SILAC and ICAT, identified peptides produce precursor ions in the MS spectra represented by a peak doublet separated the mass difference of the labels (Griffin et al., 2001). Peak area evaluation in the MS spectra allows for relative quantification. iTRAQ is fundamentally different. Here, the iTRAQ tags are all of the same molecular mass, but upon fragmentation they present reporter ions of different mass in the MS/MS spectra. The MS/MS peaks are used for relative or absolute quantification (Ross et al., 2004). In label-free relative quantification, each sample is submitted to mass spectrometry analysis separately and the peak area of individual peptides precursor ion found in the different runs are matched and used to evaluate the relative abundance of proteins (Cutillas and Vanhaesebroeck, 2007). The label-free quantification has no limitation for the number of samples that can be compared, but is less accurate than iTRAQ for quantification.

1.9.1 MALDI-Mass Spectrometry

The first report on MALDI-MS was published in 1985 describing the principle and calling the method as ‘matrix assisted desorption’ (Karas, 1985). Over the past years, MALDI has developed into indispensable tool in analytical biochemistry in particular. As with most of new technologies, MALDI evolved from a diversity of prior knowledge. During late 1960’s Beckey introduced Field desorption (FD), the first technique which opened a small road into the territory of mass spectrometry (MS) of bio-organic molecules. It was in this context, in conjunction with the first attempt to desorb organic molecules with laser irradiation, that concept of ‘matrix’ as a means of facilitating desorption and enhancing ion yield was born (Kaiser et al., 1991). The first attempts to use laser radiation to generate ions for a mass spectrometric analysis were published few years after the invention of laser. Vistola and Pirone had already demonstrated the spectra of organic compound with time of flight (TOF) mass spectrometer. Several groups continued to pursue this line of research, mainly R. Cotter at John Hopkins University in USA and P.

Kistemaker in FOM institute in Amsterdam, the Netherlands with the latter group analyzing underavatized digitonin at mass 1251Da (M + Na), using a CO_2 laser at a wavelength of 10.6μm in the far infrared (Posathumus, 1978).

1.9.2 MALDI-MS-TOF

Various combinations of ion sources (MALDI, FAB and ESI) and mass analyzers (quadruple, time-of-flight, fourier transform and ion trap) are constructed for accurate mass spectrum analyses of bio-molecules. Time-of-flight mass analyzers are coupled with MALDI due to complimentary pulsed nature of both the ion source and mass analyzer. Time-of-flight is a mass analyzer employed in modern proteomics which separates ions using time and distance as opposed to frequency used in others like quadrople, ion trap and fourier transform. Moreover, high resolution, mass accuracy and unlimited mass range detection are offered by TOF mass analyzers. A simple linear TOF mass analyzer works on the principle that if ions are accelerated with the same potential at a fixed point and a fixed initial time and are allowed to drift, the ions will separate according to their *m/z*. Ions strike the detector at different times depending on the *m/z*. A data system controls instrument parameters, acquires signal vs. time, and processes the data. In a reflector TOF mass analyzer the reflector acts as an ion mirror, extending the flight length without increasing the instrument size. The reflector also compensates for the initial energy spread of ions having the same mass showing improved resolution.

In a Bruker MALDI, TOF1 ranges from the MALDI ion source to the LIFT cell, TOF2 from the second accelerator stage in the LIFT cell to the reflector (Figure 1.7). The spots are individually targeted with a laser beam, which excites the matrix molecules. These matrix molecules then transfer energy to the peptides, leading to peptide ionization. Because the peptides are crystallized on a solid support, the same spot can be analyzed several times. However, when a spot contains too many peptides, the matrix energy is distributed over the entire sample and not enough energy is received by each peptide to ionize. This is called the ‘ionization suppression effect’ and also leads to under sampling.

1.9.2.1 Calibration

Internal and external calibration of mass spectrometer is important. In addition to the samples of interest, a standard protein for which expected spectrum is known is run, allowing the operator to externally calibrate the system and determine how well the instrument is calibrated. If trypsin is used then the advantage of this is that the masses of the resulting peptides are known exactly and can be used for internal mass calibration. Being a substrate for itself, trypsin is auto-digested into peptides that also contribute with signals in the spectra. If the trypsin peaks are found in the spectrum internal calibration should be chosen instead of external calibration. Routinely an accuracy of 50ppm (parts per million) can be obtained meaning that the differences between the measured and the exact masses are less than 0.005% of the particular peptide mass. The disadvantage of internal calibration using trypsin is that the peaks are only seen if the amount of trypsin is high enough (compared to the amount of peptides from the sample). However, too much trypsin can result in a spectrum where the signals from the interesting peptides are suppressed by the trypsin auto-digest peaks or just too low to be useful. This means that estimation of the correct amount of trypsin vs. sample is very important. The two most common intensive peptides from the porcine trypsin auto-digest are most often the peaks with the *m/z* values of 842.51 and 2211.10 (charge state MH+), respectively. In addition, a trypsin peptide giving a signal at 1045.56 can be used if either of the other two peaks is missing.

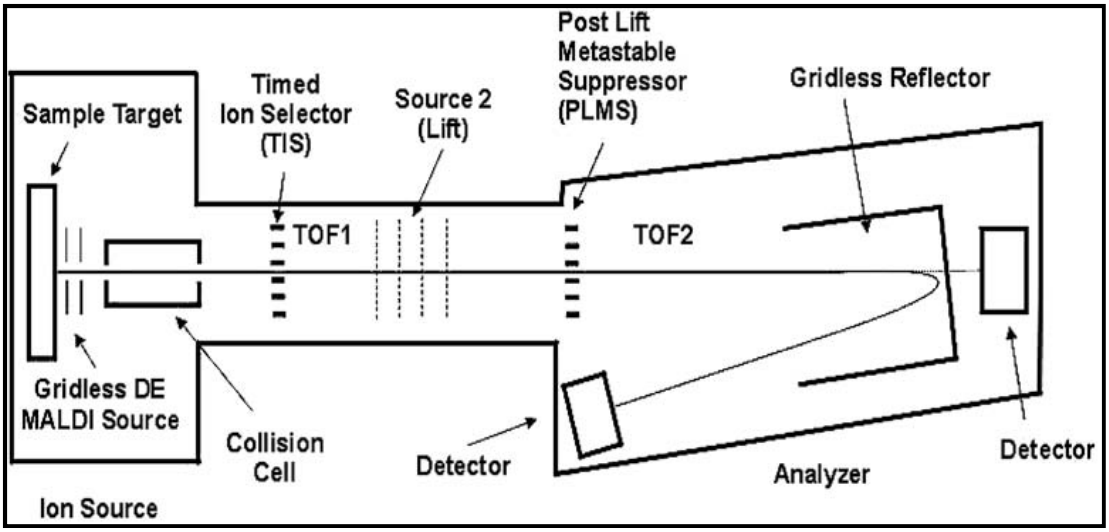

Figure 1.7 Schematic diagram of LIFT TOF/TOF MS.
Taken from Bruker Daltonics Manual.

1.9.2.2 Sequence Databases

MS and MS/MS data is transferred to a search engine such as Mascot, which then compares experimental and theoretical (*in-silico*) information in sequence databases. SwissProt developed by the SWISS-PROT groups at Swiss Institute of Bioinformatics (SIB) and European Bioinformatics Institute (EBI) is a protein sequence database that provides a description of the function of a protein, its domains structure, post-translational modifications, variants, etc., a minimal level of redundancy and high level of integration with other databases. The major available sequence databases are maintained at NCBI, EBI, SwissProt, UniProt etc. neXtProt is a resource that contains a wealth of high-quality data on all the human proteins that are produced by the 20,000 protein-coding genes found in the human genome. The content of neXtProt is continuously extended so as to provide many more carefully selected data sets and analysis tools.

The protein summary page on Mascot includes the accession number, the mass of the protein matched, the score, the number of peptides significantly matched (≤ 0.05), the protein name, the sequence of the peptides matched and their scores values and mass error values. By clicking on the accession number, a separate page ‘protein view is given, from which the isoelectric point (pI) and percentage sequence coverage is gained. The Mascot search

results may also give ‘proteins matching the same set of peptides’ or may give other protein matches with lower scores or number of peptides matched. The most appropriate protein identification can be elucidated by comparing protein masses, pI and the number of peptides in the sample matched to that protein. By clicking on the query number for a peptide, the ‘peptide view’ is given which shows a mass spectrum with labeled fragment ions and a table containing the matched fragment ions. Protein identification may be presented as a single peptide match, or may show several matched peptides. The greater number of peptides matched represents more confident protein identification. If protein identification with a single peptide match is not sufficient, extra information can be given as supporting evidence. This may include annotated spectra and/or lists of fragment ions, which can be obtained from ProteinScape within Mascot.

1.10 Proteomics

During past 5 decades research into protein biochemistry and molecular cell biology has led to the elucidation of the function and structure of many proteins. Proteins have been and continue to be explored for use in pharmacology, biotechnology and biomedical applications. Modern analytical technologies are applied to discover and develop new protein based biotechnology products. Techniques aiming at identifying the complete protein pool found in a biological sample at a given time and under a controlled set of conditions are termed ‘proteomics’ techniques. The set of proteins found in that biological sample is named its proteome. In the case of MMPs, detection of proteases and protease inhibitors at the mRNA level using microarrays gives a good indication of whether they might be found in a given biological sample. However, there is not always a good correlation between the mRNA transcript level and the protein level found in the same tissue, confirmation of expression is required at the protein level (Greenbaum et al., 2003).

For example, this is most easily seen for neutrophils storing proteases in granules and releasing these upon activation without involving mRNA synthesis (Owen and Campbell, 1999). Also, mRNA levels do not provide

any information about the levels of pre-pro-, pro- and active MMPs that are important to understand their physiological roles. Proteomics is defined by a number of new and established protein separation methods/procedures, most frequently employed in combination with mass spectrometry, for high-throughput protein identification. A number of strategies/workflows have been developed to study whole biological systems or sub-cellular organelles and quantify changes in protein expression in response external stimuli (e.g. drug administration to a cell line) or determine protein-protein interactions, post-translational modifications (PTM), etc. Some of these techniques are described briefly below.

1.10.1 Chemical Proteomics

In last few decades targeted proteome analyses has replaced global proteomic analyses with the availability of more sensitive mass spectrometers. Targeted proteomics makes use of affinity capture and termed chemical proteomics. It comprises the design of drug, cofactors, substrate or inhibitor analogues which can be immobilized on a suitable matrix support to trap specific proteins, sub-groups or families of target proteins. Affinity chromatography has been used in the past for protein isolation as part of workflows. With the advent of proteomics, like many traditional protein biochemistry techniques, affinity chromatography almost disappeared. However, as part of the advancement from global proteomics to hypothesis-driven investigation, affinity enrichment to access specific groups of proteins for mass spectrometry characterization has re-surfaced as a valuable technique (Sutton, 2011).

Different types of affinity media are commercially available, including triazine dyes (albumin, dehydrogenases), nucleotide (kinases), lectin (glycoproteins), lysine/gelatin (proteases), heparin (DNA binding proteins, growth factors, coagulation factors), Protein G/Protein A (antibodies), antibody-based (immuno-affinity and immuno-precipitation), immobilized metal affinity chromatography or IMAC (phosphopeptides), that are being used to enrich sub-proteomes based on function (Lee and Lee, 2004). One of the key differences between current affinity chromatography or chemical proteomics

and the traditional methods is scale; in general, the amounts of samples and chromatography materials are substantially lower (microlitres instead of millilitres or even litres) due to the availability of sensitive mass spectrometers and western blotting to analyze captured proteins. For chemical proteomics retaining protein functionality during protein extract/sample preparation is important. Hence, mechanical methods of protein extraction from cells and tissues such as sonication, vortexing, maceration, homogenization, extrusion are preferable to chemical methods using denaturants such as urea and guanidine, acid precipitation, and some detergents, e.g. SDS (Sutton, 2011).

The information of primary sequence of protein, type of phosphorylation (serine/threonine vs. tyrosine), or predicted phosphoacceptor sites (consensus peptide that is targeted by a kinase can be used to predict precursor and fragment ion *m/z* values for a multiple reaction monitoring (MRM) experiment. This highly sensitive MRM method of monitoring protein phosphorylation at specific phosphoacceptor sites may prove useful in understanding the physiological regulation of protein function.

1.10.2 Separation Techniques

Proteomics mass spectrometry is highly dependent on separation technologies that simplify incredibly complex biological samples prior to mass analysis. Selection of appropriate separation methods is the first step in designing the proteomic application to detect LAP that would otherwise be over-shadowed by a higher abundance signal. Therefore, both accuracy and sensitivity of a mass spectrometric experiment rely on efficient separation. Two major approaches to separation widely used in proteomics are gel-based and gel-free. Gel-based method, 2D-PAGE, have been traditionally used with pulsed ionization MALDI instruments in which the protein band can be excised, digested, and off-line sampled with MALDI source (Eckerskorn et al., 1992).

1.10.2.1 Reverse-phase High Pressure Liquid Chromatography (RP-HPLC)

Because in a mass spectrometer, proteins are identified by the *m/z* of their peptides and fragments, adequate separation is required for increased identifications. The reverse-phase high pressure liquid chromatography is as essential to LC-MS as 2D-PAGE is to gel-based proteomics. Peptides bind to beads packed into a column and binding is via hydrophobic interactions with alkyl-terminating chains covalently bound to the beads. Reverse-phase resins (C18) separate peptides based on their hydrophobicity, and a significant advantage of RP-LC is that the buffers used are compatible with MALDI. It has been shown that packing long, narrow capillary RP columns greatly improves loading capacity, sensitivity, and dynamic range of the RP-LC (Shen et al., 2005). Shen et al. have introduced long, small-particle-size (1.4μm) RP-LC columns with high peak capacity (1500 and higher, compared with an average of 400) operated in an ultra-high pressure regime (20kpsi). Using only RP-LC, they identified more than 2000 proteins that vary over six-orders of magnitude from human plasma in a single experiment. The small particle size of RP material (1.5μm) allows improved peak capacity, resolution, and reduced analysis time (Anspach et al., 2007) when using an ultra-high pressure regime.

1.10.2.2 Multidimensional Protein Identification Technology (MudPIT)

Multidimensional separation is used to address high sample complexity. By definition, the multidimensional separation approach combines several separation techniques joined to improve the resolving power. An important consideration for multidimensional separation is the orthogonality of the individual separation methods (Giddings, 1984) in which each dimension uses different (orthogonal) molecular properties of molecules as a basis for separation. One of the first 2D setups featured cation exchange chromatography coupled to a reverse phase column in line with a mass spectrometer (Opiteck et al., 1997) used for separation of *E. coli* proteins.

The overall peak capacity of the method was in excess of 2500, with femtomolar sensitivity.

1.10.3 Proteomics Approaches

Two proteomics approaches are in use based on sample preparation in which proteins are either enzymatically digested into peptides (bottom-up analysis) (Chait, 2006) or analyzed intact (top-down analysis) (Breuker et al., 2008).

1.10.3.1 Bottom-Up Analysis (LC-MALDI)

In a traditional bottom-up proteomics experiment, proteins are extracted from biological samples and digested using a specific protease, usually trypsin. The ensuing tryptic peptides are separated by chromatography techniques (described above) and submitted to tandem mass spectrometry (MS/MS), identifying proteins. In the case of LC-based MALDI-MS analysis, the peptides are injected in a capillary containing RP C18 beads and eluted using a gradient. The eluting peptides are co-deposited with MALDI matrix as discrete sequential droplets (fractions), on a MALDI target with an array of 384 spots and allowed to dry. The plate is then loaded into the mass spectrometer.

The most widely used method for bottom-up tandem MS data identification is the database search in which experimental MS/MS data are compared with the predicted, i*n-silico* generated fragmentation patterns of the peptides under investigation. Many methods have been developed that address some of the computational challenges associated with bottom-up proteomics. Some of these developments include using probabilistic scoring schemes (Sadygov and Yates, 2003) incorporating additional search criteria. LC-MALDI provides the ability to separate complex peptide mixtures into discrete fractions for more thorough analysis. Drawbacks of the bottom-up approach include limited protein sequence coverage by identified peptides, loss of labile PTMs, and ambiguity of the origin for redundant peptide sequences (Yates et al., 2009).

1.10.3.2 Top-Down Proteomics Approach

Top-down is for the analysis of PTMs which often occur in different combinations on individual proteins, and understanding these combinations is crucial for understanding biological regulation. Top-down mass spectrometry strives to preserve the post-translationally modified forms of proteins present *in vivo* by measuring them intact, rather than measuring peptides produced from them by proteolysis.

1.11 Aims and Objectives

To date MMP purification has been challenging due to the multiple steps required for each member resulting in low yields of proteins which are already low in abundance in biological samples. Targeted methods are emerging based on a chemical proteomics strategy for active forms of specific MMPs, however, there has been no method development for the purification of latent pre/pro-forms which would provide critical insights to the expression levels of these therapeutically important proteases. MMPs can be detected by antibody-based assays such as ELISA; however, these assays do not differentiate active and pro-forms. Profiling MMPs by quantifying mRNA does not predict protein activity. A shortcoming of antibody-based methods is possibility of cross-reactivity of antibodies and lack of 24 specific antibodies for each MMP. The study of active MMPs with activity assays is not 100% reliable because of the lack of specificity of substrates used. Recent advances in sensitivity and resolution of high-throughput mass spectrometric based proteomics allows detection of low abundance proteins (LAP). Hence, latent and active forms of MMPs may be detected simultaneously (Figure 1.8). Considering the number and diversity in function of MMPs, innovative approaches and tools are needed to profile expressed enzymes on a tissue-wide scale, particularly when valuable biopsies are limited in availability.

This study aims to evaluate a product, which is no longer commercially available in conjunction with proteomics methods. Procion Olive H-7G dye (Olive H-7G) has previously been used as part of a series of chromatography

steps used to purify pro-MMPs in the 80's and 90's but before proteomics techniques were widely available for MS-based identification. This project represents an opportunity to evaluate the traditional affinity purification method in conjunction with a modern LC-MALDI proteomics strategy to characterize a therapeutically important group of proteins in cancer samples.

- The first aim of the study was to optimize the preparation of a chromatography medium by immobilization of the Olive H-7G on various soft gels and magnetic beads.

- Further, to assist identification of MMPs from valuable biological samples, MS and MS/MS were performed to obtain characteristic peptide fingerprints/peptide signatures using recombinant human pro-MMPs (rhMMPs) following trypsin digestion.

- The Olive H-7G chromatography medium was screened against commercially available rhMMPs from various classes to establish the dye selectivity.

- In order to assess chromatographic performance of the Olive H-7G medium a series of complimentary and accessory techniques (SDS-PAGE, western blotting, Coomassie brilliant blue and silver staining and ELISA-based activity assays) for the analysis of MMPs from cell lines were established and optimized.

Once the pro-MMPs have been characterized and the methods optimized, protein preparations from cell lines will be applied to the chromatographic medium as a preliminary assessment of the potential for method to enable MMP enrichment from biopsies. The development of a new affinity capture tool for pro-MMPs and their subsequent MS-based characterization will provide a useful insight into their regulation prior to secretion and possible identify strategies to prevent their activation in a range of tissues and diseases.

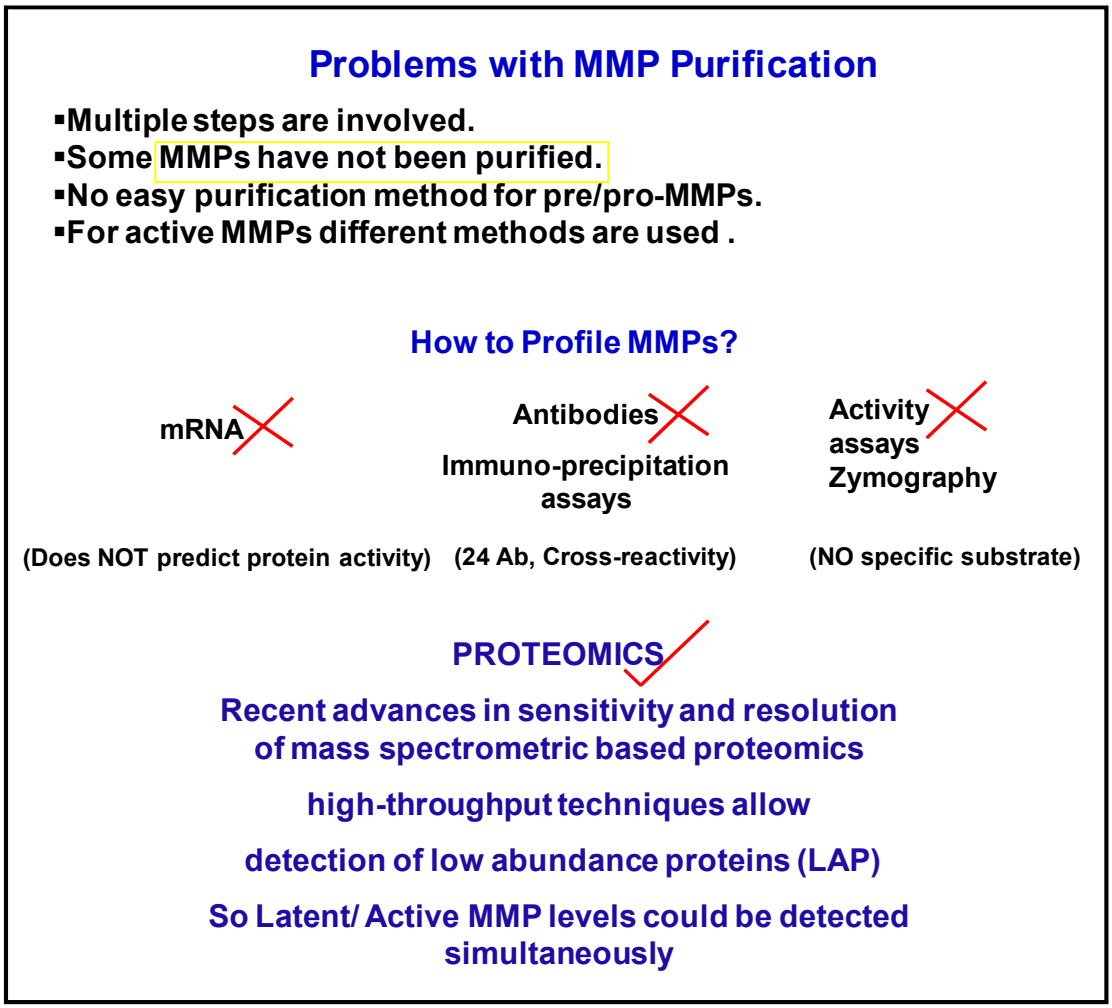

Figure 1.8 Challenges for MMP enrichment.

CHAPTER 2

MATERIALS AND METHODS

2 Materials and Methods

2.1 Reagents & Chemicals

For all proteomics work, polypropylene micro-centrifuge tubes were used, to minimize contaminations from plastics and to prevent proteins/peptides being retained on the surface of the tubes. HPLC grade water was used throughout. All chemicals were purchased from Sigma-Aldrich (Dorset, UK) unless stated.

2.2 Immobilization of OliveH-7G on Chromatography Beads: H-7G-Sepharose and H-7G-Sephadex

The Procion Olive H-7G dye (Amicon) ligand was immobilized to Sepharose-6B beads (45-165µm; fractionation range of $1x10^3$-$4x10^6$ Da for globular proteins) following the previously described method of Dean and Watson (Dean and Watson, 1979). The Procion Olive H-7G dye (10mg/mL) was added to Sepharose-6B (0.2mg/mL final) to a total volume of 25mL in HPLC grade water and mixed via rotation for 5minutes. NaCl was then added to a final concentration of 0.2mg/mL and the solution incubated at room temperature with mixing for a further 30 minutes. Following the addition of Na_2CO_3 (final concentration 333mM) the solution was incubated for 40hours at 45°C with constant mixing. After immobilization, the gel solution was poured onto a sintered glass funnel (Supelco Mobile Phase Filtration Apparatus 2) and washed with HPLC grade water under suction to remove all traces of the azide preservative from the sepharose beads. Suction was applied gently until the surface of the gel cracked. Any unbound dye was removed by washing with 1M KCl, 4M urea, and then extensive washing with HPLC grade water. The prepared beads were stored wet at 4°C in the presence of 0.1% (w/v) sodium azide when not in use. Hereafter the chromatography beads will be termed as H-7G-Sepharose or Olive H7G chromatography beads.

H-7G-Sephadex or Olive H-7G chromatography beads were synthesized using same method as described above. Sephadex bead size is 50-150µm with a bead volume of 4-6mL/g and fractionation range of $1x10^3$-$5x10^3$ Da.

2.3 Cell Culture

The cell lines were selected to represent tissue and tumour types. The human fibrosarcoma cell line (HT1080) and colon adenocarcinoma cell line (HT29) were obtained from the Institute's in-house cell line bank. Cells were grown in monolayer culture in 75mL non-vented flasks containing 50mL Rosewell Park Memorial Institute (RPMI-1640) medium supplemented with 10% foetal calf serum (FCS), 2mM L-glutamine, and 1mM sodium pyruvate (termed complete medium). The cells were maintained at 37°C in a humidified atmosphere of 5% CO_2 Haraeus Incubator (DJB Labcare Ltd, UK). Cells were grown to a maximum of 80% confluence before being passaged.

2.3.1 Cell Counting

Cells were detached using 0.25% trypsin-EDTA solution from one flask and counted using a haemocytometer. Briefly, 10µL of cell suspension was placed into the chamber of a Neubauer haemocytometer and the mean number of cells per grid of the chamber calculated, the resulting count being equivalent to the number of cells x 10^4 per mL. Cell numbers were expressed as (mean cell count) x 10^4 per mL.

2.3.2 Tumour Cell Line Growth Kinetics

To determine cell growth kinetics, cells were lifted, counted as described above and plated at a density of 1 x 10^3 cells per $25cm^2$ cell culture flask per time-point. Cells were counted every 24 hour for a total of 7 days. These values were plotted against time to generate a growth curve and determine the log phase growth period of the HT1080 and HT29 cell line. Growth curves were plotted as a mean of 3 growth curves.

2.3.3 Collection of Culture Supernatant

Cell media and the subsequent cells were collected under both serum-containing and serum-free conditions for analysis of MMP production Cells were grown to sub-confluence in complete RPMI-1640 medium (containing 10% FCS); the resultant media (henceforth referred to as serum-containing culture supernatant or S+CS) was then collected and stored at -20°C. The cell monolayer was then washed twice with Hanks balanced salt solution (HBSS) to remove residual serum prior to being incubated in serum-free RPMI-1640, containing 2mM L-glutamine and 1mM sodium pyruvate. Following further 48hours incubation at 37°C in a humidified atmosphere of 5% CO_2, media was collected (henceforth referred to as serum-free culture supernatant or SFCS) and stored at -20°C.

2.3.4 Harvesting of Cells

Cell monolayer was harvested using 0.25% trypsin-EDTA and split into further tissue culture flasks at the required density if needs to be passaged. For further protein expression studies, cell pellets were resuspended in 10mL of 1X PBS solution, centrifuged at 1000rpm for 5minutes. The supernatant was discarded and the washing was repeated until supernatant is free of the entire medium contents. The cell pellets were stored at -20°C.

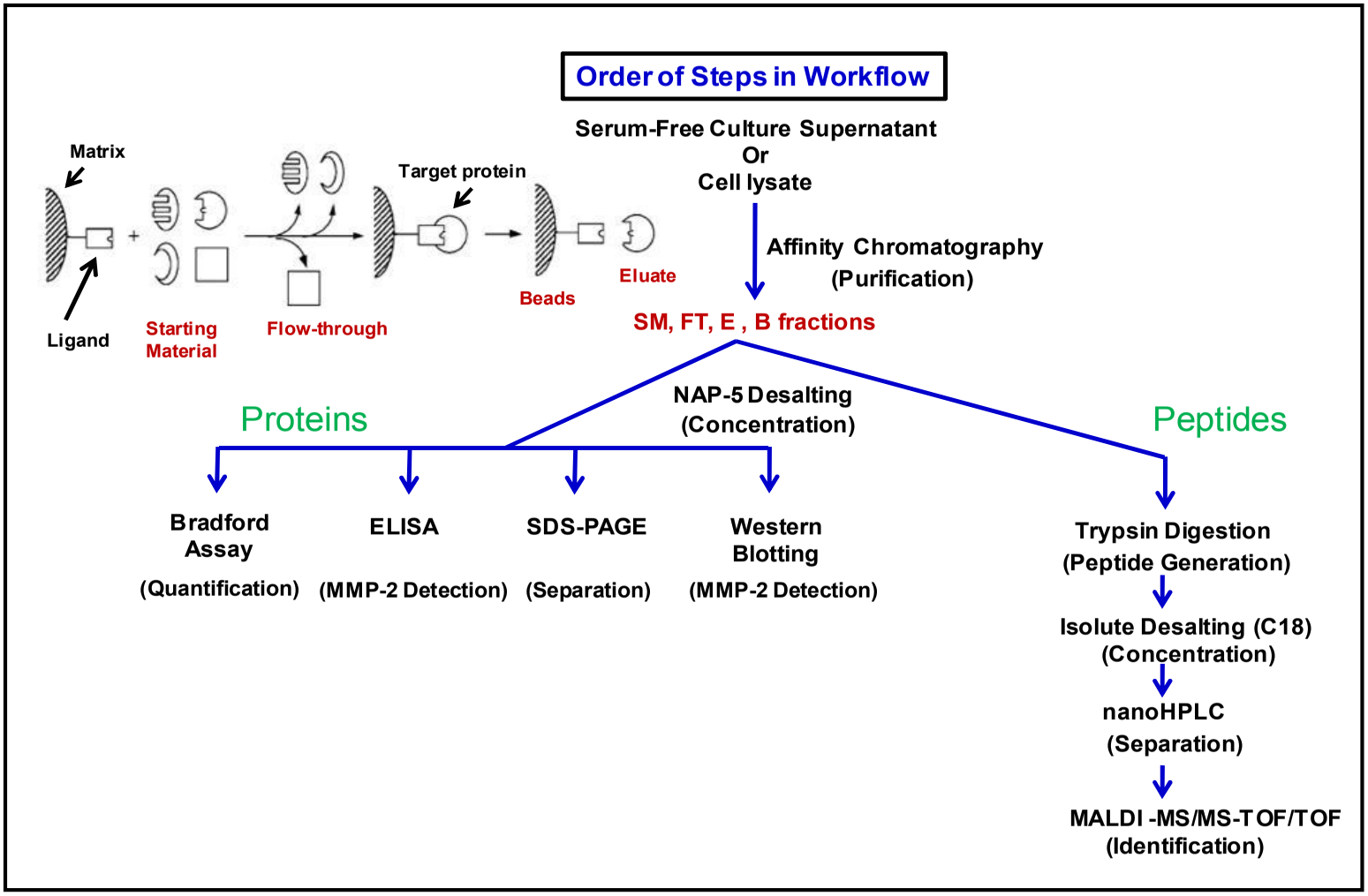

Figure 2.1 Workflow for enrichment of MMPs from cell lines.

2.4 Affinity Chromatography of Recombinant, Secreted and Cellular MMPs

An aliquot of Olive H-7G chromatography bead suspension (containing approximately 0.5mL wet volume of Olive H-7G chromatography beads) was transferred to a 15mL centrifuge tube. The chromatography beads were first equilibrated via incubation for 10-30 minutes in the following buffer: 50mM Tris-HCl (pH 7.5), 0.15M NaCl, 10mM $CaCl_2$, 0.02% (w/v) Na_3N before being centrifuged at 1200g at 4°C for 10minutes. The resultant supernatant was discarded and equilibration buffer added to the Olive H-7G chromatography beads at a final volume of 1mL. Samples (starting material or SM) were added to the Olive H-7G chromatography bead suspension and mixed with rotation for 1-4 hour at 4°C to affinity bind proteins to the Olive H-7G chromatography beads. The sample was then centrifuged at 1200g for 5-10minutes and the resultant equilibration flow-through (FT) collected. The bead-protein complex was washed 3-times in equilibration buffer (1mL each) and the individual washes collected (termed wash flow-through FT1a, FT1b and FT1c and were pooled in FT). The bead-protein complex was then washed twice with a further 10mL of equilibration buffer and the resultant FT discarded.

2.4.1 Salt Elution

Proteins were then eluted from the Olive H-7G chromatography beads via incubation for 10minutes at room temperature in 0.3M elution buffer containing: 50mM Tris-HCl (pH 7.5); 0.3M NaCl; 10mM $CaCl_2$; 0.02% (w/v) Na_3N, 0.05% (v/v) Brij-35 (if added), followed by centrifugation for 10minutes at 4°C. This was repeated 3-times and the resultant supernatants termed E1a-c. A further elution was performed in elution buffer containing high salt concentration (2M or 5M as opposed to 0.3M). This was repeated 3-times and the flow-throughs termed E2a-c. The beads were then washed twice with a further 10mL of elution buffer and the resultant FT discarded. In latter experiments the elution buffers were used without the detergent Brij-35, as described in the results. Finally, the Olive H-7G chromatography beads were

collected and stored at 4°C in 0.1% NaN_3 solution (Figure 2.2). The fractions were desalted and concentrated using NAP-5 columns (Materials and Methods section 2.5) and 10mM NH_4HCO_3 + EDTA was used to avoid autolytic degradation of MMPs during the process. The same sequence of steps of equilibration, washing and elution procedures were followed for each type of samples (recombinant human MMPs, serum-containing culture media; serum-free culture media; NaCl extract; dimethylsulfoxide (DMSO) extract and urea extract from lysed cells) used.

2.5 Protein Concentration: NAP-5 Columns and Dialysis Method

Illustrate NAP-5 columns (GE Healthcare, Piscataway, NJ, USA) were used to desalt samples. Each column was equilibrated with 3-volumes of 10mM ammonium bicarbonate solution (ambic), 0.5mL of sample added, and the desalted protein eluted and collected by loading 1mL of 10mM ambic solution. Samples were then lyophilized using Genevac EZ-Plus 2 Evaporator at 37° C, using aqueous conditions setting. The 0.5-3.0mL Slide-A-Lyzer cassettes (Thermo Scientific, USA) with a molecular weight cut off (MWCO) value of 3500Da were used for sample concentration. The cassettes slipped into the grooves of the buoy, were hydrated by immersion in 1L of 1X CAB dialysis buffer (Appendix 1). Samples were injected into the cassette using an 18-gauge needle syringe. Air was withdrawn by pulling up the syringe piston. Samples were dialyzed in dialysis buffer for 2hours at 4°C, a further 2hours in fresh buffer and then overnight in fresh buffer at 4°C. To extract the sample, air was discharged into the cassette cavity to separate membranes and the sample was withdrawn into the syringe and its volume was measured.

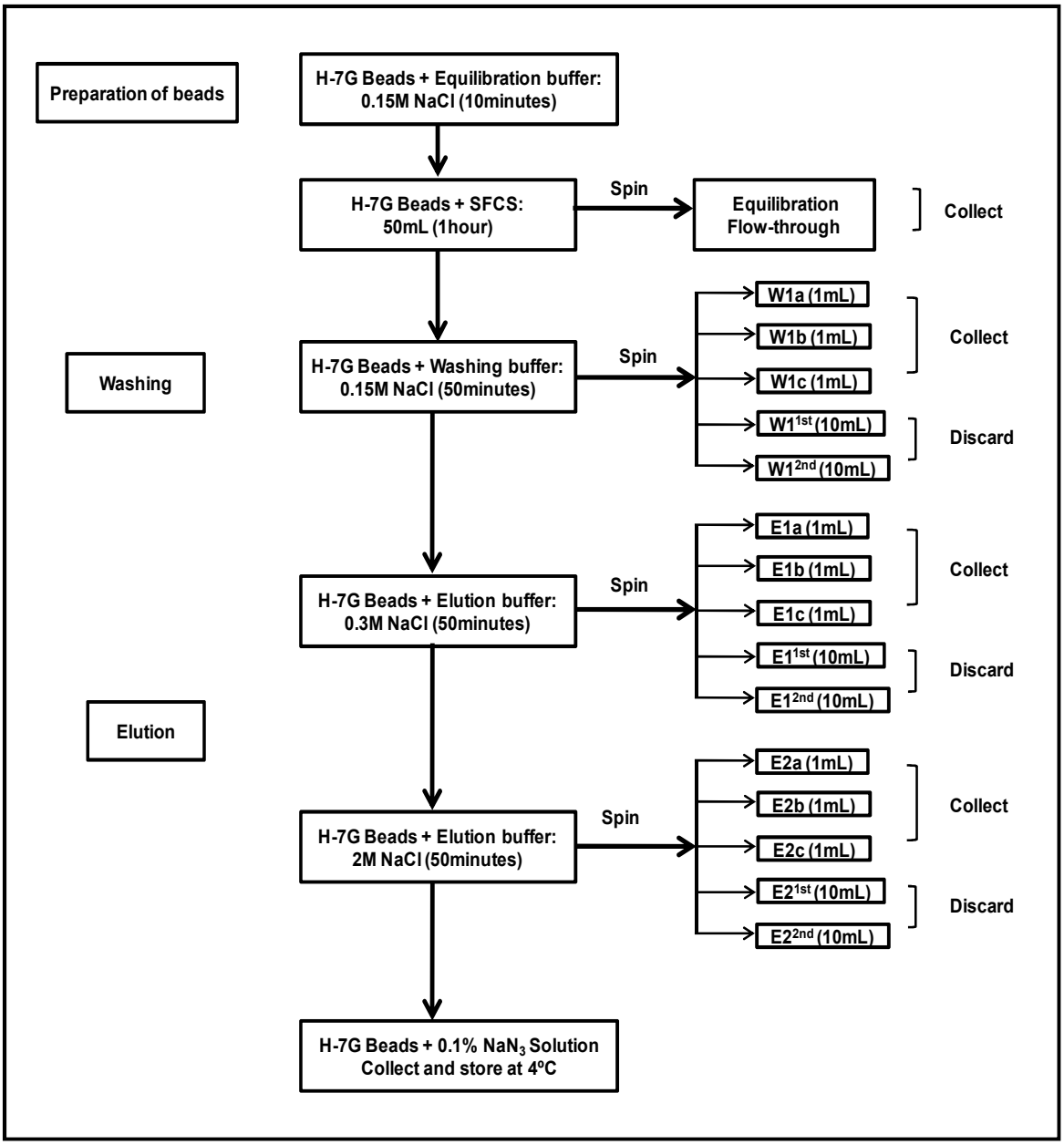

Figure 2.2 Flowchart for affinity chromatography.

2.6 Bradford Assay for Quantification of Total Proteins

Protein concentration was ascertained using the Bradford Assay (Bradford, 1976). Serial dilutions for six protein standards (62.5µg/mL-1.0mg/mL) were made up using 2mg/mL bovine serum albumin (BSA) dissolved in distilled water. These standards formed a standard curve (Figure 2.3) from which sample protein concentrations could be calculated. Each tube was vortexed and absorbance at 595nm read immediately on a spectrophotometer (Cary 50 Bio UV-Visible) using a disposable plastic cuvette.

2.7 ELISA for Quantification of MMP-2

MMP-2 amounts (pro and active) were quantified using an ELISA-based assay (R&D systems, MN, USA). The assay kit contains CHO cell expressed recombinant human MMP-2 and antibodies raised against the recombinant factor. This assay specifically recognizes recombinant and natural human MMP-2 as well as recombinant MMP-2 complexed with TIMP-2.

The mean minimum detectable dose (MDD) of MMP-2 is 0.16ng/mL. The assay was performed as per kit instructions. Briefly, serial dilutions of MMP-2 standards from 0.78ng/mL-50ng/mL were prepared in RD5-32 diluent provided in the kit. 50µL of each protein standard was applied in duplicate onto an anti-MMP2 coated microplate. Diluent RD5-32 (50µL) was used as a zero control standard and 50µL aliquots of the unknown samples were applied in duplicate into the appropriate wells.

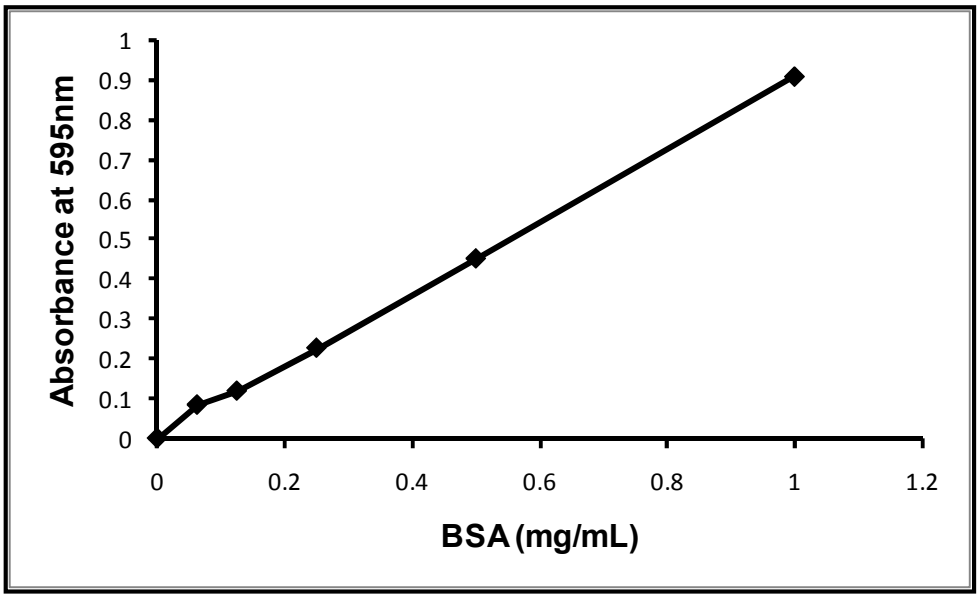

Figure 2.3 Standard curve for BSA standards.

A linear relationship between protein concentration and absorbance was confirmed between 62.5µg/mL and 1mg/mL.

The plate was then covered and shaken gently for 2hours at room temperature. All wells were washed 4-times with wash buffer and the plate blotted to remove any residual wash buffer before adding 200µL of detection antibody against MMP-2 conjugated to horseradish peroxidase to each well and incubation for a further 2hours at room temperature. Following washing, the colorimetric detection reagent (tetramethylbenzidine [TMB] and hydrogen peroxide [H_2O_2]) which is a substrate for horseradish peroxidase was added and incubated for 30 minutes at room temperature in the dark. The reaction was stopped via addition of H_2SO_4 (1N). The plate was then read at 450nm (Labsystems Multiscan Ex) to obtain the absorbance of blue product synthesized in each well. Readings were normalized by subtraction of non-specific absorbance at 540nm. Standard curves were constructed from the readings of the MMP-2 standards (Figure 2.4) and the concentrations of the unknowns calculated from these curves.

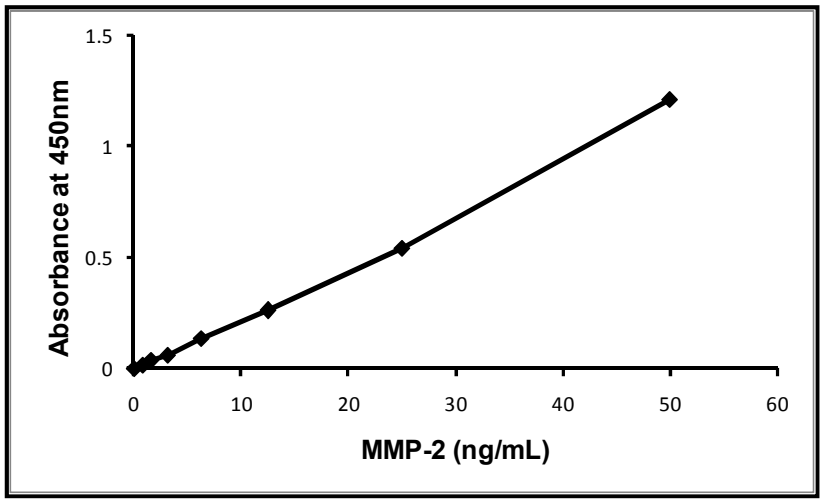

Figure 2.4 Standard curve for ELISA standards.

A linear relationship between protein concentration and absorbance was confirmed between 0.78ng/mL and 50ng/mL.

2.8 SDS-Polyacrylamide Gel Electrophoresis (SDS-PAGE)

Proteins were separated through 10% polyacrylamide SDS gels (Bio-Rad, Hertfordshire, UK). The gel was immersed in 1X running buffer (Appendix 1). Samples equivalent to 30µg protein were diluted in SDS loading buffer (Appendix 1) and were then heated at 95°C for 5minutes followed by rapid incubation on ice to denature proteins. Samples were loaded into wells at a volume of 20µL. Full range rainbow marker were loaded into the first and last well of the gel to allow for later mass determination. The electrophoresis was run at 50V until the samples reached the resolving gel, then, 125V for a further hour to separate proteins.

2.8.1 Coomassie Brilliant Blue Staining

Proteins separated on SDS-polyacrylamide gels were immersed in Coomassie brilliant blue solution (Methanol: H_20 [1:1 v/v] with 10% acetic acid) which fixed and stained it simultaneously for 1 hour. After staining the gels, a destaining solution (40% Methanol/ 10% acetic acid/ 50% water) was used to remove excess stain. Destained gels were sealed in plastic bags in water after being scanned (HP scan jet 2400).

2.8.2 Silver Staining

Gels were fully destained after Coomassie blue staining. Dodeca silver stain kit (Bio-Rad, Hertfordshire, UK) was used. Since silver salts are sensitive to temperature staining was performed at 23°C or above. After washing the gel with distilled water, a Fixing solution (8mL acetic acid, 32mL ethanol and 40mL water) was added and left for 30 minutes on a rocker. Sensitizing solution (8mL Bio-Rad SC reagent, 24mL ethanol, 800µL Bio-Rad BRC reagent and 47.2mL water) immediately after removing fixing solution was added and left on rocker for another 30 minutes at room temperature. Following three washes with 80mL of distilled water, staining solution (1.6mL Bio-Rad SRC reagent and 78.4mL water) was added and container was covered completely with aluminum foil. The gel was left on rocker for 20minutes. After removing staining solution and rinsing container quickly for few seconds with 80mL water and replacing with another 80mL of water, the gel was left for maximum of 1minute and then removed. Developing solution, (8mL Bio-Rad DBC reagent, 16µL Bio-Rad IDC reagent, 4µL Bio-Rad BRC reagent and 72mL water) was added onto the gel and left on shaker for 5-30 minutes depending on the formation of bands. The reaction was terminated by adding stopping solution (4mL acetic acid and 76mL water). The gel in container was left on shaker for 10minutes and then washed with 80mL water on the shaker for 10minutes. Water was replaced for storage.

2.8.3 Western Blotting for MMP-2

Western blotting protocol was optimized for primary antibodies for human MMP-2. The MMP-2 antibody utilized in this study was raised to bind to amino acid 107-117 of the protein. Proteins were transferred from the acrylamide gel to PVDF membrane using a Biorad transfer kit immersed in 1X transfer buffer (Appendix 1). Protein transfer was run at 300mA for 1 hour in the electrophoresis kit placed in an ice bath. After the transfer PVDF membrane was immersed in Ponceau solution to verify protein transfer. PVDF membrane was washed with 1X TBS and blocked overnight at 4°C with 10% (w/v) non-fat dried milk in Tris-buffered saline (1X TBS)-0.1%(v/v) TWEEN®20 (10X TBS: Appendix 1).

2.8.3.1 Antibody Incubations

The membrane was washed in 1X TBS without TWEEN®20 for a few seconds and then incubated with 1:1000 polyclonal rabbit anti-MMP-2 antibody in 5% (w/v) non-fat dried milk/ 1X TBS-TWEEN®20 for 2hours at room temperature. After rinsing thrice with 1X TBS-TWEEN®20, membranes were incubated with 1:2000 dilution of horseradish peroxidase conjugated polyclonal goat anti-rabbit antibody in 5% (w/v) BSA in 1X TBS-TWEEN®20 for 2hours at room temperature. The membrane was rinsed with 1X TBS-TWEEN®20 for 5minutes 3-times before protein detection. The same procedure was used for experiments set up to detect minimum amount of MMP-2 detected by using commercially available recombinant human MMP-2.

2.8.3.2 Protein Detection

The ECL plus western blotting detection system reagents A and B (Amersham™ GE Healthcare, Buckinghamshire, UK) were mixed in a 40:1 ratio and applied onto membrane for 5minutes. The membrane was then sealed using Saran™ wrap before being exposed to the Kodak scientific imaging film in dark room. Exposure times varied from 20minutes to overnight. Films were developed using Optimax X-ray film processor or in case of manual developing, developing in Ilford rapid multigrade developer (1/10 dilution) for 3minutes, rinsing with water and fixing in Ilford rapid film and paper fixer solution (1/10 dilution) for 3minutes.

2.9 Trypsin Digestion

In addition to using samples (HT1080 or HT29 culture supernatants, cell extracts, recombinant human MMPs and their corresponding affinity chromatography fractions) for total protein concentration measurement and activity assays, aliquots were used for proteomics analysis.

2.9.1 Proteomics: In-Solution Trypsin Digestion

The amounts of 8M urea, 50mM dithiothreitol (DTT) and 100mM iodoacetamide (IAC) were added depending upon the amount of protein present in the samples and will be

explained in corresponding chapters. To protein solution 8M urea in 100mM ambic was added to give a final concentration of 7.42M, vortexed and centrifuged. DTT (50mM) was added to give a final concentration of 1.85mM, vortexed and heated between 50-80^{o}C in water for 20minutes and centrifuged for 1minute. After bringing it to room temperature, 100mM IAC was added to a final concentration of 3.57mM, vortexed spun and incubated for 20minutes in the dark. HPLC grade water was added to dilute the urea concentration to 2M. Trypsin solution (20µg/mL) was added in a protein to trypsin ration of 20:1 (w/w) and incubated at 37^{o}C overnight. The reaction was stopped by freezing at -20°C. The controls -horse heart myoglobin + trypsin, myoglobin alone and trypsin alone were treated the same as the samples. Lyophilized protein samples were digested as described above, except resuspended directly in 8M urea buffer.

2.9.2 Proteomics: On-Bead Trypsin Digestion

Olive H-7G chromatography beads (100µL wet volume of Olive H-7G chromatography beads in 1:1 suspension in buffer) were equilibrated twice with 1mL of 25mM ambic, To the beads, urea was added to give an 8M concentration and vortexed. Then 50µL of 50mM DTT were added, mixed and heated to 50^{o}C for 15minutes. After bringing it to room temperature 50µL of 100mM IAC were added, vortexed, centrifuged and incubated for 15-20 minutes at room temperature in dark. To dilute the urea concentration to 2M, 50µL of HPLC grade water, were added. This was followed by the addition of 80µL of trypsin solution (20µg/mL) and incubated at 28^{o}C for 18hours. The reaction was stopped by freezing at -20°C.

2.10 Desalting of Digested Protein

Following devices were used to remove chemicals specifically detergents and salts likely to interfere with protein identification:

2.10.1 Desalting by Isolute C18 Cartridges

Digested protein samples were desalted to remove contaminants interfering with protein identification using Isolute C18 columns (Biotage, Kinesis Ltd.). To equilibrate

the column, 1mL methanol was added using a 1000µL pipette. A syringe and adaptor was attached to column to slowly force methanol through column into waste beaker stopping pressure just before total volume is eluted to prevent any air being forced through. The same process was repeated 2X with 1mL solvent A (2% CH_3CN with 0.05% triflouroacetic acid [TFA]). Then protein sample was added to column followed by toping it up to 2X with 1mL solvent A. Finally collected the sample into a labeled 1.5mL eppendorf tube by eluting with 1mL solvent B (80% CH_3CN with 0.05% TFA). Centrifuged and lyophilized the eluate at the end of the process.

2.10.2 Desalt with Zip tips

Zip tips with a C4 or C18 filter were used for desalting small volumes of fractions or for loading 2µL samples on target plate for MALDI-MS analyses. Using Gilson pipette of capacity from 2-20µL, zip tips were washed with 20µL methanol by forcing, stopping pressure just before total volume is eluted to prevent any air being forced through. The same process was repeated 2X with 20µL solvent A (2% CH_3CN with 0.05% TFA). Then 2µL protein sample was picked in zip tip followed by toping it up to 20µL with solvent A and repeated 2X with same volume of solvent A. Finally collected the sample on target plate by eluting with 2µL solvent B (80% CH_3CN with 0.05% TFA).

2.10.3 Desalt with Pierce Columns

Peptides were desalted using Pierce detergent removal spin columns (Thermo Scientific, Rockford, USA) to remove detergents which cause deleterious effects by forming adducts with peptides in MALDI-MS analyses. A 125µL spin column was placed into a 2mL collection tube. To equilibrate the column, 100µL of 10mM ambic was added using a 200µL pipette. The buffer was discarded after centrifugation at 1000g for 1minute at room temperature. As instructed, a mark was placed on the side of the column where compacted resin was slanted upwards. In all subsequent centrifugation steps, the mark was faced outwards in fixed-angle rotors since an improper orientation results in reduced detergent removal efficiency. The same process was repeated 2X with 10mM ambic. After placing the column in a new 1.5mL eppendorf

tube 10-25µL protein sample was slowly added to the top of compact resin bed and incubated for 2minutes at room temperature. The detergent free sample was collected into labeled 1.5mL eppendorf tube by centrifugating at 1000g for 2minutes.

2.11 Manual MALDI-MS of Peptides

2.11.1 Instrumentation

Mass spectrometry was performed on an Ultraflex^{TM} II MALDI-TOF/TOF instrument (Bruker Daltonics, Bremen, Germany). The MALDI-TOF-MS used a 200Hz pulsed 337nm nitrogen laser. Mass spectra were obtained after in-solution or on-bead trypsin digestion.

2.11.2 Matrix Solution Preparation

α-Cyano-4-hydroxycinnamic acid (CHCA) was used as the matrix of choice. Stock matrix solution was prepared by weighing CHCA (10mg) in a 1.5mL eppendorf tube, dissolved in 1mL of 30% CH_3CN + 0.1% TFA, vortexed for few minutes and then sonicated for 30 minutes. Stock matrix was stored at 4°C.

2.11.3 Mass Spectrum Acquisition

Samples were applied on One piece Aluminium Target with transponder MTP384 (Bruker Daltonics, Billerica, MA, USA) after cleaning the well positions with 0.5µL of 10mg/mL of CHCA. Once it was dried, each fraction (10µL) was desalted using C18 zip tips. Desalted peptides were eluted in 2µL of 80% CH_3CN + 0.05% TFA onto MTP 384 massive target plate and 0.5µL of matrix solution (10mg/mL CHCA) was applied on top of it. It was allowed to dry before placing in the mass spectrometer. A standard peptide mixture was used for calibration. Mass spectra were acquired by keeping the instrument at positive reflectron mode in the mass range of 700-4000Da using laser power from 50-80% firing 500 shots. For each sample and controls analyzed at least 5000 laser shots were added. Data was acquired by FlexControl software.

2.12 nHPLC coupled to MALDI-MS/MS for Protein Identification (LC-MS/MS)

2.12.1 Reverse phase nHPLC Fractionation of Modified Peptides

Fractions were desalted using Isolute C18 1mL columns and peptides were eluted using 1mL of 80% CH_3CN + 0.05% TFA and lyophilized. A nanoHPLC Dionex Ultimate 3000 system was used for fractionation of trypsin-digested peptides from selected chromatography fractions. The above mentioned system consists of stacked autosampler, flow manager, detector, pump and solvent rack modules. Samples were resuspended in 10% CH_3CN and (6.5µL) were transferred to Dionex vials and placed on the autosampler unit. The silica needle aspirated 5µL of sample after piercing the vial cap with a separate puncture needle. A 25µL syringe fixed at the opposite end of puncture needle helps this sample collection by creating suction. Once collected, sample was injected into the LC system via a sample loop (carrier solvent) onto a C18, 300µm x 5mm, 5µm, 100Å PepMap pre-column (LC Packings, Sunnyvale, CA). Once on the pre-column the sample was washed for 3.5minutes at a flow rate of 300nL/minute, with the carrier solvent. The sample was then transferred onto a C18, 75µm x 15cm, 3µm, 100Å PepMap column (LC Packings) which was equilibrated with 2% CH_3CN with 0.05% TFA (mobile phase A).

2.12.2 nHPLC Gradient Conditions

The peptides in the aqueous mobile phase A bind to the stationary phase in reverse phase nHPLC column. Column development (elution) was performed in a gradient manner in increasing CH_3CN buffer concentration. As autosampler injected 5µL of sample into micropump at a flow rate of 300nL/minute, 80% CH_3CN + 0.05% TFA (mobile phase B) increased by 10% in 6minutes. Between 6-81minutes it keeps increasing from 10-40% in linear fashion. At 81.1minutes it finally reaches 100%. This mobile phase composition is maintained for 5minutes and then changed to 100% mobile phase A to re-equilibrate column until the end of run at 100minutes post-injection. The detector used deuterium lamp and measured the wavelength of eluents simultaneously at two different wavelengths of 280nm and 215nm. The profile of

peptides was visualized on computer connected to the system using Hystar 3.2 software (Bruker Daltonics, Gmbh).

2.12.3 Fraction Collection

2.12.3.1 MALDI Matrix

A stock solution was prepared by solubilizing CHCA in 1mL of 30% (v/v) CH_3CN with 0.1% (v/v) TFA. CHCA was solubilized by vortexing for 2minutes and sonicating for 30 minutes to generate a saturated solution. From the stock solution a working solution is prepared by adding 1.056mL ethanol-acetone (2:1), 120µL of matrix stock supernatant, 12µL 100mM ammonium phosphate and after vortexing mixture 12µL 10% TFA was added. Working matrix solution was stored at room temperature with lid closed to prevent evaporation. The fractions (384) were collected onto a MTP AnchorChip 800/384 target plate (Bruker Daltonics, Bremen, Germany) using Proteineerfc FC fraction collector (Bruker Daltonics, Gmbh). The xyz coordinates of the robot arm were adjusted using Hystar 3.2 software. The eluate fraction volume spotted by Proteineerfc robot arm every 15seconds on each well is 1.2µL CHCA matrix + 75nL of sample.

2.12.3.2 External Calibration for MS

Peptide Calibration Standard II (Bruker Daltonics, Bremen, Germany), comprising Angiotensin I, Angiotensin II, Substrate P, Bombesin, ACTH clip 1-17, ACTH clip 18-39, Somatostatin-28, Bradykinin fragment 1-7 and Renin Substrate Tetradecapeptide porcine; covering the mass range 700-3200Da, was used for external calibration of mass spectrometer. After the collection of fractions, 0.3µL of a 1/15 dilution of Peptide Calibrant Standard II in 70% CH_3CN + 0.1%TFA was spotted between every four wells on target plate. After the calibrant dried, 1.3µL of CHCA working matrix solution was applied on top of it.

2.12.4 Mass Spectrum Acquisition

For automated MALDI-MS/MS 800 shots of laser were fired for parent ion and 1200 for the fragment ions in Ultraflex^{TM} II MALDI-TOF/TOF instrument. The details about what precursors were selected and mass range for data collection will be described in various chapters.

2.12.5 WARP-LC and Database searching

WARP-LC is a software platform for qualitative and quantitative LC-MS/MS-based protein and proteomics analysis for all ESI and MALDI mass spectrometers manufactured by Bruker, Daltonics. WARP-LC is an acronym for Workflow Administration by Result-driven Processing. Figure 2.6 shows how peaks for compounds with a certain *m/z* are selected and sent to Mascot search engine and the results are displayed on ProteinBrowser. Mass lists from MS/MS spectra of peptides were submitted to a Mascot (Matrix Science, Boston, MA) query search which used Mascot software (Perkins et al., 1999) searching against the SwissProt protein database using the Bruker Biotools (version 3.2) interface. Within the Mascot search engine, the MS tolerance was ±0.7Da and mass tolerance was 100 parts per million (ppm). The criteria also included ≤ 2partials, taxonomy human, enzyme trypsin and the variables modifications allowed were methionine oxidation and carbamidomethylation of cysteine. No global variations were selected. A 95% confidence threshold was set ($p<0.05$) for searching the MS/MS data against SwissProt. A Mascot score threshold of ≥30 was used for positive protein identification.

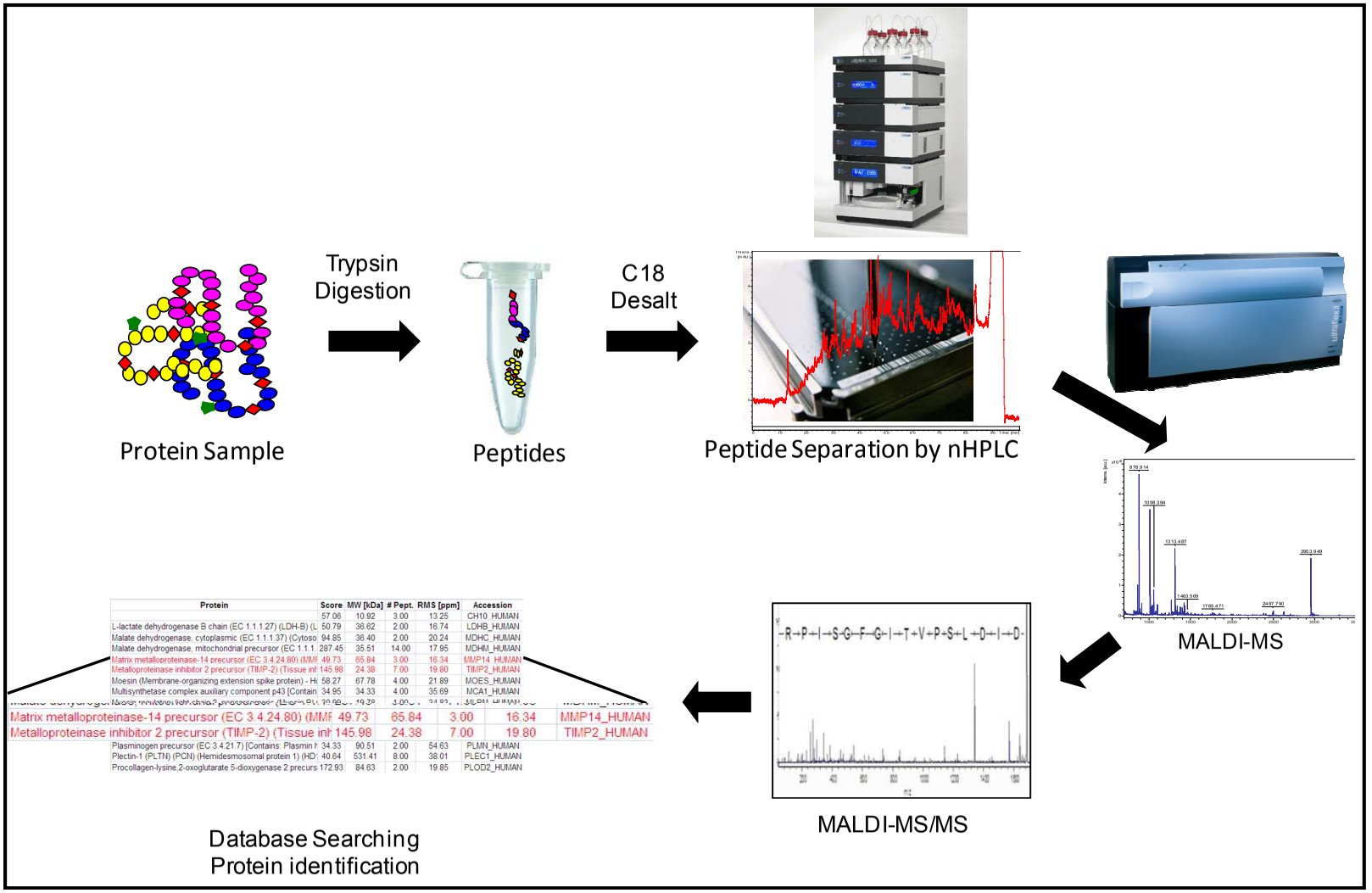

Figure 2.5 LC-MS/MS workflow.

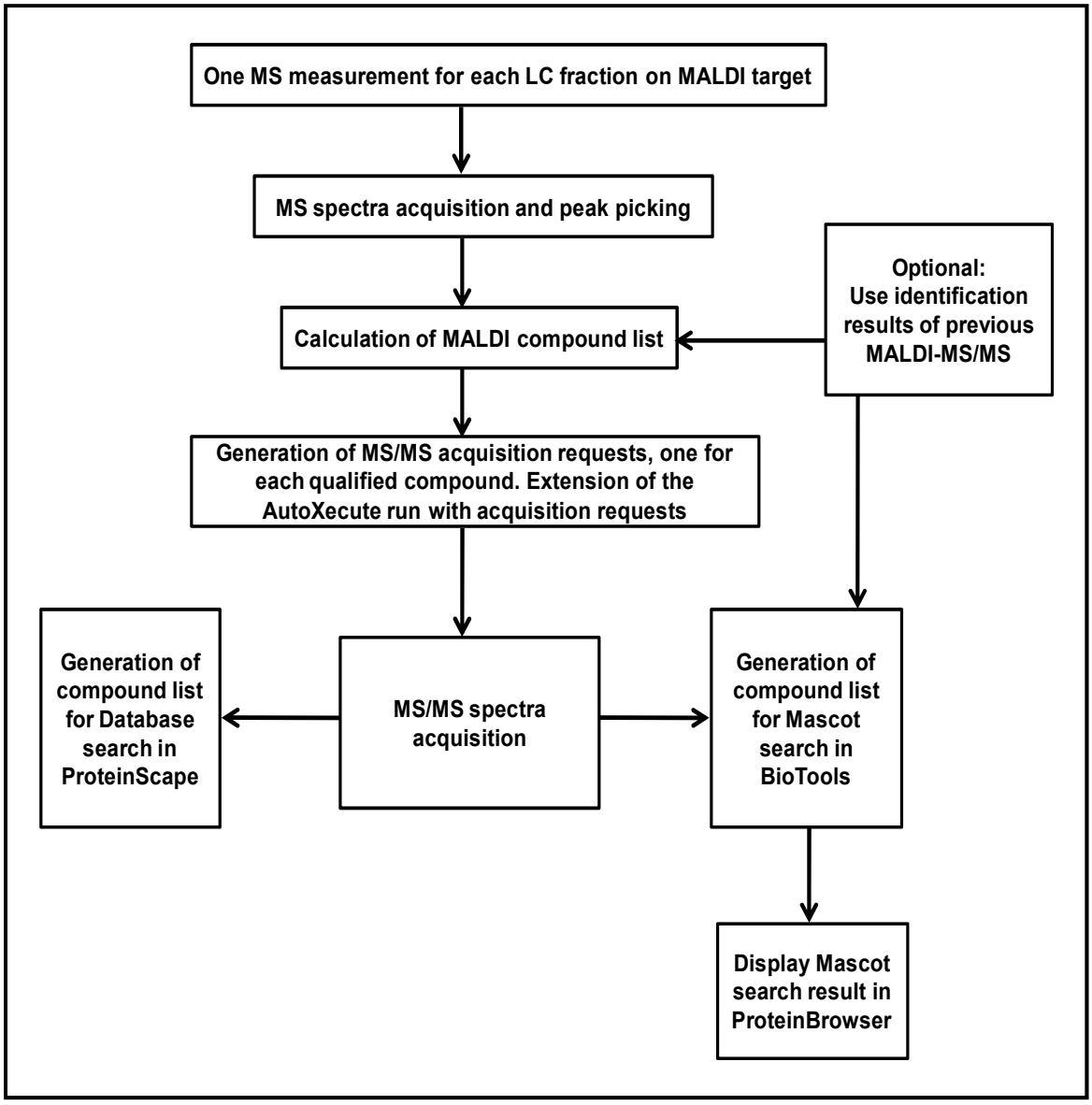

Figure 2.6 LC-MS/MS workflow supported by WARP-LC.

CHAPTER 3

PROCION OLIVE H-7G DYE CHARECTERISTICS

3 Procion Olive H-7G Dye Characteristics

3.1 Introduction

Dyematrex Reactive Green A is an azo-anthraquinone immobilized dye marketed by Amicon (Lexington, MA, USA) (Fulton, 1980) but this product is no longer commercially available. There is considerable evidence that pro-MMPs can be purified using conventional column chromatography in which the Green A Dyematrix plays an important role. This ligand had previously been demonstrated to have affinity for MMPs, specifically, pro-MMP-1, pro-MMP-2, pro-MMP-3 (Okada et al., 1986), pro-MMP-7 (Imai et al., 1995), pro-MMP-9 (Okada et al., 1992) and pro-MMP-10 (Nakamura et al., 1998). Since studies have shown that Green A Dyematrex Gel (Procion Olive H-7G or Olive H-7G) can be used for capturing multiple pro-MMPs, it suggests that there is a common binding moiety within the family of enzymes. Therefore, a detailed analysis of Olive H-7G was made to explore if it will bind other MMPs and can be used to purify all MMPs in biological sample, particularly if applied as an adjunct to proteomics methods such as MALDI mass spectrometry analysis and protein identification. A good amount of Procion Olive H-7G, the active ligand in Dyematrex Reactive Green A, is available at ICT and was provided by Millipore Inc (who acquired Amicon Inc) for these studies. Bound proteins are eluted with high salt concentrations as has been described in the literature (Imai and Okada, 2008).

This chapter comprises of experiments to determine some of the characteristics of the dye. Olive H-7G comprises of an anthraquinone moiety (Figure 3.1) with two sulphonic acid groups and an amine group. The sulphonic groups provide the desired solubility of the molecule in aqueous media (Denizli and Piskin, 2001). These groups are negatively charged at all pH values. Sodium ions increase the solubility of this dye in water. This anthraquinone moiety is linked to an azo functional group which in turn is linked to a reactive group mono-chlorotriazine ring (Figure 3.1). The presence of aromatic backbone renders it hydrophobic and helps develop interactions with hydrophobic surfaces of proteins. Like other reactive dyes,

an additional support is provided by the ionic interactions between other polar interactions of amino acid side chains with dye substituent (Denizli and Piskin, 2001). Olive H-7G is soluble in water and not soluble in methanol or ethanol. Olive H-7G dye is immobilized onto a solid support (matrix) by direct reaction between hydroxyl groups of the polysaccharide gels such as agarose or sepharose and the chloride atom on triazinyl group of the dye. This pairing is achieved at alkaline conditions by nucleophilic substitution of hydroxyl groups with the reactive chlorine on the dye molecules (Figure 3.2). The linkage between the matrix and ligand is stable during the protein absorption and elution steps of affinity chromatography. Nucleophiles are generated by the high pH, which promotes the ionization of the matrix hydroxyl groups, but pH>12 should be avoided as hydrolysis of the chlorotriazines in the aqueous media occurs (Denizli and Piskin, 2001).

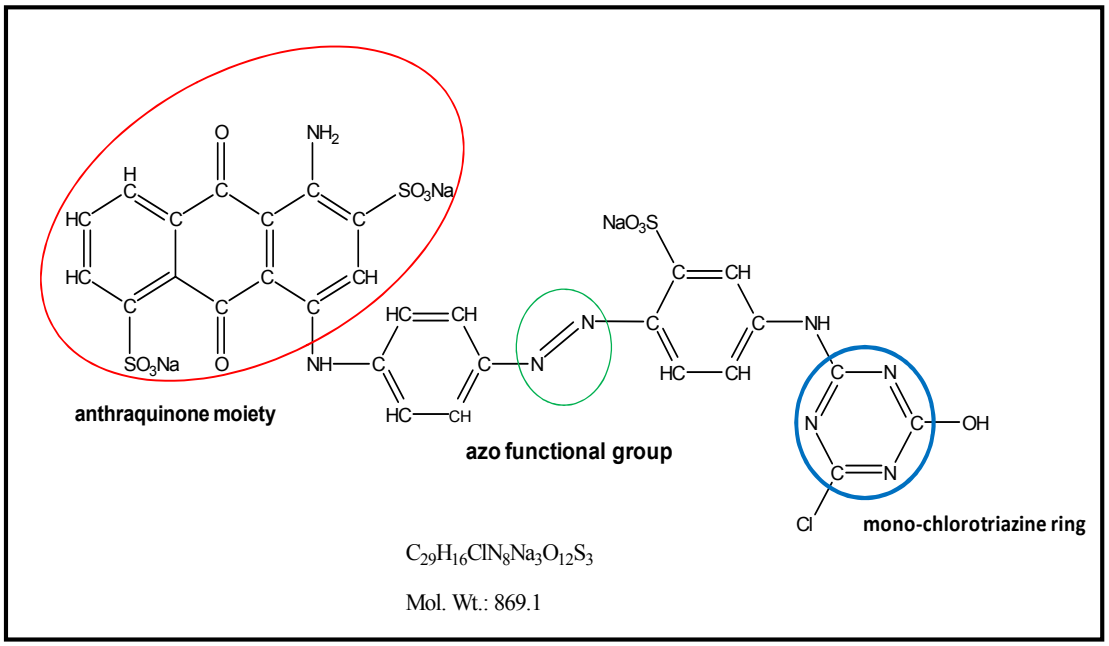

Figure 3.1 Structure of Procion Olive H-7G.

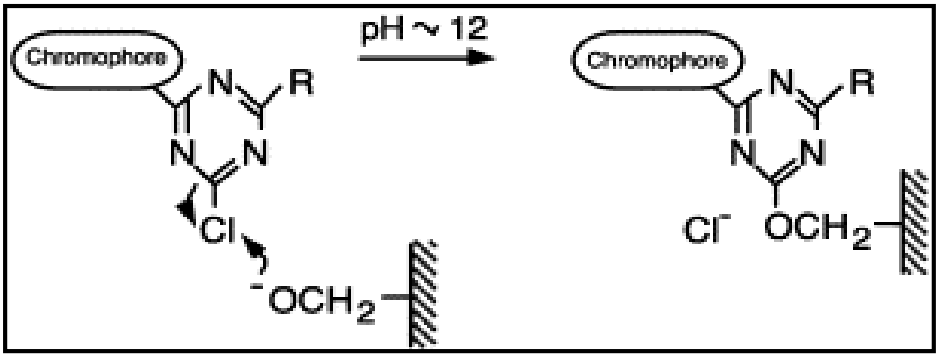

Figure 3.2 Coupling of triazinyl dyes to the matrix bearing hydroxyl groups.

Taken from (Denizli and Piskin, 2001).

3.1.1 Aims

The specific aims of this chapter are:

- To determine photometric absorbance of Olive H-7G.
- To determine limit of detection of Olive H-7G by MALDI-MS.
- To determine absorbance of Olive H-7G using nHPLC.

3.2 Materials and Methods

3.2.1 Spectrophotometery

Absorbance of Olive H-7G serial dilutions (1nM-10mM) was scanned over a range of wavelength (200nm-1000nm) with a step size of 5nm. Each dilution was vortexed and absorbance was scanned immediately on UV spectrophotometer (Multiskan Spectrum v1.2) using a disposable plastic cuvette with a path length of 1cm.

3.2.2 MALDI-MS of Olive H-7G

Mass spectrometry was performed on in-house Ultraflex^{TM} II MALDI-TOF/TOF instrument (Bruker Daltonics, Bremen, Germany) (see Chapter 2 for details) operating in reflectron, positive ion mode. The Olive H-7G dilutions (1nM-10mM) were spotted with CHCA (10mg/mL) matrix and 5000-15000 laser shots were acquired for various dilutions to achieve a stronger mass spectra.

3.2.3 nHPLC of Olive H-7G (Analytical Runs)

A nanoHPLC Dionex Ultimate 3000 system was used for Olive H-7G dilutions (0nM, 2nM, 4nM, 6nM, 8nM, 10nM, 20nM, 40nM and 80nM). Olive H-7G solutions (10µL) were transferred to Dionex vial (plastic) and placed on the autosampler unit and 2µL of samples is loaded onto the column. Elution was performed for various Olive H-7G dilutions in gradient manner using different times and increasing acetonitrile buffer concentration. The mobile phase B (80% CH_3CN + 0.05% TFA) increased finally reaching 100% and this mobile phase was changed to 100% mobile phase A (2% CH_3CN + 0.05% TFA) as shown in Table 3.1. The detector used deuterium lamp and measured the wavelength of eluents simultaneously at three different wavelengths of 215nm, 250nm and 445nm. The profiles of Olive H-7G solutions were visualized on computer connected to the system using Hystar 3.2 software (Bruker Daltonics, Gmbh).

Table 3.1 HPLC gradient parameters for analytical runs of Olive H-7G.

HPLC Gradient Parameters	
Time (minutes)	**Solvent B (%)**
0	**0**
0	**0**
5	**0**
7.5	**90**
20	**100**
25	**100**
25.1	**0**
38	**0**
48	**0**

3.3 Results

3.3.1 Spectrophotometery of Olive H-7G

Photometric absorbance scanning showed wavelengths at maximum absorbance (λ_{max}) of 250nm and 445nm in 100µM Olive H-7G solution (Figure 3.3). The multiple peaks in the 100µM dilution are because of the presence of aromatic rings in the structure of the dye. The absorbance of 1mM and 10mM dilutions was complicated and lower concentrations (1nM-1µM) were not detectable by the scanner (results not shown).

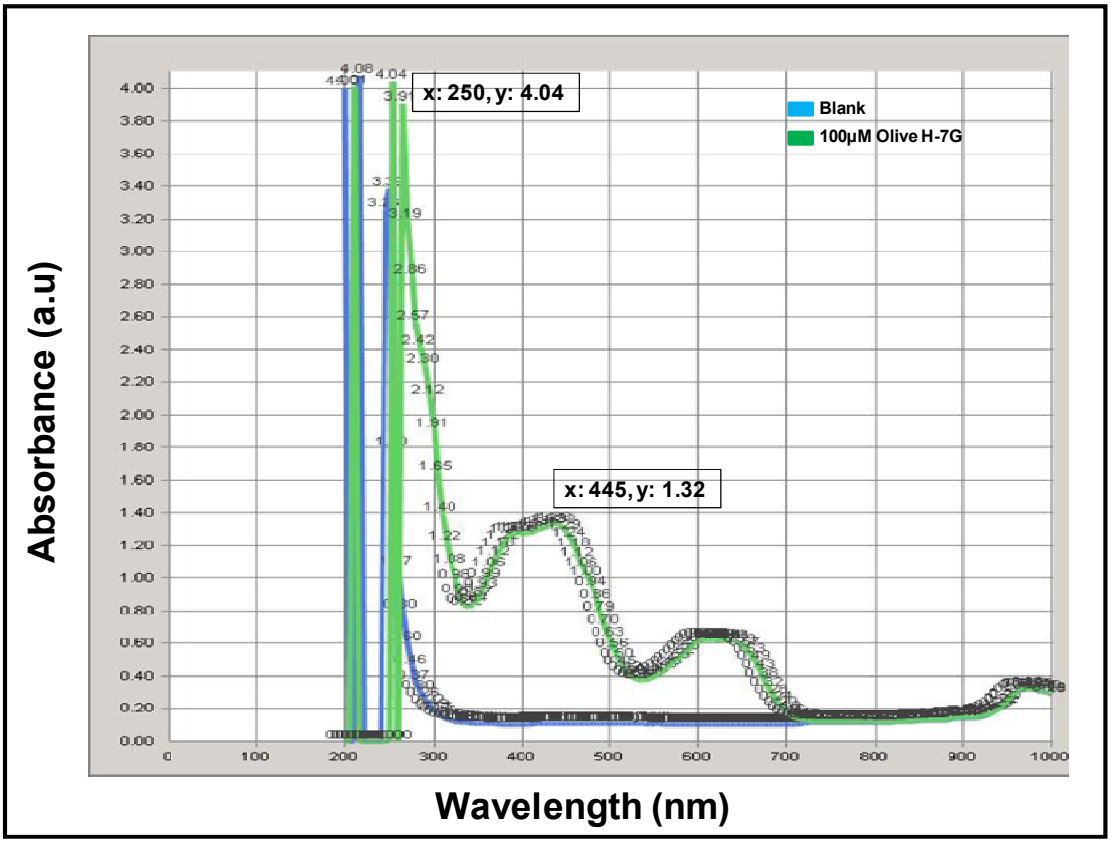

Figure 3.3 Photometric scanning (200-1000nm) of Olive H-7G to measure absorption λ (n=5).

3.3.2 Olive H-7G Molecular Mass Confirmation by MALDI-MS

Since matrix CHCA also shows low mass fragments, it was analyzed neat across a spectral range 700-4000 as shown in Figure 3.4. The calculated molecular mass of Olive H-7G is 869.1 and CHCA matrix did not show any fragment with this mass. Figure 3.5 shows that at this spectral range, Olive H-7G (10mM) showed a peak at 864.697, Olive H-7G (1mM) showed a peak at 864.873 and Olive H-7G (0.1mM) showed very weak intensity peak at this mass (result not shown). All lower concentrations (10µM-1nM) did not show any significant peaks which imply that limit of detection (LOD) of Olive H-7G compound is 0.1mM (869ng/mL). The same Olive H-7G serial dilutions were then analyzed setting a spectral range from 200-2000 and 500-1000 so that a close observation of the smaller fragments could be made. The CHCA matrix showed smaller mass peaks but no significant peak near calculated mass of Olive H-7G.

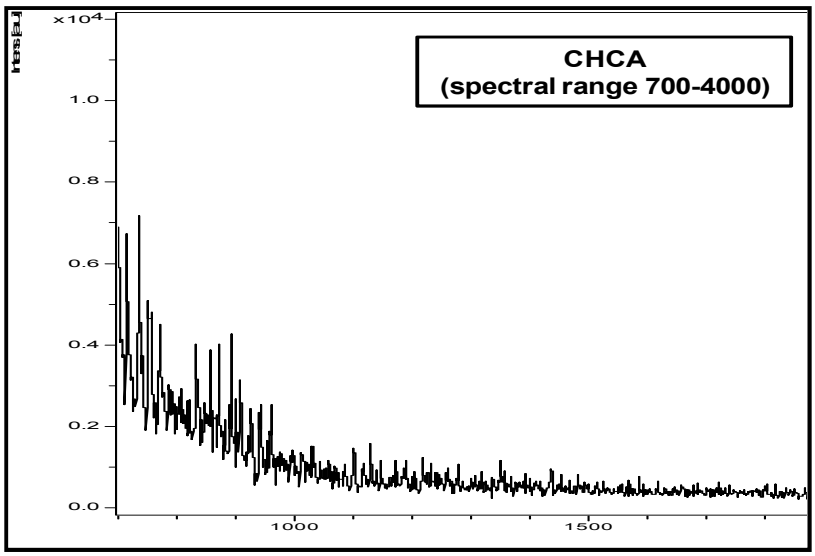

Figure 3.4 MALDI mass spectrum of CHCA matrix (spectral range 700-4000).

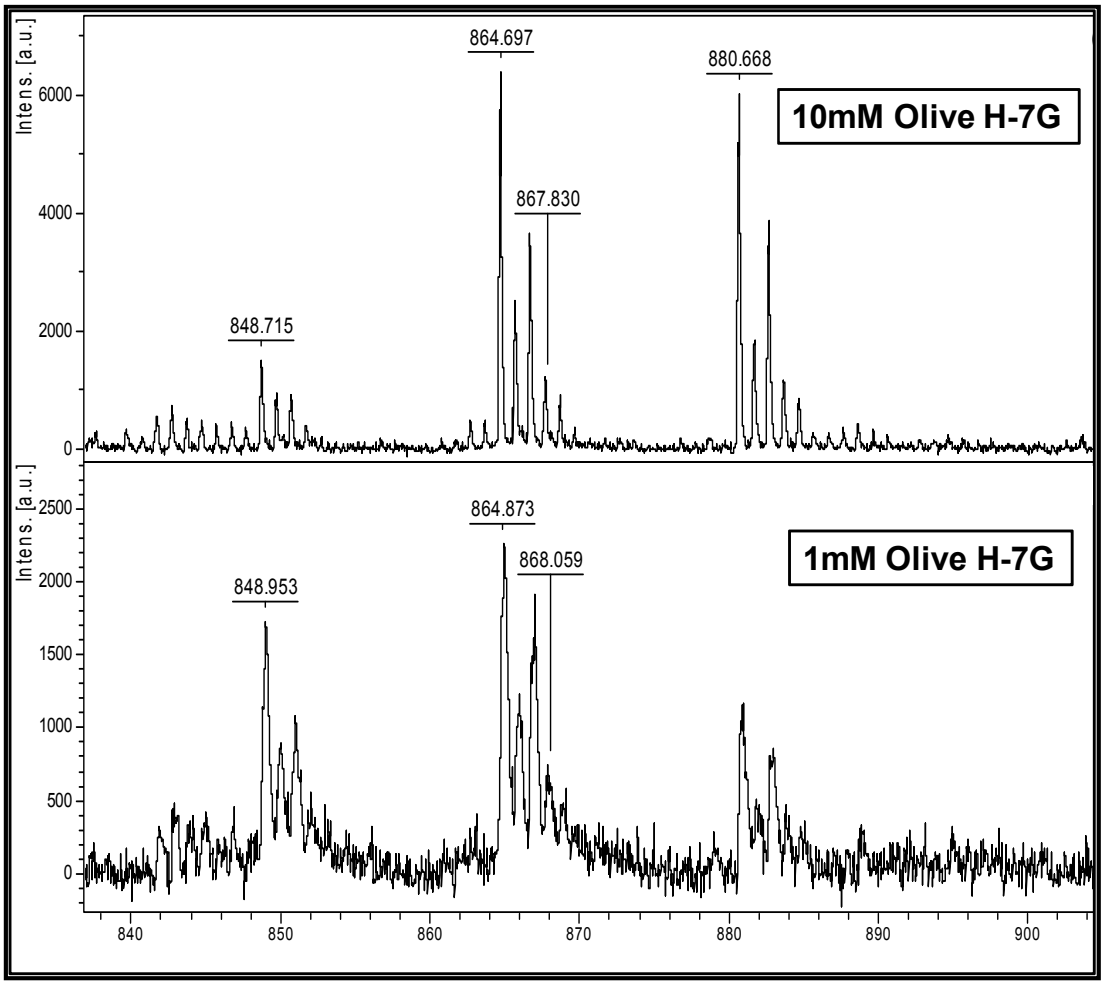

Figure 3.5 MALDI mass spectra of Olive H-7G (spectral range 700-4000).

3.3.3 nHPLC Profiles of Olive H-7G

Olive H-7G was analyzed by C18 reverse phase nanoHPLC with on-line UV detection at 215nm, 250nm and 445 over the concentration range 0-80nM. The set of parameters for HPLC analytical run are given in Table 3.1. Since Olive H-7G is more soluble in water, the gradient parameters were set so that solvent A (2% CH_3CN + 0.05% TFA) is 100% for longer time to elute the Olive H-7G dye off the HPLC column if it is bound. Within 2.5minutes solvent B (80% CH_3CN + 0.05% TFA) percentage was increased from 0-90 and then in next 12.5minutes it reached 100%. After keeping it 100% for 5minutes, solvent B percentage was decreased to 0 at time-point 25.1minute. A discrete peak was observed between 37-39minutes possibly indicating that Olive H-7G is pure and eluting in higher concentration of solvent A (2% CH_3CN + 0.05% TFA). It is also worth noticing that there is a delay in elution of a compound and its detection by UV detector in HPLC system. Once optimized, above mentioned settings were used for 80nM Olive H-7G concentration to see if discrete peak could be obtained. A more intense and similar profile was observed in three individual runs. The 80nM Olive H-7G solution shows better UV profile than for lower concentrations. The Olive H-7G did not show absorbance at 445nm.

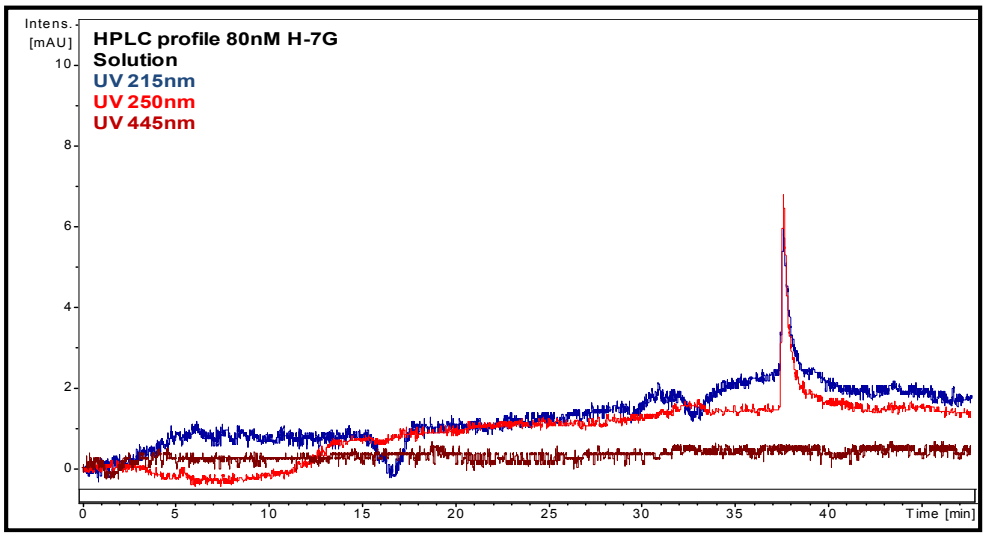

Figure 3.6 HPLC profile of 80nM Olive H-7G (n=3).

3.4 Discussion

Simple, economical and reproducible spectrophotometric methods are compared with HPLC methods for the estimation of number of components in a product to find out difference in efficiency. So that if HPLC is not available, spectrophotometer could be used. These methods were successfully applied for the determination of the two binary combinations in synthetic mixtures and in commercial tablets and syrup containing several light absorbing recipients (el-Gindy, 2003). An attempt was made to develop a UV spectrophotometric and nHPLC method for simultaneous estimation of components present in Procion Olive H-7G dye. For estimation with spectroscopy, the scanning was performed at a wavelength range from 200-1000nm. The Developed HPLC method is reverse phase chromatographic method using C18 column and acetonitrile as mobile phase. The first method involving multi-wavelength spectroscopy is specific to the instrument having software for provision of such determination. The selection of proper sampling wavelengths and concentration of components in solution is critical. Since calculations are done by the instrument itself, chances of manual error are nil; furthermore, the method is quite rapid. For nHPLC run time per sample was 48minute and it used UV detector even for visible range wavelength 445nm. Photometric absorbance scanning produced multiple wavelengths for the maximum absorbances (λ_{max}) at 250nm and 445nm because Olive H-7G has aromatic rings in its structure.

Based on the results of spectrophotometry three different wavelengths were set in HPLC system to detect the absorbance profile of various structural components of Olive H-7G. The appearance of peaks at 215nm and 250nm indicates the presence of aromatic rings. When 8nM Olive H-7G solution was fractionated using HPLC, collected on target plate and analyzed by MALDI-MS to confirm calculated mass (869.1) of Olive H-7G, very complex set of data was obtained and any conclusive observation could not be made. In HPLC, the dye was well separated and gave discrete peaks as shown in the representative chromatograms (Figure 3.6). The spectrophotometric absorbance of 100μM H-7G solution showed a profile specific to aromatic ring containing compounds and detection of discrete peaks in HPLC

chromatogram for 80nM H-7G solution might suggest that Procion Olive H-7G has one active component. However, this can not be stated with certainity that the peak at 445nm is specific to the dye. This could be attributed to weaker chromophore within the structure of the dye, low concentration of H-7G or the instrument was not specific enough.

The Olive H-7G peak profile determined by MALDI-MS did not show specific peak at 869.1+1. The dye was also analysed by ESI (facility available at IPI University of Bradford) but a conclusive result confirming structure of the dye could not be obtained suggesting complex nature of the compound.

CHAPTER 4

CHARECTERIZATION OF RECOMBINANT HUMAN MMPs (rhMMPs) BY MALDI-MS

4 Characterization of Recombinant Human MMPs (rhMMPs) by MALDI-MS

4.1 Introduction

Identification of specific peptides that are characteristic of specific proteins is one of the key principles of MS-based proteomics. In the present study MALDI-MS based strategies were used for the characterization of proteins (Figure 4.1). The MALDI-MS is suitable for purified proteins, thus any discrepancies in mass of intact purified protein from that of calculated mass as determined by amino acid sequence predicted from the cognate gene can be revealed. The individual proteins/peptides are ionized and identified searching the acquired *m/z* data against databases. The protein identification is confirmed by a score calculated by relating experimental and theoretical data. The proteins of interest for the present study are MMPs. As explained in the Introduction diverse physiological roles are played by various members of this family of enzymes in turnover of most types of the ECM proteins making them a suitable drug target for prevention of pathological tissue damage. Some of the characteristics of MMPs are summarized in Table 4.1.

4.1.1 Aims

A number of recombinant forms of human pro-MMPs (rhMMPs) are available commercially. Before studying H-7G-Sepharose chromatography for the purification of MMPs from biological samples, a set of preliminary experiments with rhMMPs using MALDI mass spectrometry for detection and identification were performed.

The aims of these experiments explained in this chapter were:

- To characterize rhMMPs by mass spectrometry using amounts equivalent to those anticipated in biological samples (a) to confirm the intact protein had the expected molecular weight and (b) to identify characteristic peptides for the ‘pro’ and ‘active’ regions of each rhMMPs after digestion with trypsin.

- Having established characteristic profiles, the region of MMPs that binds Olive H-7G dye will be identified by comparing MS spectra of trypsin-digested rhMMP in the presence and absence of soluble dye.

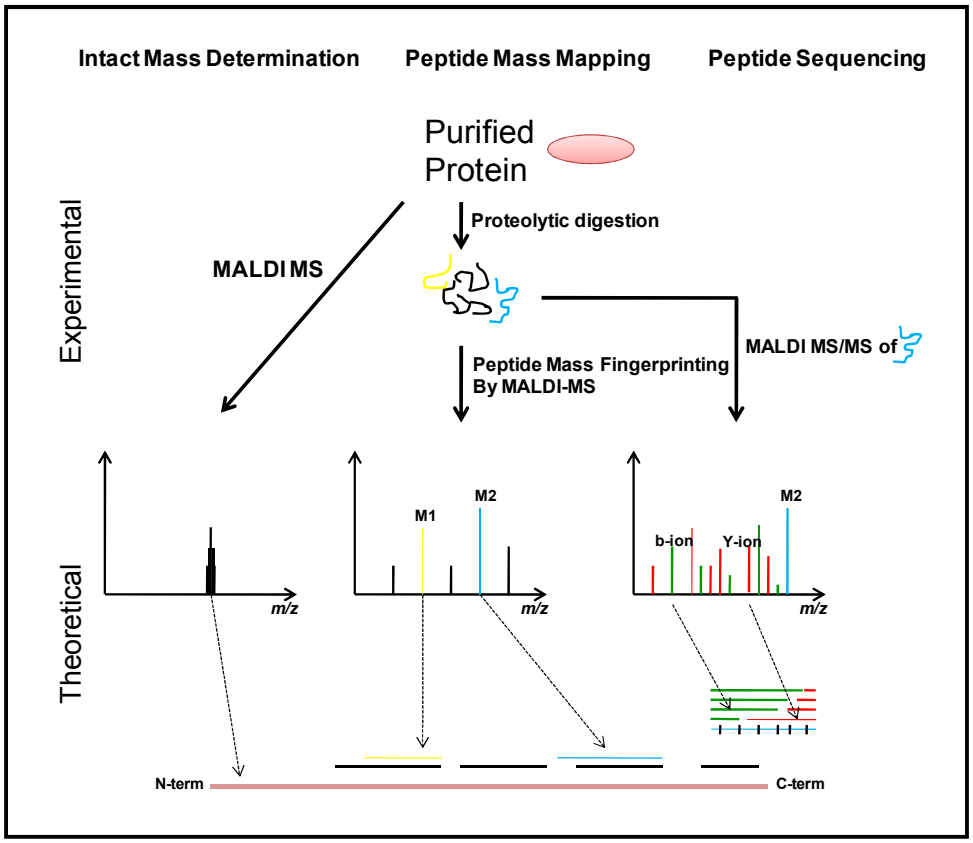

Figure 4.1 Applications of MALDI-MS in proteomics.

Table 4.1 MMP characteristics.

No.	MMP	Sequence length	Active Protease Region	Active site residue	Metal Ligands	Gene Symbol	Chromosome Locus	UniProt	Other Names
1	MMP-1	469	98-276	E219	H218, H222, H228	MMP1	11q22-q23	P03956	collagenase 1, interstitial collagenase, matrix metalloproteinase 1, vertebrate collagenase
2	MMP-2	660	108-461	E404	H403, H407, H413	MMP2	16q13	P08253	3/4 collagenase, 72 kDa gelatinase, gelatinase A, matrix metalloproteinase 5, tissue gelatinase, type IV collagenase
3	MMP-3	447	98-279	E219	H218, H222, H228	MMP3	11q23	P08254	matrix metalloproteinase 6, procollagenase activator, proteoglycanase, stromelysin 1, transin
4	MMP-7	267	94-267	E215	H214, H218, H224	MMP7	11q21-q22	P09237	matrin, matrix metalloproteinase 7, matrilysin, matrix metalloppeptidase-7, putative metalloproteinase-1, uterine metalloendopeptidase
5	MMP-8	467	97-275	E218	H217, H221, H227	MMP8	11q21-q22	P22894	collagenase 2, matrix metalloproteinase 8, neutrophil collagenase
6	MMP-9	707	105-458	E402	H401, H405, H411	MMP9	20q11.2-q13.1	P14780	92 kDa gelatinase, gelatinase B, macrophage gelatinase, matrix metalloproteinase 9, neutrophil gelatinase, type IV collagenase,
7	MMP-10	476	97-278	E218	H217, H221, H227	MMP10	11q22.3-q23	P09238	matrix metalloproteinase 10, stromelysin 2, transin-2 (Homo sapiens-type)
8	MMP-11	488	94-274	E216	H215, H219, H225	MMP11	22q11.2	P24347	matrix metalloproteinase 11, stromelysin 3
9	MMP-12	470	99-280	E219	H218, H222, H228	MMP12	11q22.2-q22.3	P39900	macrophage elastase, matrix metalloproteinase 12, metalloelastase
10	MMP-13	471	102-282	E223	H222, H226, H232	MMP13	11q22.3-q23	P45452	collagenase 3, matrix metalloproteinase 13, rat collagenase
11	MMP-14	582	108-301	E240	H239, H243, H249	MMP14	14q11-q12	P50281	matrix metalloproteinase 14, membrane-type matrix metalloproteinase 1, matrix metalloproteinase membrane-type 1, MT1-MMP, MTMMP-1

12	MMP-15	669	128-319	E260	H259, H263, H269	MMP15	16q13-q21	P51511	matrix metalloproteinase 15, membrane-type matrix metalloproteinase 2, MT2-MMP, SMCP-2, MTMMP-2
13	MMP-16	607	116-306	E247	H246, H250, H256	MMP16	8q21	P51512	matrix metalloproteinase 16, membrane-type matrix metalloproteinase 3, MT3-MMP, ovary metalloproteinase,
14	MMP-17	606	125-319	E252	H251, H255, H261	MMP17	12q24.3	Q9ULZ9	matrix metalloproteinase 17, membrane-type matrix metalloproteinase 4, MT4-MMP, MTMMP-4
15	MMP-19	508	93-282	E213	H212, H216, H222	MMP19	12q14	Q99542	matrix metalloproteinase 19, RASI-1, RASI-6
16	MMP-20	483	106-287	E227	H226, H230, H236	MMP20	11q22.3-q23	O60882	enamelysin, matrix metalloproteinase 20
17	MMP-21	569	161-353	E284	H283, H287, H293	MMP21	10q26.2	Q8N119	matrix metalloproteinase 21, XMMP (*Xenopus*)
18	MMP-23A	390	77-280	E212	H211, H215, H221	MMP23A	1p36.3	O75900-1	matrix metalloproteinase 23A
19	MMP-23	390	77-280	E212	H211, H215, H221	MMP23B	1p36.3	O75900-2	matrix metalloproteinase 23, MIFR protein (Homo sapiens), MMP-21 [obs.], MMP-22 [obs.], femalysin
20	MMP-24	645	156-645	283	H282, H285, H291	MMP24	20	Q9Y5R2	membrane-type matrix metalloproteinase 5, MT-5 MMP, matrix metalloproteinase 24, MTMMP-5
21	MMP-25	562	104-306	E234	H233, H237, H243	MMP25	16p13.3	Q9NPA2	leukolysin, membrane-type matrix metalloproteinase 6, MT-6 MMP, matrix metalloproteinase 25, MTMMP-6, myroilysin
22	MMP-26	261	88-261	E209	H208, H212, H218	MMP26	11p15	Q9NRE1	endometase, matrilysin-2, matrix metalloproteinase 26
23	MMP-27	513	95-277	E217	H216, H220, H226	MMP27	11q24	Q9H306	matrix metalloproteinase 22, MMP-22 (*Gallus domesticus*), (*Homo sapiens*), matrix metalloproteinase 27, matrix metallopeptidase 27

Source: www.uniprot.net and http://merops.sanger.ac.uk.

4.2 Materials and Methods

4.2.1 MALDI-MS of Intact Proteins

4.2.1.1 Desalting rhMMPs

Since stock rhMMPs (R & D) are in a solution containing Brij-35, C4 zip tips were used to remove the detergent where protein mass peaks were masked by detergent related peaks as will be described in Chapter 6. Depending on molecular mass and structural properties, 2-50pmoles of purified protein is required for comprehensive molecular analysis by MALDI-MS including intact mass determination.

4.2.1.2 Matrix Solution Preparation

Sinapinic acid (SA) was used as matrix. A stock solution of SA matrix (10mg/mL) was prepared in 70% CH_3CN + 0.1% TFA. rhMMPs samples (0.5µL), with or without desalting, were applied on One-piece Aluminum Target with transponder MTP384 (Bruker Daltonics, Billerica, MA, USA) and 0.5µL of matrix solution on top of it. It was allowed to dry before placing in the mass spectrometer.

4.2.1.3 Mass Spectrum Acquisition

Mass spectrometry was performed on an Ultraflex^{TM} II MALDI-TOF/TOF instrument (Bruker Daltonics, Bremen, Germany) (see Chapter 2 for details). A manual analysis was performed by keeping the instrument at positive linear mode using laser power from 70-90% firing 500 shots. For each rhMMP and controls analyzed, at least 5000 laser shots were added at a mass range of 10,000-200,000. Data was acquired by FlexControl software. The recombinant MMPs volume analyzed, stock concentrations and the volume of SA used is given in Table 4.2. All intact protein samples were analyzed before and after desalting using C4 zip tips.

Table 4.2 Concentration of intact rhMMPs for molecular mass determination.

rhMMP	Concentration (µM)	Volume (µL)	Matrix Volume (µL)
MMP-1	1.9	0.26	0.50
MMP-2	5.1	0.97	0.50
MMP-3	1.79	2.00	0.50
MMP-7	17.85	0.56	0.50
MMP-8	1.96	2.00	0.50
MMP-9	2.59	1.54	0.50
MMP-10	1.92	2.00	0.50
MMP-13	3.85	0.56	0.50
MMP-14	16.12	0.56	0.50

4.2.2 Theoretical Digests for MMPs (SequenceEditor Software)

SequenceEditor 3.2 (Bruker Daltonics, Gmbh, Germany) was used to perform *in-silico* trypsin digestion on sequences of human MMP protein. The potential peptides can be created with no modifications or by selecting cysteine modification reduced (SH), oxidised (SS), carbamidomethyl (C), N-terminal end (free hydrogen) and C-terminal side chain (free acid/ amide). The enzyme to perform the digest on protein sequence can be selected from a list of enzymes given in tab 'Edit Enzyme' in tool bar. The interface window of the software provides options to define the cleavage rules for the enzyme selected. For example, if trypsin enzyme is selected for cleaving the protein sequence, it is defined as 'allow cut after lysine (K) or arginine (R)' and 'proline (P) is not allowed after the cut'. This defines cleavage rule for trypsin as {X [K, R]‖[X X]^[P]} where X can be any amino acid. Once enzyme cleavage rules are defined, *in-silico* protein digestion can be performed by setting the extended options of mass range limit, peptide mass tolerance, partials (≤20), positive or negative ion mode, mono-isotopic or average *m/z* values as required. For present study, trypsin enzyme was selected to generate theoretical tryptic digests and no mass limit was selected with 0-2 partials. This *in-silico* digestion identified the correct amino acid sequence and *m/z.* since +1 charge was selected so it generated a list of theoretical masses of mono-isotopic tryptic peptides (MH^+) of MMPs.

4.2.3 MALDI-MS of Trypsin Digests

4.2.3.1 Preparation of rhMMPs Peptides

For the characterization study rhMMPs were prepared as described. To each rhMMP solution (in buffer provided by R&D), 4µL of 8M urea were added, vortexed and centrifuged. To each rhMMP, 1µL of 50mM DTT was added as a reducing agent, vortexed and heated between 50-80^{o}C in water for 15-20minutes and centrifuged for 1minute. After bringing it to room temperature, 1µL of 100mM IAC was added for alkylation, vortexed spun and incubated for 15-20minutes at room temperature in dark. To dilute the urea concentration to 2M, at which concentration trypsin works very effectively, 13µL of distilled water, were added. This was followed by the addition of 0.5µL of trypsin solution (20µg/mL) and incubated at 28^{o}C for 18hours. The reaction was stopped by freezing at -20°C. The controls horse heart myoglobin + trypsin, myoglobin alone and trypsin alone were treated the same as samples to assure the efficiency of trypsin enzyme.

4.2.3.2 Removal of Detergents from Peptide Solution

The peptide solutions were desalted using C18 zip tips as described in Materials and Methods section 2.10.2.

4.2.3.3 Mass Spectrum Acquisition

Mass spectra of peptides were obtained after in-solution trypsin digestion using CHCA as matrix. A manual analysis was performed by keeping the Ultraflex^{TM} II MALDI-TOF/TOF instrument (Bruker Daltonics, Bremen, Germany) (see Chapter 2 for details) at positive reflectron mode using laser power from 50-80% firing 500 shots. For each sample and controls analyzed at least 5000 laser shots were added at a mass range of 700-4000. Data was acquired by FlexControl software. External calibration of instrument was done as explained in Materials and Methods section 2.12.3.2.

4.2.4 Manual MALDI-MS/MS of rhMMP Peptides

For manual MALDI-MS/MS 800 shots of laser were fired for parent ion and 1200 for the fragment ions. The compound list of the *m/z* of parent and daughter ions were sent to Biotools manually to generate protein hit confirming the signature peptides for corresponding MMP.

4.2.5 Interaction between rhMMP-14/rhMMP-2 and Olive H-7G

Solutions of Olive H-7G (1nM), rhMMP-2 (52nM) and rhMMP-14 (33.3nM) were prepared. Constituents were added as shown in Table 4.3 to give a protein-to-dye ratio of 1:10, including horse heart myoglobin and trypsin controls and incubated on a carousel at 4°C for 4 hour.

Table 4.3 Protein to dye ratios for reaction.

Sample	rhMMP-2	rhMMP-2 + Olive H-7G	rhMMP-14	rhMMP-14 + Olive H-7G	Myo + Olive H-7G	Try + Olive H-7G	Myo + Try + Olive H-7G	Myo + Try
Component	**µL**	**µL**	**µL**	**µL**	**µL**	**µL**	**µL**	**µL**
rhMMP-2 (52nM)	19.5	19.5	-	-	-	-	-	-
rhMMP-14 (33nM)	-	-	24	24	-	-	-	-
Olive H-7G (1nM)	-	1	-	1	1	1	1	-
Myo (1mM)	-	-	-	-	2	-	2	2
Try (205nM)	1	1	1	1	-	2	2	2
Ambic (100mM)	1	-	1	-	2	2	-	1
Total Volume	21.5	21.5	26	26	5	5	5	5

4.2.6 Interaction between rhMMP Mixture and Olive H-7G

A mixture of 11 rhMMPs was reacted with 100µM Olive H-7G solution (a border-line concentration detected by MALDI-MS). To observe changes in *m/z* at peptide level, the Olive H-7G-MMPs complex was lyophilized at 37°C using evaporator. It was then trypsinized as described in Materials and Methods section 2.9.1 using trypsin (20ng/µL). The determination of mass peak shifts of Olive H-7G was accomplished by MALDI-MS of tryptic digests both with and without C18 zip tipping. In case when no zip tipping performed, 1µL of sample was spotted on MALDI target plate and 2µL when zip tipped.

The instrument was calibrated using a standard mixture of proteins and mass spectrum was acquired in a mass range of 700-4000 as described in Materials and Methods section 2.12.3.2.

4.3 Results

4.3.1 Molecular Mass of Intact rhMMPs by MALDI-MS

Table 4.4 shows the accurate molecular masses of MMPs as determined by MALDI-MS in current study and predicted molecular masses calculated based on amino acid residue recombinant protein expressed in cloned cell lines. The MALDI data for intact MMPs were obtained and shown in Figure 4.2. These mass peaks were only detectable for MMP-3, MMP-7, MMP-10 and MMP-14. No intact masses were obtained for MMP-1, MMP-2, MMP-8, MMP-9 and MMP-13. No significant results could be found after an attempt to remove the detergent using C4 zip tips.

Table 4.4 MMP theoretical and molecular masses by MALDI-MS.

MMP	rhMMP Molecular Mass (Predicted) (kDa)	MMP Theoretical Mass (Predicted) (kDa)	rhMMP Molecular Mass (MALDI-MS) (kDa)
MMP-1	52	54.007	-
MMP-2	71	73.882	-
MMP-3	52	53.977	53.16
MMP-7	20 & 28	29.677	27.70
MMP-8	51	53.412	-
MMP-9	77	78.458	-
MMP-10	43 & 52	54.51	56.09
MMP-13	52	53.820	-
MMP-14	31	65.894	31.00

*Predicted information is from R & D.

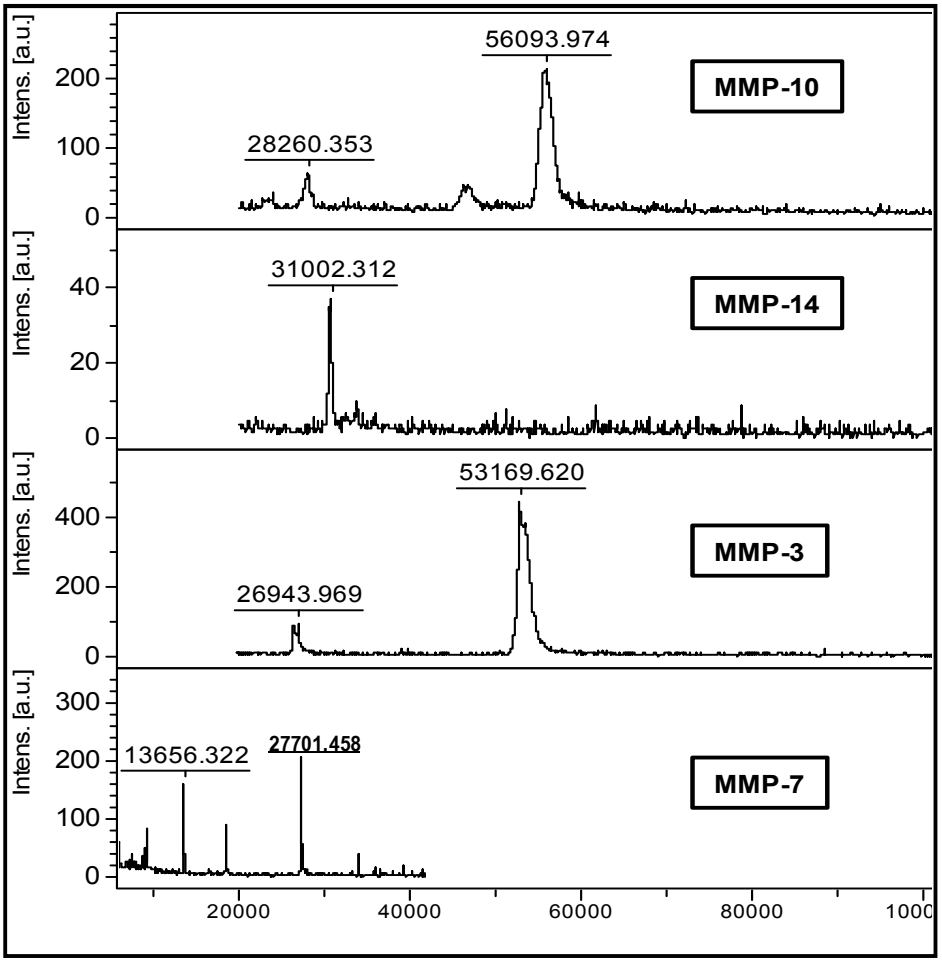

Figure 4.2 MALDI mass spectra for intact rhMMP-3, rhMMP-7, rhMMP-10 and rhMMP-14.

4.3.2 Mass Spectra for Controls in Trypsin Digestion

To assure the efficiency of trypsin, three controls (myoglobin + trypsin, myoglobin alone and trypsin alone) were run in parallel with digestion of rhMMPs for mass spectrometric analyses. Theoretical digest products of Horse heart myoglobin were generated using SequenceEditor 3.2 (Appendix 3) and masses of peaks specific to singly-charged ions were matched with those of found in analysis of digested protein samples (Figure 4.3). Horse heart myoglobin naturally removes N-terminus methionine hence first two peptides products with *m/z* 1815.90 (for peptide 2-17) and 34.03.49 (for peptide 2-32) were observed after deduction of 131Da from theoretically calculated values. There was no autolytic degradation of trypsin or

myoglobin. The mass peaks below 1000 (810.361 and 941.482) are fragments from matrix.

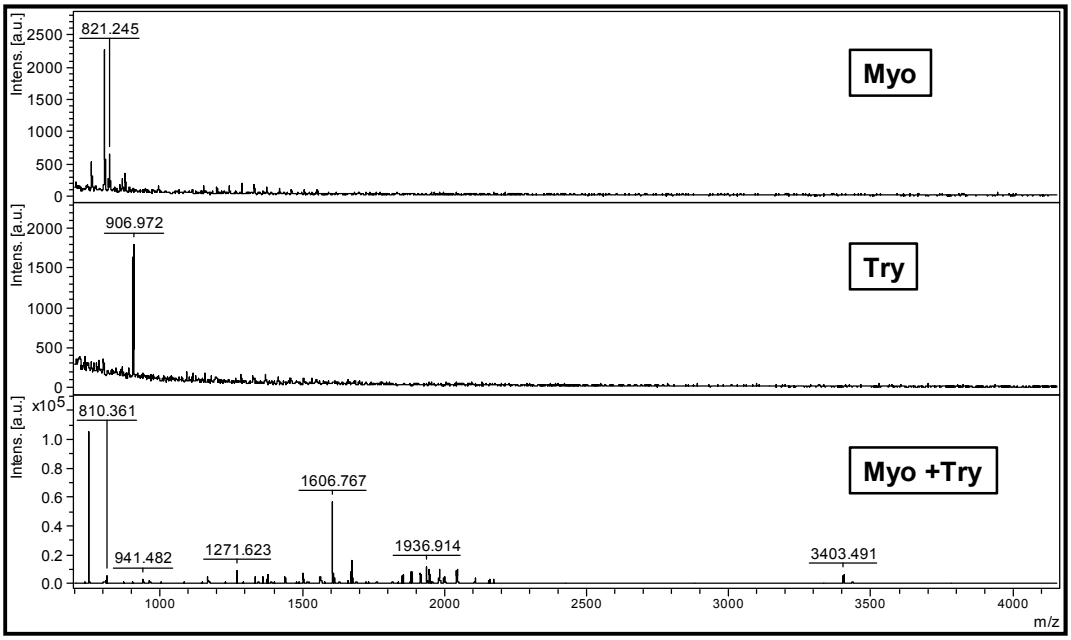

Figure 4.3 Mass spectra for Myo, Try and Myo + Try controls.

4.3.3 Peptide Mass Fingerprints (PMF) of rhMMPs

Signature peptides or PMF of MMPs were identified experimentally by manual MALDI-MS (Materials and Methods section 2.11). Several peaks were found in mass spectra of the peptides generated from rhMMP-1, rhMMP-2, rhMMP-3, rhMMP-7, rhMMP-8, rhMMP-9, rhMMP-10, rhMMP-13 and rhMMP-14 after trypsin digestion was performed. For rhMMP-12 and rhMMP-16, significant number of peaks could not be generated.

4.3.3.1 MMP-1

From the trypsin digestion of rhMMP-1, 34 signals were observed (Figure 4.4A) in the mass range of *m/z* 830.55-1900.22 (Appendix 5). The theoretical *m/z* of peptides from human MMP-1 generated by SequenceEditor 3.2 is labeled T1-T53 (Appendix 4) and matched experimental *m/z* (Figure 4.4B) highlighted red in Figure 4.4C. A number of signals corresponded to tryptic peptides were generated for the theoretical sequence. Of these peptide products, 2 were partials. The rhMMP-1 was constructed without the pre-

region (amino acids 1-19) in Murine myeloma cell line so the expressed enzyme was from Phe20-Asn469. Two peptides were detected within 'pro' region (20-99), one a partial (T2/3, *m/z* 1232.41) when trypsin skips one cleavage site (lysine in this case) and one complete (T10, *m/z* of 1127.51) (Figure 4.4C) which suggests that MMP-1 in use was not 'active' or degraded form of the enzyme before it was subjected to trypsin digestion. Other signals were detected within hemopexin-like 3 region (377-424) towards C-terminus of the active sequence but no signal was observed from the mid-section with active site residue E219 (Figure 4.4C).

4.3.3.2 MMP-2

From the trypsin digestion of rhMMP-2, 34 signals were observed (Figure 4.5A) in the mass range of *m/z* 843.38-3309.91 (Appendix 5). The theoretical *m/z* of peptides from human MMP-2 generated by SequenceEditor 3.2 is labeled T1-T68 (Appendix 4) and matched experimental *m/z* (Figure 4.5B) highlighted red in Figure 4.5C. A number of signals corresponded to tryptic peptides were generated for the theoretical sequence with a mass tolerance upto 0.33daltons. Of these peptide products, 4 were partials (T46/47, T15/16, T57/58 and T32/33) and two were with carbamidomethylation of cysteine in the sequence (T13 and T31). As there are many lysine and arginine residues in the 'pre-pro' region (1-109), many possible products of trypsin digestion could be produced (Figure 4.5C). However, this would result in many peptides with *m/z* less than 700 hence difficult to be detected by MALDI-MS. These low molecular weight molecules can also be from the matrix in use or autolytic digestion of trypsin. Two peptides were detected in 'pre-pro' region suggesting the enzyme was not active or degraded form (Figure 4.5C). Other signals corresponded to the fibronectin type-II 2 (286-334), hemopexin-like 1 (475-518), hemopexin-like 2 (520-563) and hemopexin-like 3 (568-615) of the active sequence were observed. But no signal was observed from collagenase-like 2 region with active site reside E404 (Green and enboxed in Figure 4.5C). Some tryptic peptides labeled TX could be from unexpected partials or modifications or non-trypsin cleavage products.

4.3.3.3 MMP-3

From the trypsin digestion of rhMMP-3, 65 signals were observed (Figure 4.6A) in the mass range of *m/z* 707.20-2184.74 (Appendix 5). The theoretical *m/z* of peptides from human MMP-3 generated by SequenceEditor 3.2 is labeled T1-T56 (Appendix 4) and matched experimental *m/z* (Figure 4.6B) highlighted red in Figure 4.6C. The accuracy of the peptide products was upto 0.34daltons. Of these peptide products, 8 were with 1 partial and one (T4-6) was with 2 partial. As there are many lysine and arginine residues in the 'pro' region (18-99), 15 possible products of trypsin digestion could be produced (Figure 4.6C). Two peptides were detected within 'pro' region, one a partial (T14/15, *m/z* 2122.84) when trypsin skips one cleavage site (lysine in this case) and one complete (T15, *m/z* of 1178.43) when trypsin does not skip its cleavage site (Figure 4.6C) which suggests that MMP-3 in use was not 'active' or degraded form of the enzyme before it was subjected to trypsin digestion. Other signals corresponded to the N-terminus and C-terminus of the active sequence but no signal was observed from the mid section with active site reside E219 (Figure 4.6C).

4.3.3.4 MMP-7

From the trypsin digestion of rhMMP-7, 42 signals were observed (Figure 4.7A) in the mass range of *m/z* 1065.46-2848.73 (Appendix 5). The theoretical *m/z* of peptides from human MMP-7 generated by SequenceEditor 3.2 is labeled T1-T27 (Appendix 4) and matched experimental *m/z* (Figure 4.7B) highlighted red in Figure 4.7C. A number of signals corresponded to tryptic peptides were generated for the theoretical sequence with a mass tolerance upto 0.37daltons. Of these peptide products, 2 were partials (T3/4 and T10/11). Many peptides were detected within 'pro' region (18-94), with T10/11 starting within the cysteine switch (underlined in Figure 4.7C) which suggests that MMP-7 in use was not 'active' or degraded form of the enzyme before it was subjected to trypsin digestion. None of the signals including active site residue E215 (Figure 4.7C) or corresponded to the C-terminus of the active sequence were observed.

4.3.3.5 MMP-8

From the trypsin digestion of rhMMP-8, 100 signals were observed (Figure 4.8A) in the mass range of *m/z* 714.28-3320.20 (Appendix 5). The theoretical *m/z* of peptides from human MMP-8 generated by SequenceEditor 3.2 is labeled T1-T44 (Appendix 4) and matched experimental *m/z* (Figure 4.8B) highlighted red in Figure 4.8C. A number of signals corresponded to tryptic peptides were generated for the theoretical sequence with a mass tolerance upto 0.45daltons. Of these peptide products, 8 were with one partial and one tryptic peptide T41-43 was with 2 partials skipping arginine and lysine along the sequence. None of the peptide was detected in 'pre' (1-20) or 'pro' region (21-100) suggesting the enzyme was active or degraded form (Figure 4.8, C). Other signals corresponded to the hemopexin-like 1 (285-327), hemopexin-like 3 (377-422) and hemopexin-like 4 (424-464) of the active sequence were observed. But no signal was observed from mid-section with active site reside E218 (Figure 4.8C).

4.3.3.6 MMP-9

From the trypsin digestion of rhMMP-9, 97 signals were observed (Figure 4.9A) in the mass range of *m/z* 714.26-3674.97 (Appendix 5). The theoretical *m/z* of peptides from human MMP-9 generated by SequenceEditor 3.2 is labeled T1-T67 (Appendix 4) and matched experimental *m/z* (Figure 4.9B) highlighted red in Figure 4.10C. The accuracy of matched peptides was found to be upto 3.11daltons. Of these peptide products, 11 were with one partial and 5 were with 2 partials. Two peptide products T22 and T31/32 were found to be with carbamidomethylation of cysteine based on the difference of 57.0340daltons between the detected peak *m/z* and that of the theoretical. The detection of peptides T3, T5, T6/7 and T10 within 'pro' region (20-93) suggested that enzyme in use was intact before the trypsin digestion (Figure 4.9B and Figure 4.10C). Other signals corresponded to the fibronectin type-II 1 (225-273), fibronectin type-II 2 (283-331) and fibronectin type-II 3 (342-390) were detected. Many tryptic peptides from the C-terminus of the protein were detected within the hemopexin-like 1 (521-565), hemopexin-like 2 (567-608), hemopexin-like 3 (613-659) and hemopexin-like 4 (661-704) of the active

sequence were observed. But no signal was observed from mid-section with active site reside E402 (Figure 4.10C).

4.3.3.7 MMP-10

From the trypsin digestion of rhMMP-10, 86 signals were observed (Figure 4.11A) in the mass range of *m/z* 733.15-3759.14 (Appendix 5). The theoretical *m/z* of peptides from human MMP-10 generated by SequenceEditor 3.2 is labelled T1-T49 (Appendix 4) and matched experimental *m/z* (Figure 4.11B) highlighted red in Figure 4.12C. A number of signals corresponded to tryptic peptides were generated for the theoretical sequence with a mass tolerance upto 1.29daltons. Of these peptide products, 10 were with one partial and 7 were with 2 partials. Since the rhMMP-10 in use was from Tyr18-Cys476 derived from Murine myeloma cell line so no peptide from 'pre' region (1-17) was detected. The detection of peptides T6-8, T12/3 and T14/15 within 'pro' region (18-98) suggested that enzyme in use was intact before the trypsin digestion (Figure 4.11B and Figure 4.12C). Many tryptic peptides from the C-terminus of the protein were detected within the hemopexin-like 1 (295-337), hemopexin-like 2 (339-382), hemopexin-like 3 (387-434) and hemopexin-like 4 (436-476) of the active sequence were observed. But no signal was observed with active site reside E218 (Figure 4.12C).

4.3.3.8 MMP-13

From the trypsin digestion of rhMMP-13, 100 signals were observed (Figure 4.13A) in the mass range of *m/z* 717.20-3131.86 (Appendix 5). Many of these signals were probably from the detergent which could not be removed by C18 desalting. The theoretical *m/z* of peptides from human MMP-13 generated by SequenceEditor 3.2 is labeled T1-T48 (Appendix 4) and matched experimental *m/z* (Figure 4.13B) highlighted red in Figure 4.13C. A number of signals corresponded to tryptic peptides were generated for the theoretical sequence with a mass tolerance upto 1.42daltons. Of these peptide products, 5 were with one partial and 2 were with 2 partials. Since the rhMMP-13 in use was from Leu20-Cys471 derived from Murine myeloma

cell line so no peptide from 'pre' region (1-19) was detected. The detection of peptides within 'pro' region (20-103) suggested that enzyme in use was intact before the trypsin digestion (Figure 4.13B and C). Many tryptic peptides from the C-terminus of the protein were detected within the hemopexin-like 1 (290-332), hemopexin-like 2 (334-377), hemopexin-like 3 (382-429) and hemopexin-like 4 (431-471) of the active sequence were observed. But no signal was observed from mid section with active site reside E223 (Green and enboxed in Figure 4.13C).

4.3.3.9 MMP-14

From the trypsin digestion of rhMMP-14, 48 signals were observed Figure 4.14A) in the mass range of *m/z* 715.32-2996.93 (Appendix 5). The theoretical *m/z* of peptides from human MMP-14 generated by SequenceEditor 3.2 is labeled T1-T65 (Appendix 4) and matched experimental *m/z* (Figure 4.14B) highlighted red in Figure 4.14C. A number of signals corresponded to tryptic peptides were generated for the theoretical sequence with a mass tolerance upto 0.76daltons. Of these peptide products, 7 were with one partial and 3 were with 2 partials. Only one peptide, T4, was detected within 'pro' region (21-111) suggested that enzyme in use was intact before the trypsin digestion (Figure 4.14B and C). Many tryptic peptides from the C-terminus of the protein were detected within the hemopexin-like 1 (323-366), hemopexin-like 2 (368-412), hemopexin-like 3 (415-461), hemopexin-like 4 (463-508) and cytoplasmic domain (563-582) of the active sequence were observed. But no signal was observed including active site reside E240 (Figure 4.14C).

4.3.4 MS/MS Ion Search for Peptide Fragment of rhMMPs

MS/MS analysis of parent molecule rhMMP-3 with *m/z* 1143.42 (T17 in Figure 4.6A) generated fragments and submitted to mascot search engine (human, no modifications, 1 partial) giving a mascot score of 44 (threshold significance 30 at <0.05). 72 fragments corresponded to x,y,z ions of the peptide CGVPDVGHFR within a mass accuracy of 0.7dalton (Figure 4.15). When the *m/z* of all the fragments, parent and daughter ions (PFF) were sent

to Biotools, MMP-3 (human) identification was generated. The fragment ions and parent peptides (pointed with red arrows) for rhMMP-2, rhMM-7, rhMMP-8, rhMMP-9, rhMMP-13 and rhMMP-14 are shown in Figure 4.15. The parent ions from each MMP were fragmented and data was sent to Biotools. The identification of corresponding MMP with a Mascot score greater than the threshold level (>30) proved the presence of the peptide molecule.

(A)

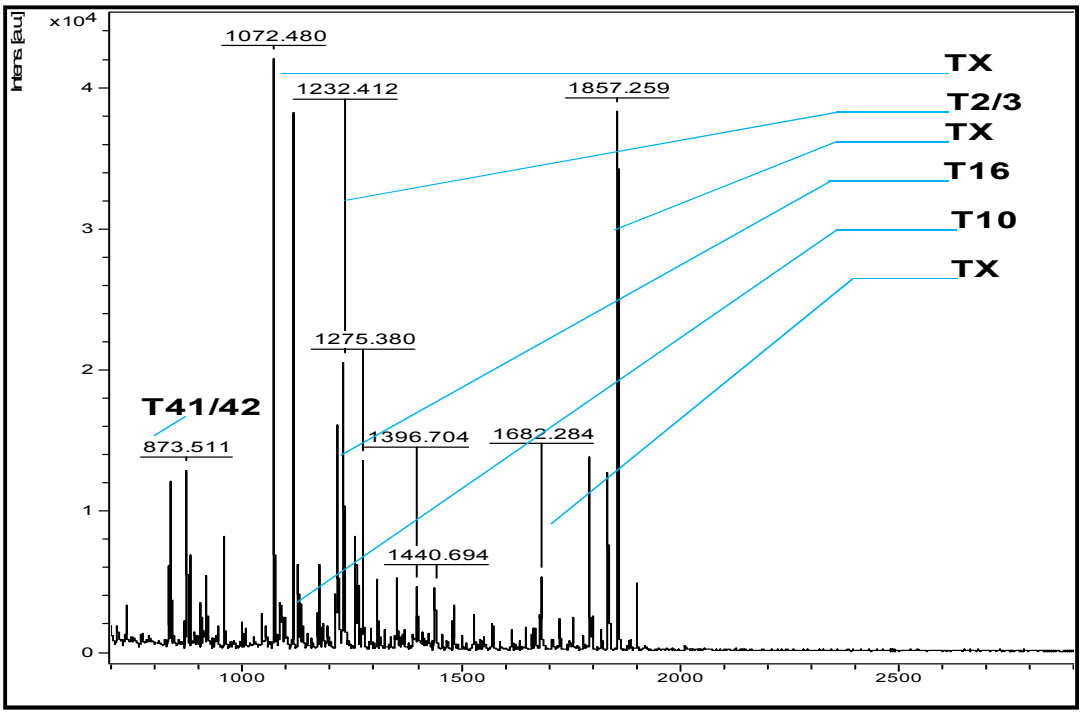

(B)

Tryptic Digests	Range	Theoretical Mono MH+	Experimental *m/z*	Accuracy (Daltons)	Partials	Sequence	Modifications
T23	[209-214]	831.41	830.55	0.86	0	EYNLHR	None
T22	[203-208]	837.40	836.53	0.87	0	WTNNFR	None
T41/42	[400-405]	873.41	873.51	-0.10	1	YDEYKR	None
T10	[66- 74]	1127.56	1127.51	0.04	0	QMQE...FGLK	None
T16	[118-127]	1217.62	1216.46	1.15	0	IENYT...DLPR	None
T40/41	[397-404]	1222.55	1220.70	1.86	1	YWRYDEYK	None
T2/3	[37- 45]	1233.65	1232.41	1.24	1	YLEKYYNLK	None

(C)

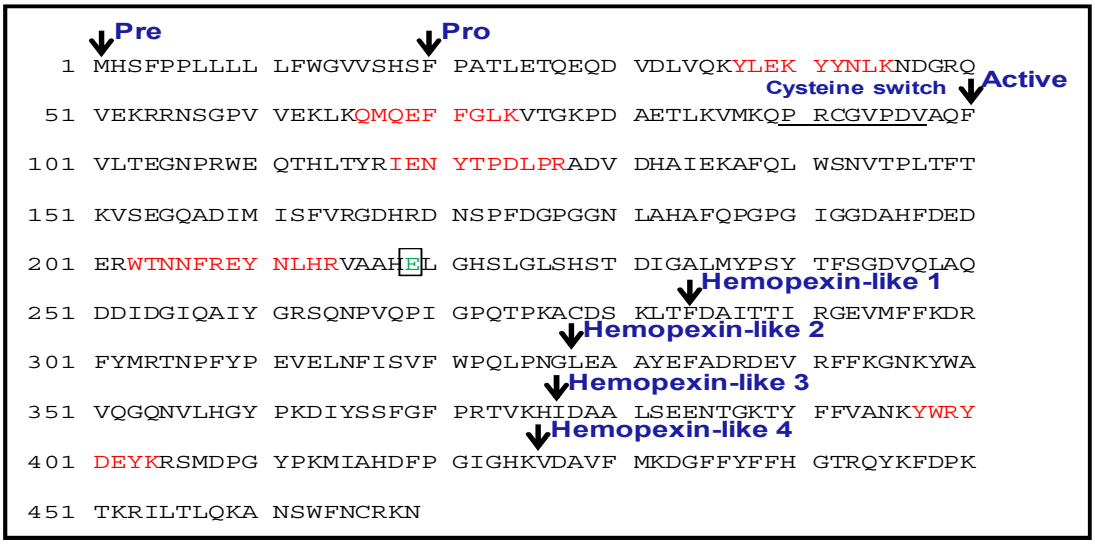

Figure 4.4 A. MS PMF of rhMMP-1 annotated tryptic peptides, B. Mass data for peptides in daltons, C. Sequence coverage, ID peptides in red, active site green and arrow heads pointing start of various regions.

(A)

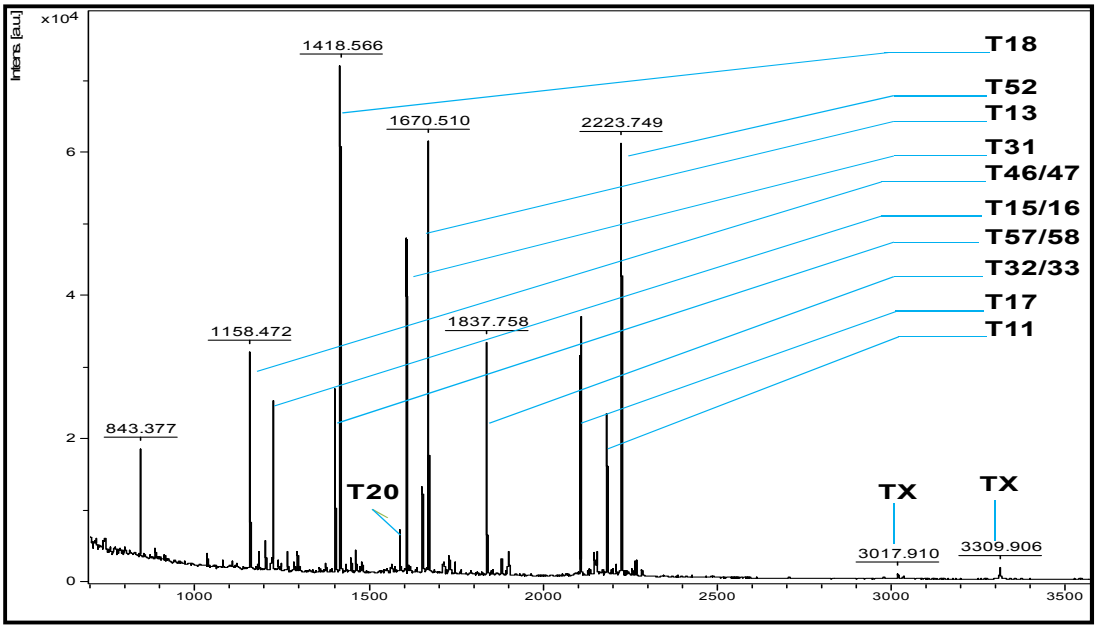

(B)

Tryptic Digests	Range	Theoretical Mono MH+	Experimental *m/z*	Accuracy (Daltons)	Partials	Sequence	Modifications
T46/47	[483-491]	1158.59	1158.47	0.12	1	GEIFFFKDR	None
T15/16	[119-127]	1223.62	1223.48	0.13	1	WDKQ...ITYR	None
T57/58	[580-590]	1403.71	1403.53	0.18	1	TYIF...KFWR	None
T18	[147-158]	1418.74	1418.57	0.18	0	AFQV...TPLR	None
T20	[162-175]	1587.76	1587.54	0.21	0	IHDG...NFGR	None
T31	[297-310]	1608.67	1608.45	0.22	0	FQGT...TEGR	Carbamidomethylation (C)
T13	[102-115]	1670.75	1670.51	0.24	0	CGNP...FFPR	Carbamidomethylation (C)
T32/33	[311-325]	1837.75	1837.76	-0.01	1	TDGY...DYDR	None
T17	[128-146]	2108.02	2107.71	0.31	0	IIGY...AFAR	None
T11	[80- 98]	2183.04	2182.72	0.33	0	FFGL...ETMR	None
T52	[532-550]	2224.07	2223.75	0.32	0	AVFF...TLER	None

(C)

Figure 4.5 A. MS PMF of rhMMP-2 annotated tryptic peptides, B. Mass data for peptides in daltons, C. Sequence coverage, ID peptides in red, active site green and arrow heads pointing start of various regions.

(A)

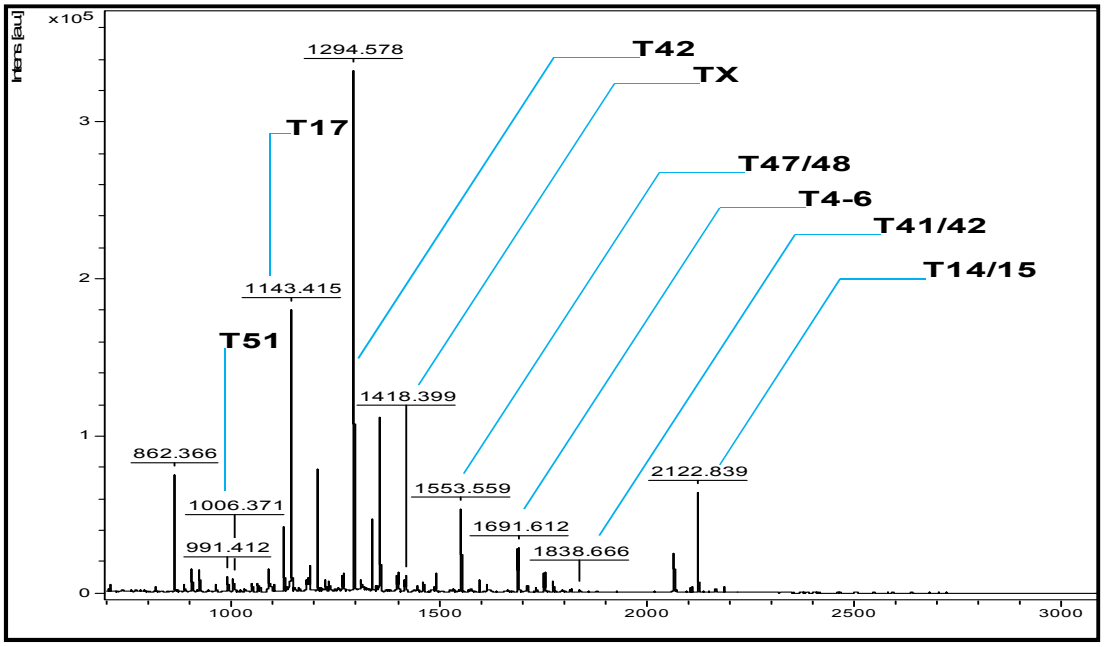

(B)

Tryptic Digests	Range	Theoretical Mono MH+	Experimental *m/z*	Accuracy (Daltons)	Partials	Sequence	Modifications
T43/44	[387-395]	960.54	961.40	-0.87	1	KIDAAISDK	None
T39	[357-364]	991.51	991.41	0.10	0	GNQFWAIR	None
T51	[416-424]	1006.47	1006.37	0.10	0	NSMEPGFPK	None
T47	[400-407]	1048.50	1049.40	-0.90	0	TYFFVEDK	None
T31/32	[304-312]	1090.63	1090.51	0.11	1	GEILIFKDR	None
T18/19	[102-110]	1101.62	1101.50	0.13	1	TFPG...PKWR	None
T15	[79- 88]	1178.57	1178.34	0.23	0	LDSD...EVMR	None
T17	[92-101]	1143.55	1143.42	0.13	0	CGVP...GHFR	Carbamidomethylation (C)
T42	[375-386]	1294.73	1294.58	0.15	0	GIHT...PTVR	None
T25	[140-151]	1463.75	1463.59	0.17	0	VWEE...TFSR	None
T47/48	[400-410]	1553.74	1553.56	0.18	1	TYFF...KYWR	None
T4-6	[37- 49]	1690.87	1691.61	-0.74	2	YLEN...KDVK	None
T26	[152-166]	1713.85	1713.64	0.21	0	LYEG...FAVR	None
T24/25	[137-151]	1775.97	1775.75	0.22	1	ALKV...TFSR	None
T41/42	[370-386]	1839.00	1838.67	0.34	1	AGYP...PTVR	None
T22/23	[118-136]	2074.07	2073.81	0.27	1	IVNY...AVEK	None
T14/15	[70- 88]	2123.11	2122.84	0.27	1	FLGL...EVMR	None

(C)

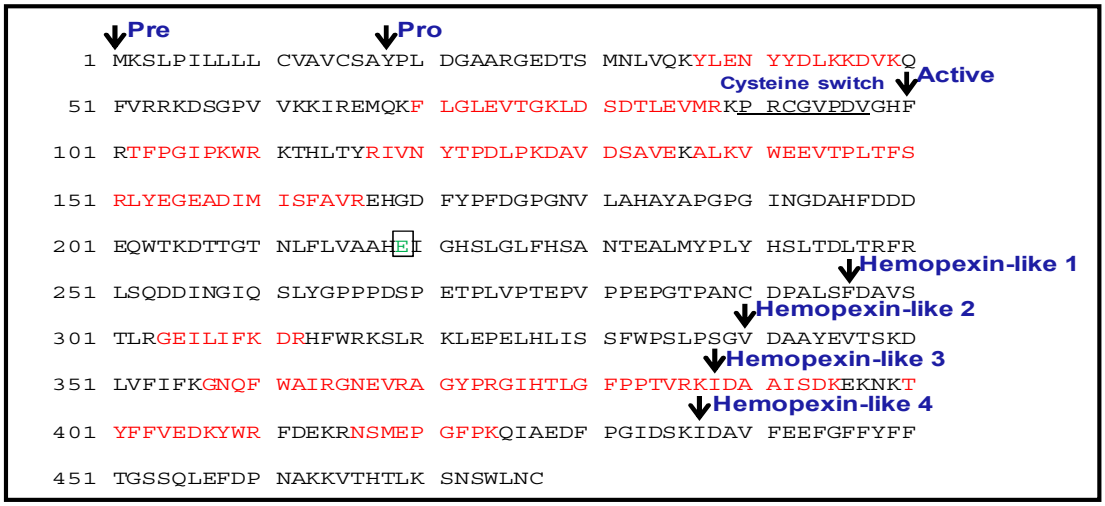

Figure 4.6 A. MS PMF of rhMMP-3 annotated tryptic peptides, B. Mass data for peptides in daltons, C. Sequence coverage, ID peptides in red, active site green and arrow heads pointing start of various regions.

(A)

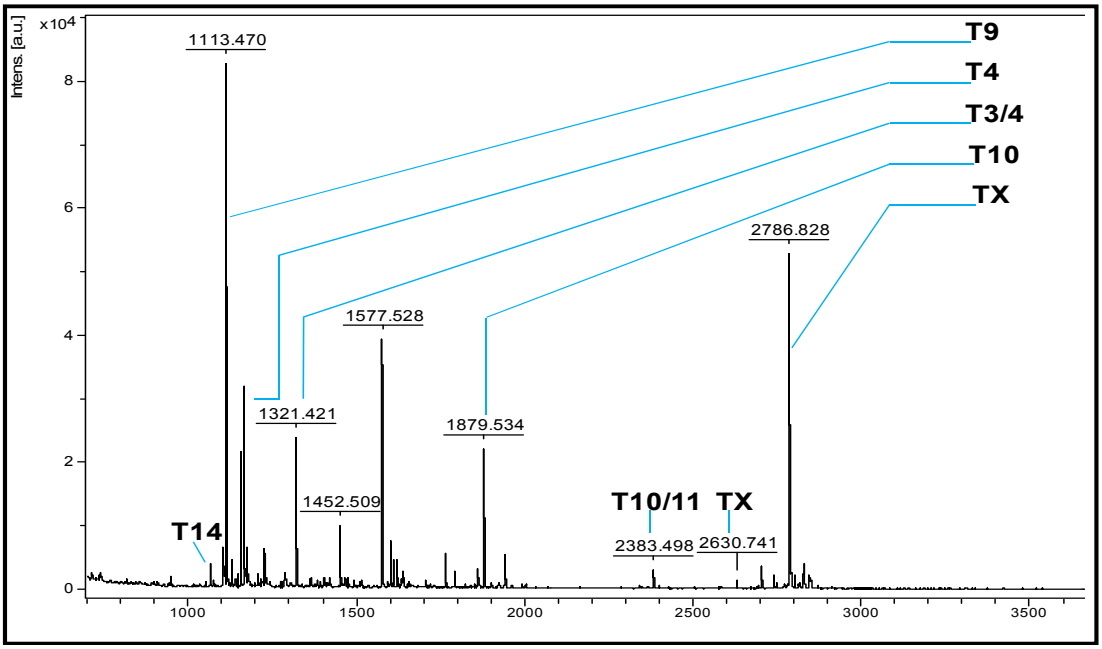

(B)

Tryptic Digests	Range	Theoretical Mono MH+	Experimental *m/z*	Accuracy (Daltons)	Partials	Sequence	Modifications
T14	[119-127]	1065.57	1065.46	0.11	0	DLPHITVDR	None
T9	[78- 86]	1113.65	1113.47	0.17	0	VIEIMQKPR	None
T4	[42- 50]	1165.54	1165.36	0.19	0	FYLYDSETK	None
T3/4	[41- 50]	1321.64	1321.42	0.22	1	RFYLYDSETK	None
T8	[65- 77]	1452.77	1452.51	0.26	0	FFGL...LNSR	None
T10	[87-103]	1879.90	1879.53	0.37	0	CGVP...NSPK	None
T10/11	[87-107]	2382.16	2383.50	-1.34	1	CGVP...WTSK	Carbamidomethylation (C)

(C)

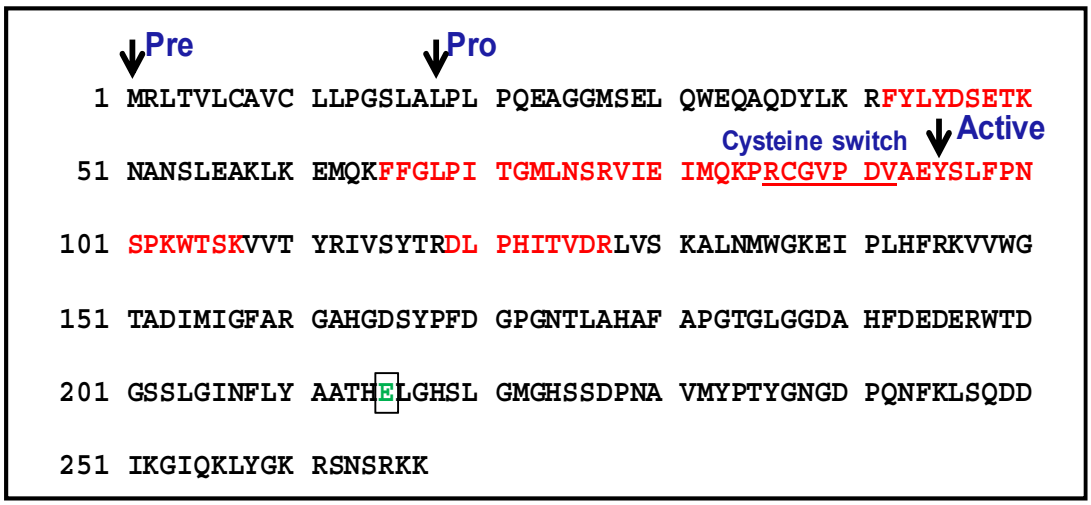

Figure 4.7 A. MS PMF of rhMMP-7 annotated tryptic peptides, B. Mass data for peptides in daltons, C. Sequence coverage, ID peptides in red, active site green and arrow heads pointing start of various regions.

(A)

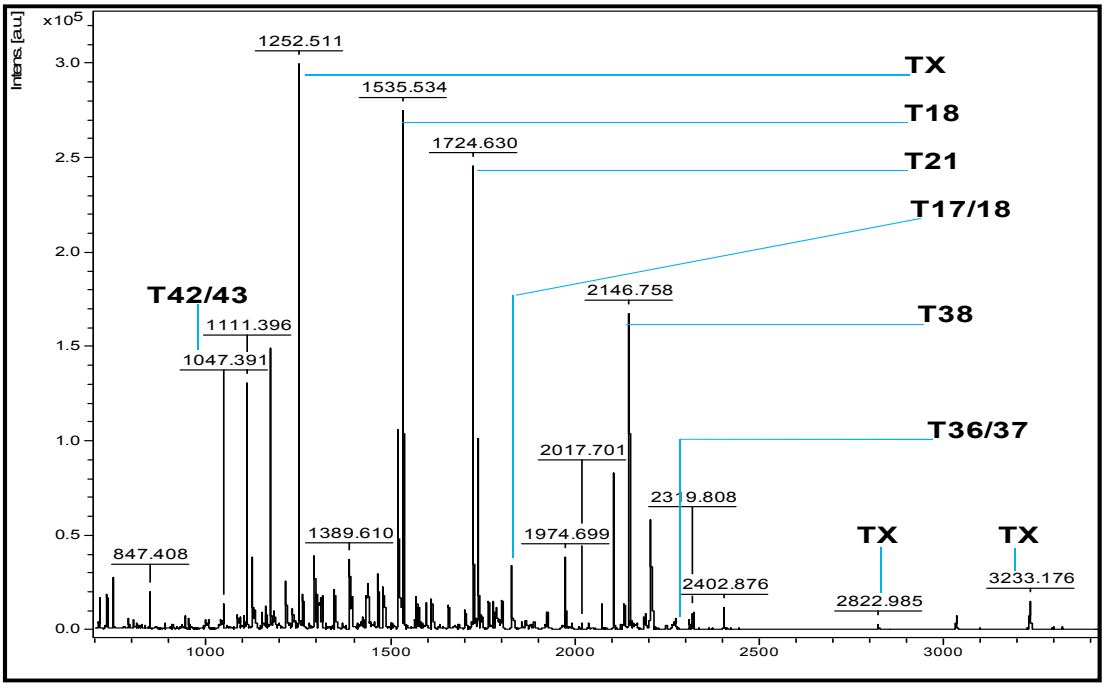

(B)

Tryptic Digests	Range	Theoretical Mono MH+	Experimental *m/z*	Accuracy (Daltons)	Partials	Sequence	Modifications
T25/26	[300-305]	942.46	942.36	0.10	1	DRYFWR	None
T42/T43	[458-465]	1047.53	1047.39	0.14	1	GNKWLNCR	None
T36	[403-411]	1096.51	1096.38	0.13	0	QFMEPGYPK	None
T24/25	[293-301]	1124.61	1124.47	0.14	1	GEILFFKDR	None
T15/16	[108-116]	1238.63	1238.38	0.25	1	WERT...LTYR	None
T41-43	[455-465]	1316.70	1316.42	0.28	2	VARG...LNCR	None
T34	[387-397]	1522.71	1522.69	0.03	0	TYFF...QFWR	None
T18	[119-131]	1535.73	1535.53	0.20	0	NYT...EVER	None
T21	[151-165]	1724.86	1724.63	0.23	0	ISQG...FYQR	None
T33/34	[385-397]	1737.84	1737.61	0.23	1	SKTY...QFWR	None
T17/18	[117-131]	1804.92	1804.68	0.24	1	IRNY...EVER	None
T38	[424-441]	2147.05	2146.76	0.29	0	VDAV...SGPR	None
T36/37	[403-423]	2270.116	2270.591	-0.47	1	QFME...IESK	None
T37/38	[412-441]	3320.65	3320.20	0.45	1	SISG...SGPR	None

(C)

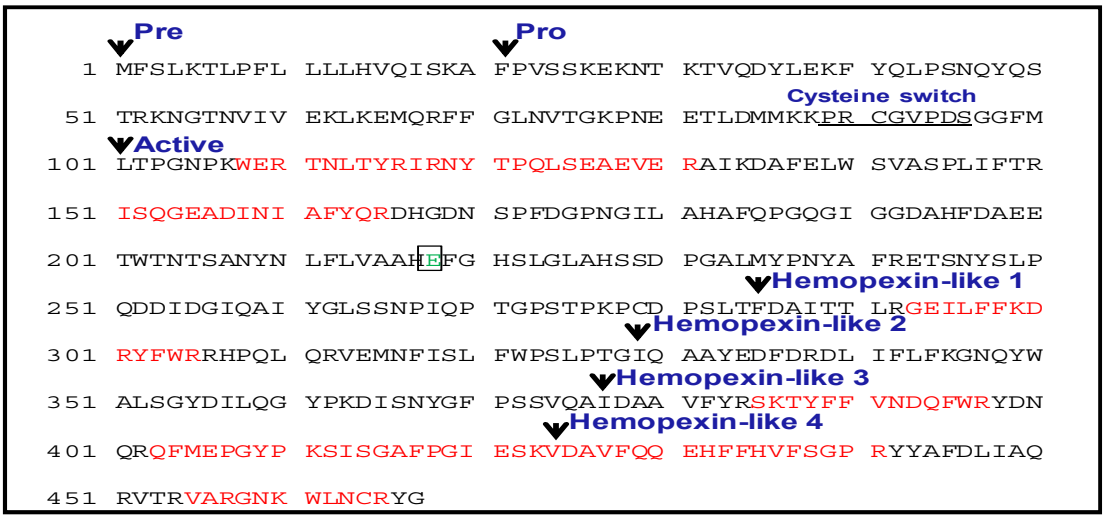

Figure 4.8 A. MS PMF of rhMMP-8 annotated tryptic peptides, B. Mass data for peptides in daltons, C. Sequence coverage, ID peptides in red, active site green and arrow heads pointing start of various regions.

(A)

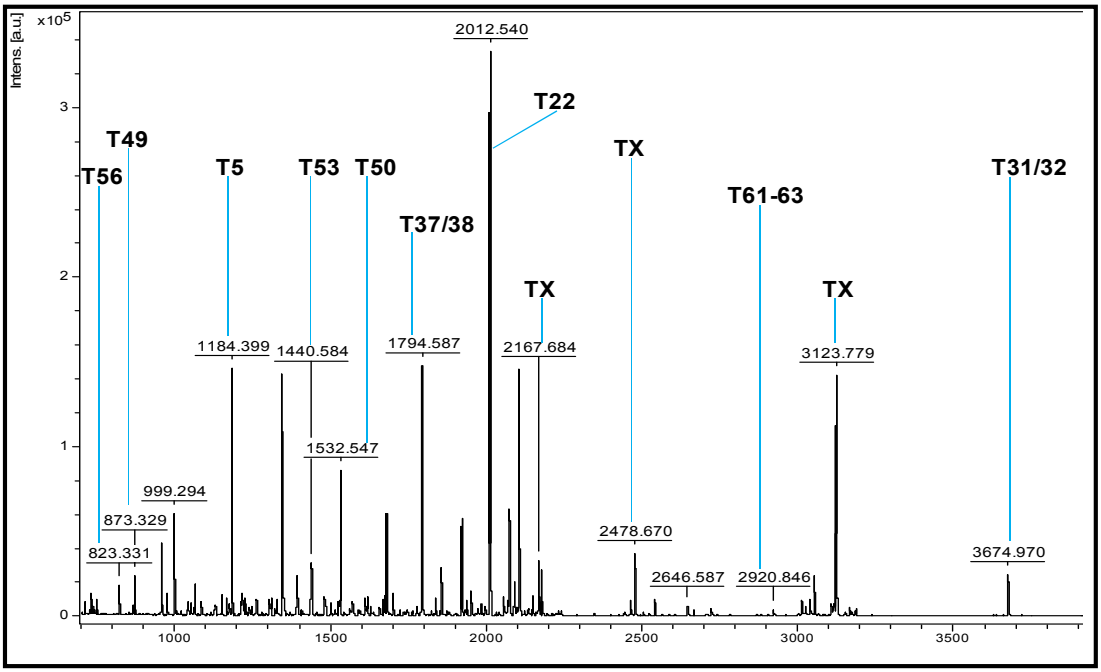

(B)

Tryptic Digests	Range	Theoretical Mono MH+	Experimental *m/z*	Accuracy (Daltons)	Partials	Sequence	Modifications
T56	[624-630]	823.45	823.33	0.12	0	MLLFSGR	None
T40/41	[536-541]	824.41	824.29	0.11	1	DGKYWR	None
T44/45	[560-566]	867.52	867.30	0.22	1	WPALPRK	None
T49	[579-585]	873.46	873.33	0.13	0	LFFFSGR	None
T16	[135-143]	977.51	977.36	0.14	0	AVIDDAFAR	None
T48/49	[578-585]	1001.56	1001.41	0.15	1	KLFFFSGR	None
T23	[240-249]	1060.44	1061.19	-0.75	0	SYSA...TDGR	None
T14	[107-115]	1084.53	1085.41	-0.88	0	FQTFEGDLK	None
T32	[357-366]	1132.46	1133.54	-1.09	0	EYST...SEGR	None
T5	[43- 51]	1184.60	1184.40	0.20	0	QLAEEYLYR	None
T6/T7	[52- 61]	1245.60	1246.30	-0.70	1	YGYT...AEMR	None
T59/60	[635-645]	1305.66	1305.53	0.13	1	FDVK...VDPR	None
T54-56	[619-630]	1308.72	1309.61	-0.89	2	SGRG...FSGR	None
T46/47	[567-577]	1322.70	1322.43	0.26	1	LDSV...RLSK	None
T47-49	[575-585]	1329.77	1328.49	1.28	2	LSKK...FSGR	None
T3	[25- 36]	1345.75	1345.51	0.23	0	QSTL...GDLR	None
T53	[604-618]	1440.82	1440.58	0.23	0	LGLG...GALR	None
T50	[586-599]	1532.82	1532.55	0.27	0	QVWV...LGPR	None
T17	[144-158]	1680.91	1680.61	0.30	0	AFAL...TFTR	None
T10	[77- 92]	1701.89	1701.60	0.29	0	QLSL...ATLK	None
T37/38	[425-440]	1794.91	1794.59	0.33	1	FTEG...NGIR	None
T52/53	[601-618]	1797.02	1798.62	-1.60	1	LDKL...GALR	None
T62	[653-668]	1921.93	1921.57	0.35	0	MFPG...FQYR	None
T51-53	[600-618]	1953.12	1952.77	0.36	2	RLDK...GALR	None
T22	[222-239]	2012.92	2012.54	0.38	0	FGNA...FEGR	Carbamidomethylation (C)
T64-66	[671-685]	1983.93	1983.47	0.46	2	AYFC...VSSR	None
T43/44	[547-565]	2106.16	2105.78	0.38	1	GSRP...ALPR	None
T41-43	[539-559]	2467.26	2464.16	3.11	2	YWRF...IADK	None
T49-51	[579-600]	2543.37	2540.58	2.79	2	LFFF...GPRR	None
T61/62	[646-668]	2666.27	2665.76	0.51	1	SASE...FQYR	None
T61-63	[646-670]	2923.40	2920.81	2.59	2	SASE...YREK	None
T20	[185-214]	3175.51	3174.93	0.58	0	DGLL...SLGK	None
T31/32	[333-366]	3675.67	3674.97	0.70	1	ADST...SEGR	Carbamidomethylation (C)

Figure 4.9 A. MS PMF of rhMMP-9 annotated tryptic peptides, B. Mass data of peptides.

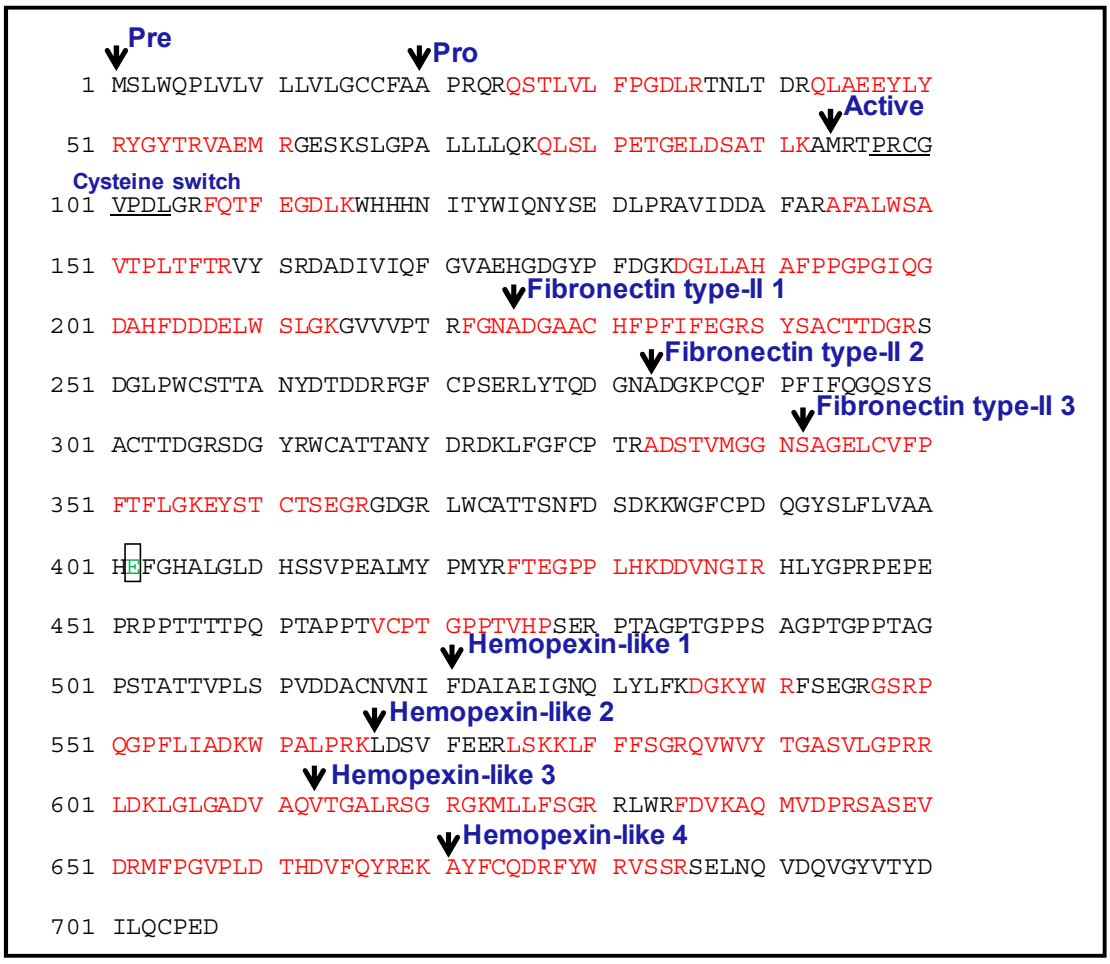

Figure 4.10 MMP-9 Sequence coverage, ID peptides in red, active site green and arrow heads pointing start of various regions.

(A)

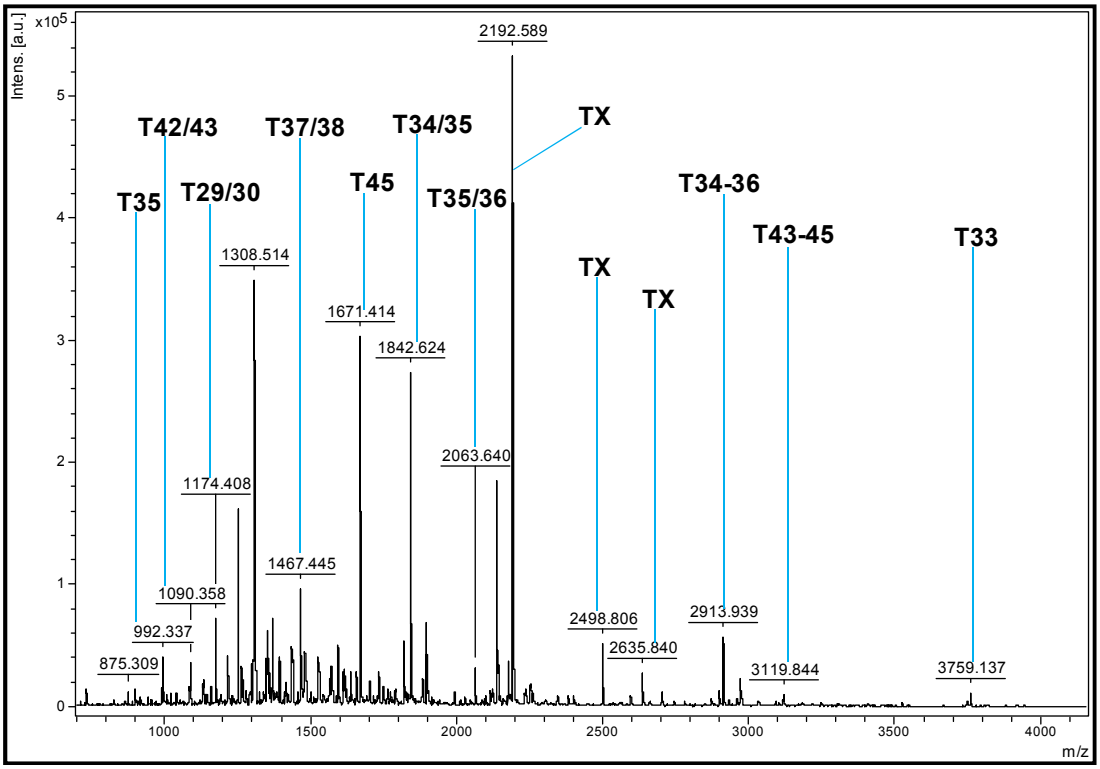

(B)

Tryptic Digests	Range	Theoretical Mono MH+	Experimental *m/z*	Accuracy (Daltons)	Partials	Sequence	Modifications
T6-8	[50- 54]	734.44	733.15	1.29	2	QFRRK	None
T30/31	[310-315]	942.46	942.32	0.14	1	DRYFWR	None
T35	[356-363]	992.50	992.34	0.16	0	GNEFWAIR	None
T42/T43	[398-406]	1090.56	1090.36	0.20	1	KTYFFAADK	None
T29/30	[303-311]	1174.59	1174.41	0.18	1	GEYLFFKDR	None
T41-43	[397-406]	1218.65	1217.45	1.20	2	KKTYFFAADK	None
T16-18	[108-116]	1260.70	1261.49	-0.79	2	WRKTHLTYR	None
T37	[374-385]	1308.74	1308.51	0.23	0	GIHT...PTIR	None
T37/38	[374-386]	1436.84	1437.55	-0.72	1	GIHT...TIRK	None
T43/44	[399-409]	1467.71	1467.45	0.26	1	TYFF...KYWR	None
T42/T44	[398-409]	1595.80	1595.51	0.30	2	KTYF...KYWR	None
T45	[410-423]	1671.71	1671.41	0.29	0	FDEN...GFPR	None
T34/35	[349-363]	1842.95	1842.62	0.33	1	DTVF...WAIR	None
T35/36	[356-373]	2064.01	2063.64	0.37	1	GNEF...GYPR	None
T12/13	[69- 87]	2137.12	2136.74	0.38	1	FLGL...EVMR	None
T14/15	[88-107]	2143.06	2142.68	0.38	1	KPRC...GMPK	None
T44/45	[407-423]	2176.95	2176.56	0.39	1	YWRF...GFPR	None
T20-22	[127-150]	2704.42	2704.70	-0.28	2	DAVD...TFSR	None
T34-36	[349-373]	2914.46	2913.94	0.52	2	DTVF...GYPR	None
T47	[436-462]	3093.44	3092.88	0.56	0	VDAV...PNAR	None
T43-45	[399-423]	3120.39	3119.84	0.55	2	TYFF...GFPR	None
T33	[317-348]	3759.79	3759.14	0.65	0	SHWN...VNSR	None

Figure 4.11 A. MS PMF of rhMMP-10 annotated tryptic peptides, B. Mass data for peptides in Daltons.

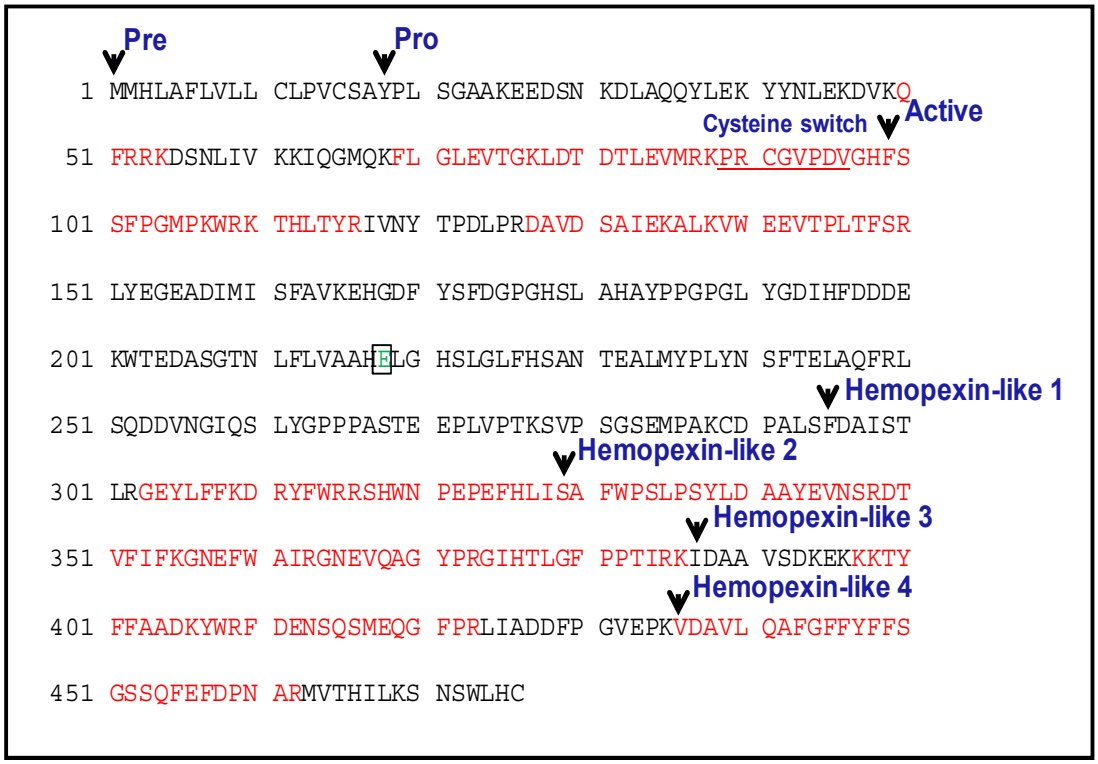

Figure 4.12 Sequence coverage for MMP-10, ID peptides in red, active site green and arrow heads pointing start of various regions.

(A)

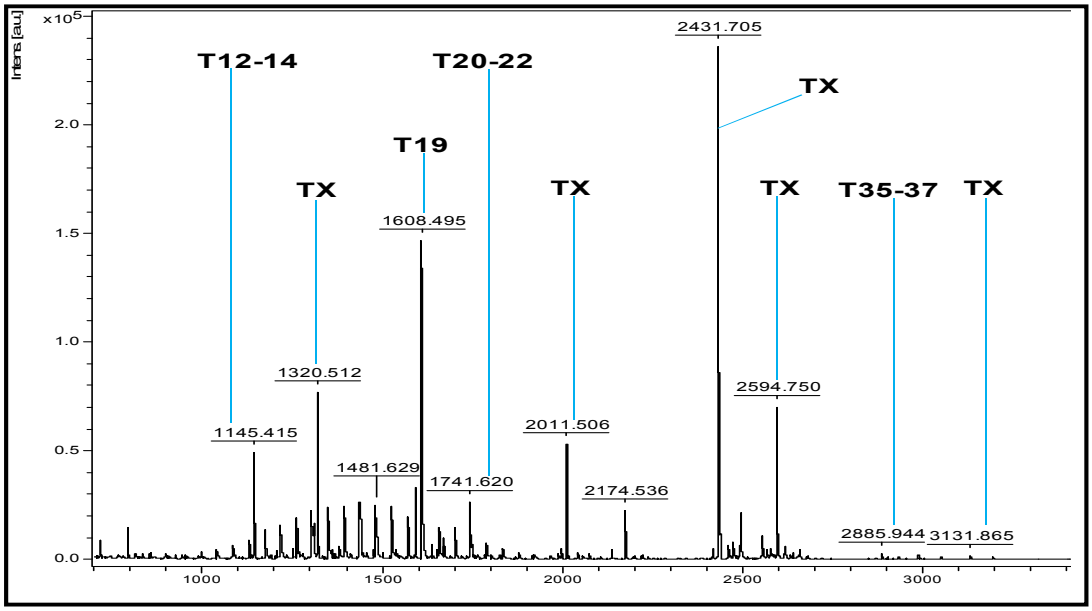

(B)

Tryptic Digests	Range	Theoretical Mono MH+	Experimental *m/z*	Accuracy (Daltons)	Partials	Sequence	Modifications
T12/13	[462-471]	1133.55	1133.56	-0.01	0	VMPA...ILWC	None
T12-14	[325-333]	1145.57	1145.42	0.16	0	SFWPELPNR	None
T16	[58- 69]	1364.66	1363.51	1.14	1	ENAA...ERLR	None
T17/18	[45- 57]	1476.79	1476.57	0.22	0	SYYH...GILK	None
T19	[96-109]	1608.76	1608.49	0.27	0	CGVP...VFPR	Carbamidomethylation (C)
T20	[235-249]	1673.82	1672.41	1.42	0	DPGA...YTGK	None
T20-22	[68- 82]	1741.89	1741.62	0.27	1	LREM...VTGK	None
T25-27	[334-350]	2044.03	2043.69	0.34	0	IDAA...FIFR	None
T27	[419-437]	2137.07	2136.72	0.35	1	LIEE...VYEK	None
T31-33	[45- 67]	2553.24	2552.81	0.43	1	SYYH...MTER	None
T32/33	[382-404]	2576.33	2575.89	0.44	1	ISAA...QVWR	None
T35-37	[68- 92]	2886.44	2885.94	0.49	2	LREM...DVMK	None
T37-39	[42- 67]	2985.49	2986.82	-1.33	2	YLRS...MTER	None

(C)

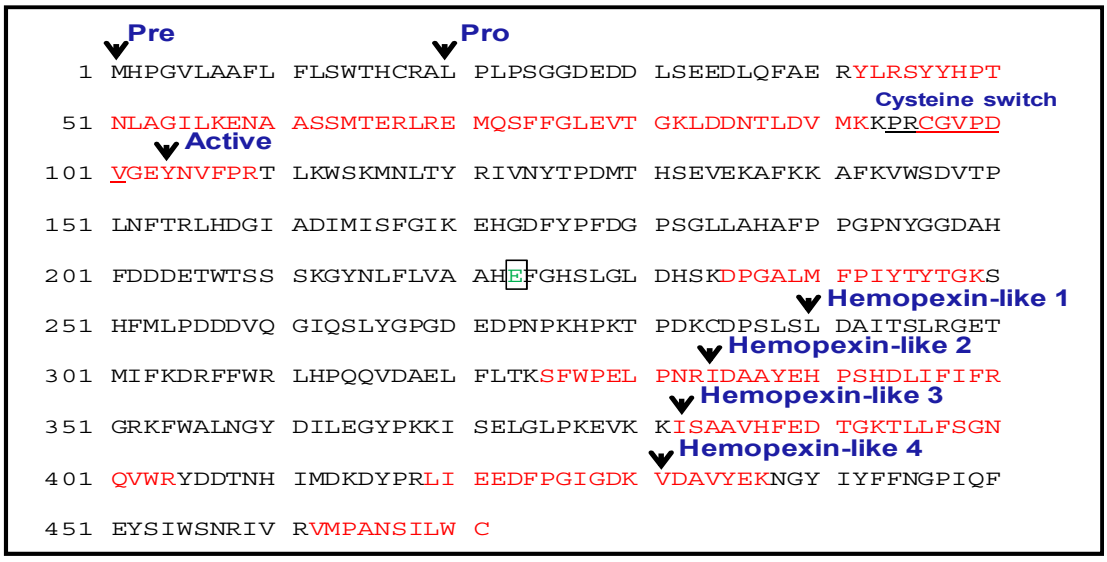

Figure 4.13 A. MS PMF of rhMMP-13 annotated tryptic peptides, B. Mass data for peptides in daltons, C. Sequence coverage, ID peptides in red, active site green and arrow heads pointing start of various regions.

(A)

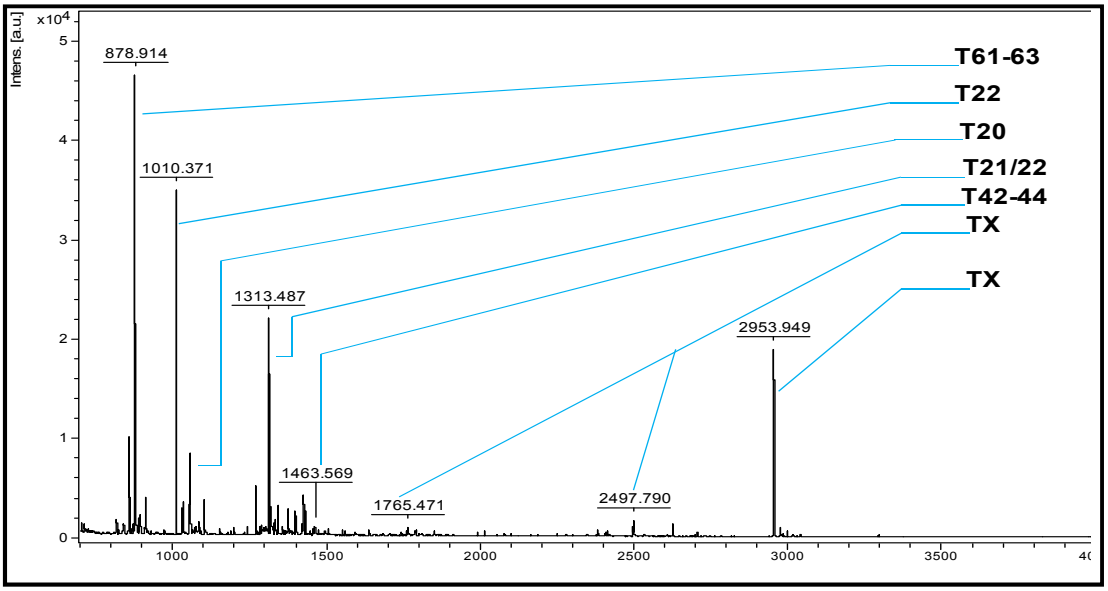

(B)

Tryptic Digests	Range	Theoretical Mono MH+	Experimental *m/z*	Accuracy (Daltons)	Partials	Sequence	Modifications
T61-63	[564-570]	879.50	878.91	0.59	2	RHGTPRR	None
T56/57	[486-492]	891.51	890.87	0.64	1	FNNQKLK	None
T22	[161-168]	1010.53	1010.37	0.16	0	EVPYAYIR	None
T46/47	[427-434]	1032.53	1032.35	0.18	1	TYFFRGNK	None
T20	[150-158]	1058.56	1058.39	0.17	0	VWESATPLR	None
T10/11	[99-108]	1104.62	1103.85	0.76	1	FGAE...ANVR	None
T17	[135-145]	1271.63	1271.42	0.21	0	VGEY...EAIR	None
T38-40	[376-386]	1287.67	1287.50	0.17	2	DGKF...KGDK	None
T21/22	[159-168]	1313.70	1313.49	0.21	1	FREV...AYIR	None
T17/18	[135-146]	1399.72	1399.49	0.23	1	VGEY...AIRK	None
T4	[57- 70]	1402.74	1402.51	0.23	0	SPQS...AMQK	None
T36/37	[363-375]	1419.76	1419.55	0.21	1	GLPA...YERK	None
T19/20	[147-158]	1432.77	1432.54	0.23	1	AFRV...TPLR	None
T42-44	[402-414]	1463.83	1463.57	0.26	2	HIKE...PTDK	None

(C)

Figure 4.14 A. MS PMF of rhMMP-14 annotated tryptic peptides, B. Mass data for peptides in daltons, C. Sequence coverage, ID peptides in red, active site green and arrow heads pointing start of various regions.

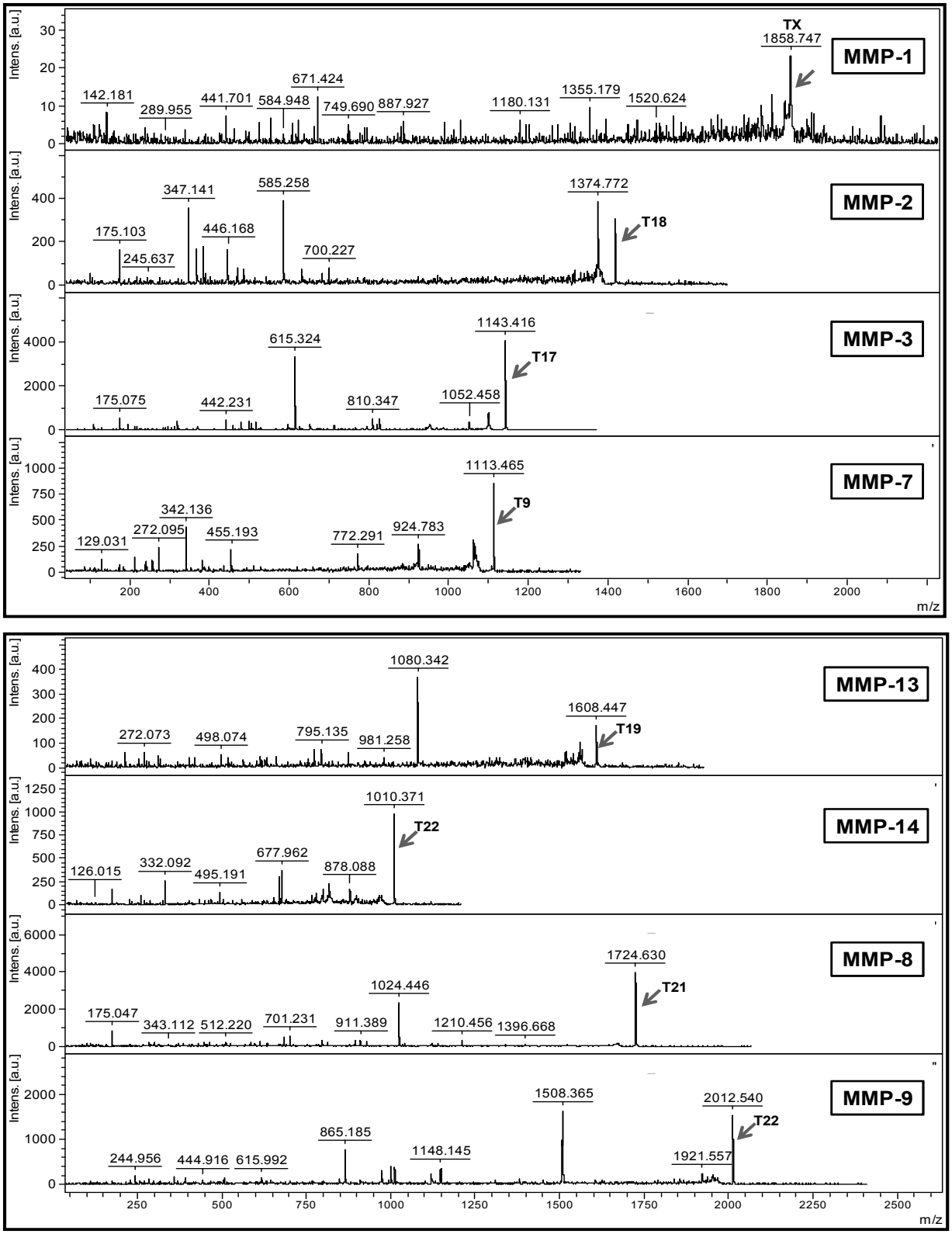

Figure 4.15 Peptide fragments of rhMMP-1, rhMMP-2, rhMMP-3, rhMMP-7, rhMMP-8, rhMMP-9, rhMMP-13 and rhMMP-14.

Red arrows pointing parent peptide ions.

4.3.5 Elastase and Lysine-N for complete Digestion of rhMMPs

To indicate a site of attachment of Olive H-7G in next set of experiments, it was important to achieve complete digestion of protein including active site residue. The digestion of rhMMP protein by trypsin might have been the reason why active site residue containing peptides could not be created as discussed in section 4.3.3. In order to achieve sufficient digestion of the protein, elastase and lysine-N were used. But efficiency of trypsin was found better than these two. Hence it was decided to keep trypsin as an enzyme for digestion.

4.3.6 Interaction between rhMMP-2/rhMMP-14 and Olive H-7G

The presence of detergent Brij-35 in rhMMP-2 did not allow noticeable shifts in specific mass peak of pure Olive H-7G (Mol. Wt. 869.1). The mass spectra of Olive H-7G solution (A) and Olive H-7G-MMP-2 complex (B) after the reaction is shown in Figure 4.16. The sample was analyzed after removal of detergent using C18 isolute columns and analyzed by MALDI mass spectrometry (Figure 4.16C) but it did not show enzyme signature peptides with an added mass of Olive H-7G indicating a site of attachment. It can be speculated that the significant signature peptides might have been lost during desalting process. Nevertheless the reaction of rhMMP-2 did change the specific profile of Olive H-7G (Figure 4.16A and C). Many *m/z* were present both in rhMMP-14 and Olive H-7G-MMP-14 complex, however, these were not matched with the theoretically digested peptide peak list created by using in-silico method. The 1/10th dilutions of rhMMP-14 and Olive H-7G-MMP-14 complex were prepared in order to get a better resolution with diluted sample. A detailed comparison of *m/z* obtained from the trypsinization of rhMM-14, rhMMP-14-Olive H-7G complex showed only one peptide 1433.478 which is closest to the theoretically determined MMP-14 specific peak 1432.770 (amino acid range 147-158 with a sequence of AFRVWESATPLUR). However, when MS/MS of the the daughter ion with m/z 1433.478 was performed and the daughter ion data was sent to Biotools, it did not generate MMP-14 identification. The Olive H-7G did not alter the *m/z* in control myoglobin + trypsin.

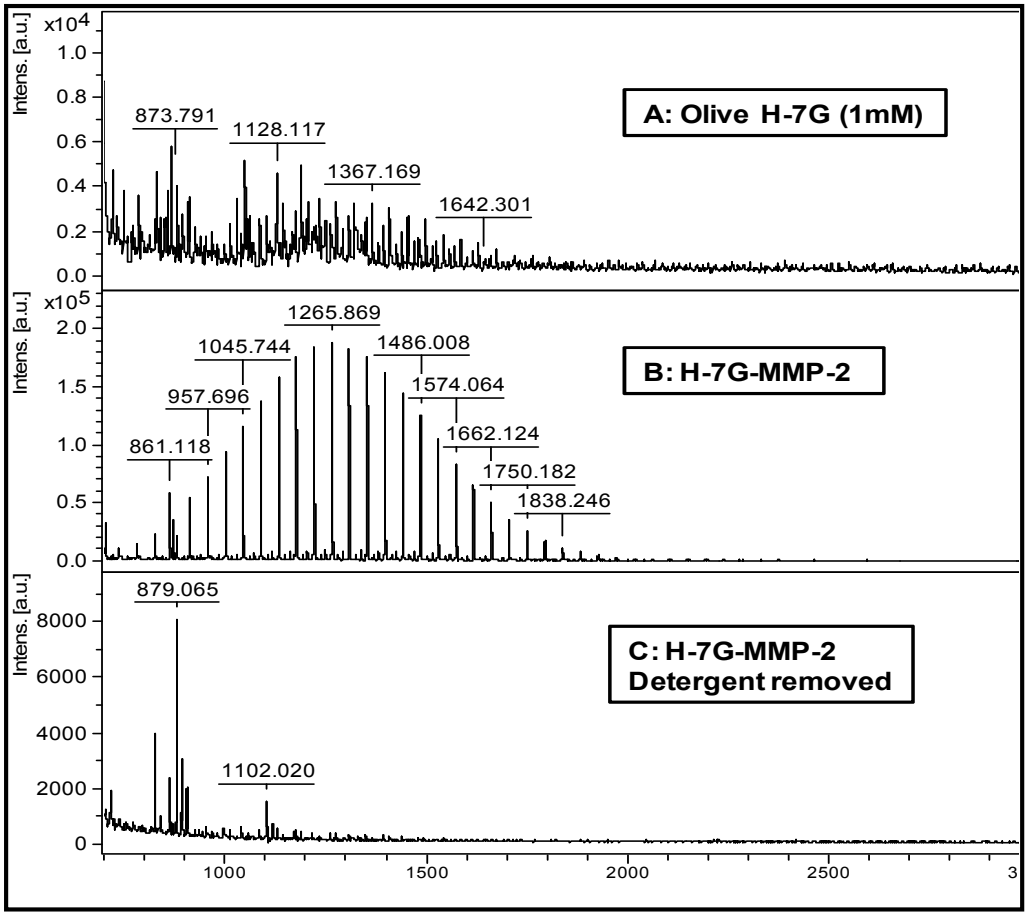

Figure 4.16 Mass Spectra of Olive H-7G and H-7G-MMP-2 complex.

4.3.7 Interaction between Mixture of 11 rhMMPs and Olive H-7G

The hypothesis that difference in the masses of peptides generated from trypsinization of MMP alone and attached to Olive H-7G will reveal site of attachment of later could not be proved because of complexity offered by detergent. Results for the reaction between Olive H-7G and MMP mixture obtained with (A) and without zip tipping (B) are shown in Figure 4.17.

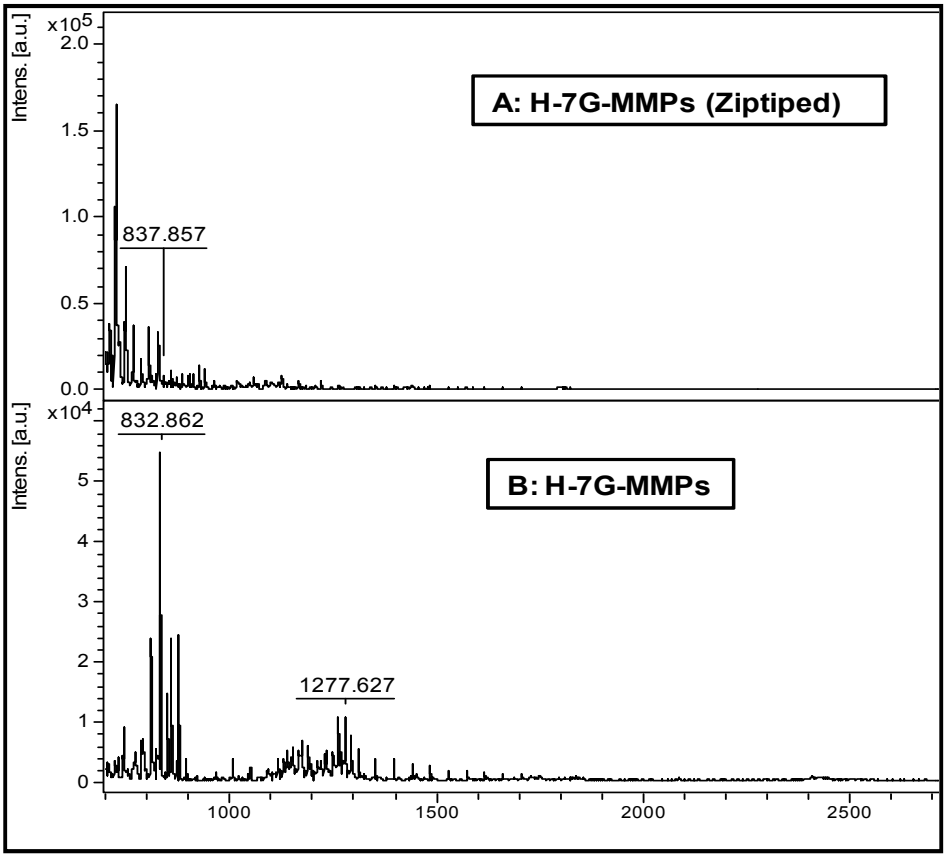

Figure 4.17 Mass spectra of Olive H-7G-MMP complex.

4.4 Discussion

The initial aim was to assess the integrity (intactness/ stability) of rhMMPs and optimize trypsin digestion assay as a part of sample preparation for mass spectrometric analysis before use in Olive H-7G chromatography.

In the current study MALDI mass spectrometry was used to establish purity and integrity of rhMMPs by detecting *m/z* of ionized proteins. An attempt was made to determine accurate molecular mass of each MMP using MALDI-MS. Conventionally, molecular weight (MW) of pure proteins is determined by SDS-PAGE. The *m/z* of the proteins cannot be measured in these gel based characterization. One of the biggest challenges during the characterization of rhMMPs was the presence of detergent Brij-35 added to the commercial enzyme solution as a surfactant to impart stability and increase solubility. Brij-35 (Mol. Wt. 1225g, aggregation No. 40) is a non-ionic polyoxyethylene surfactant, which produces mass signals with a difference of 44daltons over

a mass range, masking the peaks related to the peptides. Attempts to remove the detergent using C4 zip tips were only partially successful (MMP-3, MMP-7, MMP-10 and MMP-14) and could not be removed in the case of MMP-2, MMP-8, MMP-9, MMP-13 and MMP-16. It was anticipated that it might be the detergent (Brij-35) which is masking the specific peaks.

Characterization of MMPs by identifying their signature peptides (PMF) after trypsin digestion was attempted in this study contrary to conventional methods of characterization of proteins such as western blotting, zymography etc. Trypsin is a pancreatic serine endoprotease that cleaves proteins or peptides on the carboxyl side of arginine (R) or lysine (K) residues. The rate of hydrolysis is slower when an acidic residue is located on either side of the cleavage site and cleavage may not occur if a proline residue is on the carboxyl side (Stone et al., 1998). To optimize the assay a highly purified and chemically stabilized trypsin offering excellent performance for use in in-solution digestions was utilized. The peptide solutions were lyophilized to increase their concentration and improve digestion efficiency and denatured using 8M Urea followed by the reduction and alkylation of the cysteine present (see Figure 4.4-Figure 4.8C, Figure 4.10, Figure 4.12, Figure 4.13 and Figure 4.14C for sequences or amino acid composition). Combined urea denaturation and alkylation results in unfolding of the secondary and tertiary structure for optimal digestion by trypsin. After incubation with the trypsin, proteolytic fragments were analyzed by mass spectrometry in positive ion mode.

Mass spectrometry data can be used in three different ways for protein identification, PMF, sequence query and MS/MS ion search. PMF was the first method to be developed, and is in many ways the simplest approach. A manual comparison of experimental and theoretical peptide products was made to calculate the accuracy of acquired data and locate the sequence of amino acids in detected peptides (Figure 4.4-Figure 4.14). The selected derived *m/z* of rhMMP peptides from the list was submitted to a Mascot search engine in the present study. In this way MALDI mass spectra of rhMMPs peptides resulted in the identification of corresponding parent MMP. A Mascot search server was used because it provides option to select global

or variable modifications in protein and taxonomy filter on search form (Homo sapiens was selected) to limit the number of matches in results. Selecting variable modifications such as oxidation of methionine increase the search time because each site is tested with and without the modification. For example, if there are two methionines in a peptide, and MetOx is selected, then Mascot will try and get a match with 0 oxidised, 1 oxidised, and 2 oxidised peptides. This also increases the chance of a random match and an unnecessary variable modification decreases the score. While analyzing data from MALDI-MS it is considered that the experimental protein may be shorter than the protein mass entry in the database. The reason why better PMF for some rhMMPs were not generated could be down to many reasons such as electronic noise, ion-to-ion variation in detector response, collection efficiency of peptide ions and *m/z* dependent efficiency of detector. A large fraction of spectra acquired do not identify any peptide and remain un-used.

The MS/MS data (fragment ion masses) searching can be done either from a single peptide ion (parent ion) or from LC-MS/MS. In this study manual MS/MS from single peptide ions was done. A fragment mass tolerance of 0.7Da was used. The peptide mass fingerprint data is sent to Mascot to detect all the 'real' peaks from the spectrum. It is very important to send optimum number of peaks (30-100) with right mass range with no contaminant peaks. For each peak that fails to match, the Mascot score will be reduced, so it is important not to submit profile data or lists full of noise peaks. Since peak intensity is relative so it is not sufficient to just pick the most intense peaks. Weak as well as strong mass signals may also correspond to peptides of the protein. Some peaks may be produced by trypsin digesting itself. Trypsin has the ability to digest itself to produce autolytic peptide peaks. These peaks may have identical masses to the peptides from protein of interest. Thus removing these peaks along with noise peaks may compromise the results. Although error tolerant matches are still an open issue and one spectrum is more likely to match more than one entry, the PFF generated for rhMMPs generated identifications with good Mascot scores. As it was known already that the mass spectra were from rhMMPs, nevertheless data was searched against database to help test

possible atypical conditions, e.g. non-trypsin cleavages, more partials than expected, unexpected modifications. Such interpretation is best supported by MS/MS data.

While interpreting the results, it was kept in mind that PMF and PFF both have certain limitations. PMF is relatively simple but can be complicated because of PTMs of proteins. Although generating a list of PMF of a protein is relatively less time-consuming than MS/MS, it still needs large amounts of protein samples to start with because data is generated after manual analysis and many laser shots are fired per spot. Mass spectrometry is relatively sensitive compared to other techniques and MS/MS data is more reliable since theoretically one peptide can generate a confident protein hit. PFF makes the data more authentic and specific as in case of PMF a sequence of amino acids in a peptide in reverse order is identified the same e.g; DEFG = GFED. However, MS/MS data can be low-throughput and *de novo* sequencing is difficult to automate.

Although ionization of proteins can be achieved both by ESI and MALDI, we chose MALDI for this study. The only common thing between the two is that both can ionize intact proteins without fragmentation. The chemistry and workflow of MALDI has been explained in introduction. In ESI a liquid sample flowing, often from HPLC system, into the ESI system is aerosolized and the droplets are ionized as they exit a charged nozzle. As the liquid in these drops evaporates, the droplets shrink, until the ionic charge repulsion is sufficiently intense to overcome the surface tension holding the droplet together, producing gas-phase ions. The advantage of this arrangement is that sample is injected at the top of the column and analyzed as it emerges. However, the disadvantage during ESI-based analysis is that a very short time window is available to achieve a significant chromatographic peak of one component. The problem magnifies if column flow rate of HPLC system increases. In addition, in ESI a sample cannot be reanalyzed. In contrast in MALDI an off-line option is available in which samples are spotted on a target plate prior to ionization and can be reanalyzed. Other differences between MALDI and ESI involve the charges they impart on ions.

MALDI mostly produces ions with charge +1 along with few +2 and +3 ions. On the other hand ESI produces a range of different charge states for each molecule rendering the mass spectra to be considerably complex. This brings to one of the advantages of ESI that by producing multiply charged ions, ESI makes larger proteins accessible to analysis than does MALDI. Hence, in ESI ions will carry a range of charges corresponding to a range of *m/z*. From larger molecules, smaller *m/z* available helps getting better resolving power. In general, MALDI is faster than ESI and enables higher throughput. But ESI is more sensitive, meaning it can detect lower amounts of a given substance. Though each has its pros and cons, both are equally important and in use because some proteins will only ionize with one technique or the other. Since recombinant human pro-MMPs have theoretical molecular weights from 50 to 92kDa (active MMPs have lower molecular weights) so MALDI was selected for their characterization. MALDI is ideal for PMF study because individual MMPs can be spotted on target plate and analyzed repeatedly for longer time. Moreover, peptide molecules are very small and singly charged molecules in MALDI will generate smaller *m/z* giving better resolution. Also presence of multiple charges in ESI will create small peaks which might be masked by larger peaks from any possible contaminant or detergent. A salient feature of this study is that it was aimed to use very small quantities of MMPs (5pmoles) to emulate amounts in biological samples.

The second goal of this chapter was to identify a shift in mass of Olive H-7G because of binding of MMP. It has been shown in many kinetic studies that triazinyl dyes interact with an enzyme in a non-covalent way involving the binding site for a natural biological ligand of the enzyme such as NADH, NADPH, NAD+, NADP+, GTP, IMP, ATP, HMG-CoA, folate, etc. (Denizli and Piskin, 2001). The reason why any peptide peaks could not be seen in Olive H-7G-MMP complex could be presence of Brij35 interfered with dye binding. Another possibility is that the complex did not get ionized so could not be detected in MALDI mass spectrometer. It was hoped that extensive sequence coverage from PMFs would identify proteolytic peptides specific for the ‘pro’ and ‘active’ regions of each MMP that might be suitable for discrimination of the latent and active forms of protease captured by dye

ligand chromatography. As there were large gaps in the sequence coverage which meant that ‘loss’ of signals due to presence of Olive H7-G during trypsin digestion would not necessarily be detected or subsequent clean up resulting in sample losses and poor MS sensitivity.

CHAPTER 5

DYE LIGAND CHROMATOGRAPHY OF rhMMPs

5 Dye Ligand Chromatography of rhMMPs

5.1 Introduction

Affinity chromatography is a powerful tool for separation and enrichment of proteins. This method is based on the specific interaction between an immobilized ligand and the target protein to be separated. This study entails the use of a triazine dye Olive H-7G to purify MMPs with their subsequent identification by MALDI mass spectrometry. Pilot experiments were performed to improve chances of affinity chromatography outcome for enrichment of rhMMPs followed by identification with MALDI-MS. Mixtures comprising rhMMPs from various classes (basic, gelatinases, membrane bound and minimal domain) were used hence MALDI-MS/MS was combined with reverse phase nHPLC as a peptide separation strategy. This was attempted to provide qualitative proof that system has a potential to succeed on a full scale basis when cell line culture supernatants or biological samples are used.

5.1.1 Aims

The aims of experiments explained in this chapter were:

- To apply mixtures of rhMMPs to Olive H-7G immobilized on chromatography beads to determine potential of Olive H-7G for enriching MMPs. It was anticipated that ligand supporting matrix (sepharose or magnetic beads) would not offer any evidence of MMP binding. LC-MALDI-MS/MS was employed to characterize MMPs if present in a sample.

- Optimization of proteomics methods (LC-MS/MS) using smaller amounts of MMPs to address and overcome problems associated with the availability of small volumes of tumour biopsies in clinical set up.

- To recover rhMMPs off the chromatography beads (H-7G-Sepharose) once assured that the ligand binds the enzyme. This was achieved by employing an ELISA based assay which measured the activity of MMP-2 referred to as starting material (SM) before it was applied to H-7G-Sepharose beads (B), in flow-throughs (FT) collected after washing B and in eluates (E) combined with what was left on the beads at the end. This also proved the reversible nature of binding between protein and the ligand dye under discussion.

5.2 Materials and Methods

5.2.1 Synthesis of H-7G-Sepharose Beads

H-7G-Sepharose chromatography beads were prepared as described in Materials and Methods section 2.2.

5.2.2 Synthesis of Olive H-7G-Magnetic Beads (H-7G-MB)

Silica-coated iron oxide magnetic beads (Bioclone) with a diameter of 1µm and surface area of ~100m^2/g were used. These beads are grafted with hydroxyl group on the surface and the functional group density is ~200µmole/g of beads. Olive H-7G was immobilized on magnetic beads to synthesize H-7G-MB alongside control magnetic beads MB. To 10mg of magnetic beads 1mL of 34.6mM Olive H-7G solution (30mg/1mL of 4% NaOH) was added. Magnetic beads were then incubated at 80°C for 4 hour while constant stirring using a Fisher hotplate to create required temperature. The light brown colour of magnetic beads did not change suggesting the Olive H7-G had not bound to the beads. In order to ensure binding, the beads were transferred to glass flask and 20mL of 4% NaOH were added. The reactants were left on the shaker at 200rpm at 50°C for 45hours to allow binding of ligand on chromatography beads. The colour of the beads changed to greenish brown giving an indication that the Olive H-7G dye had bound to magnetic beads. H-7G-MB were then washed with 20mL water and centrifuged at 1200rpm for 1min at 18°C. The wash step was repeated twice

with 5mL distilled water. This was followed by another wash with 1mL distilled water. Finally 5 washes (1mL each) with methanol until non-bound dye was removed. The last wash with 1mL distilled water was given to remove any excess methanol. Beads were stored in 0.02% sodium azide solution (1:10 volume of suspension). Control beads MB (20mg) were prepared under identical conditions by adding 1mL of 4% NaOH in HPLC grade water, but absence of dye.

5.2.3 H-7G-Sepharose Capture of rhMMP Mixture

First set of experiments were performed with a mixture of 4 different rhMMPs namely MMP-1, MMP-2, MMP-3 and MMP-10. Once encouraging results indicating binding between H-7G-Sepharose were found, the number of MMPs was increased in mixture in the subsequent set of repeat experiments. Since identical temperature conditions, pH of buffers and incubations durations were tried to maintain in the repeat experiments, these will be explained simultaneously. Sepharose beads were used as a negative control and treated the same as probed beads (H-7G-Sepharose).

5.2.3.1 H-7G-Sepharose Bead Equilibration

Both beads suspension, H-7G-Sepharose and sepharose, were washed with 1mL of TNC buffer {50mM Tris-HCl (pH 7.5); 0.15M NaCl; 5mM $CaCl_2$ and 0.02% (w/v) sodium azide}. The washing was repeated thrice followed by two large washes with 10mL each to remove all residual sodium azide in which the beads are stored. Once beads were prepared these were equilibrated in TNC buffer in 2:1 ratio.

5.2.3.2 rhMMP Mixture Preparation

Mixtures comprising of 4 different MMPs (rhMMP-1, rhMMP-2, rhMMP-3 and rhMMP-10) and 9 different MMPs (rhMMP-1, rhMMP-2, rhMMP-3, rhMMP-7, rhMMP-8, rhMMP-9, rhMMP-10, rhMMP-13 and rhMMP-14) were prepared separately. In view of limit of detection of MALDI-mass spec, at least

5pmoles of each of MMPs were added. Each MMP is at less than 1µM final concentration in mixture as shown in Table 5.1.

Table 5.1 Final concentration of rhMMPs in mixtures.

MMP	MW (R&D) (kDa)	Final Conc. in 4 MMP Mixture (µM)	Final Conc. in 9 MMP Mixture (µM)
MMP-1	53	0.35	0.35
MMP-2	72	0.35	0.35
MMP-3	52	0.35	0.35
MMP-7	28	-	0.7
MMP-8	51	-	0.35
MMP-9	77	-	0.28
MMP-10	52	0.35	0.35
MMP-13	52	-	0.35
MMP-14	31	-	0.63

5.2.3.3 Reaction

The mixture of rhMMPs (SM) containing 1µg protein (4 rhMMPs) or 2.5µg protein (9 rhMMPs) was added to 125µL and 250µL H-7G-Sepharose, respectively (Figure 5.1). The negative control sepharose beads were mixed in same amounts. A part of SM was kept aside for further analyses. After rotating the mixture for 1hr at 4°C, contents were centrifuged at 1200g and flow-throughs (H-7G-Sepharose FT and sepharose FT) were collected and kept on ice. The beads (H-7G-Sepharose and sepharose) were collected and washed with 1mL TNC buffer (5-times) with each spin at 1200g at 4°C. Since this experiment was performed to validate Olive H-7G as a potential ligand for MMPs, elution was skipped and MMPs were kept bound to the beads.

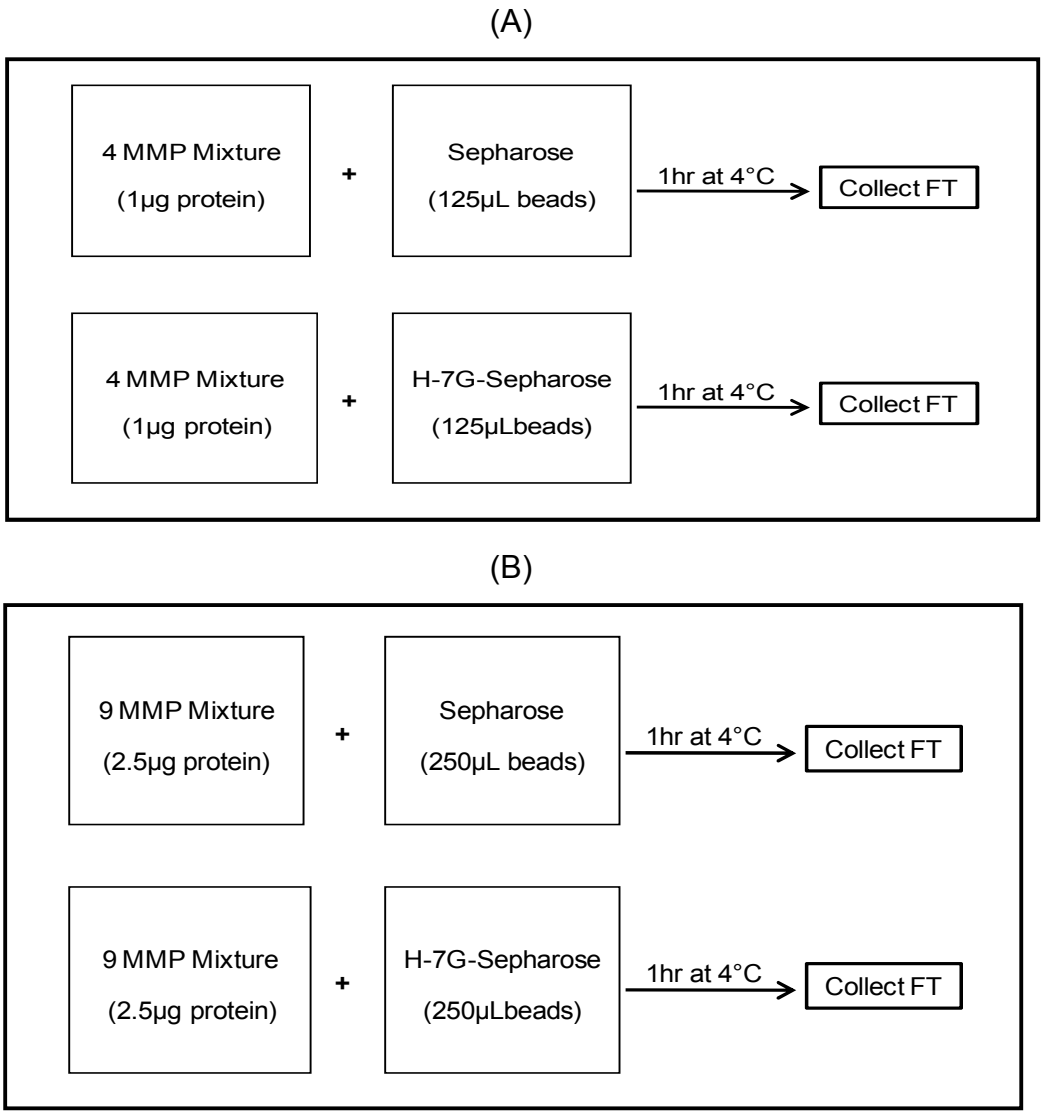

Figure 5.1 Reaction between H-7G-Sepharose beads and mixture of (A) 4 rhMMPs, (B) 9 rhMMPs.

5.2.4 H-7G-MB Capture of rhMMP Mixture

Magnetic beads were used as an alternate matrix to sepharose to improve the specificity of Olive H-7G once immobilized on their surface. A mixture of 11 rhMMPs was applied to probed and control magnetic beads synthesized as explained in section 5.2.2. The experimental design for the experiment is shown in Figure 5.2. Control magnetic beads (will be referred to as MB) were treated with TNC buffer to find their signature peaks when analyzed by MALDI mass spectrometry. Another lot of magnetic beads was treated with mixture of rhMMPs (will be referred to as MB-MMPs) to observe if these offer

any affinity to the proteins. The magnetic beads probed with Olive H-7G were mixed with rhMMP mixture (will be referred to as H-7G-MB-MMPs).

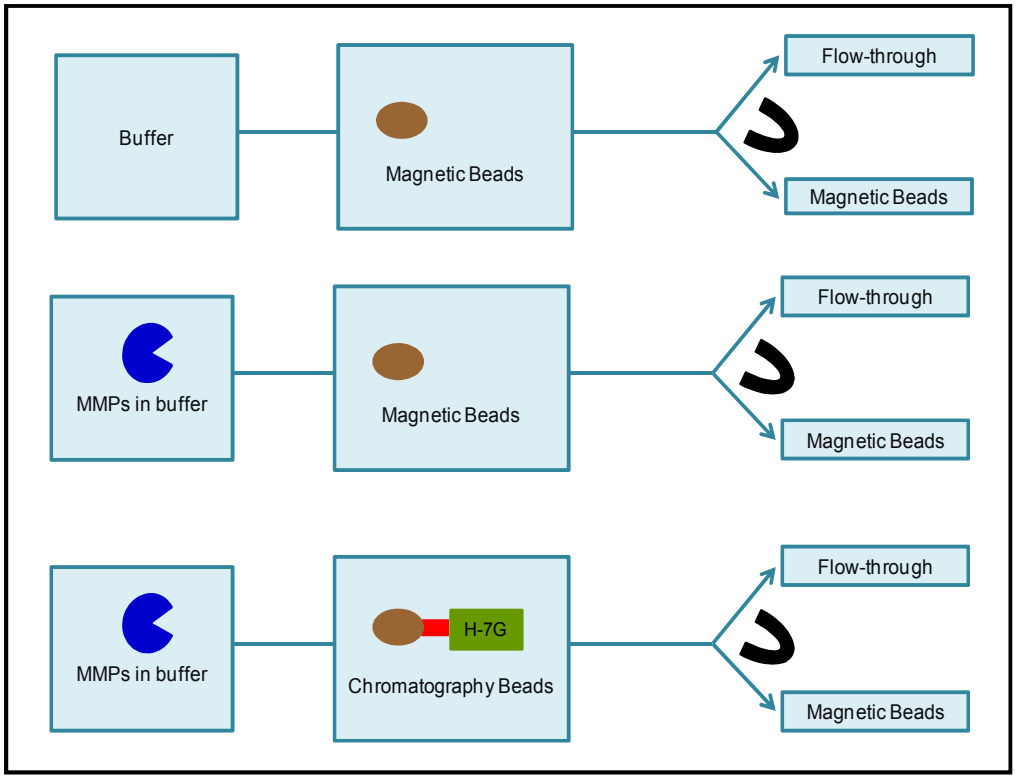

Figure 5.2 Experimental design for magnetic beads.

5.2.4.1 Magnetic Bead Equilibration

Magnetic beads were prepared by collecting with magnet and adding 1mL TNC buffer and left for 10minutes to equilibrate. After spinning at 1200g for 5minutes, supernatant was discarded and 2 further washes were followed. The magnetic beads were left in 200µL suspension.

5.2.4.2 rhMMP Mixture Preparation

Each MMP is at less than 1µM final concentration in mixture as shown in Table 5.2.

Table 5.2 Final concentration in mixture of 11 rhMMPs.

MMP	MW (R&D) (kDa)	Final Conc. In Mixture (µM)
MMP-1	53	0.35
MMP-2	71	0.35
MMP-3	52	0.35
MMP-7	28	0.7
MMP-8	51	0.35
MMP-9	77	0.28
MMP-10	52	0.35
MMP-12	52	0.35
MMP-13	52	0.35
MMP-14	31	0.63
MMP-16	31	0.63

5.2.4.3 Reaction

A mixture of 11 rhMMPs (SM) containing 3µg protein was added to 10mg of each of H-7G-MB and control beads MB (H-7G-MB-MMP and MB-MMP). Another control MB to which TNC buffer (pH7.5) was added instead of MMP were also prepared. The H-7G-MB-MMP beads, control beads MB-MMP and MB were rotated for 1 hour at 4°C at a rotator at 30rpm. The beads were attracted to bottom of polystyrene eppendorf by using a strong magnetic field and corresponding flow-throughs H-7G-MB-MMP FT, MB-MMP FT and MB FT were collected and kept in ice bucket until further analysis. All three different magnetic beads (H-7G-MB-MMP, MB-MMP and MB), were washed 5-times with 1mL TNC buffer. After the last wash, beads were not kept in any suspension. Moreover, no elution was performed because the idea of this experiment was to analyze whether MMPs bind to Olive H-7G or not.

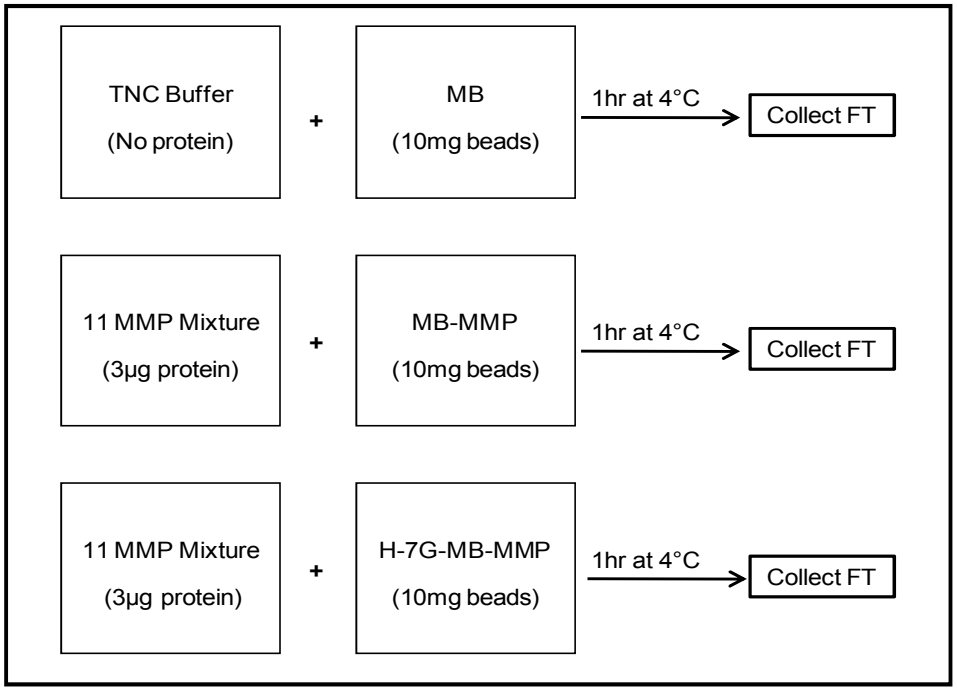

Figure 5.3 Reaction between magnetic beads and mixture of 11 rhMMPs.

5.2.5 Preparation of rhMMPs Peptides (In-solution)

To prepare samples for trypsin digestion only FT was desalted using NAP-5 (Materials and Methods section 2.5) and lyophilized at 37°C/aqueous in GenVac evaporator. In-solution trypsin digestion was performed as described in Materials and Methods section 2.9.1 with the following variations in volumes for magnetic beads SM and FT: 13µL of 8M urea, 1µL of 50mM DTT, 1µL of 100mM IAC, 36µL of HPLC grade water and 7.65µL of 20µg/mL of trypsin solution.

5.2.6 Preparation of rhMMPs Peptides (On-bead)

To the beads (H-7G-Sepharose and sepharose), 1mL of 25mM ambic was added, mixed gently, centrifuged and buffer was discarded. It was repeated to wash the beads properly. To these beads, urea was added to give an 8M concentration (48.048mg for 100µL of suspension) and vortexed. Then 25µL of 50mM DTT were added, mixed and heated to 50^{o}C for 15minutes. After bringing it to room temperature 25µL of 100mM IAC were added, vortexed,

centrifuged and incubated for 15-20minutes at room temperature in dark. To dilute the urea concentration, 250µL of HPLC grade water were added. This was followed by the addition of 6.13µL of trypsin solution (20µg/mL) and incubated at 28^{o}C for 18hours followed by addition of 50µL of trypsin solution (20µg/mL) for another 20hours at 37^{o}C for complete digestion of proteins. The reaction was stopped by freezing at -20°C. For magnetic beads (neither desalted nor lyophilized) all the steps were performed as described above with following changes in amounts of reagents: 13µL of 8M urea, 1µL of 50mM DTT, 1µL of 100mM IAC, 36µL of HPLC grade water and 7.65µL of 20µg/mL of trypsin solution were used with an overnight digestion at 28ºC.

5.2.7 Removal of Detergent from Peptide Solution

For manual MALDI mass spectrometry, peptide solutions were spotted on MALDI target plate using C18 zip tips (Materials and Methods section 2.10.2). Before nHPLC fractionation of individual peptide solutions of SM, FT and B, C18 isolute columns were used to remove detergents or salts (Materials and Methods section 2.10.1).

5.2.8 Reverse phase nHPLC coupled to MALDI-MS/MS

The peptides were successfully separated using in-house nHPLC. Separation was confirmed through the generation of unique MS spectra following manual analysis of random fractions. The overall intensities (ranging from 10^3 to 10^5 a.u) suggested sufficient peptide concentrations for duplicate automated MS/MS analysis on each single fraction. The collected fractions were analyzed as described in Materials and Methods section 2.12.

5.2.9 Enrichment of rhMMP-2

Sample (rhMMP-2) was added to the H-7G-Sepharose chromatography bead suspension and mixed with rotation for 1 hour at 4°C to affinity bind to the H-7G-Sepharose chromatography beads (Materials and Methods section 2.4) and elution of the enzyme was performed using a salt gradient of 0.3-2M NaCl buffers as described in Materials and Methods section 2.4.1.

5.2.10 Quantification of rhMMP-2 in Chromatographic Fractions

Once chromatographic fractions (FT and E) were collected, the rhMMP-2 amounts were detected (Materials and Methods section 2.7). The beads (B) collected at the end of the chromatography were also analyzed for any bound rhMMP-2.

5.3 Results

5.3.1 MALDI-MS of Mixture of 4 rhMMPs (H-7G-Sepharose Captured)

Horse myoglobin was digested into expected peptides, T1, T3, T4, etc (Appendix 3) for theoretical peptides) indicating that trypsin was working effectively. The trypsin control (in the absence of any target proteins) indicated some autolytic degradation, generating known products of the bovine enzyme {MH+ = 1045.613, 2212.15 and 2300.215 (Mooney, 2007)}. The myoglobin control (incubated in the absence of protease) was intact, exhibiting no storage related degradation products. A complex series of signals between *m/z* 700 and 4000 was observed for SM comprising the mixture of 4 rhMMPs, H-7G-Sepharose and sepharose (Figure 5.4) indicative of proteolytic digestion. The SM exhibited peptides from MMP-1, MMP-2, MMP-3 and MMP-10 (Table 5.3). On-bead digestion of H-7G-Sepharose incubated with MMPs exhibited peptides from MMP-1, MMP-2 and MMP-3, whereas the equivalent sample from the sepharose control showed none of the MMP related peaks. Only autolytic product of trypsin 843.475 in H-7G-Sepharose and 843.391 in SM was observed. Since MMPs also degrade and undergo autolysis so some signals could be from rhMMPs.

A number of signals did not correlate with expected trypsin products, especially in the sepharose control. These could be from traces of detergent Brij-35 already present in the rhMMPs. A 0.05% solution of Brij-35 was analyzed with MALDI and *m/z* are given in Appendix 6. Many of signals were matched with the peaks determined in samples. A possible contamination of keratins in the sample due to handling may have contributed towards some of the signals. The common peaks from keratin can be 1179.60, 1208.6,

1210.5, 1277.78, 1307.67, 1383.69, 1475.75, 1707.77, 1713.82, 1716.85, 1765.73, 1794.84, 1993.98, 2383.95, 2705.15 and 2872.34. Few of these were observed in SM e.g. 1713.61 and 2705.01. Some of these *m/z* can be common between the protein of interest such as MS/MS analysis of peptide with *m/z* 1713.61 identified MMP-3 in SM (Table 5.3). MS/MS analysis of *m/z* 1418.552 and 1713.945 in sample H-7G-Sepharose confirmed the signals corresponded to peptides in MMP-2 and MMP-3 respectively.

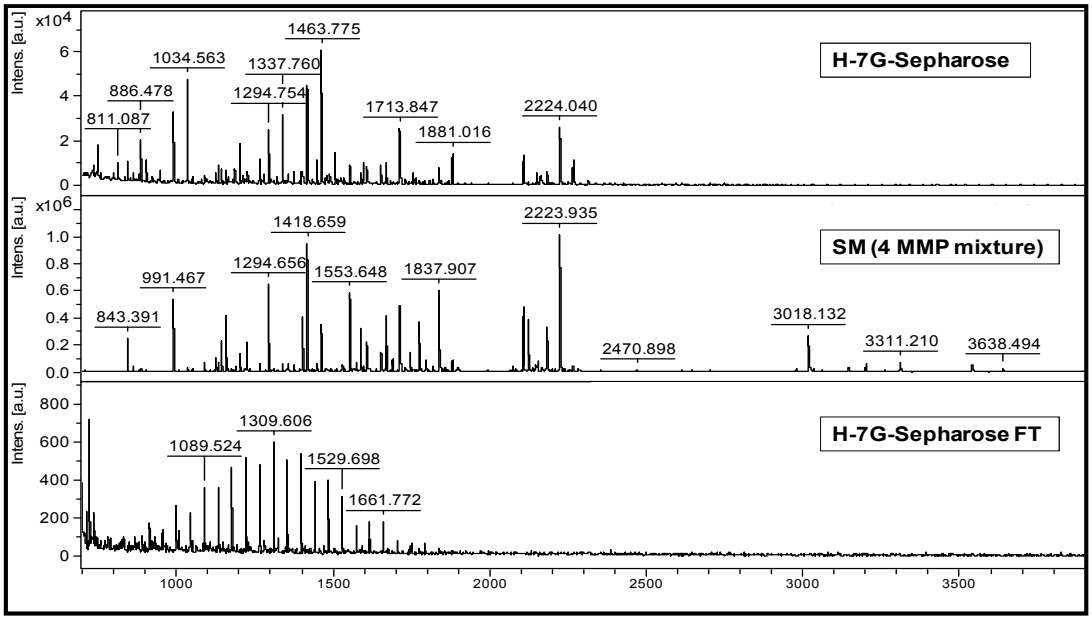

Figure 5.4 MALDI mass spectra for H-7G-Sepharose, H-7G-Sepharose FT and mixture of 4 rhMMPs.

Table 5.3 Theoretical and experimental digest peaks for 4 rhMMP mixture, H-7G-Sepharose and sepharose.

Theoretical Deigest peaks	Experimental Digest peaks				
MMP	SM		H-7G-Sepharose		Sepharose
MMP-1	m/z	Error	m/z	Error	
1158.64	1158.43	0.21	ND	-	ND
1222.55	1221.61	0.94	ND	-	ND
3016.47	3017.93	-1.46	ND	-	ND
MMP-2				-	
1418.74	1418.55	0.19	1418.55	0.19	ND
2224.07	2223.77	0.30	2223.81	0.26	ND
3146.56	3146.00	0.56	ND	-	ND
MMP-3					
1089.58	1089.54	0.04	ND	-	ND
1159.64	1158.44	1.20	ND	-	ND
1178.57	1177.59	0.98	ND	-	ND
1221.58	1221.61	-0.03	ND	-	ND
1553.74	1553.53	0.21	ND	-	ND
1713.85	1713.61	0.24	1713.65	0.20	ND
3200.65	3200.19	0.46	ND		ND
MMP-10					
1089.52	1089.60	-0.08	ND	-	ND
1573.84	1573.78	0.06	ND	-	ND
1775.97	1775.73	0.24	ND	-	ND

5.3.2 MALDI-MS of Mixture of 9 rhMMPs (H-7G-Sepharose Captured)

The number of rhMMPs was increased in the mixture against which Olive H-7G was to screen its potential as a broad-spectrum ligand. As described in section 5.2.3, after 1 hour incubation of a mixture of 9 rhMMPs with H-7G-Sepharose chromatography beads and negative control sepharose, on-bead trypsin digestion was performed. Trypsinization created peptides fragments, larger and smaller, these were ionized in MALDI mass spectrometer to demonstrate a mass peak profile. Manual MS analyses showed similar peak profile as depicted in 4 rhMMP mixture and beads. Some of these signals might be autolytic products of trypsin or rhMMPs. The detergent specific peaks were identified but lesser, both in number and intensity, than found in 4 rhMMP mixture. The peaks from keratin 1307.67, 1475.75, and 2705.15 were detected.

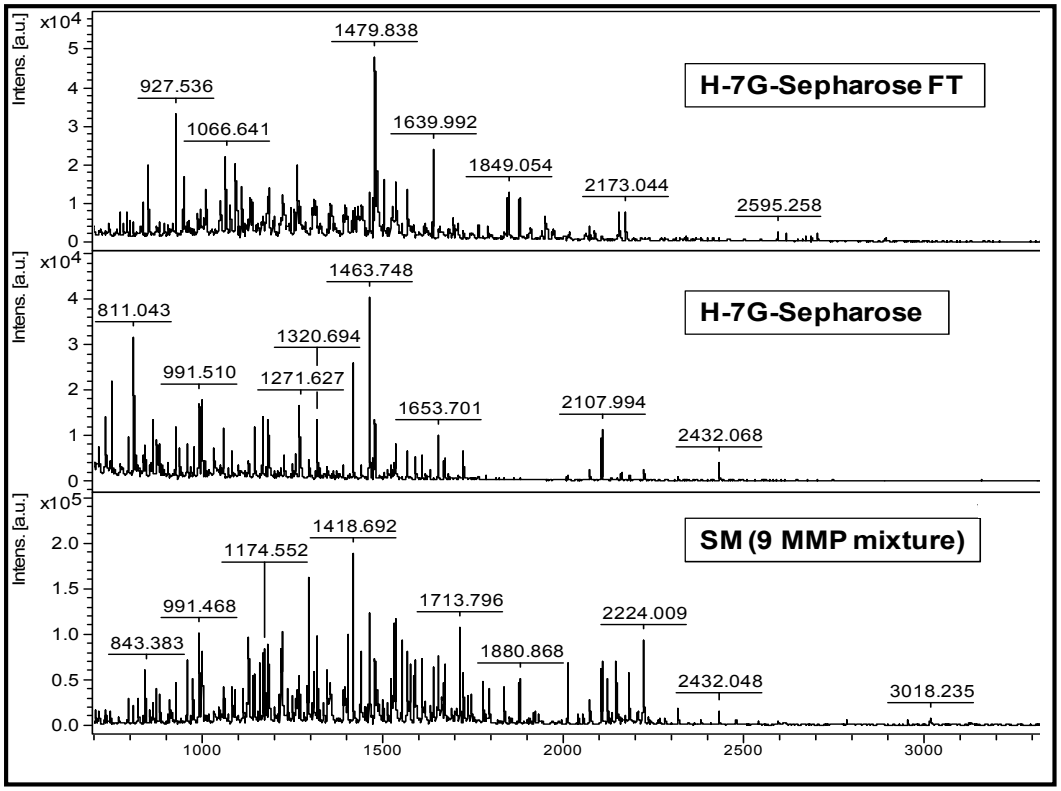

Figure 5.5 MALDI mass spectra for H-7G-Sepharose, H-7G-Sepharose FT and mixture of 9 rhMMPs (n=3).

5.3.3 MALDI-MS of Mixture of 11 rhMMPs (H-7G-MB Captured)

The negative control beads MB to which TNC buffer was added is shown in Figure 5.6. The close analysis of MB FT indicates either the solvent A used for washing zip tips or solvent B used for elution of peptides were contaminated. After MB treated with rhMMP mixture (MB-MMP in Figure 5.6) seems to bind Brij-35 specific peaks suggesting that zip tipping did not remove the detergent. The washing of the beads MB-MMPs did not remove the detergent peaks indicating stronger interaction between magnetic beads and Brij-35 micelle. A similar pattern was observed for H-7G-MB-MMP and its corresponding flow-through. Some MMP specific peaks were detected in the beads. A clear cut conclusion could not be made by observing the magnetic beads with bound Olive H-7G treated with rhMMP mixture. In an LC-MS/MS run the fraction H-7G-MB-MMPs showed 3 proteins of which MMP-8 (Mascot score 38) and MMP-12 (Mascot score 16) were identified with a sequence coverage of 2% and 1% respectively.

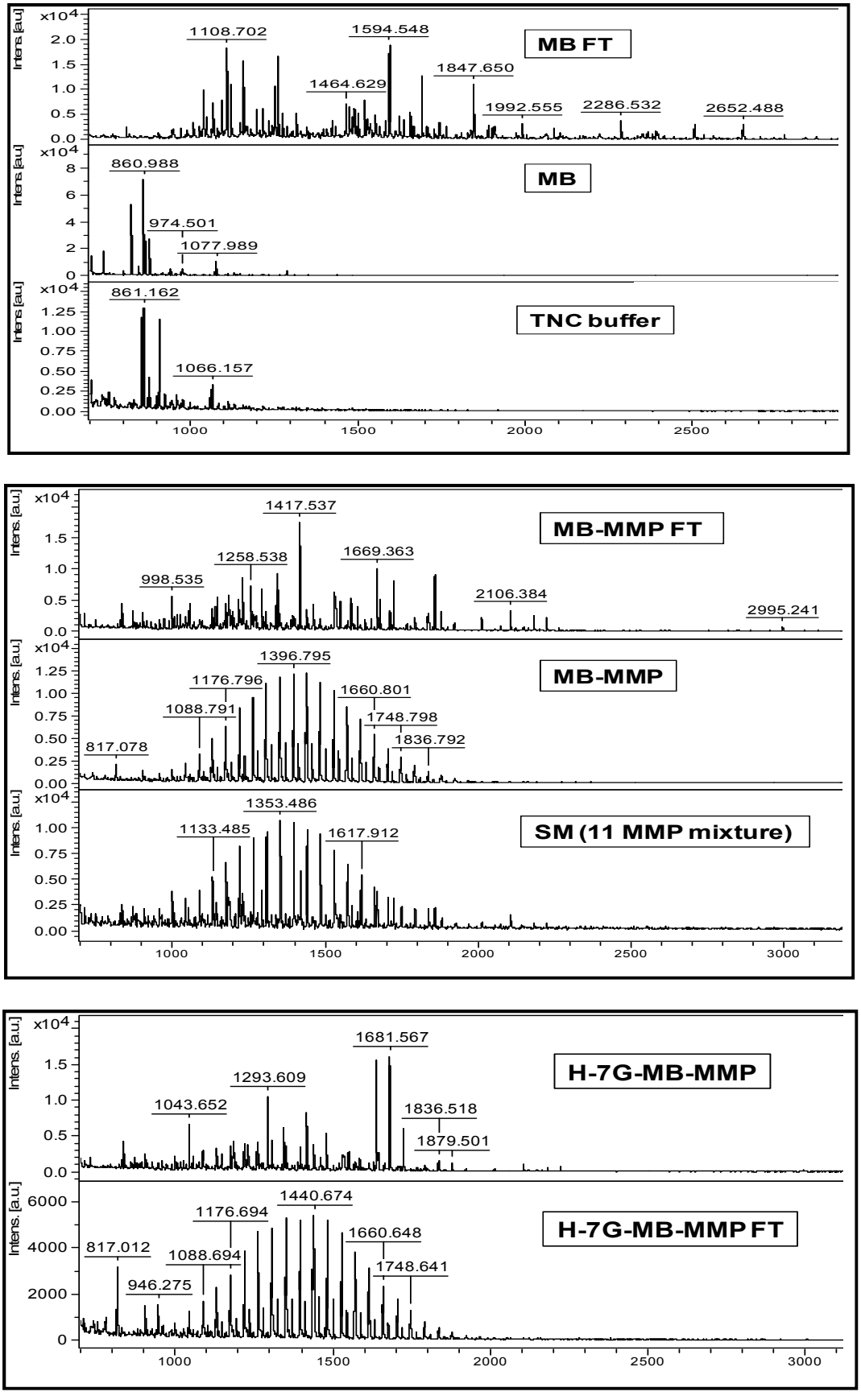

Figure 5.6 MALDI mass spectra of MB, MB-MMP, H-7G-MB-MMP and mixture of 11 rhMMPs.

5.3.4 LC-MS/MS of rhMMP Peptides

The successful separation of peptides by nHPLC was confirmed through the generation of unique MS spectra following manual analyses. The overall intensities (ranging from 10^3 to 10^5 a.u) suggested sufficient peptide concentrations for duplicate automated MS/MS analysis. The nHPLC UV profiles measured at 280nm and 215nm obtained for SM (mixture of 9 rhMMP), Beads (probed and control) and their corresponding FT are shown in Figure 5.7. The LC-MS/MS runs for each sample identified MMPs with at least 1 peptide above the Mascot significance threshold of 30 ($p<0.05$) (Table 5.4). The nHPLC profile for SM showed discrete peaks for MMP specific peptides, however, these were much weaker in the chromatographic fractions due to the presence of non-peptide contaminating peaks of unknown character. Some of these peaks were identified to be from the detergent. The comparison of probed beads H7G-Sepharose and sepharose control beads shows that it is Olive H-7G which binds MMPs since only MMP-9 was identified in later and most of the MMPs (MMP-3, MMP-8, MMP-9 and MMP-10) were leaching into sepharose FT suggesting that sepharose does not permanently trap the MMPs. A possible reason why all MMPs added to the mixture were not identified in sepharose FT could be the identification of less MMPs from same peptides generated from variable regions of different MMPs. The identification of MMP-3, MMP-7, MMP-9 and MMP-10 in H-7G-Sepharose confirms the previous findings that Olive H-7G has an affinity for MMPs and it can be used to purify these endopeptidases.

In an attempt to exploit the achieved results in this experiment to discriminate ‘pro’ and ‘active’ forms of MMPs, a comparison of sequence coverage obtained was made for the MMPs identified in H-7G-Sepharose beads and SM applied onto it. The sequence coverage as depicted by Mascot search results is shown in Table 5.5. The sequence of amino acids in red font is the peptides identified in each sample with a reliable Mascot score (≥30) confirming their identity as true signature peptides for the MMPs. For further elaboration of the results obtained, the sequence of MMPs has been enlarged to show the amino acid sequence in ‘pro’ region and the active site

'E' is highlighted green and enboxed. No peptide was detected with active site amino acid as part of its sequence. This implies that enzymes present in the SM were 'pro' form. A higher Mascot score results for an individual peptide if it is present in sufficient quantity. The lesser sequence coverage in MMPs in H-7G-Sepharose as compared to SM identified in could be for many reasons such as less affinity for Olive H-7G, degradation during trypsin digestion or lesser MS/MS fragmentation.

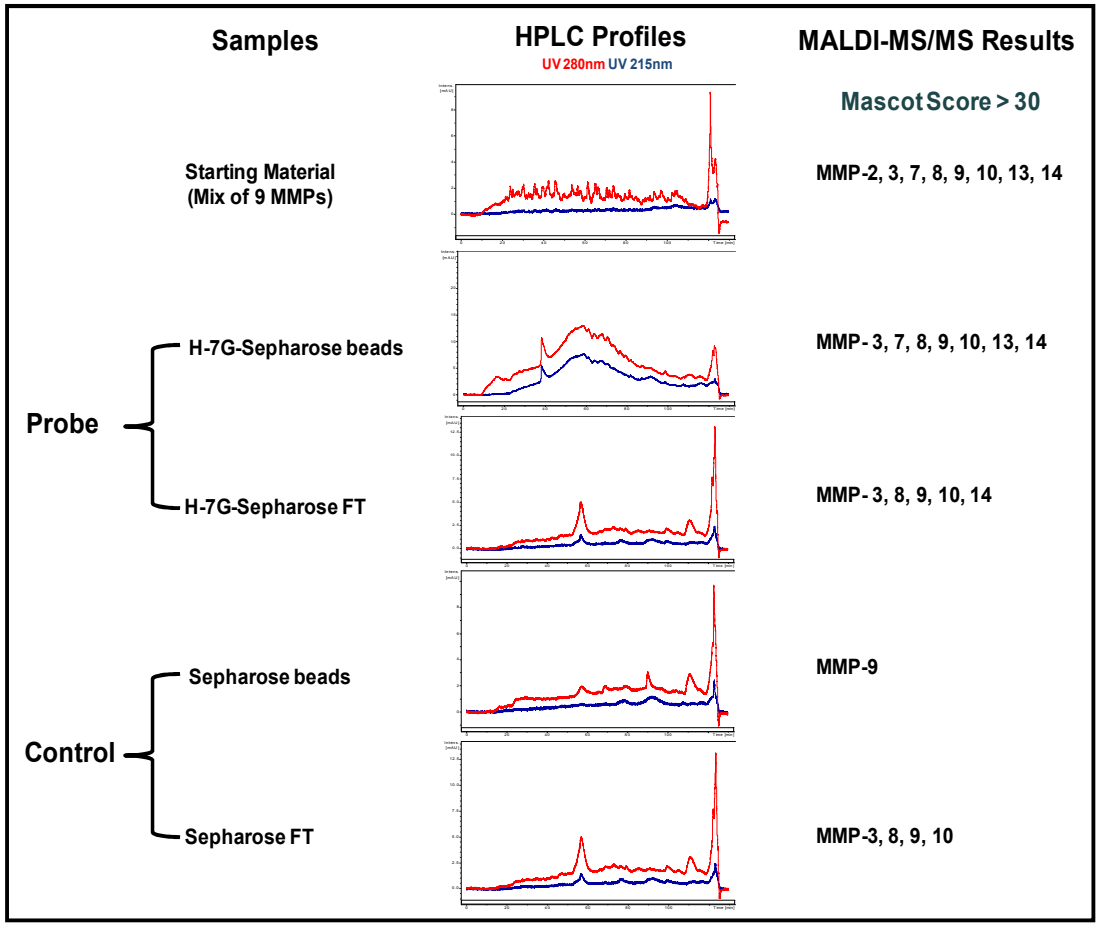

Figure 5.7 nHPLC profiles for mixture of 9 rhMMPs, H-7G-Sepharose, sepharose and corresponding FT.

Table 5.4 LC-MS/MS results.

Sample	MMP	Mascot Score	Peptides #
		(n=2)	(n=2)
SM (Mixture of 9 MMPs)	2	115.5	8
	3	306	13
	7	166	5.5
	8	419	12
	9	478	16.5
	10	501.5	16.5
	13	480.5	12
	14	161	4.5
H-7G-Sepharose Beads	3	63.5	5
	7	16.5	1
	8	45	2.5
	9	60	6
	10	178	9
	13	92.5	3.5
	14	30.5	1.5
H-7G-Sepharose FT	3	21.5	1
	8	25.5	2
	9	57	4.5
	10	91	5
	14	29	1
Sepharose	9	15.5	0.5
Sepharose FT	3		
	8		
	9		
	10		

* *Not Detected

Table 5.5 Sequence coverage of MMPs to discriminate ‘Pro’ and ‘Active’ forms.

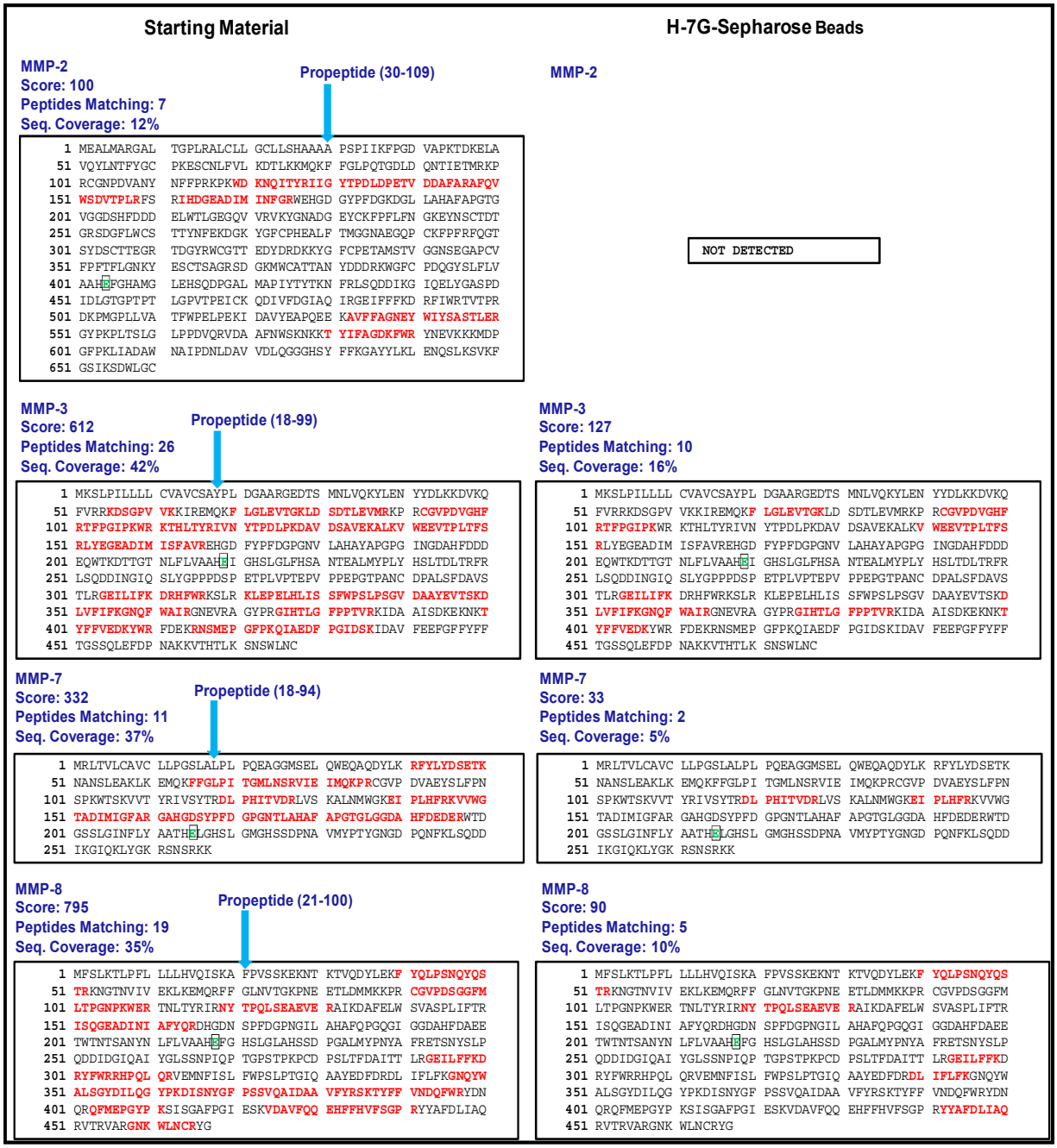


Starting Material
H-7G-Sepharose Beads
MMP-9
Score: 884
Peptides Matching: 28
Seq. Coverage: 39%
Propeptid (20-93)
MMP-9
Score: 120
Peptides Matching: 12
Seq. Coverage: 14%
MMP-10
Score: 1003
Peptides Matching: 33
Seq. Coverage: 48%
Propeptide (18-98)
MMP-10
Score: 356
Peptides Matching:18
Seq. Coverage: 27%
MMP-13
Score: 825
Peptides Matching: 19
Seq. Coverage: 43%
Propeptide (20-103)
MMP-13
Score: 185
Peptides Matching: 7
Seq. Coverage: 10%
MMP-14
Score: 322
Peptides Matching: 9
Seq. Coverage: 12%
Propeptide (21-211)
MMP-14
Score: 61
Peptides Matching: 3
Seq. Coverage: 6%

5.3.5 rhMMP Recovery from H-7G-Sepharose

MMP-2 is a well characterized, representative member of the matrix metalloproteinase family, with established assays and antibodies for its detection. Materials and Methods section 2.7 describes the validation of ELISA assay using commercially available recombinant human pro-MMP-2 (rhMMP-2). The concentration of the rhMMP-2 in SM and in H-7G-Sepharose chromatography fractions (FT, E and beads) were determined using an ELISA based quantification kit. The standard curve showing linear correlation between amounts of standards and absorbance in the range 0.78-50ng/mL is shown in Figure 2.4. To measure the MMP-2 activity within the calibration range samples were concentrated and desalted using NAP-5 columns. The eluates from NAP-5 columns were lyophilized and then resuspended in 50µL of RD5-32 ELISA buffer, performed rest of the steps as instructed by the ELISA kit and absorbance of product was measured at 450nm to calculate MMP-2 amounts (Table 5.6). The amount of rhMMP-2 in SM was 370ng based on information specified by supplier but it was detected to be 93.00ng. The results indicate that the yield of rhMMP-2 was 95.01% with 30.62% in the flow through, 43.91% eluted and 20.48% retained on the beads after elution. Therefore, within the measurement of ELISA assay, a good yield was achieved. However, the calculated amount of rhMMP-2 in starting material was 370ng hence, 24.05% of rhMMP-2 was retrieved.

Table 5.6 MMP recovery from H-7G-Sepharose based on ELISA.

Samples	rhMMP-2 (ng)		%age Retrieval	
	Mean (n=2)	SD	Mean (n=2)	SD
rhMMP-2 SM	93.00	0.16	95.01	2.04
rhMMP-2 FT	28.48	1.64		
rhMMP-2 E1	23.52	0.09		
rhMMP-2 E2	17.32	0.79		
rhMMP-2 B	19.05	0.47		

The presence of MMP-2 in FT could be because of the super saturation of beads i.e. the MMP-2 amounts were more than the capacity of beads volume. It could also be because of reversible nature of binding of MMP-2 to the dye ligand. Since the affinity between the two is not of covalent nature so MMP-2 might come off the beads during vortexing or centrifugation for washing the beads. The results obtained by ELISA of eluents (from 0.3M and 2M salt buffers) validate the findings of sections 5.3.1, 5.3.2 and 5.3.4 that Olive H-7G binds MMPs. The affinity chromatography of rh-MMP-2 comprising of binding of the enzyme to the dye and subsequent elution was performed to achieve the retrieval of the enzyme. The results obtained by ELISA quantification proved that the Olive H-7G not only bound the rhMMP-2 but also, recovery of the enzyme was possible using elution buffers containing the right salt concentrations (0.3M and 2M).

5.4 Discussion

The successful capture of MMPs with H-7G-Sepharose (section 5.3.1 and 5.3.2) as well as the successful identification of these proteins using LC-MS/MS (section 5.3.4) and the elution of these proteins based on dye ligand chromatography (section 5.3.5) paved the way for proteomic analysis of complex proteome (This will be reported in Chapter 6 and 7). Sufficient MMP amounts (in ng) very close to the sensitivity range of LC-MALDI based proteomic analysis was added to the mixture in small volumes (in µL) which allowed successful identification of the MMPs. The successful identification of MMPs after LC-MS within a small time-window was an important achievement since recombinant proteins are more prone to degradation without the stabilizing proteins found in complex proteomes. Previous studies based upon samples from cell lines have used much higher protein amounts (in µg or mg) in larger volumes (in mL or L) of cell line culture supernatants. For instance, within their study, Imai and co-workers used a four-step purification of MMPs starting from 250mL of rheumatoid synovial fibroblast culture supernantant concentrating it down to 37mL. From this, they purified different MMPs in various steps which is time-consuming (Imai and Okada, 2008).

This chapter serves to demonstrate the development of proteomics mass spectrometric method for the detection, identification and characterization of MMPs in one robust step. As described in Introduction of this chapter, the need for new and effective profiling methods for MMPs is especially pressing with respect to their role in metastasis and as a target for MMP-activated drug development. This model study attempt with rhMMPs was made in need of developing a technique using smaller amounts of MMPs in smaller volumes of biological samples for gauging the expression of 'pro' and 'active' forms of MMPs. The combination of dye ligand chromatography for MMP enrichment, nHPLC for peptide separation and MALDI tandem mass spectrometry for identification has proved to be successful system in characterizing MMPs. This will help achieve the ultimate goal of this project which is to utilize this methodology for identifying MMPs in clinical tissues and working with limited supply of tumour samples is a well-recognized challenge due to their complex proteome.

For the study of complex peptide mixtures, LC-MALDI provides an opportunity to concentrate and separate the peptides prior to analysis thereby extending time available for MS/MS interrogation resulting in increased sequence coverage. This in turn results in higher sensitivity and means that more MS/MS spectra can be generated from the sample. Rather than acquiring all the MS/MS spectra from the same spot, with the sample being depleted with each spectrum acquired, signals are collected from different positions on the MALDI target and sample depletion is less of an issue. All the samples were analyzed manually before carrying forward for LC-MALDI-MS/MS TOF/TOF. A high level of stringency was adopted to avoid false discovery. For MMP captured on beads, H-7G-Sepharose, (Table 5.5) where a better sequence coverage was not achieved from a peptide sample, this may have been due to poor peptide ionization or low sample concentration. While interpreting data and assigning protein identification, the MS/MS tolerance threshold (0.07) which states the likelihood that the peptide has been matched by chance, was considered. A lower value indicates a more confident match. It is a way of determining the quality of a match. The number of peptides matched was also considered as higher number of

matched peptides indicates more confidence in the protein. Two or more peptides were desirable for confident MMP identification. Other factors such as number of missed cleavages (2) and the variable modifications of peptides (carbamidomethylation of cysteine and oxidation of methionine in this study) were also considered.

One of the noteworthy finding of this study is that the ligand under discussion has affinity for MMP-8, MMP-13 and MMP-14 in addition to previously reported MMPs (MMP-3, MMP-7, MMP-9 and MMP-10). This finding highlights the broad applicability of Olive H-7G. The identification of these three new MMPs could be attributed to the LC-MS/MS complimentary protein identification. Ideally, there should not be any MMPs being detected in flow-through however, the identification of MMP-3, MMP-7, MMP-8, MMP-9, MMP-13 and MMP-14 in H-7G-Sepharose FT (Table 5.4) could be because of the fact that beads were saturated and excess MMPs were washed. These results are very encouraging and not only confirm the previously reported potential of the Olive H-7G affinity for MMP-3, MMP-7, MMP-9 and MMP-10 but also for MMP-8, MMP-13 and MMP-14 reported in this study.

The analysis was extended to use magnetic beads, a matrix of choice for immobilizing ligands. Recently, there has been increased interest in the use of magnetic carriers in biomolecule coupling, nucleic acid and protein purification. The magnetic character implies that they respond to a magnet, making sampling and collection easier and faster. In a study conducted by Nilgun, 2007 a triazine dye, Cibacron Blue F3GA-attached mPHEMA (2-hydroxyethylmethacrylate) beads provided an efficient method to separate lysozyme, showing high binding capacity, assuring a purity of about 87.4% with recovery about 79.6%. It was hoped that the smaller diameter of magnetic beads (1micron) as compared to sepharose (45microns) would allow minimum protein binding hence allowing immobilized ligand to enrich the MMPs. The results obtained were not clear. Possible reasons for this could be (i) Olive H-7G did not react to the hydroxyl groups on the surface of beads (ii) the pH, temperature or salt concentrations were not optimal during the capture of MMPs (iii) autolytic degradation of MMPs causing changes in 3 dimensional structure. This is in agreement with the finding of study by

Trinkle-Mulcahy that no single matrix among sepharose, agarose and magnetic beads gives required results under all conditions . Since, H-7G-Sepharose showed better results than magnetic beads so it was decided to omit the use of magnetic beads in the following experiments. Functionalized magnetic beads allow for relatively rapid and easy purification from crude biological samples, thereby eliminating the need for most of the pre-treatment steps such as centrifugation, filtration and membrane separation (Corchero and Villaverde, 2009)

The elution buffer (0.3M and 2M NaCl) were used to elute off the endopeptidases after confirming the affinity of Olive H-7G for MMPs (section 5.3.1 and 5.3.4) to gain a very fundamental information that whether bound MMPs to Olive H-7G could be retrieved or not. The ELISA assay was used to measure the MMP concentration in collected chromatography fractions and compared to the starting material (Table 5.6). The assay was optimized using recombinant form of MMP-2 to interrogate cancer cell lines selected for the study (explained in next chapters). The data offered persuasive evidence as a consequence of the observed 95.01% recovery of MMPs from Olive H-7G immobilized on sepharose. This finding appeared to be very plausible and suggested that it is worth viewing Olive H-7G as a potential probe for purification of MMPs in keeping with the previous studies. Nevertheless, it still remains vital to clarify whether it discriminates ‘pro’ form of MMPs from ‘active’. The ELISA used for determining MMP-2 levels in samples did not differentiate ‘pro’ and active forms. This draws attention to the limitations of the assay. Yet within the measurements of the assay, a good yield was achieved. The discrepancy between expected level (370ng) in the SM and actual measured (93ng) by ELISA could be for many reasons such as the potential presence of uncleaved substrate whose absorbance is measured, presence of some component (preservatives and surfactants in kit supplied reagents) interfering to the efficiency of the assay or lyophilized samples were not completely dissolved in diluent buffer could be some of the factors. The detection of rhMMP-2 on chromatography beads (19.05ng) collected at the end means that the entire bound enzyme was not eluted using salt containing buffers. Both ELISA and MALDI mass spectrometry have their

merits and limitations. For a sandwich based ELISA assay, an enzyme label such as HRP is conjugated to antibody raised against the antigen of the target protein. The assay involves washing steps which remove unbound material and leaves behind the specific protein bound to the capture antibody coated to the polystyrene micro-titre pate. In MALDI, there is no need to adjust the wavelength to match absorption frequency of each analyte because matrix is used. Also, matrix does not allow the formation of cluster of molecules which helps increase accuracy and resolution. The sensitivity of MALDI MS is down to the attomole concentrations as opposed to ELISA where micromolar concentrations are vital. ELISA is restricted to the proteins for which antibodies have been raised to a smaller part of the protein structure. In case of MALDI, many proteins can be identified simultaneously because databases have theoretical profiles for all the known proteins.

Taken together these data add weight to the validity of Olive H-7G as a potential affinity tool for the separation of MMPs from complex proteome. This compelling data was viewed as a further justification of the choice of Olive H-7G as a potentially useful purifying tool for MMPs. This pilot study with rhMMPs helped to scale up the amount of MMPs in samples of low total protein content for later analyses with MALDI-MS since most of the proteins are lost during preparation for final analysis. Moreover, there is no published data of using a mixture of recombinant human MMPs (basic, gelatinases, membrane bound and minimal domain) shown to bind to one dye ligand (Olive H-7G) and identified by LC-MS/MS presented in this study. To the best of my knowledge, the binding of MMP-8, MMP13 and MMP-14 to Olive H-7G is reported for the first time in this study.

CHAPTER 6

PURIFICATION OF SECRETED AND CELLULAR MMPs FROM PRE-CLINICAL CANCER MODEL AND PROTEOMIC MASS SPECTROMETRY

6 Purification of Secreted and Cellular MMPs from Pre-clinical Cancer Model and Proteomic Mass Spectrometry

6.1 Introduction

The expression of MMPs is related to the progression of various cancers such as the breast and colorectal cancer (Garbett et al., 1999), human gastric carcinoma (Nomura et al., 1996) and oral squamous cell carcinomas (Patel et al., 2007) and the metastases of endometrial and gastrointestinal carcinomas (Shiomi and Okada, 2003). The role of MMPs in cancer has been covered in detail in Introduction (Introduction section 1.5). Compartmentalization, that is where and how in the pericellular environment an MMP is released and held is important (Ra and Parks, 2007). The architectural complexity of natural site of action of MMPs, the ECM into which MMPs are secreted, is maintained by a large portfolio of matrix proteins, signaling molecules, proteases, and cell types that play a fundamental role in the remodeling process. Membrane bound MMPs can serve as a localized, pericellular site of ECM proteolytic activity.

In vitro cell lines have been in use to facilitate the characterization of new molecular targets (Bibby, 1999). The fibrosarcoma cell line HT1080 has been used for the purification of pro-MMP-9 and its mechanism of activation (Okada et al., 1992). The characterization of MMPs and more specifically expression of active MMPs in tumour cell lines have been used as a means of elucidating disease state. In a study, the expression pattern of the 23 human MMPs was investigated in different gynecological cancer cell lines from three endometrium carcinomas (Ishikawa, HEC-1-A, AN-3 CA), three cervical carcinomas (HeLa, Caski, SiHa), three chorioncarcinomas (JEG, JAR, BeWo), two ovarian cancers (BG-1, OAW-42) and one eratocarcinoma (PA-1). The expression of MMPs was analyzed by RT-PCR, western blot and gelatin zymography. The major findings of the study were that Ishikawa, Caski, OAW-42 and BeWo cell lines could be the best choice for experiments on MMP regulation and their role in endometrial, cervical, ovarian or choriocarcinoma development, whereas the teratocarcinoma cell line PA-1 in

which a broad range of 16 MMPs could be found and could be used as a positive control for general MMP experiments (Schropfer et al., 2010).

Despite this a dearth of data exists with respect to pro/active/TIMP complexed MMP expression in various pathological conditions at a given time point. The ruling out of one gene-one protein dogma due to the presence of post-translational modifications (PTMs) has rendered the proteome analysis difficult using standardized methodologies such as western blotting and activity assays. Examples of more than 100 PTMs have been reported for a single protein (O'Donovan et al., 2001). Protein structural diversity is one of the major analytical challenges in detecting low abundance proteins (Gross and Lapiere, 1962). The fact that biological samples contain mixture of proteins, most of which are high abundance proteins (HAP), offers a great deal of obstacle in characterizing target proteins.

Back in 80's, triazine based reactive dye were more frequently used for protein purification as explained in Introduction section 1.8.4.1. Affinity chromatography is based on highly specific biological interactions between two molecules and provide significant time savings and several hundred-fold or higher purification (Urh et al., 2009). With the growing popularity of affinity purification, many of the commonly used ligands attached to affinity matrices are now commercially available and are ready to use. However, in some cases new affinity chromatographic material may need to be developed by pairing the ligand onto the matrix such that the ligand retains specific binding affinity for the protein of interest. Thus, it is important to optimize the purification protocol to achieve efficient capture and maximum recovery of the target protein. The recent development of mass spectrometry and use of proteomic approaches has allowed the rapid, high-throughput identification of proteins including those secreted in culture supernatant and cell extracts. Successful application of proteome analysis is accomplished by tandem mass spectrometry (MS/MS) because of its tremendous power of protein identification and sequencing by analyzing signature peptides. Identification of MMPs with mass spectrometry based methods is challenging because of their membership of low abundance proteins (LAP).

For LAP, chromatography enrichment helps bring their concentration high enough for detection and quantification. For example, a 1000-fold Immuno-affinity enrichment of proteins can achieve 1ng/mL limit of MS quantification (Berna and Ackermann, 2009). The problems with the identification of LAP such as MMPs can be overcome if appropriate enrichment and separation techniques both at protein and peptide level are combined with tandem mass spectrometry. This is achieved by devising affinity based chromatography systems which segregate and enrich proteins of interest followed by controlled digestion of proteins and separating the corresponding peptides by liquid chromatography. In the present study an attempt was made to make these various techniques compatible with each other starting with lowest possible amounts of biological samples and optimize tandem mass spectrometry to detect MMPs. For enrichment, H-7G-Sepharose chromatography beads were synthesized. Following demonstration of signature peptides of MMPs (Chapter 4), H-7G-Sepharose chromatography beads showed evidence of capture of rhMMPs and were successfully identified by LC-MS/MS (Chapter 5). This gave confidence to proceed for the purification of these endopeptidases from a mixture of proteins. Hence, culture supernatants and cell lysates from HT1080 and HT29, fibrosarcoma and colon carcinoma cell lines, respectively, known to express MMP-2, MMP-9, MMP-7 and MMP-14 etc, were used as a source of MMPs. The affinity chromatography was performed following standard protocol using 0.3M and 2M NaCl buffers (Okada et al., 1990; Okada et al., 1986) and with the variation in the composition of elution buffers. Once chromatography fractions were generated, a series of experiments were performed which will be explained in detail in this chapter. Briefly, presence of purified proteins was confirmed by performing SDS-PAGE and staining either with Coomassie blue or silver stain to get a better visual. The recovery of MMP-2, as a representative of MMPs, from H-7G-Sepharose chromatography beads was measured by ELISA. The results were validated by western blotting as well. Finally tandem mass spectrometry was performed on selected chromatography fractions to identify MMPs.

6.1.1 Aims

The specific goals could be summarized as:

- The first aim of this chapter was maintaining a continuous source of MMPs so selected immortalized HT1080 and HT29 cell lines were cultured to create culture supernatants and cell extracts for chromatography method development and additional material for supplementary tests such as MMP-2 ELISA assays and western blotting to corroborate results. It was aimed to avoid the known problems caused by proteins present in the foetal calf serum (FCS) added to the growing cells, it was decided to replace serum-containing culture supernatant (S+CS) with serum-free RPMI-1640 media and allowed the cells to grow for 48hours so that enough MMPs could be secreted into the culture supernatant. This serum-free culture supernatant (SFCS) was used for subsequent experiments. Cell lysates were prepared extracting MMPs in three sequential steps using salt (NaCl) containing buffers, dimethyl sulphoxide (DMSO) containing buffers and urea containing buffers as described by (Davis et al., 1998). Salt and DMSO remove matrix bound MMPs and urea removes soluble MMPs.

- FCS was trypsinized and subjected to LC-MS/MS for identifying proteins present in it.

- A major issue that tumour biopsies are available in small amounts was kept in mind while optimizing various methods. Hence, SFCS in small volumes such as 50mL in comparison to larger volumes (250-500mL) in previous studies (Okada et al., 1992; Okada et al., 1990) and cell lysates from $7x10^6$ cells, which possibly expressed MMPs in nanogram amounts, were applied to H-7G-Sepharose chromatography beads. The idea was to use affinity chromatography (H-7G-Sepharose beads) as enrichment means as well as specifically elute MMPs in sufficient amounts that beside potential losses at

subsequent sample preparations, nHPLC fractionation should still enable detection and identification of each MMP in amounts close to the limit of detection of MALDI mass spectrometer. Chromatography optimization included variation in salt concentration (0.3-5M NaCl) and addition or exclusion of inhibitors such as EDTA. Additional optimization included handling of chromatographic fractions to enable compatibility with MALDI-MS analyses, such as concentrating, desalting (NAP-5 GPC columns, Isolute RP C18 columns and proteolysis (trypsin, lysine and elastase) methods.

- HT1080 cell lysate analyses using all above methods to compare their MMP profile with that of culture supernatant.

In conclusion this chapter aims to demonstrate the application of H-7G-Sepharose chromatography with biological samples in amounts that will emulate the limited amounts of materials expected from tumour biopsy collection. Consequently tumour cell lines previously reported to express high levels of MMPs were examined.

6.2 Materials and Methods

6.2.1 Preparation of Foetal Calf Serum (FCS) for LC-MS/MS

Heat inactivated FCS (4mg/µL) was desalted through NAP-5 column and lyophilized at 37°C in evaporator. To lyophilized protein, 20µL of 8M urea was added, vortexed and spun for 1minute. 5µL of 50mM DTT was added and heated for 20minutes at 80°C. After bringing it to room temperature, 5µL of 100mM IAC was added, centrifuged at 14000g for 1minute and left in dark for the reaction completion. A 1mg/µL trypsin solution was added after diluting the contents with HPLC grade water to bring down the urea concentration to 2M. An overnight incubation in water bath at 37°C was set up to complete the digestion. The peptide solution was desalted with C18 columns and lyophilized 37°C. The lyophilized peptides were resuspended in 10% CH_3CN and a 25µg equivalent of protein digest was run through nHPLC

as described in Materials and Methods section 2.12.1. An automated MALDI-MS/MS (Materials and Methods section 2.12) was followed to detect the proteins present in serum.

6.2.2 Preparation of Culture Supernatants (Serum+ and Serum-free)

The collected HT1080 and HT29 culture supernatants S+CS and SFCS (Materials and Methods section 2.3.3) were desalted using NAP-5 columns at 4°C to ensure minimal protein degradation and lyophilized at 37ºC. Work following this was carried out as quickly as possible in sterile conditions to avoid keratin contamination.

6.2.3 Specific variations in Olive H-7G Chromatography applied for Culture Supernatants

The standard protocol using salt containing buffers (0.3M and 2M NaCl) was followed for the isolation of MMPs from HT1080 and HT29 culture supernatants as described in Material and Methods section 2.4. However, following modifications in elution buffers were applied to achieve specific elution of MMPs.

6.2.3.1 EDTA Elution

After washing the equilibrated beads {50mM Tris-HCl (pH 7.5); 0.15M NaCl; 5mM $CaCl_2$ and 0.02% (w/v) sodium azide} elution was performed mixing the beads in 1mL of 10mM EDTA solution {50mM Tris-HCl (pH 7.5); 0.15M NaCl; 10mM EDTA; 5mM $CaCl_2$ and 0.02% (w/v) sodium azide} for 1-2minutes and centrifuged at 4°C for 5minutes and collected supernatant termed E1a. This was repeated to collect E1b and E1c followed by washing (2-times) the beads with 10mL of same elution buffer and discarded the supernatant. A further elution was performed using 100mM EDTA {50mM Tris-HCl (pH 7.5); 0.15M NaCl; 100mM EDTA; 5mM $CaCl_2$ and 0.02% (w/v) sodium azide} and eluates E2a-c collected. The beads were stored in 0.02% sodium azide solution after washing in elution buffer and discarded the supernatants. The fractions were desalted and concentrated using NAP-5 columns and 10mM

NH_4HCO_3 + 20µM EDTA was used to avoid autolytic degradation of MMPs during the process. After concentration each of the fractions were lyophilized at 37°C in evaporator. The trypsin-digested samples prepared (Materials and Methods section 2.9.1) using amounts shown in Table 6.1 were pooled during the process so as that E2c was kept separate because of high salt and to assure the protein resuspension. The peptide solution was then desalted using C18 columns and lyophilized at 37ºC in evaporator.

Table 6.1 Trypsin digestion for EDTA eluates.

Samples		8M Urea	50mM DTT	100mM IAC	HPLC H_2O	Trypsin
SM	(Lyophilized)	20 µL	2 µL	2µL	112µL	5µL
FT	(Lyophilized)	30 µL	3 µL	3µL	84µL	5µL
SFCS E1a+b+c	(Lyophilized)	30 µL	3 µL	3 µL	84µL	5µL
SFCS E2a+b	(Lyophilized)	40 µL	4 µL	4 µL	112µL	5µL
SFCS E2c	(Lyophilized)	20 µL	2 µL	2µL	112µL	5µL

6.2.3.2 Salt + EDTA Elution

Following washing the equilibrated beads, elution was performed incubating them in elution buffer containing 50mM Tris-HCl (pH 7.5); 0.15M NaCl; 5mM EDTA; 5mM EGTA; 1µM $ZnCl_2$; 0.5mM $CaCl_2$ and 0.02% (w/v) sodium azide. The supernatant E1a was collected after centrifugation at 4°C for 5minutes. This was repeated twice to collect E1b and E1c. A further elution was performed in elution buffer containing high salt concentration (0.3M, 2M or 5M as opposed to 0.15M). This was repeated three times and the flow-throughs termed E2a-c, E3a-c, and E4a-c. The beads were then washed twice with a further 10mL of elution buffer and the resultant flow-through discarded. The fractions E1a-c, E2a-c, E3a-c and E4a-c were pooled and labeled as E1, E2, E3 and E4, respectively. While desalting the fractions using NAP-5 columns, 10mM NH_4HCO_3 + 20µM EDTA was used to avoid

autolytic degradation of MMPs during the process. After lyophlization at 37ºC each fraction was resuspended in 20µL of HPLC grade water for further analyses.

6.2.4 Protein Extraction from Cells

6.2.4.1 Method I

The resulting cell pellet (HT1080 grown in serum-free medium) prepared as described in Materials and Methods section 2.3 was incubated in lysis buffer containing 50mM Tris-HCl (pH 7.5); 150mM NaCl; 10mM $CaCl_2$; 0.02% (w/v) NaN_3; 0.05% (v/v) Brij-35; 2mM PMSF for 10minutes at room temperature with vortexing to homogenize the sample. The cell homogenate was centrifuged at 12000g for 10minutes and the resultant supernatant containing the soluble MMPs collected (termed extract SE). The cell pellet was then incubated in lysis buffer containing 2% (v/v) DMSO for 10minutes, centrifuged at 12000g and the supernatant containing matrix- and membrane-bound MMPs (termed extract DE). The cell pellet was then further incubated in lysis buffer containing 10M urea for 10minutes, centrifuged at 12000g, and the supernatant containing the remaining MMPs collected (termed extract UE). The subsequent cell pellet was then stored at -20°C until further analyses.

6.2.4.2 Method II

The HT1080 cell pellet (grown in serum-free medium) prepared as described in Materials and Methods section 2.3 was incubated in lysis buffer containing 50mM Tris-HCl (pH 7.5); 150mM NaCl; 2% (v/v) DMSO; 10M urea; 10mM $CaCl_2$; 0.02% (w/v) NaN_3; 0.05% (v/v) Brij-35; 2mM PMSF for 10minutes at room temperature with vortexing to homogenize the sample. The cell homogenate was centrifuged at 12000g for 10minutes and the resultant supernatant collected. The cell pellet was then incubated in above lysis buffer for 10minutes, centrifuged at 12000g and the supernatant. The step was repeated one more time to ensure extraction of soluble and matrix MMPs and

collected supernatants pooled. The subsequent cell pellet was then stored at -20°C until further analyses.

6.2.5 Olive H-7G Chromatography of Cell Extracts

The proteins were purified from HT1080 cell extracts using 0.3M and 2M NaCl buffers without Brij-5 as described in Materials and Methods section 2.4 and 2.4.1.

6.3 Results

6.3.1 *In vitro* Models

In order to ensure that cells were harvested during their exponential growth phase, growth patterns were studied. Growth curves and a summary of growth characteristics of the HT1080 fibrosarcoma cell line and colon cancer cell line HT29 used in this study is presented in Figure 6.1. The HT1080 cells entered log phase of growth at day 2 with a lag phase of 1 day. The doubling time for the cells in log phase growth was calculated as 8.6hours. Following 4 days of growth, cells entered a plateau phase of growth. Growth rates varied between two cell lines as demonstrated by their doubling times. Although HT29 entered log phase at day 2 the number of cells was lower than that of HT1080 suggesting HT29 has a slower growth rate. From these data the optimum time of harvesting for both cell lines was identified.

6.3.2 LC-MS/MS of Foetal Calf Serum (FCS)

FCS generated 36 proteins (n=2) from automated LC-MALDI with search parameters (Taxonomy: Mammals, Partials: 2, MS/MS tolerance: 100ppm). The protein list from one of the repeats is shown in Appendix 7. These proteins will be deducted from the results obtained from various fraction produced from cell line culture supernatants assuming that trace amounts of serum left in the culture supernatant might have contributed towards the identification of the bovine proteins. Serum albumin (Accession No.: ALBU_BOVIN; Mass: 69.25) was observed with a Mascot score of 1654

(n=2). The number of peptides contributed towards the identification was 34 (n=2). The sequence of the peptides collectively identifying bovine serum albumin is shown in Appendix 8. These sequences will be matched/compared with peptides of MMPs identified in later experiments to find the sequence of competing parts of the two proteins to bind to Olive H-7G. The peptides highlighted in yellow were different in two separate LC-MALDI runs. The peptide RHPEYAVSVLLR in FCS (Repeat 1) appearing 3-times is because of the reason that it is detected on 3 different positions on target plate (J16, F1 and F8). The MH+ of the peptide is the same (1439.81) but individual ion scores (38.55, 79.2 and 74.5) are different.

6.3.3 HT1080 and HT29- S+CS vs. SFCS

6.3.3.1 Protein Quantification

Prior to isolating MMPs using H-7G-Sepharose chromatography beads and detecting with mass spectrometry, it was necessary to confirm the suitability of HT1080 and HT29 cell lines for the production of MMPs. Accurate and reproducible determination of protein concentration is a central requirement for proteomic analysis. HT1080 and HT29 cell lines were cultured and S+CS, SFCS (from HT1080 and HT29) and cell lysates (from HT1080 in serum-free media) were obtained as described in Materials and Methods sections 2.3 and 6.2.4, respectively. In order to determine the protein concentrations of test samples it was necessary to standardize sample dilution at 20-fold, to remove inaccuracies of the assay caused by high salt concentrations or detergents. Initially, protein concentrations were below the level of detection of the assay (62.5µg/mL), therefore it was necessary to concentrate the samples after desalting using NAP-5 columns. Following NAP-5 column enrichment, samples were then within the accurate range of the assay and concentrations could be calculated by interpolation of the standard curves. The gene expression studies on HT1080 and HT29 cell lines and their xenografts were determined using RT-PCR (by a colleague, Jennifer Atkinson at ICT) and they exhibited expression of a number of MMPs at different levels from low to very high (Figure 6.2). To confirm this data the

amounts of proteins in HT1080 and HT29 culture supernatants (50mL for each) and lysates (from 6million HT1080 cells) were determined by Bradford assay (Materials and Methods section 2.6; standard curve Figure 2.3) and results are shown in Table 6.2 and Table 6.3. Serum-containing culture supernatants contained a total of 64.43mg (±0.51mg) in a total volume of 50mL (n=3), whereas serum-free supernatants contained a total of 41.29mg (±1.64mg) in a total volume of 50mL (n=9). The amount of protein was much higher than expected which may be due to serum carry over. A strong albumin band (66kDa) in Coomassie blue-stained SDS-PAGE gels confirms this (Figure 6.6).

(A)

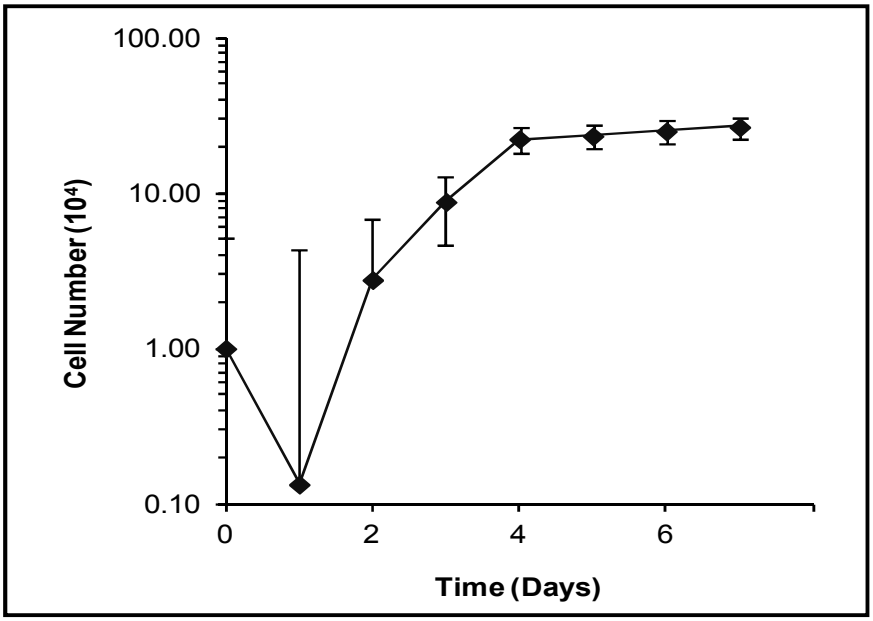

(B)

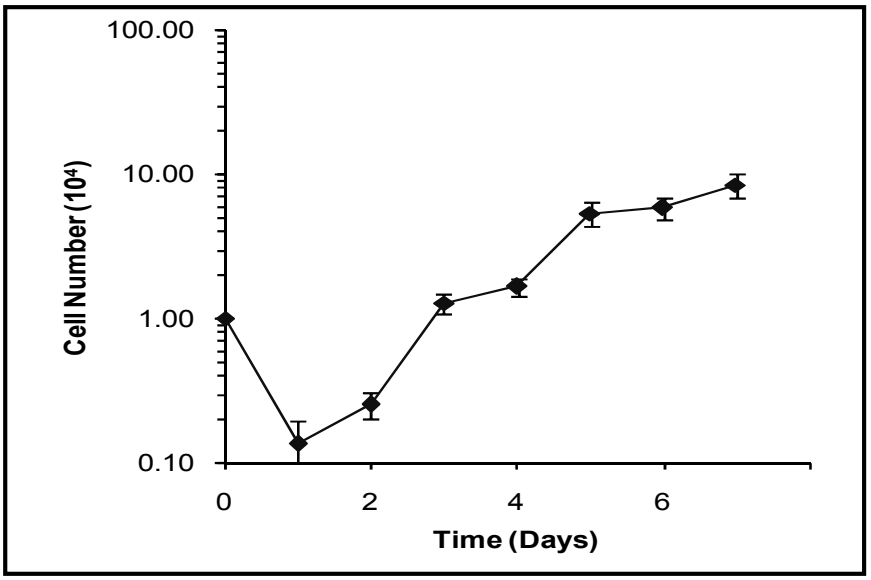

Figure 6.1 Tumour cell line growth curves.

HT1080 (A) and HT29 (B) cells growth curves. Cells were plated on day 0 at $1x10^3$ cells per flask. At daily intervals, a flask of cells was trypsinized and the total number of cells calculated.

Data representative of the mean ±SD of 3 independent experiments.

6.3.3.2 MMP-2 Production by HT1080 and HT29 Cell Lines

To confirm gene expression data the secreted and extracted MMP-2 amounts in the culture supernatants (S+CS, SFCS) and lysates (SE, DE and UE) were determined by ELISA assay (Materials and Methods section 2.7). The presence of MMP-2 in these samples was used as an indicator of the presence of a wide range of MMPs in HT1080 and HT29 cell lines. The standard curves for the assay were highly reproducible (n=25) showing linear correlation between amounts of standards and absorbance in the range 0.78-50ng/mL (Standard curve Figure 2.4). Preliminary analyses of culture supernatants indicated that the MMP-2 amounts were below the level of detection. Using NAP-5 columns to desalt and concentrate the samples, it was possible to measure the MMP-2 activity within the calibration range. The eluates from NAP-5 columns were lyophilized and then resuspended in minimum possible diluent (50µL of RD5-32 diluent). Another desalting device, Slide-A-Lyzer Dialysis Cassettes, was used to see if it is a better approach to enrich proteins. But it diluted the samples instead since it involves an overnight immersion of dialysis cassettes in dialysis buffer (Appendix 1). So, it was decided to desalt chromatography fractions using NAP-5 columns. Results for secreted and extracted MMP-2 are shown in Table 6.2 and Table 6.3, respectively. Interestingly, cell lysates (SE, DE and UE) showed MMP-2 activity which reflects the successful extraction of cellular MMPs. This is encouraging for profiling cellular MMPs. As predicted by gene expression data (Figure 6.2), MMP-2 was not detected in HT29 culture supernatants because the cell line is negative for the expression of the enzyme.

6.3.3.3 Protein Separation (SDS-PAGE)

Using Coomassie detection and silver staining, proteins were detectable in all serum-containing and serum-free culture supernatants of HT1080 (Figure 6.6) and HT29. No bands corresponding to pro-MMP-2 were detectable because possibly presence of albumin band corresponding to 66kDa hides the expression of closely resolved proteins. Although, NAP-5 concentrated

samples were loaded still MMPs amounts could be less than the detection limits for the stains in use.

6.3.3.4 Western Blotting of MMP-2

Analysis of gels in parallel to staining, using immuno-blotting were undertaken to determine the presence of MMP-2 in starting material (S+CS and SFCS). In order to determine whether MMP-2 was absent from these media, 30µg of protein was loaded on gels after being concentrated by NAP-5 columns. Immuno-blotting of these samples (SM) resulted in no identification of a band corresponding to molecular weight of 72kDa both in serum-containing and serum-free culture supernatants (Figure 6.8). MMP-2 could be present in amounts less than the detection limit of anti-MMP-2 antibody which was determined to be 0.3µg/mL. Immuno-blotting of HT29 culture supernatants using anti-MMP-2 antibody was not performed since it does not express MMP-2.

6.3.3.5 MALDI-MS

Based on the presence of proteins as shown by SDS-PAGE gels (some shown) and concentration found in ELISA (Table 6.2 and Table 6.3), S+CS, SFCS, SE, DE, UE (used as starting materials to apply on the H-7G-Sepharose chromatography beads) were analyzed manually by MALDI-MS. The S+CS showed very high expression of peptides as shown in Figure 6.3 which could be explained by the contribution of proteins from the FCS added to the media for cell culturing. Since the mass spectra were complicated with the serum present hence for the following experiments serum-free culture supernatants were used as a starting material hoping that the peptides, even though with lower intensity as compared to S+CS, are from the proteins secreted by the HT1080 cells into the media. Many of these mass peaks were found to be specific to proteins such as TIMPs, MMPs, kellikerin-6 etc. This was confirmed when these proteins were identified in SFCS subjected to automated analyses. A similar mass peak profile for the manual MALDI-MS of HT29 SFCS showed two signals (*m/z* 1156.29 and 1639.59) specific to MMP-7 as identified in rhMMP-7 (Appendix 5) with mass error of 0.17 and -

0.1, respectively. Mass spectra of cell extracts, SE, DE and UE, were gained from manual MALDI-MS analyses (Materials and Methods section.2.11) but specific peaks to MMPs could not be found. However, amounts of protein and MMP-2 in SE, DE and UE (Table 6.3) suggest that cell lysate extraction (method I) was successful but MALDI-MS methods need to be optimized to gain a better mass peak profile.

6.3.3.6 LC-MS/MS

To avoid proteins from FCS, HT1080 SFCS were selected as a starting material to apply on the H-7G-Sepharose chromatography beads. A sample was selected for LC-MS/MS in which 431ng/50mL of MMP-2 was detected by ELISA. However, among 69 proteins identified, only TIMP-1 (Mascot: score 112, No. of peptides: 5) and TIMP-2 (Mascot score: 86, No. of peptides: 1) were detected. In the following experiments, TIMP-1 and TIMP-2 were identified in HT1080 SFCS with significant Mascot scores. It was anticipated that enrichment through chromatography (reported later in this chapter) will bring the concentration of MMPs up to be compatible with LC-MS/MS. Since HT29 expresses MMP-7 in very high amounts, the MMP-7 (Mascot score: 126, No. of peptides: 8) was identified in HT29 SFCS by LC-MS/MS. Among 124 proteins, TIMP-1 was detected Mascot score 30 (No. of peptide: 2) which is border line significant. Although other proteins were also being identified, the detection of TIMP-2 and MMP-7 gave a confidence that as low volume as 50mL of the culture supernatant from the selected cell lines could be used and LC-MALDI methods could be optimized for screening the MMP enrichment capability of H-7G-Sepharose chromatography beads.

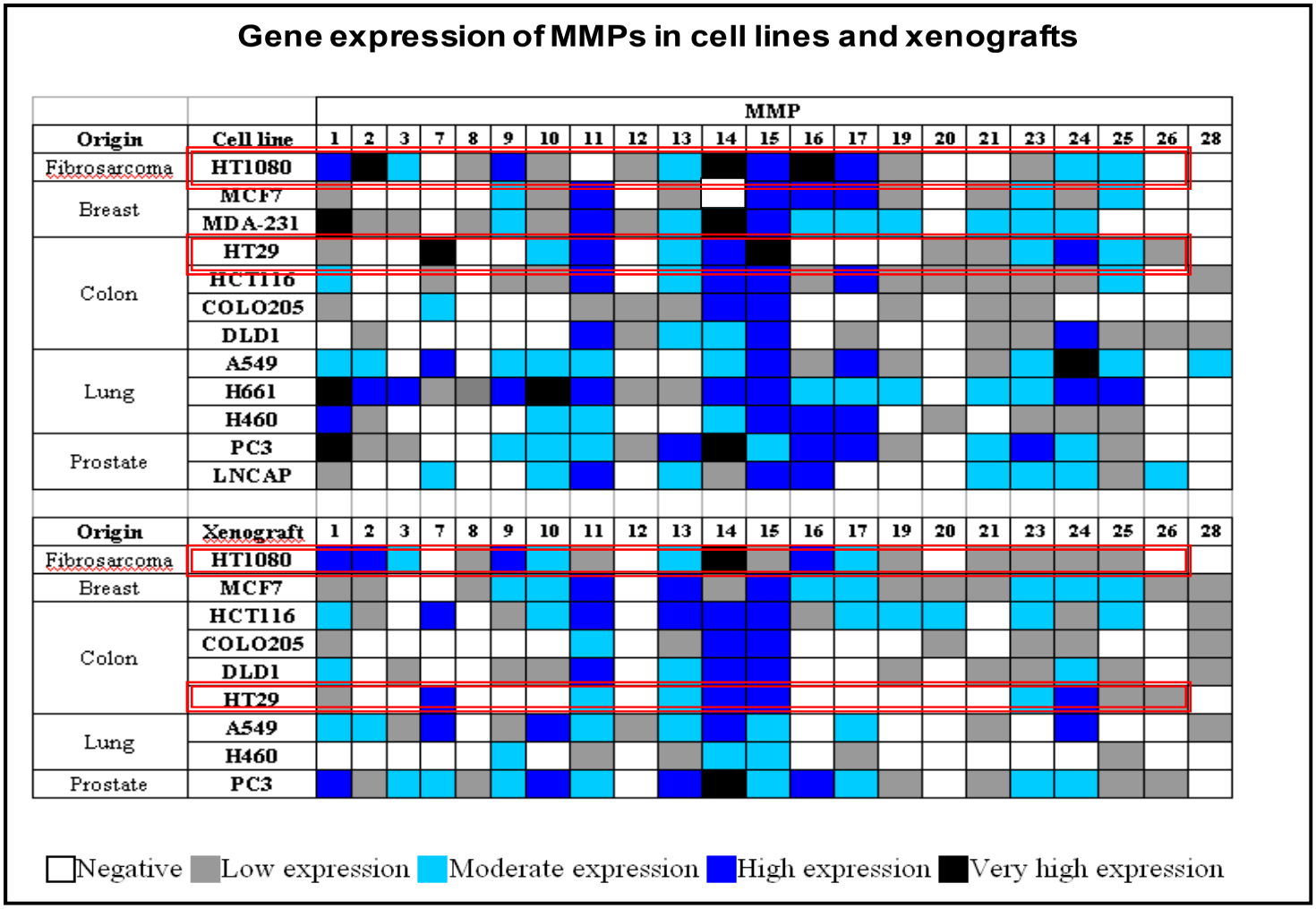

Figure 6.2 Gene expression of MMPs in cell lines. Rreproduced courtesy of Jenifer Atkinson, (Atkinson, Pennington et al. 2007).

Table 6.2 MMP-2 production by HT1080 and HT29 culture supernatants.

Cell Line	Sample	Protein Amount (Bradford Assay)		MMP-2 Amount (ELISA)	
		(mg)		(ng)	
	(50mL)	Mean	SD	Mean	SD
HT1080	S+CS	64.43 (n=3)	0.51	3447.33 (n=3)	1339.73
	SFCS	41.29 (n=9)	1.64	196.38 (n=9)	165.89
HT29	SFCS	43.35 (n=2)	1.05	ND	ND

S+CS: Serum-containing culture supernatant; SFCS: Serum-free culture supernatant; ND: Not detected.

Table 6.3 MMP-2 production by HT1080 cell lysates.

Cell Line	Sample	Protein Amount (Bradford Assay)		MMP-2 Amount (ELISA)	
		(mg)		(ng)	
	$6x10^6$	Mean (n=3)	SD	Mean (n=3)	SD
HT1080	SE	1.95	1.16	21.31	16.81
	DE	0.56	0.97	3.80	0.72
	UE	2.73	2.4	16.19	15.32

SE: Salt extract; DE: DMSO extract; UE: Urea extract.

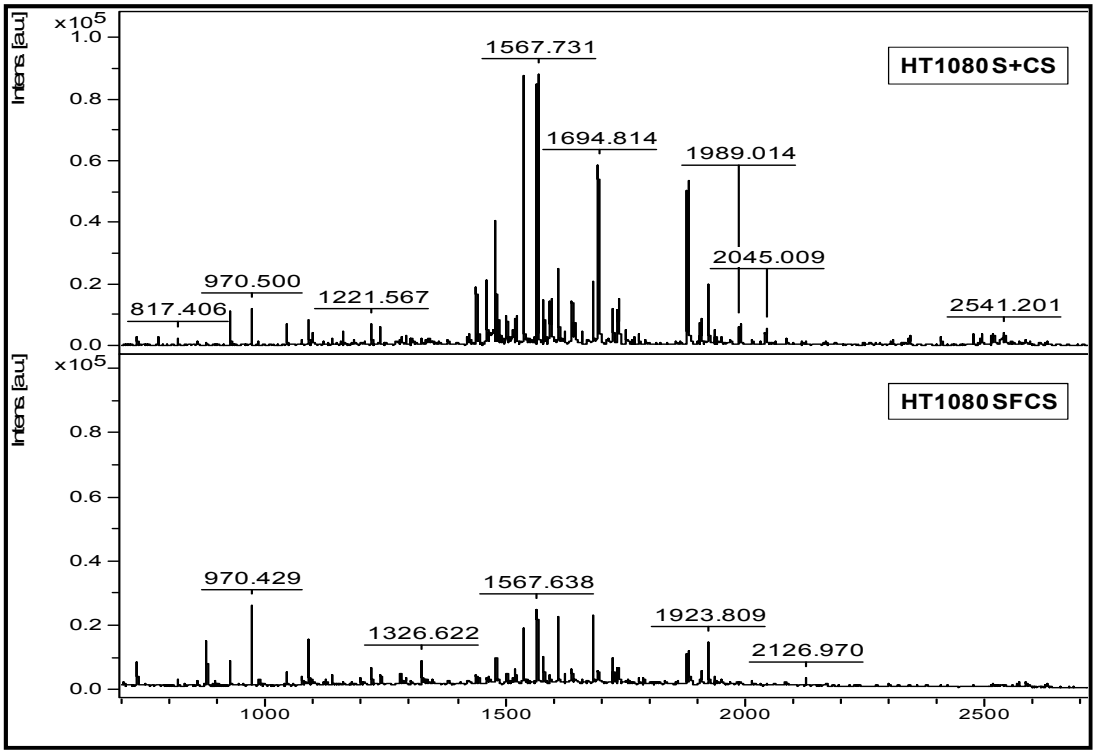

Figure 6.3 MALDI mass spectra of HT1080 S+CS and SFCS.

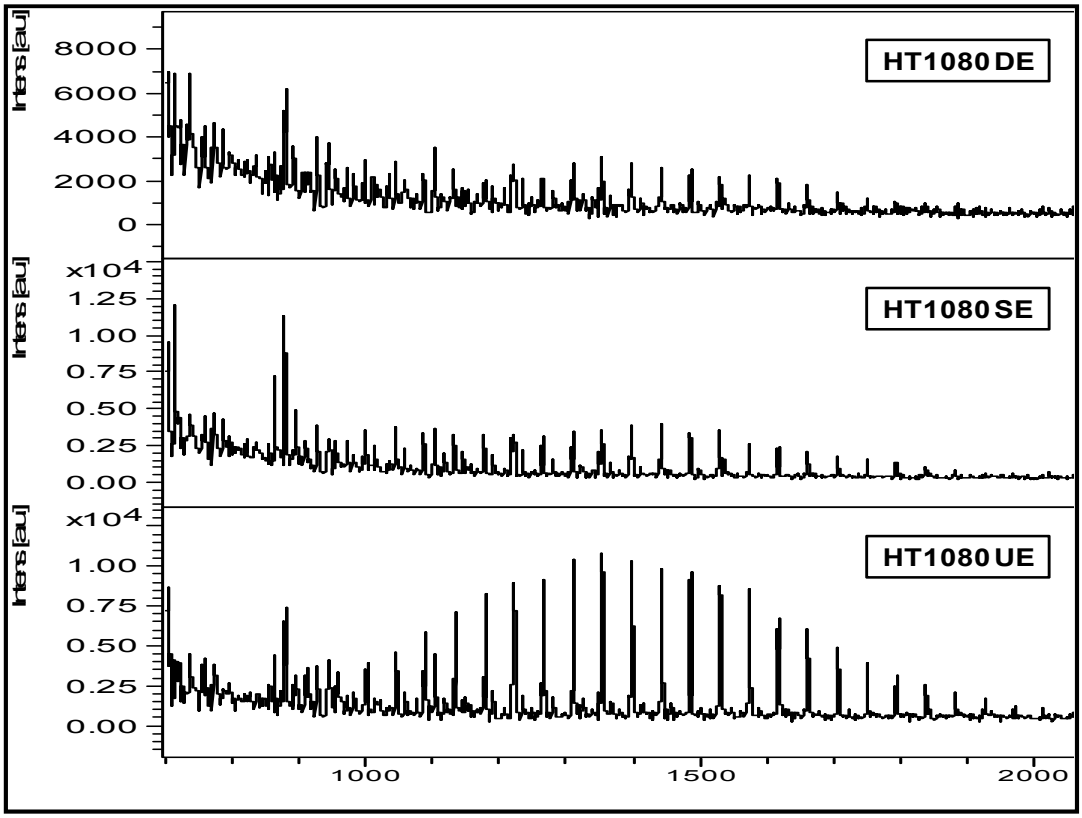

Figure 6.4 MALDI mass spectra of HT1080 cell lysates (SFCS).

6.3.4 Olive H-7G Chromatography- HT1080 S+CS vs. SFCS (Salt Elution)

6.3.4.1 Protein Quantification

In case of SFCS, due to the selective nature of binding by dye chromatography, most of the protein was in the flow-through. Proteins were detected in fractions eluted with various Brij-35 free elution buffers (0.3M and 2M NaCl). In each case most protein was eluted with the initial addition of salt (E1a and E2a), decreasing with each elution. Therefore, three volumes of eluate were sufficient to remove proteins at each salt concentration. The results of a representative H-7G-Sepharose chromatography are shown in Table 6.4. Some serum proteins were still present even after replacing serum-containing media and allowing cells to grow in serum-free conditions. Despite the selectivity of the Olive H-7G, the complex nature of serum means that some serum proteins may also compete with MMPs for binding sites and therefore limit the effectiveness of the chromatography. Protein yields could not be calculated in H-7G-Sepharose chromatography fractions since starting material SFCS has lower amount of protein (40.11mg) than determined in combined H-7G-Sepharose chromatography fractions. This could be because of handling error or starting material was too diluted.

6.3.4.2 MMP-2 Quantification (%age yield by H-7G-Sepharose Beads)

The concentration of the secreted MMP-2 in SM (HT1080 SFCS) and in H-7G-Sepharose chromatography fractions were determined using an ELISA based quantification kit to assure the reproducibility of chromatography. The standard curves for four chromatography experiments to confirm the reproducibility (n=4) showed linear correlation between amounts of standards and absorbance in the range 0.78-50ng/mL. The recovery of MMP-2 determined by ELISA in SFCS eluates by H-7G-Sepharose chromatography beads is 14.47% (Table 6.5). The data shown was generated by performing four independent experiments with fresh stock of HT1080 SFCS. As shown, most of the MMP-2 activity is being lost in wash flow-throughs and eluates

(E1a-c and E2a-c) but some is still bound to the H-7G-Sepharose chromatography beads. The yield is 14.47% if calculated by combining all the lost MMP-2 in wash flow-throughs and beads. This very low yield could possibly be because of the over-loading of ligand Olive H-7G with MMP-2 as there will be specific number of sites available for binding. Another reason might be that MMP-2 was degrading during extensive steps of washings.

Table 6.4 Protein amounts in HT1080 SFCS and H-7G-Sepharose chromatography fractions (Detergent-free elution buffers).

HT1080 SFCS	Volume	Protein Amount (Bradford Assay)
	(mL)	(mg) (n=1)
SM	50	40.11
FT	50	124.86
W1a	1	4.01
E1a	1	20.22
E1b	1	2.62
E1c	1	ND
E2a	1	3.03
E2b	1	2.37
E2c	1	ND
Beads	1	1.02

6.3.4.3 Protein Separation (SDS-PAGE)

SDS-PAGE and immuno-blotting was performed as a second approach to detect proteins if present. The capture of proteins by H-7G-Sepharose chromatography beads was confirmed by Coomassie and silver staining (Figure 6.5). Although these beads had been treated with elution buffers (0.3M and 2M NaCl), many proteins were still bound to the beads. In Coomassie detection of proteins in HT1080 cell culture media (in the presence and absence of serum) and in all fractions of chromatography performed using detergent-free elution buffers, many protein bands were detectable (Figure 6.6). It is clear that silver staining is more sensitive than Coomassie staining and better band visibility is attained. The presence of 66kDa albumin in S+CS and its corresponding chromatography fraction

masks the presence of other proteins in the similar mass range. Hence the use of serum was omitted in the following experiments and SFCS eluates did not show any sign of albumin as shown. This is not clear whether albumin binds to the Olive H-7G or leeching off the beads. No bands corresponding to MMP-2 were detectable in HT1080 cell culture media and in all fractions of chromatography performed using detergent-free elution buffers.

Table 6.5 MMP-2 amounts in HT1080 SFCS to show yield in H-7G-Sepharose chromatography.

HT1080 SFCS	MMP-2 Amounts (ELISA) (ng)		%age Yield Individual Fractions		%age Yield Total	
	Mean (n=4)	SD	Mean (n=4)	SD	Mean (n=4)	SD
SM	8377.70	711.70				
FT	234.88	1.84	2.80	0.26	14.47	0.26
W1a	44.80	5.61	0.53	0.79		
W1b	33.84	4.18	0.40	0.59		
E1a	26.60	53.19	0.32	7.47		
E1b	229.32	2.04	2.74	0.29		
E1c	209.09	11.77	2.50	1.65		
E2a	252.37	25.61	3.01	3.60		
E2b	131.93	14.23	1.57	2.00		
E2c	34.30	18.97	0.41	2.67		
Beads	15.27	9.40	0.18	1.32		

6.3.4.4 Western blotting of MMP-2

Immuno-blotting was performed to determine the presence of MMP-2 in starting material (S+CS and SFCS) and the fractions in which this protein is eluted. Protein (30µg) was loaded on gels after being concentrated by NAP-5 columns. Immuno-blotting of these samples resulted in the identification of a band corresponding to an approximate molecular weight of 72kDa in H-7G-Sepharose chromatography beads treated with S+CS after the 0.3M and 2M salt elution (Figure 6.7). The H-7G-Sepharose beads treated with SFCS did not show MMP-2 either due to elution of all the MMP-2 off the beads or very small amounts in SFCS to begin with. The success of H-7G-Sepharose chromatography is revealed by the immuno-blotting of MMP-2 that although levels in SFCS are below detection in the starting material or on beads,

elution with salt (0.3M) concentrated MMP-2 and demonstrated a band of the correct mass in eluates E1a and E1b (Figure 6.8). The SM however did not show any band. This suggests that chromatography concentrated the eluates while SM was too dilute hence not enough MMP-2 to be detected by the anti-MMP-2 antibody which requires at least 0.3µg/mL MMP-2.

6.3.4.5 MALDI-MS

As mentioned earlier, based on the peak pattern in mass spectrum from S+CS and presence of more albumin shown by gels, it was decided to analyze SFCS only for LC-MS/MS analyses. Initial experiments were performed using Brij-35 in elution buffers because it helps break the affinity between the proteins and the dye as reported in literature (Imai and Okada, 2008). But the mass peaks from the detergent were interfering with the data analysis (Figure 6.9). For removing detergent, samples were diluted 10-fold before desalting still there was detergent left to interfere with the specific pattern of peaks in spectra. The detergent could not be removed even after desalting sample dilutions twice, first using 1mL C18 columns and then using C18 zip tips to desalt when spotting sample on target plate for manual MALDI-MS analysis. Since presence of Brij-35 in elution buffers was causing problems in acquisition of specific mass spectra, it was decided to omit its use. Although literature supports the use of this detergent for the elution of MMPs off the ligand (Imai and Okada, 2008) yet we performed chromatography successfully using elution buffers without any detergent. To avoid any traces of detergents from distilled water, all buffers were prepared in HPLC grade water. The H-7G-Sepharose chromatography fractions and beads obtained were trypsinized as described in Materials and Methods section 2.9 and analyzed by manual MALDI-MS after desalting using C18 columns to see if there are any peaks showing presence of peptides. Based on the detection of peak pattern specific to peptides, the fractions were selected for LC-MS/MS analyses.

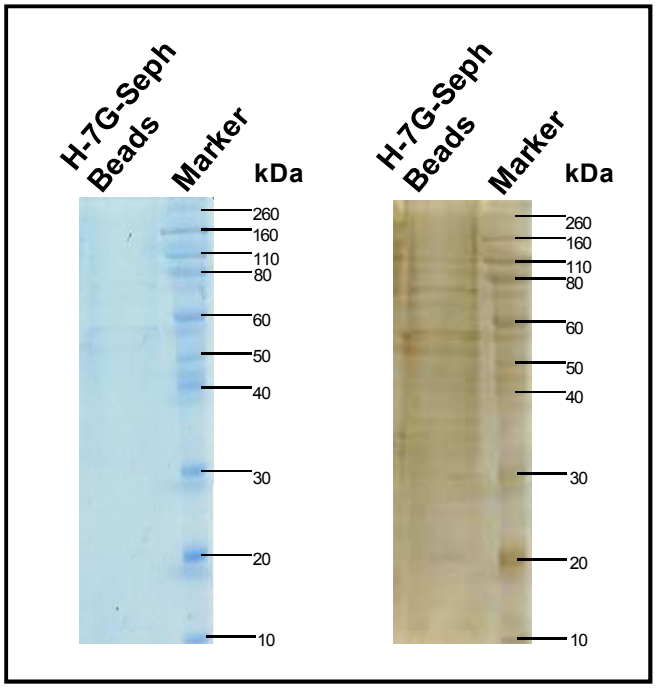

Figure 6.5 SDS-PAGE to show capture of proteins by H-7G-Sepharose chromatography beads.

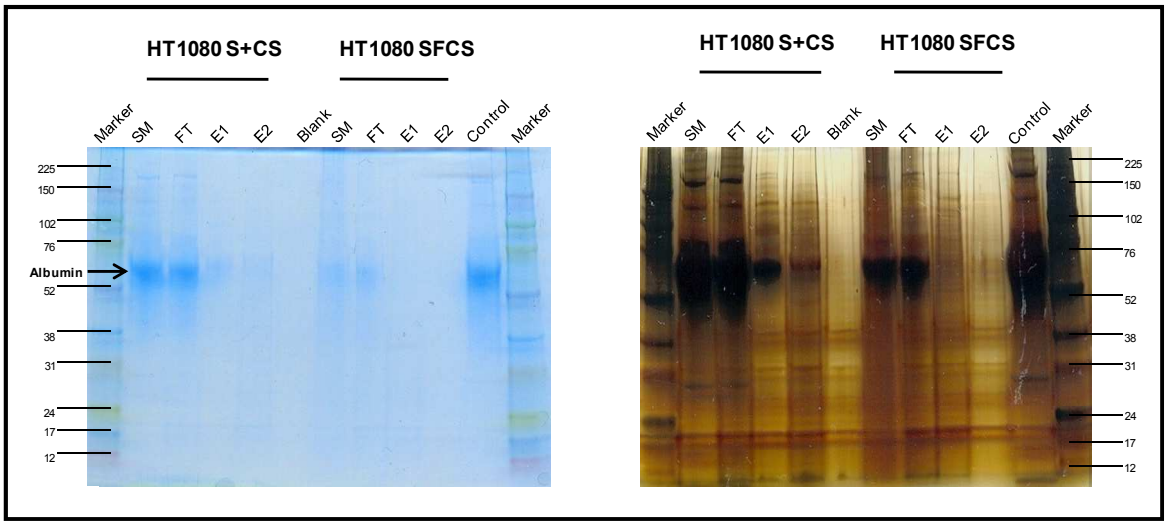

Figure 6.6 Staining of S+CS and SFCS H-7G-Sepharose chromatography fractions to show recovery of proteins.

Control: Concentrated HT1080 serum-containing culture supernatant.

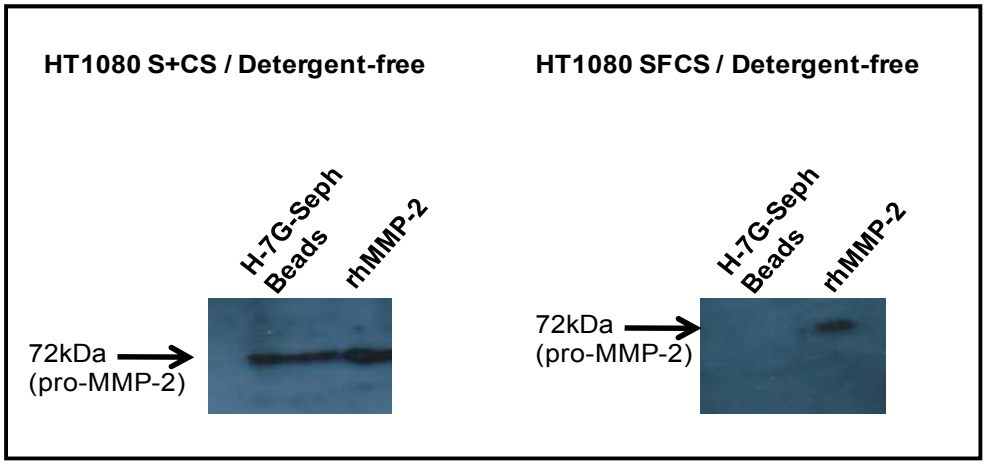

Figure 6.7 Immuno-blotting to show MMP-2 capture by H-7G-Sepharose chromatography beads (after elution) from HT1080 S+CS and SFCS.

rhMMP-2 (12.5ng/µL) was used as positive control.

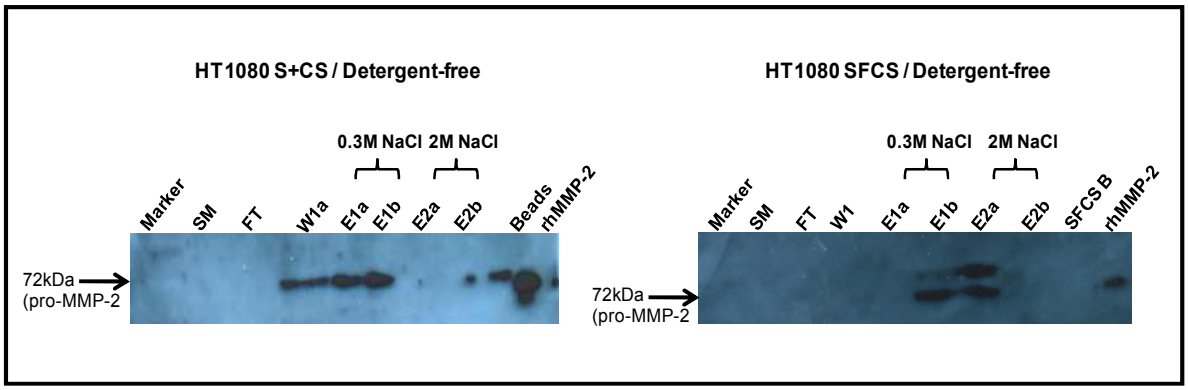

Figure 6.8 Immuno-blotting of HT1080 culture cupernatants and Olive H-7G chromatography fractions.

SM: Starting material, FT: Equilibration flow-through, W1a: Wash flow-through, E1a: Eluate1a, E1b: Eluate1b, E2a: Eluate 2a, E2b: Eluate2b, B: Beads, MMP-2: Recombinant human MMP-2 (12.5ng/µL) used as positive control.

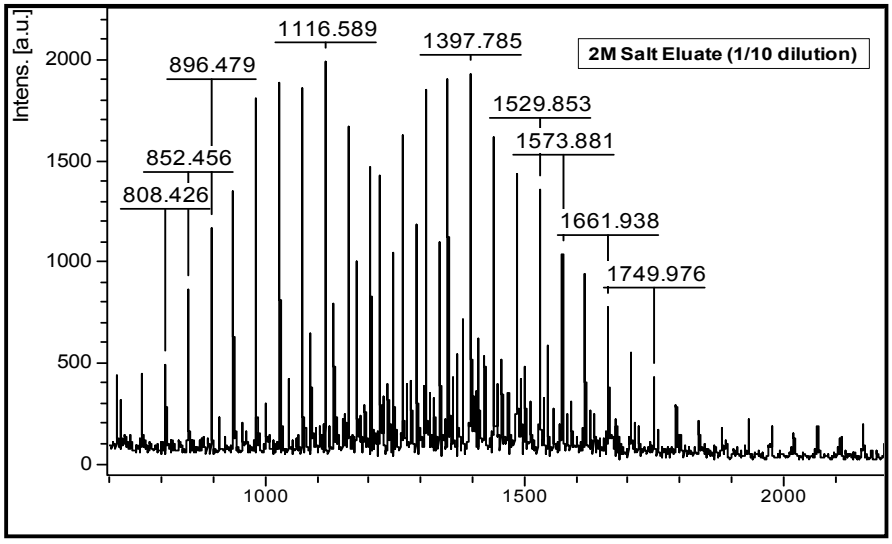

Figure 6.9 MALDI mass spectra of HT1080 eluate showing detergent peaks.

6.3.4.6 LC-MS/MS

The H-7G-Sepharose chromatography fraction from 2M NaCl (HT1080 SFCS E2a) was selected for LC-MS/MS because Coomassie stained gel and Bradford assay (1.25µg/mL) showed presence of proteins in the fraction. After the completion of MS/MS analysis, although a tissue inhibitor of metalloproteinases 1 (TIMP-1) was found; there was no MMP among 13 proteins in the sample. The Mascot score for TIMP-1 was 41 and was identified with two signature peptides (Table 6.6). Malate dehydrogenase which has been reported to bind to triazine dyes was considered as an in-house protein control assuming Olive H-7G bound to the protein and elution buffers reversed the affinity. The mitochondrial precursor of Malate dehydrogenase (MDHM) was identified with Mascot score 40 from 5 peptides in the same fraction. LC-MS/MS of the 2M NaCl eluate (HT1080 SFCS E2c) identified 57 proteins including tissue inhibitor of metalloproteinases 2 (TIMP-2) with a Mascot score = 146 (No. of peptides: 7) and MMP-14, Mascot score = 50 (No. of peptides: 3). The MDHM was detected with Mascot score 287 (No. of peptides: 13). Once subjected to LC-MS/MS analysis, 0.3M NaCl eluate (HT1080 SFCS E1a-c) identified 121 proteins including TIMP-1, TIMP-2 and matrix metalloproteinase-14 precursor (MMP-14 or MT-1-MMP). The

sequence and amino acid range of the peptides identifying these proteins is shown in Table 6.6. The peptides for MMPs are from hemopexin-like domains within the protein structure which is a part of the active enzyme. MMP-2 was identified in 0.3M NaCl eluate with a Mascot score of 145 with 3 peptides greater than threshold.

Table 6.6 Sequence of signature peptides in MMP-2, MMP-14, TIMP-1 and TIMP-2 detected in HT1080 SFCS eluates from 0.3 and 2M NaCl containing buffers.

Experiment No.	Chromatography fractions	Protein	Mascot Score	Peptide No.	Sequence	Modification
1	HT1080 SFCS 2M Eluate a	TIMP-1	41	2	GFQALGDAADIR	No modification
					EPGLCTWQSLR	No modification
		MDHM	40	4	GCDVVVIPAGVPR	Carbamidomethyl (C)
					TIIPLISQCTPK	Carbamidomethyl (C)
					AGAGSATLSMAYAGAR	Oxidation (M)
					VDFPQDQLTALTGR	
2	HT1080 SFCS 2M Eluate c	MMP-14	50	3	VWEGIPESPR	No modification
					GLPASINTAYER	No modification
					NIKVWEGIPESPR	No modification
		TIMP-2	146	7	FFACIK	Carbamidomethyl (C)
					IQYEIK	No modification
					FFACIKR	Carbamidomethyl (C)
					SDGSCAWYR	Carbamidomethyl (C)
					RSDGSCAWYR	Carbamidomethyl (C)
					EVDSGNDIYGNPIKR	No modification
					AVSEKEVDSGNDIYGNPIKR	No modification
		MDHM	287	13	ANTFVAELK	No modification
					IQEAGTEVVK	No modification
					MISDAIPELK	Oxidation (M)
					VNVPVIGGHAGK	No modification
					TIIPLISQCTPK	Carbamidomethyl (C)
					NLGIGKVSSFEEK	No modification
					AGAGSATLSMAYAGAR	Oxidation (M)
					GYLGPEQLPDCLK	Carbamidomethyl (C)
					VDFPQDQLTALTGR	No modification
					ANTFVAELKGLDPAR	No modification
					GLDPARVNVPVIGGHAGK	No modification
					GIEKNLGIGKVSSFEEK	No modification
					LTLYDIAHTPGVAADLSHIETK	No modification

3	HT1080 SFCS 0.3M Eluate 1-c	MMP-14	33	1	VWEGIPESPR	Carbamidomethyl (C)
		TMP-1	41	4	HLACLPR	Carbamidomethyl (C)
					FVYTPAMESVCGYFHR	2Carbamidomethyl (C)
					ACTCVPPHPQTAFCNSDLVIR	Carbamidomethyl (C)
					LQDGLLHITTCSFVAPWNSLSLAQR	No modification
		TIMP-2	83	2	EVDSGNDIYGNPIKR	No modification
					AVSEKEVDSGNDIYGNPIKR	No modification
		MDHM	131	4	IFGVTTLDIVR	No modification
					GCDVVVIPAGVPR	Carbamidomethyl (C)
					VDFPQDQLTALTGR	No modification
					LTLYDIAHTPGVAADLSHIETK	No modification
4	HT1080 SFCS 0.3M Eluate 1-c	MMP-2	145	3	AFQVWSDVTPLR	No modification
					IIGYTPDLDPETVDDAFAR	No modification
					FFGLPQTGDLDQNTIETMR	Oxidation (M)
		TIMP-1	276	8	HLACLPR	No modification
					GFQALGDAADIR	No modification
					EPGLCTWQSLR	No modification
					FVYTPAMESVCGYFHR	No modification
					FVYTPAMESVCGYFHR	Oxidation (M)
					HLACLPREPGLCTWQSLR	No modification
					LQSGTHCLWTDQLLQGSEK	No modification
					LQSGTHCLWTDQLLQGSEKGFQSR	No modification
		TIMP-2	177	7	FFACIK	No modification
					FFACIKR	No modification
					SDGSCAWYR	No modification
					RSDGSCAWYR	No modification
					GAAPPKQEFLDIEDP	No modification
					EVDSGNDIYGNPIKR	No modification
					AVSEKEVDSGNDIYGNPIKR	No modification
		MDHM	251	6	IFGVTTLDIVR	No modification
					GCDVVVIPAGVPR	No modification
					VDFPQDQLTALTGR	No modification
					HGVYNPNKIFGVTTLDIVR	No modification
					LTLYDIAHTPGVAADLSHIETK	No modification
					GYLGPEQLPDCLKGCDVVVIPAGVPR	No modification

6.3.5 H-7G Chromatography of HT1080 SFCS (EDTA Elution)

6.3.5.1 LC-MS/MS

When EDTA was used, as an alternative to NaCl, to elute proteins bound to H-7G-Sepharose, TIMP-1 and TIMP-2 were detected in tandem mass spectrometry of the chromatography fractions (Table 6.7). Although ELISA indicated an MMP-2 concentration of 9.94ng/mL in the SM (HT1080 SFCS), proteomics analysis did not detect the enzyme (Table 6.7). The smaller number of proteins in SM and FT than in eluates shows that affinity chromatography is an enrichment method. Neither method detected MMP-2 in the FT, 10mM (E1a-c) or 100mM EDTA eluates (E2a+b and E2c) as shown in Table 6.7. TIMP-1 and TIMP-2 were detected by proteomics analysis in the SM and eluted in E2, but not in the FT and E1. However, 17 and 38 proteins were also detected along with TIMPs in 100mM EDTA sequential fractions E2a+b and E2c respectively, indicating elution was not specific. Moreover, the protein Malate dehydrogenase is eluting off in 100mM EDTA buffer. The list of the proteins (human) in all the eluate fractions from 10mM and 100mM EDTA elution buffers is shown in Table 6.8. As anticipated, albumin was detected in all the eluates (highlighted blue in Table 6.8). The green highlighted proteins are only coming off the chromatography beads with 100mM EDTA. Of these proteins, kellikerin-6 is a potential serum cancer biomarker. Galectin-3 is used in studies where tumours are resistant to chemotherapy. The un-highlighted proteins are specific to the EDTA concentration in which these are being identified.

Table 6.7 Protein (BA) and MMP-2 amounts (ELISA) in EDTA eluates (10mM, 100mM) and LC-MS/MS results.

HT1080 SFCS	BA	ELISA	LC-MS/MS	TIMP-1		TIMP-2	
	Protein (mg/50mL)	MMP-2 (ng/50mL)	No. of Proteins	Mascot Score	Peptide #	Mascot Score	Peptide #
SM	41.3	497	17	112	5	86	1
FT	ND	ND	4	-	-	-	-
10mM E1a-c	ND	ND	15	-	-	-	-
100mM E2a+b	ND	ND	17	44	2	48	2
100mM E2c	ND	ND	38	82	7	71	2

ND: Note detected

Table 6.8 Proteins eluted in 10mM and 100mM EDTA.

SM	FT	E1-c (10mM EDTA elution)	E2a+b (100mM EDTA elution)	E2c (100mM EDTA elution)
60S ribosomal protein L30	Non-histone chromosomal protein HMG-17	Serum albumin	Keratin, type II cytoskeletal 1	Cystatin-C
C-X-C motif chemokine 5	Serum albumin OS=Homo sapiens	High mobility group protein B1	Serum albumin	Kallikrein-6
Cystatin-C	High mobility group nucleosome-binding domain-containing protein 3	Keratin, type II cytoskeletal 1	Cystatin-C	Serum albumin
Fibronectin	Protein MON2 homolog OS=Homo sapiens	Non-histone chromosomal protein HMG-17	Alpha-enolase	Alpha-enolase
Growth/differentiation factor 15		Keratin, type II cytoskeletal 2 epidermal	Lactotransferrin	10 kDa heat shock protein, mitochondrial
Histone H1.5		Angiogenin	Kallikrein-6	Peptidyl-prolyl cis-trans isomerase A
Histone H2A type 1-A		High mobility group nucleosome-binding domain-containing protein 4	Metalloproteinase inhibitor 2	Stathmin
Kallikrein-10		Insulin-like growth factor-binding protein 7	10 kDa heat shock protein, mitochondrial	Metalloproteinase inhibitor 1
Keratin, type I cuticular Ha1		Keratin, type I cytoskeletal 9	Metalloproteinase inhibitor 1	Malate dehydrogenase, cytoplasmic
Keratin, type I cuticular Ha3-II		Cadherin-23	Protein disulfide-isomerase A3	Non-histone chromosomal protein HMG-17
Proteasome subunit beta type-1		Amyloid beta A4 protein	Methyl-CpG-binding protein 2	Metalloproteinase inhibitor 2
Pyruvate kinase isozymes M1/M2		Myotubularin-related protein 9	Phosphoglycerate kinase 1	Insulin-like growth factor-binding protein 2
Serum albumin		Roquin	Galectin-3	Eukaryotic translation initiation factor 5A-1
Signal recognition particle 9 kDa protein		Keratin, type I cytoskeletal 10	Fructose-bisphosphate aldolase A	Lactotransferrin
Small nuclear ribonucleoprotein Sm D3		Mesencephalic astrocyte-derived neurotrophic factor	Cadherin-23	Polypyrimidine tract-binding protein 1
Splicing factor, proline- and glutamine-rich			Kininogen-1	Galectin-3
Uncharacterized protein C10orf68			Peroxiredoxin-1	Keratin, type II cytoskeletal 1
				Protein disulfide-isomerase A3
				Inter-alpha-trypsin inhibitor heavy chain H2
				Malate dehydrogenase, mitochondrial
Common between E1a-c and E2a+b				Abhydrolase domain-containing protein 8
Common between E2a+b and E2c				Nucleosome-remodeling factor subunit BPTF
Common among E1a-c, E2a+b and E2c				Protein piccolo
				Filamin-A
				Alpha-fetoprotein
				Antithrombin-III
				Tetraspanin-14
				Transcription termination factor 2
				Fructose-bisphosphate aldolase A
				Sperm-associated antigen 1
				Methyl-CpG-binding protein 2
				Vinculin
				Kininogen-1
				Cadherin-23
				Glutathione S-transferase P
				Peroxiredoxin-1
				Heterogeneous nuclear ribonucleoprotein A1
				High mobility group nucleosome-binding domain-containing protein 3

6.3.6 H-7G Chromatography of HT1080 SFCS (Salt + EDTA Elution)

6.3.6.1 LC-MS/MS

The higher number of proteins in eluate E1 (75) and E4 (82) suggest that neither a lower salt concentration of 0.15M nor a very high concentration of 5M NaCl is optimum for binding of proteins to Olive H-7G (Table 6.9). On the other hand, 0.3M and 2M salt concentration elute proteins specifically as 16 proteins were common in all the four eluates. The proteins shown in Table 6.10 were identified in eluates E1, E2, E3 and E4 from 0.15M, 0.3M, 2M and 5M NaCl buffers containing EDTA, respectively. These salt concentrations seem to help proteins to disengage from beads and go into solution. Although no MMPs were identified however, with increasing salt concentration in elution buffers, TIMPs were being identified with better Mascot scores (Table 6.9).

Table 6.9 TIMP-1 and TIMP-2 Mascot scores in Salt + EDTA eluates.

HT1080 SFCS	BA	ELISA	LC-MS/MS	TIMP-1		TIMP-2	
	Protein (mg/50mL)	MMP-2 (ng/50mL)	No. of Proteins	Mascot Score	Peptide #	Mascot Score	Peptide #
SM	39.14	164.04	19	-	-	34	2
FT	ND	ND	12	-	-	-	-
0.15 M NaCl E1	ND	ND	75	-	-	53	3
0.3 M NaCl E2	ND	ND	47	56	4	95	2
2M NaCl E3	ND	ND	41	58	3	106	5
5M NaCl E4	ND	ND	82	185	4	193	6

ND: Not detected

Table 6.10 Proteins eluted in Salt + EDTA elution buffers.

SM	FT	E1 (0.15M NaCl elution)	E2 (0.3M NaCl elution)	E3 (2M NaCl elution)	E4 (5M NaCl elution)
14-3-3 protein sigma	Alpha-2-antiplasmin	10 kDa heat shock protein, mitochondrial	10 kDa heat shock protein, mitochondrial		10 kDa heat shock protein, mitochondrial
14-3-3 protein zeta/delta	Alpha-2-HS-glycoprotein	5'-nucleotidase domain-containing protein 3			60S ribosomal protein L30
Calsyntenin-1	Amyloid beta A4 protein	78 kDa glucose-regulated protein	78 kDa glucose-regulated protein	78 kDa glucose-regulated protein	78 kDa glucose-regulated protein
DNA replication licensing factor MCM4	CASP8-associated protein 2	Actin, cytoplasmic 1	Actin, cytoplasmic 1	Actin, cytoplasmic 1	Actin, cytoplasmic 1
Fibronectin	CD44 antigen	Agrin	Alpha-enolase	Amyloid beta A4 protein	Activated RNA polymerase II transcriptional coactivator p15
Galectin-3-binding protein	Clusterin	Alpha-enolase	Amyloid beta A4 protein	Annexin A2	Adenylate kinase 2, mitochondrial
Heat shock 70 kDa protein 6	Cystatin-C	Amyloid beta A4 protein	Annexin A2	Antileukoproteinase	Agrin
Heat shock cognate 71 kDa protein	Fibulin-1	Annexin A2	Anterior gradient protein 2 homolog	Cadherin-1	Amyloid beta A4 protein
Heat shock protein 75 kDa, mitochondrial	Galectin-3-binding protein	Antileukoproteinase	Beta-2-syntrophin	DNA-(apurinic or apyrimidinic site) lyase	Angiogenin
Heat shock protein HSP 90-alpha	Heat shock cognate 71 kDa protein	ATP synthase subunit alpha, mitochondrial	Calreticulin	Endoplasmic reticulum resident protein 29	Annexin A1
Heat shock protein HSP 90-beta	Hemoglobin subunit alpha	Beta-enolase	Chitinase-3-like protein 1	Ezrin	Annexin A2
Histone H4	Hemoglobin subunit beta	Blood vessel epicardial substance	Collagen alpha-2(IV) chain	Fibroblast growth factor-binding protein 1	Antileukoproteinase
Metalloproteinase inhibitor 2	Histone H2A type 1-A	Calmodulin	DNA-(apurinic or apyrimidinic site) lyase	Fibronectin	Cadherin-1
Neuralized-like protein 4	Inter-alpha-trypsin inhibitor heavy chain H2	Calreticulin	EGF-containing fibulin-like extracellular matrix P1	Fructose-bisphosphate aldolase A	Calreticulin
POTE ankyrin domain family member E	Inter-alpha-trypsin inhibitor heavy chain H3	Calsyntenin-1	Elongation factor 1-alpha 1	Heat shock protein HSP 90-alpha	Citrate synthase, mitochondrial
Serum albumin	Keratin, type II cytoskeletal 1	Chloride intracellular channel protein 1	Endoplasmin	Heterogeneous nuclear ribonucleoprotein D0	Coproporphyrinogen-III oxidase, mitochondrial
SPARC	Kininogen-1	Clusterin	Ezrin	Heterogeneous nuclear ribonucleoprotein G	DNA-(apurinic or apyrimidinic site) lyase
Tetraspanin-14	Lactotransferrin	Coiled-coil domain-containing protein 157	Fibronectin	Heterogeneous nuclear ribonucleoproteins A2/B1	Dystrophin-related protein 2
Triosephosphate isomerase	Liprin-alpha-3	Collagen alpha-2(IV) chain	Galectin-3	Histone H2A type 1-A	Endoplasmic reticulum resident protein 29
	Metalloproteinase inhibitor 1	Complement component 1 Q subcomponent-binding protein	Glutaminyl-peptide cyclotransferase	Histone H4	Extracellular matrix protein 1
	Midasin	DNA-(apurinic or apyrimidinic site) lyase	Glutathione reductase, mitochondrial	Insulin-like growth factor-binding protein 7	Ezrin
	Peroxiredoxin-1	EGF-containing fibulin-like extracellular matrix protein 1	Heat shock cognate 71 kDa protein	Kallikrein-10	Fibroblast growth factor-binding protein 1
	POTE ankyrin domain family member E	Elongation factor 1-alpha 1	Heat shock protein 75 kDa, mitochondrial	L-lactate dehydrogenase A chain	Fibronectin
Common between E1 & E2	Probable 3-hydroxymethyl-3-methylglutaryl-CoA lyase 2	Elongation factor 1-alpha 2	Heat shock protein HSP 90-alpha	L-lactate dehydrogenase B chain	Filamin-A
Common between E1 & E3	Protein MON2 homolog	Elongation factor 2	Heterogeneous nuclear ribonucleoprotein A1	Malate dehydrogenase, cytoplasmic	Fructose-bisphosphate aldolase A
Common between E1 & E4	Protein piccolo	Endoplasmin	Histone H2A type 1-A	Malate dehydrogenase, mitochondrial	Galectin-3
Common between E2 & E3	Protein TANC1	Fibronectin	Histone H4	Metalloproteinase inhibitor 1	Gelsolin
Common between E2 & E4	Putative beta-actin-like protein 3	Filamin-A	Lamin-A/C	Metalloproteinase inhibitor 2	Glucose-6-phosphate 1-dehydrogenase
Common between E3 & E4	Serum albumin	Filamin-B	L-lactate dehydrogenase A chain	Nucleoside diphosphate kinase B	GMP reductase 2
Common among E1, E2 & E3	SPARC	Galectin-3	L-lactate dehydrogenase B chain	Peptidyl-prolyl cis-trans isomerase B	Growth/differentiation factor 15
Common among E1, E2 & E4	Sulfhydryl oxidase 1	Galectin-3-binding protein	Malate dehydrogenase, cytoplasmic	Peroxiredoxin-1	Heat shock cognate 71 kDa protein
Common among E1, E3 & E4	Thrombospondin-1	Gamma-glutamyl hydrolase	Malate dehydrogenase, mitochondrial	POTE ankyrin domain family member E	Heat shock protein HSP 90-alpha
Common among E2, E3 & E4	Triosephosphate isomerase	Glucosidase 2 subunit beta	Metalloproteinase inhibitor 1	Procollagen-lysine,2-oxoglutarate 5-dioxygenase 3	Heat shock protein HSP 90-beta
Common among E1, E2, E3, E4	Ubiquitin	Glutaminyl-peptide cyclotransferase	Metalloproteinase inhibitor 2	Protein disulfide-isomerase A3	Heterogeneous nuclear ribonucleoproteins A2/B1
	Vitamin D-binding protein	Glutathione reductase, mitochondrial	Neuropilin-1	Protein disulfide-isomerase A6	High mobility group protein B1
		Glyceraldehyde-3-phosphate dehydrogenase	Nucleolin	Putative heterogeneous nuclear ribonucleoprotein A1-like 3	Histone H2A
		Glypican-1	Peptidyl-prolyl cis-trans isomerase B	Quinone oxidoreductase	Histone H4
		Heat shock 70 kDa protein 1A/1B	Peroxiredoxin-1	Small nuclear ribonucleoprotein Sm D1	Insulin-like growth factor-binding protein 7
		Heat shock cognate 71 kDa protein	Procollagen-lysine,2-oxoglutarate 5-dioxygenase 3	Small nuclear ribonucleoprotein Sm D3	Kallikrein-10
		Heat shock protein 75 kDa, mitochondrial	Protein disulfide-isomerase A3	Sulfhydryl oxidase 1	Kunitz-type protease inhibitor 1
		Heat shock protein HSP 90-alpha	Protein disulfide-isomerase A4	Thioredoxin domain-containing protein 5	Filamin-A
		Heat shock protein HSP 90-beta	Serum albumin	Thrombospondin-1	L-lactate dehydrogenase A chain
		Histone H2A type 1-A	Small nuclear ribonucleoprotein Sm D3	Voltage-dependent L-type calcium channel subunit b-2	L-lactate dehydrogenase B chain
		Histone H3-like	Sulfhydryl oxidase 1		Malate dehydrogenase, cytoplasmic
		Histone H4	Suppressor of tumorigenicity 14 protein		Malate dehydrogenase, mitochondrial
		Kallikrein-6	Suprabasin		Mesencephalic astrocyte-derived neurotrophic factor
		Keratin, type II cytoskeletal 8	Thioredoxin-dependent peroxide reductase		Metalloproteinase inhibitor 1
		L-lactate dehydrogenase A chain	Thrombospondin-1		Metalloproteinase inhibitor 2
		L-lactate dehydrogenase B chain			Moesin
		Lysosome-associated membrane glycoprotein 2			Neutral alpha-glucosidase AB
		Malate dehydrogenase, cytoplasmic			Non-histone chromosomal protein HMG-17
		Malate dehydrogenase, mitochondrial			Nucleoside diphosphate kinase A
		Metalloproteinase inhibitor 2			Nucleoside diphosphate kinase B
		Moesin			Nucleosome assembly protein 1-like 1
		Neutrophil gelatinase-associated lipocalin			Peptidyl-prolyl cis-trans isomerase B
		Olfactory receptor 8J2			Peroxiredoxin-1
		Peptidyl-prolyl cis-trans isomerase A			POTE ankyrin domain family member E
		Peptidyl-prolyl cis-trans isomerase B			Procollagen-lysine,2-oxoglutarate 5-dioxygenase 3
		Proteasome subunit alpha type-1			Protein disulfide-isomerase A3
		Proteasome subunit alpha type-6			Protein disulfide-isomerase A4
		Protein disulfide-isomerase			Protein disulfide-isomerase A6
		Protein disulfide-isomerase A3			Putative heterogeneous nuclear ribonucleoprotein A1-like 3
		Receptor-type tyrosine-protein phosphatase kappa			Quinone oxidoreductase
		S-adenosylmethionine synthetase isoform type-2			Radixin
		Serine/threonine-protein kinase TAO3			Ras-GEF domain-containing family member 1A
		Serum albumin			Rho GTPase-activating protein 30
		Stress-70 protein, mitochondrial			Ribonuclease 4
		Sulfhydryl oxidase 1			RNA-binding protein EWS
		Syndecan-1			Small nuclear ribonucleoprotein G-like protein
		Thioredoxin reductase 1, cytoplasmic			Small nuclear ribonucleoprotein Sm D1
		Thrombospondin-1			Small nuclear ribonucleoprotein Sm D2
		Transforming growth factor-beta-induced protein ig-h3			Small nuclear ribonucleoprotein Sm D3
		Tubulin alpha-1A chai			Small nuclear ribonucleoprotein-associated proteins B and B
		Tyrosine-protein phosphatase non-receptor type 21			Splicing factor, arginine/serine-rich 1
		Ubiquitin			Splicing factor, arginine/serine-rich 3
					Sulfhydryl oxidase 1
					Thioredoxin domain-containing protein 5
					Thrombospondin-1
					Transferrin receptor protein 1
					Transforming growth factor-beta-induced protein ig-h3
					Voltage-dependent L-type calcium channel subunit alpha-1F

6.3.7 H-7G Chromatography of HT1080 SF Cell Extract

6.3.7.1 Protein Quantification

The HT1080 cell lysates (salt extract, DMSO extract and urea extract) prepared by method I as described in section 6.2.4.1 showed a significant protein yield. Lower protein amount in SE (1.95mg/mL) than in flow-through (2.6mg/mL) (Table 6.11) could be explained by the fact that binding of Bradford reagent and proteins is occurring only in chromatography fractions because chromatography beads might remove interfering components in original lysate. Urea extract showed maximum amount (2.73mg/mL) of proteins measured by Bradford assay (Table 6.13) and an 84.24% yield was achieved from combined fractions.

6.3.7.2 MMP-2 Quantification

The results for salt extract (prepared as Method I; section 6.2.4.1) and its corresponding chromatography fractions (Table 6.11) showed that most of the proteins were not binding to the beads and leaching off in equilibration flow-through and washes (4.43ng + 5.35ng respectively out of 21.31ng in salt extract). MMP-2 amounts were measured in salt extract fractions showing a 59.17% yield when calculated by combining all the activities including flow-through (or column washes). MMP-2 activities measured in DMSO extract (prepared as Method I; section 6.2.4.1) and H-7G-Sepharose chromatography beads (Table 6.12) showed same response as there was more enzyme in flow-through fractions (3.40ng + 4.18ng) than in the SM (3.80ng) as seen for SE (Table 6.11). MMP-2 amounts in urea extract (prepared as Method I; section 6.2.4.1) measured by ELISA (50.60% yield from combined fractions) are in accordance with the expected profile for chromatography where some proteins are lost in the washes (4.60ng + 1.58ng), then eluted in elution buffers (0.85ng + 1.05ng) with no proteins left bound to the beads (0.12ng).

Table 6.11 Protein (BA) and MMP-2 (ELISA) amounts in HT1080 cells Salt Extract and H-7G-Sepharose chromatography fractions.

Sample	Protein Amount (Bradford Assay) (mg)		MMP-2 Amount (ELISA) (ng)	
	Mean (n=3)	SD	Mean (n=3)	SD
SE	1.95	1.16	21.31	16.81
SE Beads	0.00	0.00	1.28	1.34
SE FT	2.60	2.25	4.43	4.68
SE W	0.10	0.17	5.35	4.28
SE 0.3M NaCl E	0.00	0.00	0.98	0.98
SE 2M NaCl E	0.01	0.02	0.57	0.35

Table 6.12 Protein (BA) and MMP-2 (ELISA) amounts in HT1080 cells DMSO Extract and H-7G-Sepharose chromatography fractions.

Sample	Protein Amount (Bradford Assay) (mg)		MMP-2 Amount (ELISA) (ng)	
	Mean (n=3)	SD	Mean (n=3)	SD
DE	0.56	0.97	3.80	0.72
DE Beads	0.08	0.14	0.23	0.29
DE FT	1.48	2.43	3.40	2.97
DE W	1.57	1.36	4.18	0.83
DE 0.3M NaCl E	0.26	0.45	0.94	0.62
DE 2M NaCl E	0.23	0.39	0.94	0.73

Table 6.13 Protein (BA) and MMP-2 (ELISA) amounts in HT1080 cells Urea Extract and H-7G-Sepharose chromatography fractions.

Sample	Protein Amount (Bradford Assay) (mg)		MMP-2 Amount (ELISA) (ng)	
	Mean (n=3)	SD	Mean (n=3)	SD
UE	2.73	2.40	16.19	15.32
UE Beads	0.00	0.00	0.12	0.20
UE FT	0.00	0.00	4.60	4.68
UE W	1.50	2.60	1.58	1.25
UE 0.3M NaCl E	0.80	1.39	0.85	0.70
UE 2M NaCl E	0.00	0.00	1.05	0.66

6.3.7.3 Protein Separation (SDS-PAGE)

To isolate membrane bound MMPs, HT1080 cell lysis was performed and cell extracts were subjected to affinity chromatography. All the H-7G-Sepharose chromatography fractions were analyzed by silver staining to identify presence of proteins and western blotting for MMP-2. As evident from silver stained gel (Figure 6.10A-F), beads (SE B and DE B) lost bound proteins after NAP-5 desalting (SE B NAP-5 and DE B NAP-5). This loss of proteins is also evident in case of urea extract (UE B vs. UE B NAP-5). These stained gels showed that cell lysis occurred since there are many proteins in starting cell extracts (SE panel A, DE panel B and UE panel C) but most of proteins did not bind to the beads and went into the flow-through fractions (SE/DE/UE FT).

6.3.7.4 Western Blotting of MMP-2

Once bands were developed and identified in western blotting for culture supernatants, MMP-2 expression in HT1080 cell lysates (prepared as Method I; section 6.2.4.1) and corresponding chromatography fractions were analyzed (Figure 6.10G-I). The results obtained in this case showed that MMP-2 expression in supernatants is more than observed in cell lysates. The western blots showed interesting results as DMSO starting material and chromatography fractions showed a band near 72kDa molecular weight showing the presence of MMP-2. A distinct band visible in blots where standard rh-MMP-2 (12.5ng/µL) was loaded, indicates that antibody to MMP-2 was specific and conditions for western blotting allowed proper binding of antibody to proteins. Salt extracts and urea extract however only showed bands of 35kDa in starting material and flow-through (Figure 6.10G and I). Immuno-bloting of cell lysates prepared by Method II (section 6.2.4.2) did not show MMP-2 specific bands (results not shown).

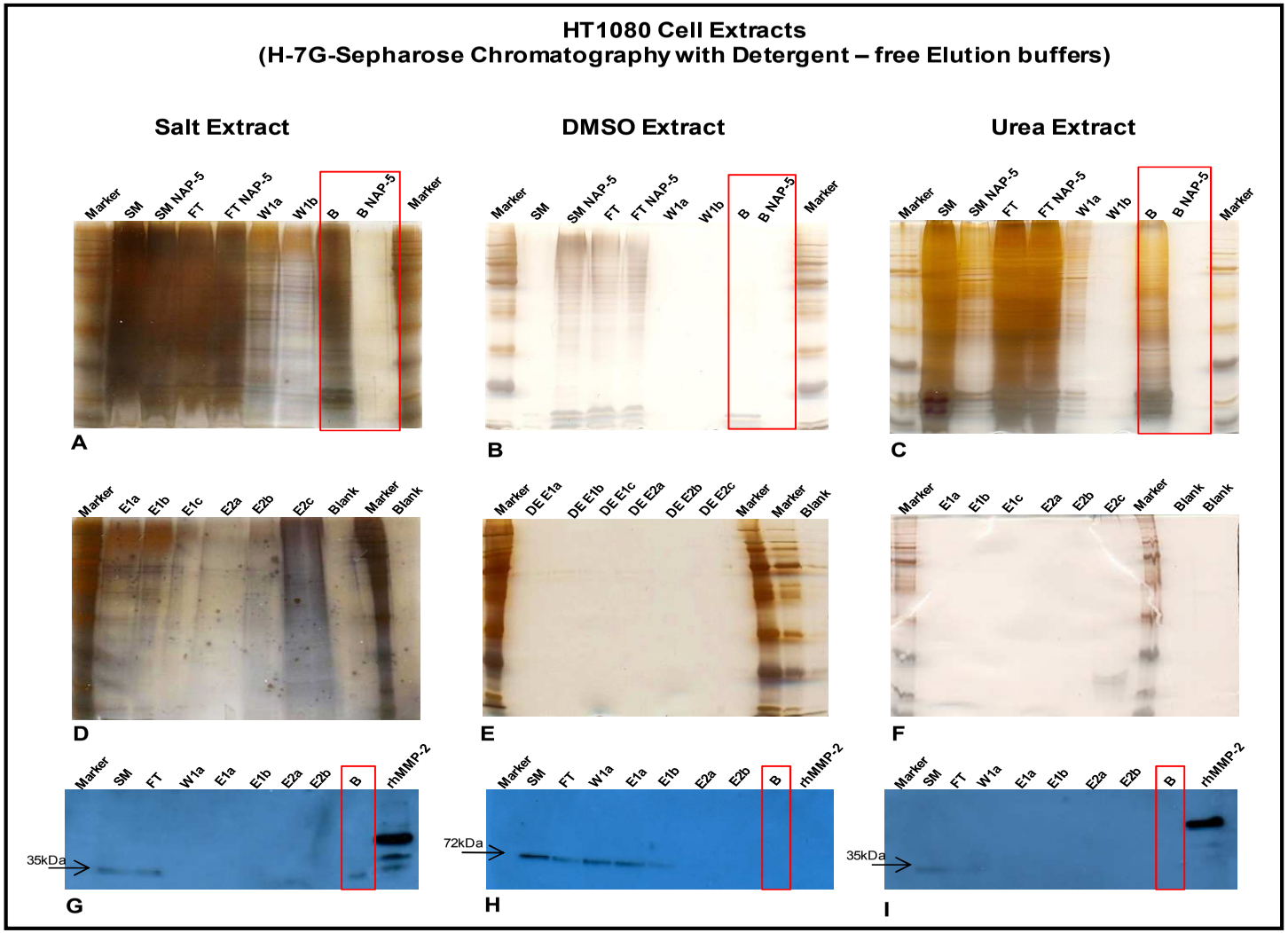

Figure 6.10 Protein expression of HT1080 cell extracts (Method I) and H-7G-Sepharose chromatography fractions.

Salt extract chromatography - SE: Salt Extract starting material, **SE NAP-5:** Starting material NAP-5 desalted, **SE FT:** Equilibration flow-through, **SE FT NAP-5:** Equilibration flow-through NAP-5 desalted, **SE W1a:** Wash flow-through1a, **SE W1b:** Wash flow-through1b, **SE B:** Beads (Not desalted by NAP-5), **SE B NAP-5:** Beads (NAP-5 desalted), **SE E1a:** Eluate1a, **SE E1b:** Eluate1b, **SE E1c:** Eluate1c, **SE E2a:** Eluate2a, **SE E2b:** Eluate2b, **SE E2c:** Eluate2c, **Blank:** SDS Loading dye.

DMSO extract chromatography - DE: DMSO Extract starting material, **DE NAP-5:** Starting material NAP-5 desalted, **DE FT:** Equilibration flow-through, **DE FT NAP-5:** Equilibration flow-through NAP-5 desalted, **DE W1a:** Wash flow-through1a, **DE W1b:** Wash flow-through1b, **DE B:** Beads (Not desalted by NAP-5), **DE B NAP-5:** Beads (NAP-5 desalted), **DE E1a:** Eluate1a, **DE E1b:** Eluate1b, **DE E1c:** Eluate1c, **DE E2a:** Eluate2a, **DE E2b:** Eluate2b, **DE E2c:** Eluate2c.

Urea extract chromatography - UE: Urea Extract starting material, U**E NAP-5:** Starting material NAP-5 desalted, **UE FT:** Equilibration flow-through, **UE FT NAP-5:** Equilibration flow-through NAP-5 desalted, **UE W1a:** Wash flow-through1a, **UE W1b:** Wash flow-through1b, **UE B:** Beads (Not desalted by NAP-5), **UE B NAP-5:** Beads (NAP-5 desalted), **UE E1a:** Eluate1a, **UE E1b:** Eluate1b, **UE E1c:** Eluate1c, **UE E2a:** Eluate2a, **UE E2b:** Eluate2b, **UE E2c:** Eluate2c, rhMMP-2: Recombinant human MMP-2 (12.5ng/mL).

6.3.7.5 MALDI-MS

Mass spectra of salt extract, DMSO or urea extracts or H-7G-Sepharose chromatography fractions with or without C18 (zip tip or Isolute columns) clean-up, no peptide were detected following trypsin digestion. However, the cell lysates prepared by Method II (section 6.2.4.2) showed mass signals in the MALDI mass spectra with some peaks specific to proteins. Based on these mass spectra, fractions were selected for LC-MS/MS.

6.3.7.6 LC-MS/MS

The number of proteins identified by LC-MS/MS of cell extracts and corresponding chromatography fractions was from 155-294 but none of the MMPs or TIMPs was detected suggesting the method of preparation of these fractions need to be optimized. There were some MMP related peaks in the MS/MS data but the Mascot score for the peptides were not high enough to identify any MMPs.

Table 6.14 Protein (BA) and MMP-2 (ELISA) amounts in cell lysates (Method II) and Olive H-7G chromatography fractions and LC-MS/MS results.

HT1080 Cell Lysate (Method II)	Protein Amount (Bradford Assay) (mg)		MMP-2 Amount (ELISA) (ng)		LC-MALDI-MS/MS
	Mean (n=2)	SD	Mean (n=2)	SD	No. of Proteins
SM	1.15	0.01	0.24	0.00	172
FT	0.59	0.00	0.31	0.00	-
0.3M NaCl E1	0.55	0.01	0.03	0.00	155
2M NaCl E2	0.57	0.00	0.03	0.00	164
Beads	0.57	0.01	ND	-	294

6.3.8 Olive H-7G Chromatography of HT29 SFCS (Salt Elution)

The serum-free culture supernatants (50mL) from HT29 cell line were treated with H-7G-Sepharose chromatography beads to isolate MMP-7 and MMP-14 which have been reported to be expressed by the cell line. For elution of

proteins, 0.3M and 2M NaCl buffers were used as described in Materials and Methods section 2.4.

6.3.8.1 MMP-2 Quantification

Since MMP-2 is not expressed by the cell line, hence ELISA for MMP-2 did not detect show any absorbance for the chromatography fractions.

6.3.8.2 MALDI-MS

The mass spectra of experiments performed using HT29 SFCS as a SM confirming successful trypsinization. The SFCS was also treated with sepharose as a negative control. The mass spectra for SM, 0.3M NaCl eluate (E1) and 2M NaCl eluate (E2) showed that eluates have more peaks common to SM when compared to the eluates from sepharose control. This quick manual MALDI-MS analysis gave evidence that ligand Olive H-7G bound to the sepharose was responsible for the concentration of peptides. Many of these peaks were showing *m/z* as found for rhMMP-7 and rhMMP-14 (Chapter 4). None of the MMPs were identified by LC-MS/MS of chromatography fractions indicating lower amounts of MMPs.

6.4 Discussion

The aim of this chapter was to use H-7G-Sepharose chromatography beads to purify MMPs and detect their expression in cell line culture supernatants that have previously been shown to express MMPs. The ELISA assay employed to examine MMP activity in HT1080 the lung fibrosarcoma cell line utilized antibody coated to the surface of wells. A yield of MMP-2 (14.4% ±0.26) was found and this low yield could possibly be because of the over-loading of ligand Olive H-7G with MMP-2 as there will be specific number of sites available for binding. Another reason might be that MMP-2 was degrading during extensive steps of washings. The MMP-2 amounts detected by ELISA showed high standard deviation (SD) in some of the chromatography fractions. The high SD indicates that the data points are spread out over a large range of values.

Coomassie brilliant blue binds to proteins stoichiometrically and is therefore, a quantitative method for determination of differential protein expression. This method is quick, quantitative and convenient. Separated proteins being detected as blue bands on a clear background, can be simultaneously fixed and stained in the same solution. Although convenient, the major disadvantage of this method is less sensitivity as it needs 3µg of protein to be detected. A more sensitive method than Coomassie staining for protein detection is silver staining. This process relies on differential reduction of silver ions that are bound to the side chains of amino acids (Oakley et al., 1980; Switzer et al., 1979). This method is 100-fold more sensitive to Coomassie staining (Merril et al., 1981). Although, this method can detect trace amounts of proteins from 0.1-1ng, it employs solutions which are light sensitive and do not work if left for a long time thus increasing the cost. Another disadvantage of this method is that some proteins cannot be stained with silver salts well stained with Coomassie brilliant blue (Merril et al., 1981).

Examination of western blot data for HT1080 revealed varying expression levels in serum-containing and serum-free fractions as measured by primary anti-MMP-2 antibodies. The immune-blots of eluate fractions from 0.3M and 2M NaCl buffers from both (S+CS and SFCS) showed 72kDa bands specific to MMP-2 (Figure 6.8). However, no bands could be detected in starting material and corresponding chromatography flow-through fractions suggesting that level of MMP-2 were close to the lower limits of detection or samples were too diluted. In initial experiments when Brij-35 detergent was used to elute MMPs, primary anti-MMP-2 antibody did not show specific bands to MMP-2. However when Brij-35 was omitted from elution buffers, antibody worked. The chromatography beads treated S+CS showed MMP-2 specific bands but not with SFCS probably for the reason that when cells were well nourished in the presence of serum, these secreted more MMP-2 while during 48hours of depletion of serum, MMP-2 productivity of cells decreased as shown in the MMP-2 ELISA data in Table 6.2.

Cursory and detailed examination of chromatography fractions with highly sophisticated technique MALDI-MS served to reveal the nature of samples to be containing enormous number of non-specific proteins. Despite the

evidence presented in Chapter 5 that rhMMPs were binding to H7-G dye ligand, the tumour cell line SFCS demonstrated least binding primarily because of complex nature of sample. Moreover, with respect to MMPs, the samples most commonly exhibited low to undetectable levels. The data shown in Appendix 9, Table 6.8 and Table 6.10 indicates that the ligand Olive H-7G is not specific to MMPs and has affinity towards other proteins including heterogeneous nuclear ribonucleoproteins and histones. These data questioned the effective use of Olive H-7G as a specific probe for MMPs. This highlights the importance of introducing structural changes in Procion Olive H-7G dye so as to enhance its selectivity towards MMPs.

Since many proteins were binding to Olive H-7G beads, specific elution of MMPs off the beads was pursued leaving other proteins on the beads. For this purpose EDTA which is a potent inhibitor of MMPs was used as it has been reported to act as a competitor to bind to MMPs (Alberto Passo, 1999). The proteins eluting in 100mM EDTA solution shown in Table 6.8 include TIMPs which are natural inhibitors of MMPs. Although the main goal of this project was isolating MMPs yet the identification of TIMP-1 and TIMP-2 with high Mascot scores suggests the possibility of using EDTA elution to purify TIMPs using Olive H-7G to concentrate them from the biological sources. The identification of some other biologically significant proteins such as kellikerin-6, galactin-3 and 10kDa heat shock protein that eluted with EDTA qualifies Olive H-7G as a ligand of choice if these proteins need to be isolated. The internal control of Olive H-7G, MDHM, was also detected confirming the activity of the ligand under discussion. These results were further confirmed when EDTA was used in buffers with increasing NaCl concentration from 0.15-5M to enhance the reversibility of bound proteins. Although EDTA was added to reduce the autolytic degradation of MMPs, it might have helped in elution off the Olive H-7G ligand immobilized on the chromatography beads. The identification of TIMP-1 and TIMP-2 in eluates from 0.15-5M (Table 6.10) with high Mascot scores approves the use of the dye for their isolation. Moreover, galactin-3, MDHM, thrombospondin-1, heat shock proteins (10kDa and 70kDa) and many other proteins of biological

importance were identified proving the potential of Olive H-7G as a purifying tool for these proteins.

Cell lysates of HT1080 human fibrosarcoma cells were utilized to optimize the MALDI-MS protocol. In order to eliminate the possibility of competition from enormous number of proteins other than MMPs for finding room on chromatography beads, cell lysates were washed with 1X PBS to remove cell debris, centrifuged several times and filtered using 0.45micron syringe filters. Although cell pellets yielded poor definition, it did however demonstrate that MMP expression could be illustrated by MALDI-MS means. In cell lysates it was expected that there would be high enough levels of membrane bound MMPs which would be sufficient for the capacity of Olive H-7G immobilized chromatography beads. The unaccountable expression pattern of other cellular proteins (172 proteins in cell extract identified by LC-MS/MS in this study) may have been made it unlikely for MMPs to bind to their ligand. Further evidence of the specificity of the primary antibody for MMP-2 was provided by the western blotting of the cellular fractions. Significantly, in the present study western blot analysis using MMP-2 antibody exhibited bands representative of high MMP-2 expression (Figure 6.10). These western blot and ELISA data (Table 6.11, Table 6.12 and Table 6.13) did not concur with the data acquired from both manual MALDI-MS and automated LC-MS/MS (Table 6.14). This could be for the reason that in contrast to western blotting, MALDI-MS involves strong denaturation conditions (8M Urea) and an overnight trypsin digestion. As a consequence, it can be hypothesized that signature peptides for MMPs could be degraded/lysed in a way that does not allow the protein identification after being fragmented by laser within MALDI mass spectrometer. Furthermore, ionization process within source of the instrument holds a complex chemistry. To the best of my knowledge, currently there is no published data referring to the purification of cellular MMPs from human cell lines and consequent analysis by MALDI-MS.

Research has highlighted the potential shortcomings of MALDI-MS and has emphasized on the need for caution in the interpretation of resulting data. Variables such as level of expression of protein under investigation, quality of matrix in use, ionization potential of peptides and calibration of instrument

have all been implicated in jeopardizing the quality of data. Moreover, the exhaustive optimization of procedure and performance of replicate experiments should have limited the probable errors implicit within the investigation.

MMPs (MMP-2 and MMP-14) were identified among many of the attempts of LC-MS/MS of SFCS eluates hence the HT1080 cell line showed low levels of MMPs quite frequently. The reason is unclear but a possible explanation could be that MMPs were lower than sensitivity limit of detection of MALDI mass spectrometer; this requires further elucidation of other cell lines. The cell line HT29 was used in the present study but significant results could not be generated. Another reason could be that a small volume (50mL) of starting material was used and the potential loss of the protein during various steps along the preparation of samples for final analysis might have failed the techniques used. It is possible that presence of other proteins which have affinity towards the Olive H-7G may have interfered with the true outcome of the methodology under discussion. The issue of non-specific binding found in this study is in keeping with the published data by other groups (Trinkle-Mulcahy et al., 2008). The data presented here strongly resemble to the findings of Trinkle-Mulcahy study that both qualitative and quantitative mass spectrometry results were affected by most commonly used affinity matrices because of non-specific binding of proteins. Many of the proteins enlisted by Trinkle-Mulcahy study binding non-specifically to sepharose matrix were similar to those found in present study. Although promising results were found for Olive H-7G dye ligand when mixture of rhMMPs were used (Chapter 5), due to the issues of non-specific binding and limit of detection of MALDI mass spectrometer it was not possible to make clear-cut conclusion when cell culture supernatants were used. Currently there is no published data since previous studies have not addressed this issue.

Alternative approaches were considered and it was decided to synthesize more MMP specific ligands. Of great importance to this project was the synthesis of economical compounds using in-house resources within ICT. Unfortunately the synthesis of MMP inhibitor illomastat-based chromatography beads attempted encountered many problems so it was not

used within the time-frame of this project. In view of understanding the site of attachment of Olive H-7G ligand and the part of the MMPs (and TIMPs) where it binds, NMR analysis of the ligand was conducted, but did not yield any interpretable results (results not shown).

In short, the findings of the study indicate that the triazine dye-based ligand (Olive H-7G, Reactive Green-8) immobilized on chromatography beads can be utilized to purify latent MMPs and TIMPs (possibly complexed with MMPs). Results suggest the ligand interacts with a site common to both latent and active forms of MMPs, the later being preferential, allowing their isolation using gradient salt buffers. Using this methodology, the MS/MS spectral peaks specific to MMPs (MMP-2, MMP-14), and two endogenous inhibitors (TIMP-1 and TIMP-2) were found in cell culture supernatants. Although detergent-free elution buffers improved MALDI analysis, recovery of MMPs from biological samples was sub-optimal. Taken together these observations suggest that MMPs can be identified using a smaller volume (50mL) of cell line culture supernatant as starting material. In terms of the development of MMP targeted purifying tools, the data presented in this chapter suggests that this would not be an easily achievable goal. The detection of MMP-2 activity (ELISA) and identification of MMPs in highly sensitive tandem mass spectrometry reinforces the potential of this strategy but lack of ability of specifically identifying MMPs in complex protein mixture remains an issue. These findings though promising, the diagnostic use of this methodology needs further optimization to remove non-specific binding of proteins. Although, none of the MMPs could be identified nevertheless, EDTA containing buffers could be of use if target proteins are TIMPs. These data are fundamental to this study. However, next chapter will entail the attempts to remove non-specific binding of proteins.

CHAPTER 7

STRATEGIES TO REMOVE NON-SPECIFIC BINDING AND ENHANCE MMP ENRICHMENT

7 Strategies to remove Non-specific binding and Enhance MMP Enrichment

7.1 Introduction

This chapter describes the attempts made to reduce biological sample complexity and selective isolation of target protein family (MMPs). The proteome is a highly complex mixture of diverse proteins and peptides varying in concentration and states. To understand the time-dependant interplay of the different pathways, and the structure and function of all involved proteins is a challenging task. Post-translational modifications such as glycosylation, phosphorylation etc. add an extra layer of complexity and are important in development of certain diseases. The challenges posed by a large range (Abrahams et al., 1996) of proteins binding non-specifically to affinity matrices has been described previously (Sutton, 2011). Such components binding non-specifically to affinity matrices, can affect the experimental outcome by reducing the possibility of low abundance target proteins bound specifically being suppressed in proteomics analysis. Research, to date, has not provided a single simple solution to preventing or interpreting non-specific binding. Methods that have been tried often relate to the specific affinity interaction between the target protein and the immobilized capture compound (e.g. an analogue of the compound that is known not to recognize the target proteins) or adapting the stringency conditions for binding.

The mesenchyme-derived dermal papilla plays a major regulatory role in the complex cell biology of the hair follicle. The ability to culture dermal papilla cells from a range of species and particularly a range of normal and disordered human hair follicles has enabled the development of a powerful new model system for investigating hair follicle biology (Randall, 1996). The dermal papilla is a cluster of specialized mesenchymal cells at the bottom of the mammalian hair follicle, embedded in a loose extracellular matrix. These cells have the capability to induce and support hair growth via close epithelial-mesenchymal interactions with the keratinocytes surrounding the

hair matrix. The extracellular matrix of the dermal papilla differs markedly from the interfollicular matrix. In a study the expression pattern and activity of MMP-1, MMP-2, MMP-3, MMP-9, TIMP-1, TIMP-2 and MT1-MMP in *in vitro* cultures of cells derived from scalp dermal papilla and fibrous sheath were reported (de Almeida et al., 2005). Zymographic analysis showed activation of MMP-2 in all cells grown in three-dimensional collagen lattices whereas MMP-9 was activated only in three-dimensional collagen cultures of dermal fibroblasts and weakly in follicular cells. Expression of MMP-1, TIMP-1, TIMP-2 and MT1-MMP was similar in all cells, in both culture conditions, whereas expression of MMP-3 was absent in dermal papilla cells (de Almeida et al., 2005). Many studies have been conducted to understand dermal abnormalities and many MMPs have been reported to play important roles. Neutrophil elastase has been reported to be associated with solar elastosis. Photo aging of skin or solar elastosis (which is probably an end product of elastic fiber degradation) results from an influx of neutrophils on exposure of human skin to a certain threshold of UV, infrared radiation (IR), and heat. In this study the neutrophils, packed with potent proteolytic enzymes capable of degrading collagen and, particularly, elastic fibers responsible for ECM damage were observed in several non-dermatological conditions. Taken together with their data this group proposed that MMPs generated by sub-erythemogenic doses of UV and low doses of IR/heat are involved in cellular processes other than ECM degradation (Rijken and Bruijnzeel, 2009).

7.1.1 Aims

In the present study various strategies were explored to remove proteins, other than MMPs, binding non-specifically to sepharose (results from Chapter 6). The strategies followed were:

- To sweep abundant proteins in culture supernatant using sepharose followed by use of H-7G-Sepharose beads to bind MMPs.

- To add ADP/GDP in culture supernatant so that proteins having affinity for these nucleotides could be engaged giving opportunity to MMPs for binding to Olive H-7G supported on matrix.

- To use sephadex as a matrix as opposed to conventional sepharose to reduce the chances of getting MMPs trapped in porous soft gel hence enhancing likelihood of binding to Olive H-7G.

7.2 Materials and Methods

7.2.1 Pre-clearing Dermal Papilla Culture Supernatant using Sepahrose (Non-Cancer source of MMPs)

Dermal papilla culture supernatant (henceforth referred to as CS) was kindly provided by one of the colleagues Heero Rehman at the University of Bradford. The 'CS' was divided into two 15mL tubes (5mL each). To one labeled 'CS-1 H-7G-Sepharose' 1mL of 'H-7G-Sepharose' beads (washed and equilibrated Materials and Methods section 2.4) were added and to other tube labeled 'CS-2 Sepharose' 1mL of 'Sepharose' control beads were added. The workflow for the experiment is depicted in Figure 7.1. The contents of both tubes were rotated on a rotator at 30rpm for 2hours at 4°C. The corresponding flow-throughs were collected and frozen at -20°C. The flow-through 'CS-2 FT 2' was presumably cleared by 'Sepharose' since this is the trapping net for proteins. To this cleared flow-through, 'H-7G-Sepharose' beads were added and left on a rotator at 30rpm for 2hours at 4°C for binding any proteins which were not swept by Sepharose or were in excess. The beads were collected in the end and divided into two 1.5mL eppendorfs. To one part elution was performed using 0.3M and 2M NaCl buffers as described in Materials and Methods section 2.4.1. On-bead trypsin digestion was performed keeping in view the amount of proteins, 50µL of trypsin solution (10µg/mL) was added and incubated at 28^{o}C for 18hours followed by desalting peptide solution (Materials and Methods section 2.10.1).

7.2.2 ADP/GDP use in HT1080 SFCS

ADP and GDP bind to most of the proteins. HT1080 SFCS was mixed with 1mM ADP and 1mM GDP to remove non-specific binding. The affinity chromatography was performed as described in Materials and Methods section 2.4. All fractions were NAP-5 desalted and lyophilized at 37°C.

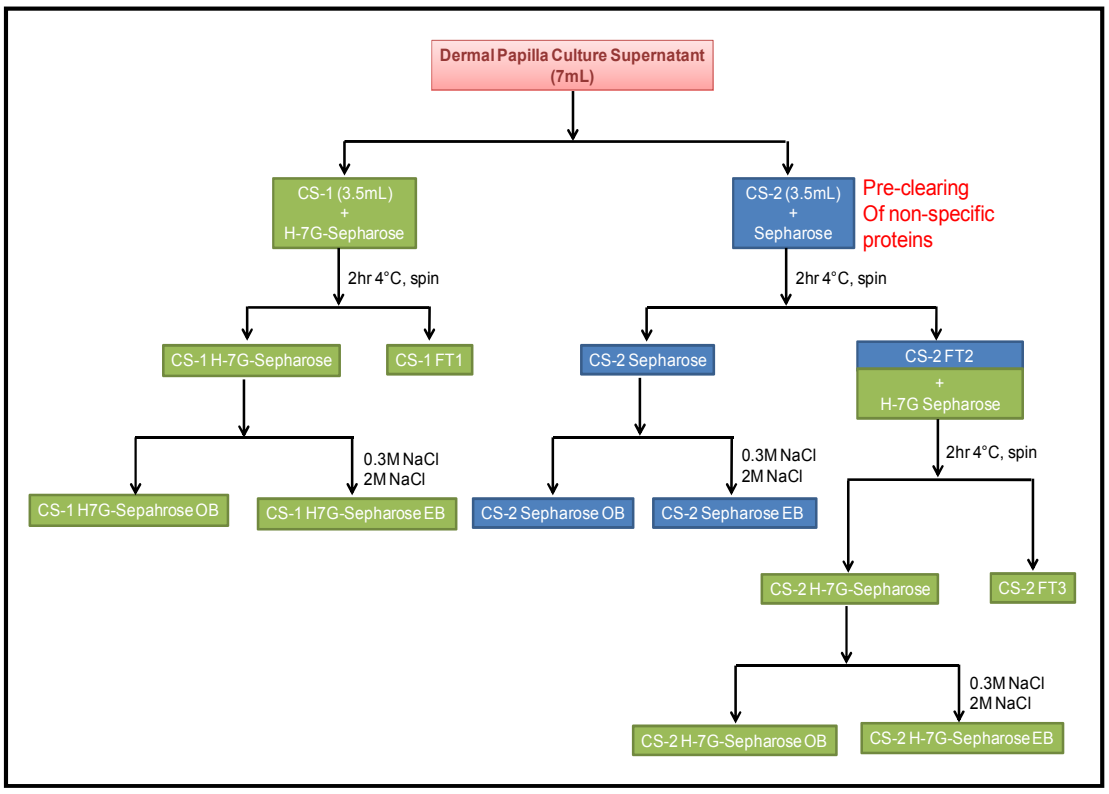

Figure 7.1 Affinity chromatography of dermal papilla culture supernatant before and after sepharose pre-clearing.

7.2.3 Low Porosity Beads (Sephadex)

H-7G-Sephadex chromatography beads were synthesized (Materials and Methods section 2.2) and treated with HT1080 SFCS for affinity chromatography (Materials and Methods section 2.4). The chromatography fractions were subjected to NAP-5 concentration and lyophlization. In-soultion trypsin digestion was performed (Materials and Methods section 2.9.1) with the variations in volumes of reagents shown in Figure 7.2.

Samples		8M Urea	50mM DTT	100mM IAC	HPLC H_2O	Trypsin
SM	(Lyophilized)	20 µL	2 µL	2µL	112µL	5µL
FT	(Lyophilized)	30 µL	3 µL	3µL	84µL	5µL
SFCS E1a+b+c	(Lyophilized)	30 µL	3 µL	3 µL	84µL	5µL
SFCS E2a+b	(Lyophilized)	40 µL	4 µL	4 µL	112µL	5µL
SFCS E2c	(Lyophilized)	20 µL	2 µL	2µL	112µL	5µL

Figure 7.2 Trypsin digestion for H-7G-Sephadex chromatography fractions.

7.3 Results

7.3.1 LC-MS/MS of Dermal Papilla Culture Supernatant Fractions

Significant but not complete depletion of abundant proteins was observed in spectra and increased numbers of peaks were detected. Most of the peptides were removed from beads during elution with 0.3M and 2M salt buffer as depicted by the HPLC profiles (Figure 7.3A and B). The HPLC profile for the fraction 'CS-1 H-7G Sepharose OB' (beads mixed in culture supernatant 1 and on-bead trypsinized) shows discrete peaks hence more proteins (47) detected by LC-MS/MS where 3271 compounds were scheduled for fragmentation out of 6911 leading to the identification of MMP-1, MMP-2 and MMP-3 along with TIMP-1 with Mascot scores > 30 (Figure 7.3). The HPLC profile for 'CS-2 Sepharose OB' (sepharose mixed with culture supernatant 2 and on-bead trypsinized) and the one after elution using 0.3M and 2M salt buffer (Figure 7.3C and D) show half the intensity observed in 'CS-1 H-7G-Sepharose OB' and 'CS-1 H-7G-Sepharose EB' (panels A and B). Identification of comparatively lower number of proteins (9 and 2 in CS-2 Sepharose OB and CS-2 Sepharose EB, respectively) suggests some proteins do bind to matrix. For the fraction 'CS-2 Sepharose OB' (Figure 7.3C) the number of compounds scheduled to MS/MS was 2561 out of 6810 but identification of just 9 proteins suggests that most of the compounds were

not peptides. Similarly, 7138 compounds in the fraction 'CS-2 Sepharose EB' indicate lack of real signal because only six proteins were identified (Figure 7.3D). The profiles for 'CS-2 H-7G-Sepharose OB' (Figure 7.3E) and 'CS-2 H-7G-Sepharose EB' (Figure 7.3F) shows very high intensity HPLC peaks. As described in methods section and shown in Figure 7.1 the 'CS-2 FT2' cleared culture supernatant by pre-treating proteins with sepharose. The comparison of results of beads fractions 'CS-1 H-7G-Sepharose and 'CS-2 H-7G-Sepharose' (Figure 7.3, equivalent fractions before and after sepharose pre-treatment) shows that there is a reduction in the number of proteins from 47 to 10. Therefore, pre-clearing method was non-specific and did not enhance MMP enrichment.

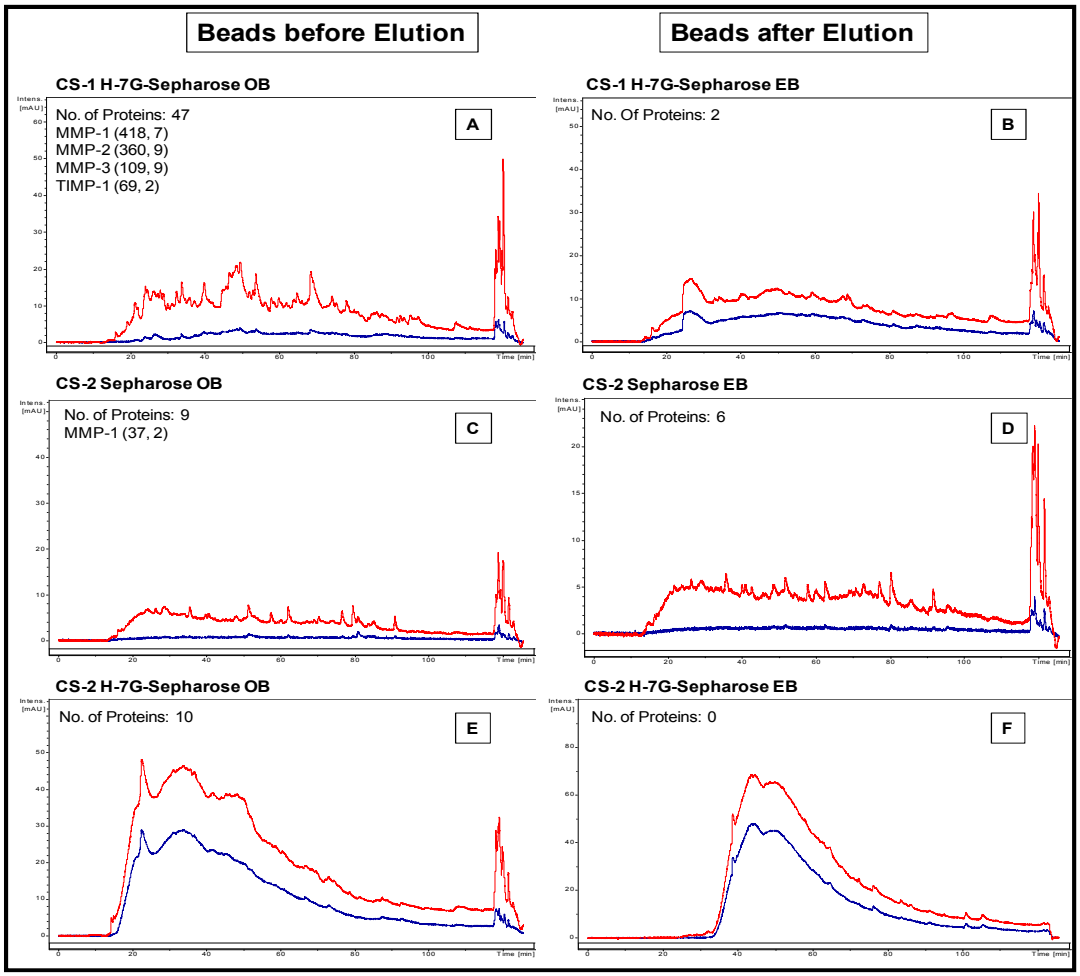

Figure 7.3 HPLC profiles and LC-MS/MS results for sepharose pre-clearing experiment (n=1).

OB: on-bead trypsin digest; EB: on-bead trypsin digest after elution. Numbers is parentheses are Mascot scores and peptides identifying the proteins.

7.3.2 ADP/GDP use in HT1080 SFCS

7.3.2.1 Protein Separation (SDS-PAGE)

The protein expression for HT1080 SFCS and corresponding chromatography fractions was the same before and after adding ADP and GDP (Figure 7.4A). The beads collected after the elution of proteins showed similar protein profile suggesting proteins did not bind to ADP and GDP. The control sepharose beads did not show bound proteins before and after adding ADP and GDP (Figure 7.4B).

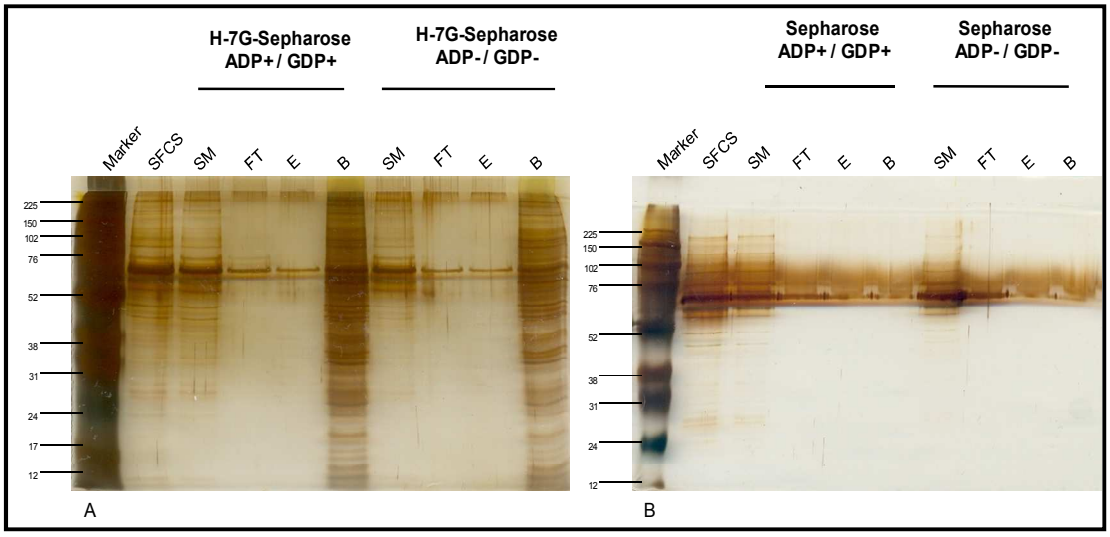

Figure 7.4 Protein expression of HT1080 SFCS and chromatography fractions after removal of ADP/GDP binding proteins.

7.3.2.2 LC-MS/MS

Amongst the 140 identified proteins in the starting material were high abundant background proteins such as actin, hemoglobin, serum albumin, heat shock proteins, keratins and TIMPs (Table 7.1). Several proteins in the 0.3M NaCl eluates were identified in the probed and control sepharose, i.e. wherein ADP/GDP was added to the HT1080 SFCS prior to the chromatography. Those included keratins, serum albumins but none of the MMPs were identified.

Table 7.1 LC-MS/MS of HT1080 SFCS chromatography fractions after ADP/GDP suppression of proteins.

HT1080 SFCS	LC-MS/MS	TIMP-1		TIMP-2	
	No. of Proteins	Mascot Score	Peptide #	Mascot Score	Peptide #
SM	140	37	3	146	4
H-7G-Sepharose ADP+/ GDP+ 0.3M NaCl E	40	-	-	62	1
Sepharose ADP+/ GDP+ 0.3MNaCl E	7	-	-	-	-

7.3.3 LC-MS/MS for H-7G-Sephadex Fractions

To analyze the number of proteins binding non-specifically to sephadex, HT1080 SFCS was sieved with sephadex and H-7G-Sephadex beads. No proteins were eluted and on-bead digestion was performed. LC-MS/MS of culture supernatant and the beads did not identify MMPs or TIMPs (Table 7.2). Since number of proteins was reduced when compared to results obtained with sepharose (Chapter 6) so sephadex was considered as better matrix than sepharose.

Table 7.2 Proteins binding non-specifically to H-7G-Sephadex (No elution).

HT1080 SFCS (50mL)	BA	ELISA	LC-MS/MS
	Protein (mg/50mL) (n=3)	MMP-2 (ng/50mL) (n=3)	No. of Proteins (n=3)
SM	42.94	149.66	40-69
H-7G-Sephadex	ND	ND	2-17
Sephadex	ND	ND	0-14

Further experiments were set up to elute proteins from H-7G-Sephadex and control sephadex using 0.3 and 5M NaCl buffer {50mM Tris-HCl (pH 7.5); 0.3M or 5M NaCl; 10mM $CaCl_2$; 0.02% (w/v) Na_3N}. In previous experiments using sepharose as matrix, 5M NaCl buffer eluted more proteins than 2M

NaCl buffer. In view of eluting all proteins possibly trapped in sephadex, 5M salt buffer was used. The trypsin-digested samples were then desalted using C18 columns followed by lyophilization at 37ºC in evaporator. In one of the experiments to elute proteins off the H-7G-Sephadex, elution buffers were mixed with beads for 30 minutes before centrifugation. The results are shown in Table 7.3 presenting elution of TIMP-1 (Mascot score 57) in 0.3M salt buffer and TIMP-2 (Mascot score 68) in 5M salt buffer. Although, any MMP could not be identified but there were MMP-14 specific peptide peaks observed with a low Mascot score. Detailed list of proteins identified in pooled eluate fractions of 0.3M salt buffer (E1a-c) and 5M salt buffer (E2a+b and E2c) is shown in Table 7.4. MDH in eluates of 0.3M salt buffer are internal control for Olive H-7G and have been reported to bind to the dye.

Table 7.3 Proteins eluted from H-7G-Sephadex using 0.3M and 5M NaCl buffers.

HT1080 SFCS	BA	ELISA	LC-MS/MS	TIMP-1		TIMP-2	
	Protein (mg/50mL)	MMP-2 (ng/50mL)	No. of Proteins	Mascot Score	Peptide #	Mascot Score	Peptide #
SM	39.71	59.55	69	112	5	86	1
FT	ND	ND	35	32	2	-	-
0.3 M NaCl E1a-c	ND	ND	4	57	1	-	-
5M NaCl E2a+b	ND	ND	24	-	-	68	1
5M NaCl E2c	ND	ND	8	-	-	-	-

ND: Not detected

Table 7.4 Proteins in eluates of H-7G-Sephadex.

SM	FT	E1-c (0.3M NaCl elution)	E2a+b (5M NaCl elution)	E2c (5M NaCl elution)
Protein	Protein	Protein	Protein	Protein
Serum albumin	Alpha-2-antiplasmin	Keratin, type II cytoskeletal 1	Serum albumin	Serum albumin
Keratin, type II cytoskeletal 1	Alpha-2-HS-glycoprotein	Keratin, type I cytoskeletal 9	Actin, cytoplasmic 1	Inter-alpha-trypsin inhibitor heavy chain H2
Actin, cytoplasmic 1	Amyloid beta A4 protein	Tubulin alpha-1A chain	Annexin A2	Histone H2A type 1-A
Heat shock cognate 71 kDa protein	CASP8-associated protein 2	Serum albumin	Moesin	Histone H3.1t
Metalloproteinase inhibitor 1	CD44 antigen	Histone H2A type 1-B/E	Protein disulfide-isomerase A3	Kallikrein-10
Peptidyl-prolyl cis-trans isomerase A	Clusterin	Histone H4	Malate dehydrogenase, mitochondrial	Histone H1.5
Inter-alpha-trypsin inhibitor heavy chain H2	Cystatin-C	Fibronectin	Metalloproteinase inhibitor 2	Cystatin-C
Alpha-2-HS-glycoprotein	Fibulin-1	Actin, cytoplasmic 1	Non-histone chromosomal protein HMG-17	Histone H4
Clusterin	Galectin-3-binding protein	Heterogeneous nuclear ribonucleoproteins C1/C2	Inter-alpha-trypsin inhibitor heavy chain H2	
Peroxiredoxin-1	Heat shock cognate 71 kDa protein	Histone H2B type 1-B	Histone H4	
Cystatin-C	Hemoglobin subunit alpha	60S ribosomal protein L6	Thrombospondin-1	
Tubulin alpha-1A chain	Hemoglobin subunit beta	Histone H2B type 1-C/E/F/G/I	Ceramide glucosyltransferase	
Metalloproteinase inhibitor 2	Histone H2A type 1-A	Protein disulfide-isomerase A3	Histone H2A type 1-A	
Alpha-enolase	Inter-alpha-trypsin inhibitor heavy chain H2	Annexin A2	Sulfhydryl oxidase 1	
Sulfhydryl oxidase 1	Inter-alpha-trypsin inhibitor heavy chain H3	Keratin, type I cytoskeletal 10	Malate dehydrogenase, cytoplasmic	
SPARC	Keratin, type II cytoskeletal 1	Heterogeneous nuclear ribonucleoproteins A2/B1	Histone H3.1t	
Hemoglobin subunit alpha	Kininogen-1	Thrombospondin-1	Transforming growth factor-beta-induced protein ig-h3	
Tubulin beta chain	Lactotransferrin	Histone H2B type 1-A	Keratin, type I cytoskeletal 10	
Vitronectin	Liprin-alpha-3	Keratin, type I cytoskeletal 18	Stathmin	
Inter-alpha-trypsin inhibitor heavy chain H3	Metalloproteinase inhibitor 1	Ezrin	Cystatin-C	
Triosephosphate isomerase	Midasin	Endoplasmin	Kallikrein-6	
Hemoglobin subunit beta	Peroxiredoxin-1	Enhancer of polycomb homolog 2	Keratin, type II cytoskeletal 1	
Vitamin D-binding protein	POTE ankyrin domain family member E		Keratin, type I cytoskeletal 18	
Neurosecretory protein VGF	Probable 3-hydroxymethyl-3-methylglutaryl-CoA lyase 2		Olfactomedin-like protein 3	
Galectin-3-binding protein	Protein MON2 homolog			
Thrombospondin-1	Protein piccolo			
Lactotransferrin	Protein TANC1			
Pyruvate kinase isozymes M1/M2	Putative beta-actin-like protein 3			
Glyceraldehyde-3-phosphate dehydrogenase	Serum albumin			
Alpha-2-antiplasmin	SPARC			
Alpha-2-macroglobulin	Sulfhydryl oxidase 1			
78 kDa glucose-regulated protein	Thrombospondin-1			
Amyloid beta A4 protein	Triosephosphate isomerase			
Sperm-associated antigen 1	Ubiquitin			
Kininogen-1	Vitamin D-binding protein			
Elongation factor 2				
WD repeat-containing protein 7				
Cadherin-23				
Keratin, type II cytoskeletal 2 epidermal				
Retinol-binding protein 4	**Common between E1a-c and E2a+b**			
Histone H2A type 1-D	**Common between E2a+b and E2c**			
Stathmin	**Common among E1a-c, E2a+b and E2c**			
Laminin subunit beta-2				
Putative C-type lectin domain-containing protein				
Guanine nucleotide-binding protein subunit alpha-12				
CASP8-associated protein 2				
Keratin, type I cytoskeletal 10				
Keratin, type I cytoskeletal 18				
Rab proteins geranylgeranyltransferase component A 1				
Complement C4-A				
Nucleolin				
Ecto-ADP-ribosyltransferase 4				
Insulin-like growth factor-binding protein 2				
Nebulin				
Abhydrolase domain-containing protein 12B				
Ribosomal protein S6 modification-like protein B				
Macrophage migration inhibitory factor				
Abhydrolase domain-containing protein 15				
Gelsolin				
Kallikrein-6				
Borealin				
Caspase recruitment domain-containing protein 11				
Kinesin-like protein KIF2C				
CD44 antigen				
Tetraspanin-14				
Midasin				
Tax1-binding protein 1				
Zinc finger protein 611				

7.4 Discussion

Matrices constitute a major source of non-specific binding. High resolution separation is achieved by chromatographic protein purification systems yet colloidal contaminants in biological samples such as cell debris often plug soft gel matrices such as highly porous sepharose.

Since dermal papilla cells have been reported to express MMPs in high amounts along with other proteins, their culture supernatant was used in the current study as a source of MMPs. An attempt was made to deplete high abundance proteins by adding un-derivatized sepharose to dermal papilla culture supernatant with the aim of filtering out proteins that bind non-specifically to affinity matrix while increasing the likelihood of binding of MMPs to Olive H-7G and identification by MALDI-MS profiling. In addition an attempt was made to elute the bound proteins. The resulting fractions were assayed for the presence and purity of the target of interest. The results showed that depletion of high abundance proteins also removed low abundance proteins including MMPs. However, the comparison of results of beads fractions 'CS-1 H-7G-Sepharose and 'CS-2 H-7G-Sepharose' (Figure 7.3, equivalent fractions before and after sepharose pre-treatment) showed that there is a reduction in the number of background proteins from 47 to 10.

Dadvar et al developed an enrichment protocol by using a combination of pre-clearing and competitive blocking of proteins in mouse lung tissue lysate with nucleotides (ADP and GDP) which reduced the binding of nucleotide binding proteins (especially serum albumin) to the beads (Dadvar et al., 2009). Therefore, we opted for this strategy and used high concentration ADP and GDP to suppress nucleotide binding proteins (Actin, endoplasmin, tubulin) in the HT1080 SFCS before pull-down affinity assay with H-7G-Sepharose chromatography beads. However, no change was observed in the protein expression for HT1080 SFCS and corresponding chromatography fractions before and after adding ADP and GDP (Figure 7.4A). It was expected that ADP and GDP will engage proteins leaving les number of proteins to bind to the chromatography beads. The beads collected after the elution of proteins showed similar protein profile suggesting proteins did not

bind to ADP and GDP. The control sepharose beads did not show bound proteins before and after adding ADP and GDP (Figure 7.4B). These results were confirmed when HT1080 SFCS and corresponding chromatography fractions were analysed by MALDI-MS/MS. Amongst the 140 identified proteins in the starting material were high abundant background proteins such as actin, hemoglobin, serum albumin, heat shock proteins, keratins and TIMPs (Table 7.1). Several proteins in the 0.3M NaCl eluates were identified in the probed and control sepharose, i.e. wherein ADP/GDP was added to the HT1080 SFCS prior to the chromatography. Those included keratins, serum albumins but none of the MMPs were identified.

Sepharose has particle size 45-200μm (wet) and a fractionation range of $1x10^4$-$4x10^7$ Da for globular proteins (Sigma and GE healthcare). This is composed of cross-linked (through lysine or cysteine side chains) beaded agarose more resistant to denaturing conditions and thus offers more versatility in the choice of sample buffer and eluent. Because of the porosity characteristic to the polymer proteins get trapped in it and keep leaching out with every elution buffer used. Its brand name is derived from **Se**paration-**Pha**rmacia-Aga**rose**. Sepharose is a registered trademark of GE Healthcare and its common application is gel filtration (separation by size) of biomolecules.

Sephadex has a fractionation range ≤700-$6x10^6$ and bead sizes fall in discrete ranges between 20-300μm (Sigma) on the other hand has cross-linking in its structure resulting in fine pores hence the number of proteins getting stuck is lesser. Sephadex has a fractionation range of $1x10^3$-$5x10^3$ Da and bead size 20-300μm (GE healthcare). Sephadex is a trademark for cross-linked polysaccharide dextran gel commonly used for gel filtration in bead form. By varying the degree of cross-linking, the fractionation properties of the gel can be altered. It was launched by Pharmacia in 1959 and the name is derived from **se**paration **Pha**rmacia **dex**tran. The organic chains are cross-linked to give a three dimensional network having functional ionic groups attached by ether linkages to glucose units of the polysaccharide chains. Moreover, sephadex is used in commercially available desalting columns, size exclusion chromatography (SEC) or gel permeation

chromatography (GPC). Proteins slide alongside the bead structure and only proteins having affinity for the ligand immobilized on beads bind hence specifically eluted afterwards. One of the most significant reasons sephadex was selected is that the Olive H-7G dye binds to hydroxyl groups. To analyze the number of proteins binding non-specifically to sephadex, HT1080 SFCS was sieved with sephadex and H-7G-Sephadex beads. The number of proteins identified when sepharose was used as a matrix higher (from 70-170) but when sephadex was used it was reduced to 40 so sephadex was considered as better matrix than sepharose. However, no MMP was identified before or after elution using salt containing buffers (Table 7.2 and Table 7.3). A set of experiments was performed changing samples:beads ratio but noteworthy differences were not observed.

In conclusion, the strategies adopted in this study did not eradicate the non-specific binding of proteins to affinity matrices. Hence, further possibilities need to be explored.

CHAPTER 8

CONCLUSIONS

8 Conclusions

Identification of proteolytic enzyme expression, activity and localization in human cancers is important to improving our knowledge of cancer, its diagnosis and treatment. The detection and function of these enzymes, particularly MMPs, in cancer may result in new diagnostic markers or new therapeutic targets. There are contradictory findings with regard to the role played by MMPs in promotion and inhibition of the tumour growth as well as tumour progression. It is therefore essential to investigate expression profiles and associated high proteolytic activity in cancer tissue to improve understanding of their role and potential. The purification and isolation of biologically active or inactive proteases from complex mixtures remains a challenging task, and is a major objective of this study. Quantification of the activity state of proteases promises to reveal the functions of proteases in homeostasis and in disease states. This will indicate which proteases participate in defined pathologies and will help targeting specific proteases for disease treatments.

Owing to the expanding knowledge of complex roles for MMPs both in normal and diseased cells, there has been an increasing interest in their identification and functional characterization in human. More information about the profile of these proteases will prove useful in the molecular diagnosis of disease, with the calibration of protease level to disease severity or tumour grade enabling more accurate prognosis for patients. It will help find out their state (active or latent) at the time of secretion and understand their role in tumour progression and metastasis in cancer. The approach described will help progress in the detection of endogenous active, latent forms of MMPs and complexed with TIMPs in complex proteomes, an important objective with many diagnostic applications. This MALDI-MS based MMP profile characterization in turn will help monitor the efficacy of a drug administered causing changes in MMP quantities being secreted. The development of new affinity capture tool for pro-MMPs and their subsequent characterization will provide a useful insight into their regulation prior to

secretion and possible strategies to stop their activation on the onset of disease.

A major drawback of previous protein purification methods is the lack of specificity. One approach to address this problem is to select a relatively specific ligand and make use of it as a broad spectrum purifying tool for a class of closely related proteases. Keeping this in view, the first aim of the study was synthesis of chromatography material by immobilization of previously reported MMP ligand Procion Olive H-7G on hydroxyl polymer beads. As a supporting matrix, different gel media for immobilization Olive H-7G were investigated. This project has attempted to profile MMPs by combining principles of affinity chromatography and soft ionization high-throughput MALDI mass spectrometry. This work has focused on human recombinant forms and in particular on cell lines which are known sources of MMPs. Current identification methods are not specific enough and there is the need for a novel more specific one. The rational design for this study entails two stages: enrichment of MMPs followed by an assessment of the efficiency of chromatography system using MALDI mass spectrometry. This study aimed to achieve these goals with a view to demonstrate Olive H-7G dye as a potential ligand for MMPs.

In order for chromatography to perform its role, it was necessary to demonstrate MMPs were expressed and active in cell lines. For this, analysis of protein expression using proteomic techniques, SDS-PAGE, western blotting, Coomassie brilliant blue and silver staining and ELISA based activity assays were performed. The MALDI-MS peptide fingerprints/peptide signatures of recombinant human MMPs were identified using trypsin (and other proteases). To determine which pro-MMPs bind Olive H-7G, the chromatography system Olive H-7G-Sepharose was evaluated using commercially available latent recombinant human MMPs (Chapter 5). Further elucidation of separation potential of Olive H-7G was achieved by LC-MS/MS analysis of purified MMPs from serum-free culture supernatant of cancer cell lines.

One of the objectives of studying rhMMPs was to handle the enzymes as levels expected to be similar to those occurring in biological samples.

rhMMPs were analyzed using MALDI-MS for their integrity and show mass peaks specific to intact protein. It was anticipated that it might be the detergent (Brij-35) which is masking the specific peaks of intact rhMMPs. Attempts to remove the detergent from rhMMPs using C4 zip tips were only partially successful (MMP-3, MMP-7, MMP-10 and MMP-14) and could not be removed in the case of MMP-2, MMP-8, MMP-9, MMP-13 and MMP-16.

The identification of MMP-8, MMP-13 and MMP-14 (Figure 5.7) in addition to previously reported MMPs (MMP-3, MMP-7, MMP-9 and MMP-10) highlighted the broad applicability of Olive H-7G. The identification of these three new MMPs could be credited to the LC-MS/MS complimentary protein identification. Nevertheless, these results are very encouraging and not only confirm the previously reported potential of the Olive H-7G affinity for MMP-3, MMP-7, MMP-9 and MMP-10 but also for MMP-8, MMP-13 and MMP-14 reported in this study. Once the affinity of Olive H-7G was confirmed (Chapter 5, section 5.3.1 and 5.3.4), a very fundamental information that whether bound MMPs to Olive H-7G could be retrieved or not, 0.3M and 2M NaCl buffers were used to elute off the endopeptidases. The ELISA assay measured 95.01% recovery of the MMP-2 from Olive H-7G immobilized on sepharose (Table 5.6) offering a persuasive evidence. This finding appeared to be very plausible and suggested that it is worth viewing Olive H-7G as a potential probe for purification of MMPs in keeping with the previous studies. The results obtained by ELISA quantification proved that the Olive H-7G not only bound the rhMMP-2 but also, recovery of the enzyme was possible using elution buffers containing right salt concentrations (0.3M and 2M NaCl).

The major aim of this study was to develop a method for detection of both intracellular and secreted MMPs applicable for use with both pre-clinical and clinical material. The main output of the project to date has been the development of an affinity chromatographic method utilizing the Procion Olive H-7G dye ligand and its use to purify secreted and cellular MMPs. The present study utilized the affinity of Olive H-7G to purify both inactive and active MMPs from a biological matrix and analyzed by proteomic mass spectrometry. This methodology was initially performed using MMP-2 as a

representative target, due to the previous reports of MMP-2 purification using this dye (Okada et al., 1986). In order to develop this methodology the HT1080 fibrosarcoma model was used, which was previously demonstrated to express high levels of MMPs (Atkinson et al., 2007) particularly MMP-2, MMP-9 (Roomi et al., 2009), MMP-14 (Koshikawa et al., 2000; Takino et al., 2004). Also HT29 cell line was used which has been reported to express MMP-7 and MMP-14 in high amounts (Atkinson et al., 2007). Binding of Olive H-7G to different support matrices (sepharose, sephadex and magnetic beads) to synthesize an affinity system was successful as there was no leaching off of the Olive H-7G dye from beads even when the suspension was kept for more than 3 months at 4°C.

Initially, the yield of MMP-2 from chromatography was low (<10%), irrespective of the presence of serum or detergent. A substantial amount of MMP-2 being present in the flow-through fraction suggested a lack of binding of MMP-2 to the column. One explanation could be that MMP-2 is being processed prior to the chromatography, either by MMP-2 auto-activation (Makowski and Ramsby, 2005) or via the trypsin used for cell harvesting as previously suggested (Okada et al., 1992). This proteolysis of MMP-2 was unlikely since MMP-2 was detectable by ELISA, which detects both active and inactive MMP-2. A more likely explanation was that other non-MMP proteins were binding to the Olive H-7G-Matrix chromatography beads thereby blocking access of MMP-2, a hypothesis reinforced by the number of non-MMP proteins present in the eluates when analyzed by LC-MS/MS (Appendix 9).

Analyses of the starting material and chromatography eluates by SDS-PAGE demonstrated that a high level of albumin was present from cells grown in serum-containing media, and potentially masking the MMP-2 signal (Figure 6.6). Therefore, although MMP-2 levels were higher in serum-containing culture supernatants, the six-fold lower level of total protein from serum-free media meant that this would be advantageous for chromatography and reduced contamination from non-MMP proteins in the fractions. In this context it is interesting to note that although cells were grown in serum-free media that albumin was still present, as identified by its presence by LC-

MS/MS in NaCl eluate HT1080 SFCS E2a (Appendix 9) with significant Mascot scores. The complete removal of albumin is therefore not possible, unless cells are grown completely without serum, an unfeasible situation.

Analysis of cell lysates and their corresponding chromatographic eluates by western blotting demonstrated the presence of MMP-2 in these fractions. Samples prepared using either salt or urea buffers did not demonstrate bands corresponding to either pro- or active MMP-2. Alternatively, a band was evident at 35kDa in salt and urea lysates (Figure 6.10G and I) but not corresponding eluates, suggesting MMP-2 proteolysis in these systems. In contrast, MMP-2 was present with a mass of 72kDa, corresponding to latent MMP-2, in lysates and 0.3M salt eluates isolated in DMSO (Figure 6.10H). This result therefore indicated the potential for this chromatographic methodology to isolate MMP-2, a finding which provides a strong base for further optimization of this method and potentially detection of other forms of MMP-2 and other MMPs.

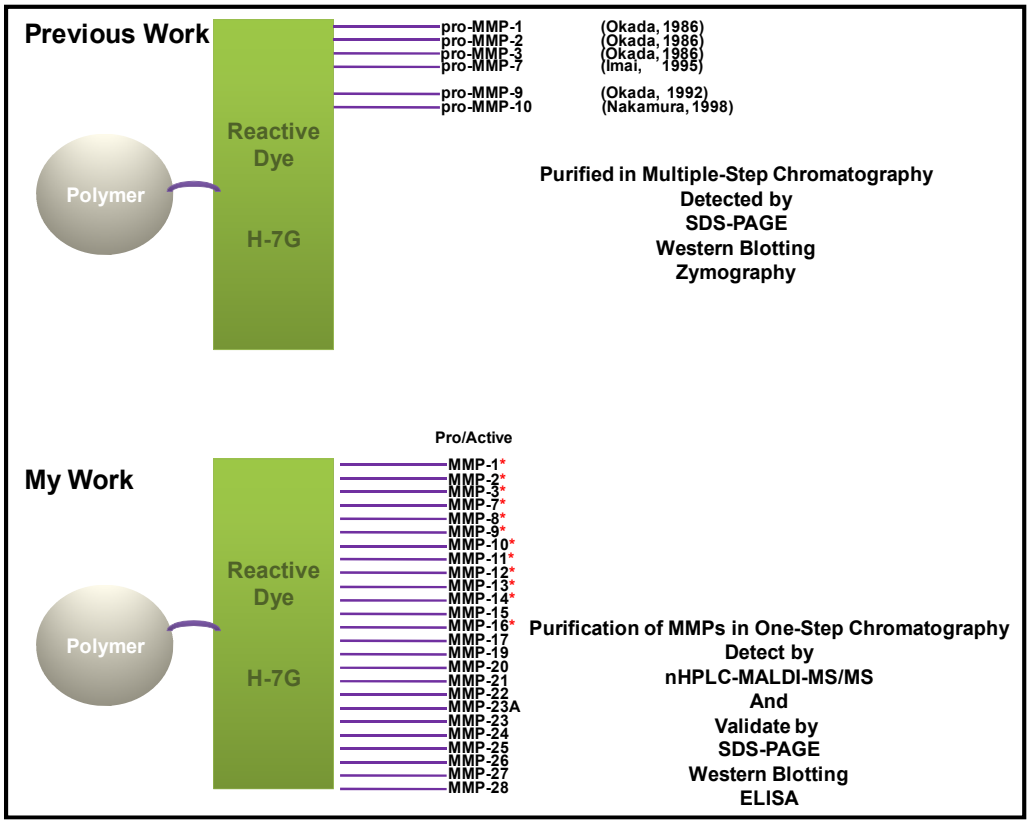

Figure 8.1 Screening rhMMPs for Olive H-7G in present study.
Reactive dye Olive H-7G was screened for MMPs with asterisk.

Conversely to cell lysates, initial analysis of MMP-2 in culture supernatant by western blotting did not yield positive results from any fraction (results not shown). In order to confirm the presence or absence of MMP-2 (and other MMPs) in cell culture supernatants, and the previous demonstration that MMP-2 can bind to the chromatography material (albeit at a low yield), samples were prepared for mass spectrometric analysis. Due to interference with MALDI-MS/MS, samples have to be prepared in the absence of Brij-35 detergent. Following this preparation, samples were once again screened by gel chromatography and western blotting to indicate the presence of sufficient proteins and any MMP-2 proteins. Unexpectedly, MMP-2 was now detectable by western blotting in the culture supernatants (Figure 6.8) and cell lysates (Figure 6.10G-I), suggesting that Brij-35 may also interfere with antibody recognition of MMP-2.

Analysis of chromatography fractions by LC-MS/MS demonstrated the presence of various proteins in all eluates and fractions (Appendix 9). Comparative results were also obtained from four fractions shown in Table 6.6 from four independent HT1080 serum-free culture supernatants, with the identification of common proteins such as placental anti-coagulant protein (PAPIV), malate dehydrogenase mitochondrial precursor, lung cancer antigen NY-LU-1, serum albumin precursor and protein disulfide-isomerase A-3 precursor. Thus demonstrating the reproducibility of this assay.

Importantly for the aims of this project, signature peptides from MMPs (Chapter 4) and related proteins were detectable in chromatographic eluates from serum-free culture supernatants, specifically for MMP-2, MMP-14, TIMP-1 and TIMP-2 (Table 6.6). The detection of the MMP inhibitors TIMP-1 (HT1080 SFCS eluates: E1-c and E2a) and TIMP-2 (HT1080 SFCS eluates: E1-c, E2a and E2c) strongly supports the utility of this method for identification of MMPs, particularly considering that these proteins are central to activation protein complex of MMPs.

This is the first demonstration that this methodology has applicability for detection of MMPs. The membrane-bound MMP-14 was identified from both eluates from 0.3M salt (HT1080 SFCS E1-c) and 2M salt (HT1080 SFCS E2c). This either supports the suggestion that MMP-14 is bound weakly to

the beads, or implies that MMP-14 was present at high levels and so exceeds the capacity of the chromatography beads. The detection of MMP-14 in culture supernatant rather than its expected localization within the cellular membrane was an unexpected observation. One explanation for this is that MMP-14 is cleaved from the membrane during sample processing, either as a consequence of trypsinization during routine cell culture or due to MMP-14 mediated auto-conversion (Rozanov et al., 2008), thereby appearing in the supernatant. Alternatively, MMP-14 is also known to exist in a soluble form, albeit at low levels, and so this may reflect this observation (Hakulinen et al., 2008). Interestingly, although MMP-2 was not detected in many of analyses, the fact MMP-2 requires both MMP-14 and TIMP-2 binding for its activation (Butler et al., 1998; Sounni et al., 2003), and the detection of both these species in the chromatography, may imply that MMP-2 was present but not directly bound to the chromatography beads and so undetected in most attempts. This is a hypothesis that obviously needs further investigation. Since TIMPs inhibit all the MMPs (Murphy and Nagase, 2008a), this suggests that other MMPs complexed with TIMPs are not being detected for the same reason. An interesting observation was the elution of TIMP-1 and TIMP-2 with EDTA containing elution buffers (Table 6.8 and Table 6.10) suggesting TIMPs might have more affinity towards Olive H-7G and the binding is reversed by EDTA. This highlights use of the dye ligand under discussion for the purification and identification of TIMPs.

These results therefore strongly support that Procion Olive H-7G (also known as Dyematrex Reactive Green A) is a suitable chromatography medium for purifying MMPs. This is in agreement with the previous studies indicating the binding of this dye to several pro-MMPs but also extends these studies by demonstrating that this dye can actually be used for isolation of further MMPs and has strong potential for affinity chromatography of MMPs from biological systems. With optimization of the chromatography procedures, it is hoped that other MMPs can also be detected. The data would have been more compelling if non-specific binding of proteins could be resolved completely.

In conclusion, this study has highlighted the challenges encountered in whole cell and culture supernatant based assays, particularly the issues of

sensitivity and specificity. From the results of the present work, it is concluded that simultaneous use of different protein separation techniques (MudPIT) performed at protein extraction level (cell fractionation) at protein isolation level (affinity chromatography) and at peptide level (nHPLC) allows MS and MS/MS analysis for MMP identification. The presence of detergent and albumin poses a problem in data interpretation in whole cell and culture supernatant based assays and was found to be detrimental in mass spectrum data acquisition. The results obtained so far are encouraging for the identification of latent and possibly active forms of MMPs by LC-MS/MS analysis (Table 5.5).

This study has acknowledged the challenges of developing a robust purification and identification method for MMPs exploiting the protease binding ability of Olive H-7G. Issues of selectivity and sensitivity within the context of techniques (MALDI-MS) utilized which by implication do not bode well for the low abundance protein identification. Hence, demonstration of non-specific proteins and lack of selectivity of Olive H-7G it is unlikely to translate the MMP purification success within clinical settings and further work needs to be done. Monitoring active MMPs using approaches described in this study will prove valuable in terms of our understanding of cancer and its treatment.

This study aimed to evaluate a previously commercially available method in conjunction with proteomics methods. Procion Olive H-7G dye was used as part of a series of chromatography steps used to purify pro-MMPs in the 80's and 90's but before proteomics techniques were widely available and before affinity capture had been re-introduced as a valuable method to enrich LAP for MS-based identification in the 00's. This project represents an opportunity to evaluate the traditional affinity purification method in conjunction with a modern LC-MALDI proteomics strategy to characterize a therapeutically important group of proteins in cancer samples. As opposed to previous studies, Olive H-7G was screened against more MMPs from various classes to find its broad range selectivity (Figure 8.1). The primary objective of this project is to develop affinity based methods, based on common

physicochemical and functional properties, for unambiguous detection by proteomic profiling of human pro-MMPs within a range of biological samples.

One of the outcomes of the approach described will help to progress in the detection of endogenous active and latent forms of MMPs in complex proteomes, an important objective with many diagnostic applications. It will help find out their state (active or latent) at the time of secretion and understand their role in tumour progression and metastasis in cancer. A long term outcome of MALDI-MS based MMP profile characterization proposed in this study is that it will help monitor the efficacy of a drug administered causing changes in MMP quantities being secreted. The development of new affinity capture tool for pro-MMPs and their subsequent characterization will provide a useful insight into their regulation prior to secretion and possible strategies to stop their activation on the onset of disease.

In summary, major findings of the study are:

- Pro-MMPs bind to H-7G-Sepharose chromatography beads.
- H7-G also binds other proteins (MDH) specifically as previously reported.
- Chromatography matrices constitute a major source of non-specific protein binding and no single type of bead is ideally suited.
- MMPs purified from biological sources and identified by LC-MS/MS are:

Cell Line		MMPs Identified
HT1080	Culture supernatant	MMP-2 MMP-14
	Cell extract	ND
HT29	Culture supernatant	MMP-7 (SM)
	Cell extract	ND
Dermal papilla	Culture supernatant	MMP-1 MMP-2 MMP-3 (Beads)

ND: Not detected

Future Work

- Potential use of signature peptides from pro- and active region for each MMP in MRM analysis in future studies.

- Introducing structural changes in Procion Olive H-7G dye so as to improve its selectivity towards MMPs.

- Since Olive H-7G is a small molecule, it might have a better chance of binding to smaller peptide molecules instead of larger 3D proteins. One possible approach can be affinity purification of peptides of MMPs using Olive H-7G instead of MMP affinity chromatography because of the difference in molecular sizes between protein and peptide.

- Introducing structural modifications (phosphorylation or glycosylation) in MMP's highly conserved region and see if the Olive H-7G dye has better specificity for phosph- or glyco- peptides.

- Design and synthesis of inhibitor based analogues as an alternative method for increased selectivity towards MMPs and reduce non-specific binding.

- Use of other affinity based ligands such as Procion Red HE-3B to compare its efficiency with Olive H-7G ligand.

- Identification of pro- or active form of MMP with greater sequence coverage using more than one digestion enzymes for increased confidence in protein identification from the MALDI-MS and database searching.

- Determination of changes in MMP levels under stressed physiological conditions, during tumourigenesis or following drug treatment.

References

Abrahams, T.P., Faust, M.L., and Varner, K.J. (1996). The depletion of monoamines blocks the sympathoinhibitory response to cocaine. J Auton Nerv Syst *58*, 170-176.

Amour, A., Knight, C.G., Webster, A., Slocombe, P.M., Stephens, P.E., Knauper, V., Docherty, A.J., and Murphy, G. (2000). The in vitro activity of ADAM-10 is inhibited by TIMP-1 and TIMP-3. FEBS Lett *473*, 275-279.

Anspach, J.A., Maloney, T.D., and Colon, L.A. (2007). Ultrahigh-pressure liquid chromatography using a 1-mm id column packed with 1.5-microm porous particles. Journal of separation science *30*, 1207-1213.

Atkinson, J.M., Pennington, C.J., Martin, S.W., Anikin, V.A., Mearns, A.J., Loadman, P.M., Edwards, D.R., and Gill, J.H. (2007). Membrane type matrix metalloproteinases (MMPs) show differential expression in non-small cell lung cancer (NSCLC) compared to normal lung: correlation of MMP-14 mRNA expression and proteolytic activity. Eur J Cancer *43*, 1764-1771.

Bayne, E.K., Hutchinson, N.I., Walakovits, L.A., Donatelli, S., MacNaul, K.L., Harper, C.F., Cameron, P., Moore, V.L., and Lark, M.W. (1992). Production, purification and characterization of canine prostromelysin. Matrix *12*, 173-184.

Becker, J.W., Marcy, A.I., Rokosz, L.L., Axel, M.G., Burbaum, J.J., Fitzgerald, P.M., Cameron, P.M., Esser, C.K., Hagmann, W.K., Hermes, J.D.*, et al.* (1995). Stromelysin-1: three-dimensional structure of the inhibited catalytic domain and of the C-truncated proenzyme. Protein Sci *4*, 1966-1976.

Bergers, G., and Benjamin, L.E. (2003). Tumorigenesis and the angiogenic switch. Nat Rev Cancer *3*, 401-410.

Bergers, G., Brekken, R., McMahon, G., Vu, T.H., Itoh, T., Tamaki, K., Tanzawa, K., Thorpe, P., Itohara, S., Werb, Z.*, et al.* (2000). Matrix metalloproteinase-9 triggers the angiogenic switch during carcinogenesis. Nat Cell Biol *2*, 737-744.

Berna, M., and Ackermann, B. (2009). Increased throughput for low-abundance protein biomarker verification by liquid chromatography/tandem mass spectrometry. Anal Chem *81*, 3950-3956.

Bernardo, M.M., Brown, S., Li, Z.H., Fridman, R., and Mobashery, S. (2002). Design, synthesis, and characterization of potent, slow-binding inhibitors that are selective for gelatinases. J Biol Chem *277*, 11201-11207.

Bibby, M.C. (1999). Making the most of rodent tumour systems in cancer drug discovery. Br J Cancer *79*, 1633-1640.

Blackburn, E.H. (2005). Telomeres and telomerase: their mechanisms of action and the effects of altering their functions. FEBS Lett *579*, 859-862.

Bode, W., Gomis-Ruth, F.X., and Stockler, W. (1993). Astacins, serralysins, snake venom and matrix metalloproteinases exhibit identical zinc-binding

environments (HEXXHXXGXXH and Met-turn) and topologies and should be grouped into a common family, the 'metzincins'. FEBS Lett *331*, 134-140.

Bradford, M.M. (1976). A rapid and sensitive method for the quantitation of microgram quantities of protein utilizing the principle of protein-dye binding. Anal Biochem *72*, 248-254.

Breuker, K., Jin, M., Han, X., Jiang, H., and McLafferty, F.W. (2008). Top-down identification and characterization of biomolecules by mass spectrometry. Journal of the American Society for Mass Spectrometry *19*, 1045-1053.

Butler, G.S., Butler, M.J., Atkinson, S.J., Will, H., Tamura, T., Schade van Westrum, S., Crabbe, T., Clements, J., d'Ortho, M.P., and Murphy, G. (1998). The TIMP2 membrane type 1 metalloproteinase "receptor" regulates the concentration and efficient activation of progelatinase A. A kinetic study. J Biol Chem *273*, 871-880.

Butler, G.S., Dean, R.A., Tam, E.M., and Overall, C.M. (2008). Pharmacoproteomics of a metalloproteinase hydroxamate inhibitor in breast cancer cells: dynamics of membrane type 1 matrix metalloproteinase-mediated membrane protein shedding. Mol Cell Biol *28*, 4896-4914.

Butler, G.S., and Overall, C.M. (2009). Updated biological roles for matrix metalloproteinases and new "intracellular" substrates revealed by degradomics. Biochemistry *48*, 10830-10845.

Carmeliet, P., and Jain, R.K. (2000). Angiogenesis in cancer and other diseases. Nature *407*, 249-257.

Cawston, T.E., and Wilson, A.J. (2006). Understanding the role of tissue degrading enzymes and their inhibitors in development and disease. Best Pract Res Clin Rheumatol *20*, 983-1002.

Chait, B.T. (2006). Chemistry. Mass spectrometry: bottom-up or top-down? Science *314*, 65-66.

Chase, A.J., and Newby, A.C. (2003). Regulation of matrix metalloproteinase (matrixin) genes in blood vessels: a multi-step recruitment model for pathological remodelling. J Vasc Res *40*, 329-343.

Choi, J., Choi, K., Benveniste, E.N., Rho, S.B., Hong, Y.S., Lee, J.H., Kim, J., and Park, K. (2005). Bcl-2 promotes invasion and lung metastasis by inducing matrix metalloproteinase-2. Cancer Res *65*, 5554-5560.

Chung, L., Dinakarpandian, D., Yoshida, N., Lauer-Fields, J.L., Fields, G.B., Visse, R., and Nagase, H. (2004). Collagenase unwinds triple-helical collagen prior to peptide bond hydrolysis. EMBO J *23*, 3020-3030.

Corchero, J.L., and Villaverde, A. (2009). Biomedical applications of distally controlled magnetic nanoparticles. Trends in biotechnology *27*, 468-476.

Cuatrecasas, P., and Wilchek, M. (1968). Single-step purification of avidine from egg white by affinity chromatography on biocytin-Sepharose columns. Biochem Biophys Res Commun *33*, 235-239.

Cuatrecasas, P., Wilchek, M., and Anfinsen, C.B. (1968). Selective enzyme purification by affinity chromatography. Proc Natl Acad Sci U S A *61*, 636-643.

Cuniasse, P., Devel, L., Makaritis, A., Beau, F., Georgiadis, D., Matziari, M., Yiotakis, A., and Dive, V. (2005). Future challenges facing the development of specific active-site-directed synthetic inhibitors of MMPs. Biochimie *87*, 393-402.

Cutillas, P.R., and Vanhaesebroeck, B. (2007). Quantitative profile of five murine core proteomes using label-free functional proteomics. Mol Cell Proteomics *6*, 1560-1573.

Dadvar, P., O'Flaherty, M., Scholten, A., Rumpel, K., and Heck, A.J. (2009). A chemical proteomics based enrichment technique targeting the interactome of the PDE5 inhibitor PF-4540124. Molecular bioSystems *5*, 472-482.

Dameron, K.M., Volpert, O.V., Tainsky, M.A., and Bouck, N. (1994). The p53 tumor suppressor gene inhibits angiogenesis by stimulating the production of thrombospondin. Cold Spring Harb Symp Quant Biol *59*, 483-489.

Datar, R.V., Cartwright, T., and Rosen, C.G. (1993). Process economics of animal cell and bacterial fermentations: a case study analysis of tissue plasminogen activator. Biotechnology (N Y) *11*, 349-357.

Davis, V., Persidskaia, R., Baca-Regen, L., Itoh, Y., Nagase, H., Persidsky, Y., Ghorpade, A., and Baxter, B.T. (1998). Matrix metalloproteinase-2 production and its binding to the matrix are increased in abdominal aortic aneurysms. Arterioscler Thromb Vasc Biol *18*, 1625-1633.

de Almeida, H., Jr., Zigrino, P., Muller, F., Krieg, T., Korge, B., and Mauch, C. (2005). Human scalp dermal papilla and fibrous sheath cells have a different expression profile of matrix metalloproteinases in vitro when compared to scalp dermal fibroblasts. Archives of dermatological research *297*, 121-126.

Dean, P.D., and Watson, D.H. (1979). Protein purification using immobilised triazine dyes. J Chromatogr *165*, 301-319.

Denizli, A., and Piskin, E. (2001). Dye-ligand affinity systems. J Biochem Biophys Methods *49*, 391-416.

Deschamps, A.M., Yarbrough, W.M., Squires, C.E., Allen, R.A., McClister, D.M., Dowdy, K.B., McLean, J.E., Mingoia, J.T., Sample, J.A., Mukherjee, R., *et al.* (2005). Trafficking of the membrane type-1 matrix metalloproteinase in ischemia and reperfusion: relation to interstitial membrane type-1 matrix metalloproteinase activity. Circulation *111*, 1166-1174.

Devel, L., Rogakos, V., David, A., Makaritis, A., Beau, F., Cuniasse, P., Yiotakis, A., and Dive, V. (2006). Development of selective inhibitors and substrate of matrix metalloproteinase-12. J Biol Chem *281*, 11152-11160.

Eckerskorn, C., Strupat, K., Karas, M., Hillenkamp, F., and Lottspeich, F. (1992). Mass spectrometric analysis of blotted proteins after gel electrophoretic separation by matrix-assisted laser desorption/ionization. Electrophoresis *13*, 664-665.

Egeblad, M., and Werb, Z. (2002). New functions for the matrix metalloproteinases in cancer progression. Nat Rev Cancer *2*, 161-174.

Eickelberg, O., Kohler, E., Reichenberger, F., Bertschin, S., Woodtli, T., Erne, P., Perruchoud, A.P., and Roth, M. (1999). Extracellular matrix deposition by primary human lung fibroblasts in response to TGF-beta1 and TGF-beta3. The American journal of physiology *276*, L814-824.

el-Gindy, A. (2003). Spectrophotometric and LC determination of two binary mixtures containing pyridoxine hydrochloride. J Pharm Biomed Anal *32*, 277-286.

Elkins, P.A., Ho, Y.S., Smith, W.W., Janson, C.A., D'Alessio, K.J., McQueney, M.S., Cummings, M.D., and Romanic, A.M. (2002). Structure of the C-terminally truncated human ProMMP9, a gelatin-binding matrix metalloproteinase. Acta Crystallogr D Biol Crystallogr *58*, 1182-1192.

Enghild, J.J., Salvesen, G., Brew, K., and Nagase, H. (1989). Interaction of human rheumatoid synovial collagenase (matrix metalloproteinase 1) and stromelysin (matrix metalloproteinase 3) with human alpha 2-macroglobulin and chicken ovostatin. Binding kinetics and identification of matrix metalloproteinase cleavage sites. J Biol Chem *264*, 8779-8785.

English, W.R., Holtz, B., Vogt, G., Knauper, V., and Murphy, G. (2001). Characterization of the role of the "MT-loop": an eight-amino acid insertion specific to progelatinase A (MMP2) activating membrane-type matrix metalloproteinases. J Biol Chem *276*, 42018-42026.

Evan, G., and Littlewood, T. (1998). A matter of life and cell death. Science *281*, 1317-1322.

Fearon, E.R., and Vogelstein, B. (1990). A genetic model for colorectal tumorigenesis. Cell *61*, 759-767.

Foley, K.P., and Eisenman, R.N. (1999). Two MAD tails: what the recent knockouts of Mad1 and Mxi1 tell us about the MYC/MAX/MAD network. Biochim Biophys Acta *1423*, M37-47.

Folkman, J. (1997). Addressing tumor blood vessels. Nat Biotechnol *15*, 510.

Ford, C.F., Suominen, I., and Glatz, C.E. (1991). Fusion tails for the recovery and purification of recombinant proteins. Protein Expr Purif *2*, 95-107.

Fynan, T.M., and Reiss, M. (1993). Resistance to inhibition of cell growth by transforming growth factor-beta and its role in oncogenesis. Crit Rev Oncog *4*, 493-540.

Garbett, E.A., Reed, M.W., and Brown, N.J. (1999). Proteolysis in human breast and colorectal cancer. Br J Cancer *81*, 287-293.

Gianazza, E., and Arnaud, P. (1982). A general method for fractionation of plasma proteins. Dye-ligand affinity chromatography on immobilized Cibacron blue F3-GA. Biochem J *201*, 129-136.

Giddings, J.C. (1984). Two-dimensional separations: concept and promise. Anal Chem *56*, 1258A-1260A, 1262A, 1264A passim.

Gomis-Ruth, F.X., Gohlke, U., Betz, M., Knauper, V., Murphy, G., Lopez-Otin, C., and Bode, W. (1996). The helping hand of collagenase-3 (MMP-13): 2.7 A crystal structure of its C-terminal haemopexin-like domain. J Mol Biol *264*, 556-566.

Gomis-Ruth, F.X., Maskos, K., Betz, M., Bergner, A., Huber, R., Suzuki, K., Yoshida, N., Nagase, H., Brew, K., Bourenkov, G.P.*, et al.* (1997). Mechanism of inhibition of the human matrix metalloproteinase stromelysin-1 by TIMP-1. Nature *389*, 77-81.

Greenbaum, D., Colangelo, C., Williams, K., and Gerstein, M. (2003). Comparing protein abundance and mRNA expression levels on a genomic scale. Genome Biol *4*, 117.

Greenlee, K.J., Werb, Z., and Kheradmand, F. (2007). Matrix metalloproteinases in lung: multiple, multifarious, and multifaceted. Physiological reviews *87*, 69-98.

Griffin, T.J., Gygi, S.P., Rist, B., Aebersold, R., Loboda, A., Jilkine, A., Ens, W., and Standing, K.G. (2001). Quantitative proteomic analysis using a MALDI quadrupole time-of-flight mass spectrometer. Anal Chem *73*, 978-986.

Gross, J., and Lapiere, C.M. (1962). Collagenolytic activity in amphibian tissues: a tissue culture assay. Proc Natl Acad Sci U S A *48*, 1014-1022.

Gunzer, G., and Hennrich, N. (1984). Purification of alpha 1-proteinase inhibitor by triazine dye affinity chromatography, ion-exchange chromatography and gel filtration on Fractogel TSK. J Chromatogr *296*, 221-229.

Gygi, S.P., Rist, B., Gerber, S.A., Turecek, F., Gelb, M.H., and Aebersold, R. (1999). Quantitative analysis of complex protein mixtures using isotope-coded affinity tags. Nat Biotechnol *17*, 994-999.

Haas, T.L. (2005). Endothelial cell regulation of matrix metalloproteinases. Canadian journal of physiology and pharmacology *83*, 1-7.

Hakulinen, J., Sankkila, L., Sugiyama, N., Lehti, K., and Keski-Oja, J. (2008). Secretion of active membrane type 1 matrix metalloproteinase (MMP-14) into extracellular space in microvesicular exosomes. J Cell Biochem *105*, 1211-1218.

Hamano, Y., Zeisberg, M., Sugimoto, H., Lively, J.C., Maeshima, Y., Yang, C., Hynes, R.O., Werb, Z., Sudhakar, A., and Kalluri, R. (2003). Physiological levels of tumstatin, a fragment of collagen IV alpha3 chain, are generated by MMP-9 proteolysis and suppress angiogenesis via alphaV beta3 integrin. Cancer Cell *3*, 589-601.

Han, X., Boyd, P.J., Colgan, S., Madri, J.A., and Haas, T.L. (2003). Transcriptional up-regulation of endothelial cell matrix metalloproteinase-2 in response to extracellular cues involves GATA-2. J Biol Chem *278*, 47785-47791.

Hanahan, D., and Weinberg, R.A. (2000). The hallmarks of cancer. Cell *100*, 57-70.

Hanahan, D., and Weinberg, R.A. (2011). Hallmarks of cancer: the next generation. Cell *144*, 646-674.

Hayashidani, S., Tsutsui, H., Ikeuchi, M., Shiomi, T., Matsusaka, H., Kubota, T., Imanaka-Yoshida, K., Itoh, T., and Takeshita, A. (2003). Targeted deletion

of MMP-2 attenuates early LV rupture and late remodeling after experimental myocardial infarction. Am J Physiol Heart Circ Physiol *285*, H1229-1235.

Hiraoka, N., Allen, E., Apel, I.J., Gyetko, M.R., and Weiss, S.J. (1998). Matrix metalloproteinases regulate neovascularization by acting as pericellular fibrinolysins. Cell *95*, 365-377.

Hudson, J.D., Shoaibi, M.A., Maestro, R., Carnero, A., Hannon, G.J., and Beach, D.H. (1999). A proinflammatory cytokine inhibits p53 tumor suppressor activity. J Exp Med *190*, 1375-1382.

Imai, K., and Okada, Y. (2008). Purification of matrix metalloproteinases by column chromatography. Nat Protoc *3*, 1111-1124.

Imai, K., Yokohama, Y., Nakanishi, I., Ohuchi, E., Fujii, Y., Nakai, N., and Okada, Y. (1995). Matrix metalloproteinase 7 (matrilysin) from human rectal carcinoma cells. Activation of the precursor, interaction with other matrix metalloproteinases and enzymic properties. J Biol Chem *270*, 6691-6697.

Itoh, T., Tanioka, M., Yoshida, H., Yoshioka, T., Nishimoto, H., and Itohara, S. (1998). Reduced angiogenesis and tumor progression in gelatinase A-deficient mice. Cancer Res *58*, 1048-1051.

Itoh, Y., Ito, N., Nagase, H., Evans, R.D., Bird, S.A., and Seiki, M. (2006). Cell surface collagenolysis requires homodimerization of the membrane-bound collagenase MT1-MMP. Mol Biol Cell *17*, 5390-5399.

Itoh, Y., Takamura, A., Ito, N., Maru, Y., Sato, H., Suenaga, N., Aoki, T., and Seiki, M. (2001). Homophilic complex formation of MT1-MMP facilitates proMMP-2 activation on the cell surface and promotes tumor cell invasion. EMBO J *20*, 4782-4793.

Iyer, S., Visse, R., Nagase, H., and Acharya, K.R. (2006). Crystal structure of an active form of human MMP-1. J Mol Biol *362*, 78-88.

Jessani, N., and Cravatt, B.F. (2004). The development and application of methods for activity-based protein profiling. Curr Opin Chem Biol *8*, 54-59.

Jozic, D., Bourenkov, G., Lim, N.H., Visse, R., Nagase, H., Bode, W., and Maskos, K. (2005). X-ray structure of human proMMP-1: new insights into procollagenase activation and collagen binding. J Biol Chem *280*, 9578-9585.

Kaiser, R.E., Jr., Williams, J.D., Lammert, S.A., Cooks, R.G., and Zakett, D. (1991). Thermospray liquid chromatography-mass spectrometry with a quadrupole ion trap mass spectrometer. J Chromatogr *562*, 3-11.

Kelleher, N.L. (2004). Top-down proteomics. Anal Chem *76*, 197A-203A.

Kheradmand, F., Werner, E., Tremble, P., Symons, M., and Werb, Z. (1998). Role of Rac1 and oxygen radicals in collagenase-1 expression induced by cell shape change. Science *280*, 898-902.

Kinoshita, T., Sato, H., Okada, A., Ohuchi, E., Imai, K., Okada, Y., and Seiki, M. (1998). TIMP-2 promotes activation of progelatinase A by membrane-type 1 matrix metalloproteinase immobilized on agarose beads. J Biol Chem *273*, 16098-16103.

Kinzler, K.W., and Vogelstein, B. (1996). Life (and death) in a malignant tumour. Nature *379*, 19-20.

Kleno, T.G., Andreasen, C.M., Kjeldal, H.O., Leonardsen, L.R., Krogh, T.N., Nielsen, P.F., Sorensen, M.V., and Jensen, O.N. (2004). MALDI MS peptide mapping performance by in-gel digestion on a probe with prestructured sample supports. Anal Chem *76*, 3576-3583.

Klier, C.M., Nelson, E.L., Cohen, C.D., Horuk, R., Schlondorff, D., and Nelson, P.J. (2001). Chemokine-Induced secretion of gelatinase B in primary human monocytes. Biological chemistry *382*, 1405-1410.

Knauper, V., Docherty, A.J., Smith, B., Tschesche, H., and Murphy, G. (1997). Analysis of the contribution of the hinge region of human neutrophil collagenase (HNC, MMP-8) to stability and collagenolytic activity by alanine scanning mutagenesis. FEBS Lett *405*, 60-64.

Koklitis, P.A., Murphy, G., Sutton, C., and Angal, S. (1991). Purification of recombinant human prostromelysin. Studies on heat activation to give high-Mr and low-Mr active forms, and a comparison of recombinant with natural stromelysin activities. Biochem J *276 (Pt 1)*, 217-221.

Koshikawa, N., Giannelli, G., Cirulli, V., Miyazaki, K., and Quaranta, V. (2000). Role of cell surface metalloprotease MT1-MMP in epithelial cell migration over laminin-5. J Cell Biol *148*, 615-624.

Lark, M.W., Walakovits, L.A., Shah, T.K., Vanmiddlesworth, J., Cameron, P.M., and Lin, T.Y. (1990). Production and purification of prostromelysin and procollagenase from IL-1 beta-stimulated human gingival fibroblasts. Connect Tissue Res *25*, 49-65.

Lee, W.C., and Lee, K.H. (2004). Applications of affinity chromatography in proteomics. Analytical biochemistry *324*, 1-10.

Li, R., Dowd, V., Stewart, D.J., Burton, S.J., and Lowe, C.R. (1998). Design, synthesis, and application of a protein A mimetic. Nat Biotechnol *16*, 190-195.

Longo, G.M., Xiong, W., Greiner, T.C., Zhao, Y., Fiotti, N., and Baxter, B.T. (2002). Matrix metalloproteinases 2 and 9 work in concert to produce aortic aneurysms. J Clin Invest *110*, 625-632.

Lopez-Otin, C., and Overall, C.M. (2002). Protease degradomics: a new challenge for proteomics. Nat Rev Mol Cell Biol *3*, 509-519.

Luo, D., Mari, B., Stoll, I., and Anglard, P. (2002). Alternative splicing and promoter usage generates an intracellular stromelysin 3 isoform directly translated as an active matrix metalloproteinase. J Biol Chem *277*, 25527-25536.

Madhusudan, and Vijayan, M. (1992). Additional binding sites in lysozyme. X-ray analysis of lysozyme complexes with bromophenol red and bromophenol blue. Protein Eng *5*, 399-404.

Makowski, G.S., and Ramsby, M.L. (2005). Autoactivation profiles of calcium-dependent matrix metalloproteinase-2 and -9 in inflammatory synovial fluid: effect of pyrophosphate and bisphosphonates. Clin Chim Acta *358*, 182-191.

Marchenko, G.N., Ratnikov, B.I., Rozanov, D.V., Godzik, A., Deryugina, E.I., and Strongin, A.Y. (2001). Characterization of matrix metalloproteinase-26, a

novel metalloproteinase widely expressed in cancer cells of epithelial origin. Biochem J *356*, 705-718.

Maskos, K. (2005). Crystal structures of MMPs in complex with physiological and pharmacological inhibitors. Biochimie *87*, 249-263.

Matsumura, S., Iwanaga, S., Mochizuki, S., Okamoto, H., Ogawa, S., and Okada, Y. (2005). Targeted deletion or pharmacological inhibition of MMP-2 prevents cardiac rupture after myocardial infarction in mice. J Clin Invest *115*, 599-609.

Merril, C.R., Dunau, M.L., and Goldman, D. (1981). A rapid sensitive silver stain for polypeptides in polyacrylamide gels. Anal Biochem *110*, 201-207.

Mix, K.S., Mengshol, J.A., Benbow, U., Vincenti, M.P., Sporn, M.B., and Brinckerhoff, C.E. (2001). A synthetic triterpenoid selectively inhibits the induction of matrix metalloproteinases 1 and 13 by inflammatory cytokines. Arthritis Rheum *44*, 1096-1104.

Mookhtiar, K.A., and Van Wart, H.E. (1990). Purification to homogeneity of latent and active 58-kilodalton forms of human neutrophil collagenase. Biochemistry *29*, 10620-10627.

Morgunova, E., Tuuttila, A., Bergmann, U., Isupov, M., Lindqvist, Y., Schneider, G., and Tryggvason, K. (1999). Structure of human pro-matrix metalloproteinase-2: activation mechanism revealed. Science *284*, 1667-1670.

Morgunova, E., Tuuttila, A., Bergmann, U., and Tryggvason, K. (2002). Structural insight into the complex formation of latent matrix metalloproteinase 2 with tissue inhibitor of metalloproteinase 2. Proc Natl Acad Sci U S A *99*, 7414-7419.

Moutsiakis, D., Mancuso, P., Krutzsch, H., Stetler-Stevenson, W., and Zucker, S. (1992). Characterization of metalloproteinases and tissue inhibitors of metalloproteinases in human plasma. Connect Tissue Res *28*, 213-230.

Muddiman, D.C., Anderson, G.A., Hofstadler, S.A., and Smith, R.D. (1997). Length and base composition of PCR-amplified nucleic acids using mass measurements from electrospray ionization mass spectrometry. Anal Chem *69*, 1543-1549.

Murphy, G., Allan, J.A., Willenbrock, F., Cockett, M.I., O'Connell, J.P., and Docherty, A.J. (1992). The role of the C-terminal domain in collagenase and stromelysin specificity. J Biol Chem *267*, 9612-9618.

Murphy, G., and Nagase, H. (2008a). Progress in matrix metalloproteinase research. Mol Aspects Med *29*, 290-308.

Murphy, G., and Nagase, H. (2008b). Reappraising metalloproteinases in rheumatoid arthritis and osteoarthritis: destruction or repair? Nat Clin Pract Rheumatol *4*, 128-135.

Murphy, G., Reynolds, J.J., Bretz, U., and Baggiolini, M. (1982). Partial purification of collagenase and gelatinase from human polymorphonuclear leucocytes. Analysis of their actions on soluble and insoluble collagens. Biochem J *203*, 209-221.

Nagase, H., Enghild, J.J., Suzuki, K., and Salvesen, G. (1990). Stepwise activation mechanisms of the precursor of matrix metalloproteinase 3 (stromelysin) by proteinases and (4-aminophenyl)mercuric acetate. Biochemistry *29*, 5783-5789.

Nakamura, H., Fujii, Y., Ohuchi, E., Yamamoto, E., and Okada, Y. (1998). Activation of the precursor of human stromelysin 2 and its interactions with other matrix metalloproteinases. Eur J Biochem *253*, 67-75.

Nelson, K.K., and Melendez, J.A. (2004). Mitochondrial redox control of matrix metalloproteinases. Free radical biology & medicine *37*, 768-784.

Noel, A., Jost, M., and Maquoi, E. (2008). Matrix metalloproteinases at cancer tumor-host interface. Semin Cell Dev Biol *19*, 52-60.

Nomura, H., Fujimoto, N., Seiki, M., Mai, M., and Okada, Y. (1996). Enhanced production of matrix metalloproteinases and activation of matrix metalloproteinase 2 (gelatinase A) in human gastric carcinomas. Int J Cancer *69*, 9-16.

O'Donovan, C., Apweiler, R., and Bairoch, A. (2001). The human proteomics initiative (HPI). Trends in biotechnology *19*, 178-181.

Oakley, B.R., Kirsch, D.R., and Morris, N.R. (1980). A simplified ultrasensitive silver stain for detecting proteins in polyacrylamide gels. Anal Biochem *105*, 361-363.

Okada, Y., Gonoji, Y., Naka, K., Tomita, K., Nakanishi, I., Iwata, K., Yamashita, K., and Hayakawa, T. (1992). Matrix metalloproteinase 9 (92-kDa gelatinase/type IV collagenase) from HT 1080 human fibrosarcoma cells. Purification and activation of the precursor and enzymic properties. J Biol Chem *267*, 21712-21719.

Okada, Y., Harris, E.D., Jr., and Nagase, H. (1988). The precursor of a metalloendopeptidase from human rheumatoid synovial fibroblasts. Purification and mechanisms of activation by endopeptidases and 4-aminophenylmercuric acetate. Biochem J *254*, 731-741.

Okada, Y., Morodomi, T., Enghild, J.J., Suzuki, K., Yasui, A., Nakanishi, I., Salvesen, G., and Nagase, H. (1990). Matrix metalloproteinase 2 from human rheumatoid synovial fibroblasts. Purification and activation of the precursor and enzymic properties. Eur J Biochem *194*, 721-730.

Okada, Y., Nagase, H., and Harris, E.D., Jr. (1986). A metalloproteinase from human rheumatoid synovial fibroblasts that digests connective tissue matrix components. Purification and characterization. J Biol Chem *261*, 14245-14255.

Ong, S.E., Blagoev, B., Kratchmarova, I., Kristensen, D.B., Steen, H., Pandey, A., and Mann, M. (2002). Stable isotope labeling by amino acids in cell culture, SILAC, as a simple and accurate approach to expression proteomics. Mol Cell Proteomics *1*, 376-386.

Opiteck, G.J., Lewis, K.C., Jorgenson, J.W., and Anderegg, R.J. (1997). Comprehensive on-line LC/LC/MS of proteins. Anal Chem *69*, 1518-1524.

Overall, C.M., and Blobel, C.P. (2007). In search of partners: linking extracellular proteases to substrates. Nat Rev Mol Cell Biol *8*, 245-257.

Overall, C.M., and Dean, R.A. (2006). Degradomics: systems biology of the protease web. Pleiotropic roles of MMPs in cancer. Cancer Metastasis Rev *25*, 69-75.

Overall, C.M., and Lopez-Otin, C. (2002). Strategies for MMP inhibition in cancer: innovations for the post-trial era. Nat Rev Cancer *2*, 657-672.

Overall, C.M., Wrana, J.L., and Sodek, J. (1991). Transcriptional and post-transcriptional regulation of 72-kDa gelatinase/type IV collagenase by transforming growth factor-beta 1 in human fibroblasts. Comparisons with collagenase and tissue inhibitor of matrix metalloproteinase gene expression. J Biol Chem *266*, 14064-14071.

Owen, C.A., and Campbell, E.J. (1999). The cell biology of leukocyte-mediated proteolysis. J Leukoc Biol *65*, 137-150.

Owen, C.A., Hu, Z., Barrick, B., and Shapiro, S.D. (2003). Inducible expression of tissue inhibitor of metalloproteinases-resistant matrix metalloproteinase-9 on the cell surface of neutrophils. American journal of respiratory cell and molecular biology *29*, 283-294.

Pardo, A., Ramirez, R., Gutierrez-Kobeh, L., Mendoza, F., Bauer, E., and Selman, M. (1991). Purification of a procollagenase-activator present in medium of cultured guinea pig carrageenin granuloma. Connect Tissue Res *26*, 259-269.

Patel, B.P., Shah, S.V., Shukla, S.N., Shah, P.M., and Patel, P.S. (2007). Clinical significance of MMP-2 and MMP-9 in patients with oral cancer. Head & neck *29*, 564-572.

Pei, D., and Weiss, S.J. (1995). Furin-dependent intracellular activation of the human stromelysin-3 zymogen. Nature *375*, 244-247.

Perkins, D.N., Pappin, D.J., Creasy, D.M., and Cottrell, J.S. (1999). Probability-based protein identification by searching sequence databases using mass spectrometry data. Electrophoresis *20*, 3551-3567.

Pitti, R.M., Marsters, S.A., Lawrence, D.A., Roy, M., Kischkel, F.C., Dowd, P., Huang, A., Donahue, C.J., Sherwood, S.W., Baldwin, D.T.*, et al.* (1998). Genomic amplification of a decoy receptor for Fas ligand in lung and colon cancer. Nature *396*, 699-703.

Plantner, J.J., and Quinn, T.A. (1997). Association of matrix metalloproteinases with interphotoreceptor retinoid binding protein. Current eye research *16*, 51-55.

Puente, X.S., and Lopez-Otin, C. (2004). A genomic analysis of rat proteases and protease inhibitors. Genome Res *14*, 609-622.

Puente, X.S., Sanchez, L.M., Overall, C.M., and Lopez-Otin, C. (2003). Human and mouse proteases: a comparative genomic approach. Nat Rev Genet *4*, 544-558.

Qoronfleh, M.W., Chowdhury, S.K., Eshraghi, J., Ho, T., Brake, P.G., Banks, T., Huang, J., Pulvino, T., and Jones, B.N. (1997). Identification of new autolytic sites of recombinant truncated mature human fibroblast stromelysin by mass spectrometry. The journal of peptide research : official journal of the American Peptide Society *49*, 612-619.

Ra, H.J., and Parks, W.C. (2007). Control of matrix metalloproteinase catalytic activity. Matrix Biol *26*, 587-596.

Randall, V.A. (1996). The use of dermal papilla cells in studies of normal and abnormal hair follicle biology. Dermatologic clinics *14*, 585-594.

Rijken, F., and Bruijnzeel, P.L. (2009). The pathogenesis of photoaging: the role of neutrophils and neutrophil-derived enzymes. The journal of investigative dermatology Symposium proceedings / the Society for Investigative Dermatology, Inc [and] European Society for Dermatological Research *14*, 67-72.

Roomi, M.W., Monterrey, J.C., Kalinovsky, T., Rath, M., and Niedzwiecki, A. (2009). Patterns of MMP-2 and MMP-9 expression in human cancer cell lines. Oncol Rep *21*, 1323-1333.

Roschlau, P., and Hess, B. (1972). Affinity chromatography of yeast pyruvate kinase with Cibacronblau bound to Sephadex G-200. Hoppe Seylers Z Physiol Chem *353*, 441-443.

Rosenblum, G., Van den Steen, P.E., Cohen, S.R., Grossmann, J.G., Frenkel, J., Sertchook, R., Slack, N., Strange, R.W., Opdenakker, G., and Sagi, I. (2007). Insights into the structure and domain flexibility of full-length pro-matrix metalloproteinase-9/gelatinase B. Structure *15*, 1227-1236.

Ross, P.L., Huang, Y.N., Marchese, J.N., Williamson, B., Parker, K., Hattan, S., Khainovski, N., Pillai, S., Dey, S., Daniels, S.*, et al.* (2004). Multiplexed protein quantitation in Saccharomyces cerevisiae using amine-reactive isobaric tagging reagents. Mol Cell Proteomics *3*, 1154-1169.

Rozanov, D.V., Savinov, A.Y., Williams, R., Liu, K., Golubkov, V.S., Krajewski, S., and Strongin, A.Y. (2008). Molecular signature of MT1-MMP: transactivation of the downstream universal gene network in cancer. Cancer Res *68*, 4086-4096.

Sadygov, R.G., and Yates, J.R., 3rd (2003). A hypergeometric probability model for protein identification and validation using tandem mass spectral data and protein sequence databases. Anal Chem *75*, 3792-3798.

Saghatelian, A., Jessani, N., Joseph, A., Humphrey, M., and Cravatt, B.F. (2004). Activity-based probes for the proteomic profiling of metalloproteases. Proc Natl Acad Sci U S A *101*, 10000-10005.

Sarkissian, G., Fergelot, P., Lamy, P.J., Patard, J.J., Culine, S., Jouin, P., Rioux-Leclercq, N., and Darbouret, B. (2008). Identification of pro-MMP-7 as a serum marker for renal cell carcinoma by use of proteomic analysis. Clin Chem *54*, 574-581.

Schropfer, A., Kammerer, U., Kapp, M., Dietl, J., Feix, S., and Anacker, J. (2010). Expression pattern of matrix metalloproteinases in human gynecological cancer cell lines. BMC cancer *10*, 553.

Seltzer, J.L., Eschbach, M.L., and Eisen, A.Z. (1985). Purification of gelatin-specific neutral protease from human skin by conventional and high-performance liquid chromatography. J Chromatogr *326*, 147-155.

Shen, Y., Zhang, R., Moore, R.J., Kim, J., Metz, T.O., Hixson, K.K., Zhao, R., Livesay, E.A., Udseth, H.R., and Smith, R.D. (2005). Automated 20 kpsi

RPLC-MS and MS/MS with chromatographic peak capacities of 1000-1500 and capabilities in proteomics and metabolomics. Anal Chem *77*, 3090-3100.

Shi, Y.B., Li, Q., Damjanovski, S., Amano, T., and Ishizuya-Oka, A. (1998). Regulation of apoptosis during development: input from the extracellular matrix (review). Int J Mol Med *2*, 273-282.

Shiomi, T., and Okada, Y. (2003). MT1-MMP and MMP-7 in invasion and metastasis of human cancers. Cancer Metastasis Rev *22*, 145-152.

Smeets, T.J., Kraan, M.C., Galjaard, S., Youssef, P.P., Smith, M.D., and Tak, P.P. (2001). Analysis of the cell infiltrate and expression of matrix metalloproteinases and granzyme B in paired synovial biopsy specimens from the cartilage-pannus junction in patients with RA. Ann Rheum Dis *60*, 561-565.

Sobott, F., Hernandez, H., McCammon, M.G., Tito, M.A., and Robinson, C.V. (2002). A tandem mass spectrometer for improved transmission and analysis of large macromolecular assemblies. Anal Chem *74*, 1402-1407.

Sounni, N.E., Janssen, M., Foidart, J.M., and Noel, A. (2003). Membrane type-1 matrix metalloproteinase and TIMP-2 in tumor angiogenesis. Matrix Biol *22*, 55-61.

Stack, M.S., Emberts, C.G., and Gray, R.D. (1991). Application of N-carboxyalkyl peptides to the inhibition and affinity purification of the porcine matrix metalloproteinases collagenase, gelatinase, and stromelysin. Arch Biochem Biophys *287*, 240-249.

Stahl, S., and Nygren, P.A. (1997). The use of gene fusions to protein A and protein G in immunology and biotechnology. Pathol Biol (Paris) *45*, 66-76.

Steeg, P.S., and Theodorescu, D. (2008). Metastasis: a therapeutic target for cancer. Nat Clin Pract Oncol *5*, 206-219.

Stetler-Stevenson, W.G. (1999). Matrix metalloproteinases in angiogenesis: a moving target for therapeutic intervention. J Clin Invest *103*, 1237-1241.

Stone, K.L., DeAngelis, R., LoPresti, M., Jones, J., Papov, V.V., and Williams, K.R. (1998). Use of liquid chromatography-electrospray ionization-tandem mass spectrometry (LC-ESI-MS/MS) for routine identification of enzymatically digested proteins separated by sodium dodecyl sulfate-polyacrylamide gel electrophoresis. Electrophoresis *19*, 1046-1052.

Stratmann, B., Farr, M., and Tschesche, H. (2001). Characterization of C-terminally truncated human tissue inhibitor of metalloproteinases-4 expressed in Pichia pastoris. Biological chemistry *382*, 987-991.

Strongin, A.Y., Collier, I., Bannikov, G., Marmer, B.L., Grant, G.A., and Goldberg, G.I. (1995). Mechanism of cell surface activation of 72-kDa type IV collagenase. Isolation of the activated form of the membrane metalloprotease. J Biol Chem *270*, 5331-5338.

Sun, H.B., and Yokota, H. (2001). Messenger-RNA expression of matrix metalloproteinases, tissue inhibitors of metalloproteinases, and transcription factors in rheumatic synovial cells under mechanical stimuli. Bone *28*, 303-309.

Sutton, C.W. (2011). The role of targeted chemical proteomics in pharmacology. British journal of pharmacology.

Swaminathan, S., and Khanna, N. (1999). Affinity purification of recombinant interferon-alpha on a mimetic ligand adsorbent. Protein Expr Purif *15*, 236-242.

Switzer, R.C., 3rd, Merril, C.R., and Shifrin, S. (1979). A highly sensitive silver stain for detecting proteins and peptides in polyacrylamide gels. Anal Biochem *98*, 231-237.

Symonds, H., Krall, L., Remington, L., Saenz-Robles, M., Lowe, S., Jacks, T., and Van Dyke, T. (1994). p53-dependent apoptosis suppresses tumor growth and progression in vivo. Cell *78*, 703-711.

Takino, T., Miyamori, H., Watanabe, Y., Yoshioka, K., Seiki, M., and Sato, H. (2004). Membrane type 1 matrix metalloproteinase regulates collagen-dependent mitogen-activated protein/extracellular signal-related kinase activation and cell migration. Cancer Res *64*, 1044-1049.

Tao, W.A., and Aebersold, R. (2003). Advances in quantitative proteomics via stable isotope tagging and mass spectrometry. Curr Opin Biotechnol *14*, 110-118.

Trinkle-Mulcahy, L., Boulon, S., Lam, Y.W., Urcia, R., Boisvert, F.M., Vandermoere, F., Morrice, N.A., Swift, S., Rothbauer, U., Leonhardt, H.*, et al.* (2008). Identifying specific protein interaction partners using quantitative mass spectrometry and bead proteomes. J Cell Biol *183*, 223-239.

Tsukada, H., and Pourmotabbed, T. (2002). Unexpected crucial role of residue 272 in substrate specificity of fibroblast collagenase. J Biol Chem *277*, 27378-27384.

Urh, M., Simpson, D., and Zhao, K. (2009). Affinity chromatography: general methods. Methods Enzymol *463*, 417-438.

Van den Steen, P.E., Van Aelst, I., Hvidberg, V., Piccard, H., Fiten, P., Jacobsen, C., Moestrup, S.K., Fry, S., Royle, L., Wormald, M.R.*, et al.* (2006). The hemopexin and O-glycosylated domains tune gelatinase B/MMP-9 bioavailability via inhibition and binding to cargo receptors. J Biol Chem *281*, 18626-18637.

Van Wart, H.E., and Birkedal-Hansen, H. (1990). The cysteine switch: a principle of regulation of metalloproteinase activity with potential applicability to the entire matrix metalloproteinase gene family. Proc Natl Acad Sci U S A *87*, 5578-5582.

Varmus, H. (2006). The new era in cancer research. Science *312*, 1162-1165.

Visse, R., and Nagase, H. (2003). Matrix metalloproteinases and tissue inhibitors of metalloproteinases: structure, function, and biochemistry. Circ Res *92*, 827-839.

Volpert, O.V., Dameron, K.M., and Bouck, N. (1997). Sequential development of an angiogenic phenotype by human fibroblasts progressing to tumorigenicity. Oncogene *14*, 1495-1502.

Wang, W.M., Ge, G., Lim, N.H., Nagase, H., and Greenspan, D.S. (2006). TIMP-3 inhibits the procollagen N-proteinase ADAMTS-2. Biochem J *398*, 515-519.

Wang, X., Yi, J., Lei, J., and Pei, D. (1999). Expression, purification and characterization of recombinant mouse MT5-MMP protein products. FEBS Lett *462*, 261-266.

Watson, D.H., Harvey, M.J., and Dean, P.D. (1978). The selective retardation of NADP+-dependent dehydrogenases by immobilized procion red HE-3B. Biochem J *173*, 591-596.

Weiss, L., Orr, F.W., and Honn, K.V. (1988). Interactions of cancer cells with the microvasculature during metastasis. FASEB J *2*, 12-21.

Werner, R.G., and Berthold, W. (1988). Purification of proteins produced by biotechnological process. Arzneimittel-Forschung *38*, 422-428.

Wright, W.E., Pereira-Smith, O.M., and Shay, J.W. (1989). Reversible cellular senescence: implications for immortalization of normal human diploid fibroblasts. Mol Cell Biol *9*, 3088-3092.

Wu, Y.I., Munshi, H.G., Sen, R., Snipas, S.J., Salvesen, G.S., Fridman, R., and Stack, M.S. (2004). Glycosylation broadens the substrate profile of membrane type 1 matrix metalloproteinase. J Biol Chem *279*, 8278-8289.

Yarden, Y., and Ullrich, A. (1988). Growth factor receptor tyrosine kinases. Annu Rev Biochem *57*, 443-478.

Yates, J.R., 3rd (1998). Mass spectrometry and the age of the proteome. J Mass Spectrom *33*, 1-19.

Yates, J.R., Ruse, C.I., and Nakorchevsky, A. (2009). Proteomics by mass spectrometry: approaches, advances, and applications. Annual review of biomedical engineering *11*, 49-79.

Zhou, Z., Apte, S.S., Soininen, R., Cao, R., Baaklini, G.Y., Rauser, R.W., Wang, J., Cao, Y., and Tryggvason, K. (2000). Impaired endochondral ossification and angiogenesis in mice deficient in membrane-type matrix metalloproteinase I. Proc Natl Acad Sci U S A *97*, 4052-4057.

Zoon, K.C., Smith, M.E., Bridgen, P.J., zur Nedden, D., and Anfinsen, C.B. (1979). Purification and partial characterization of human lymphoblast interferon. Proc Natl Acad Sci U S A *76*, 5601-5605.

Books:

Harvey, M. J., (1980). The application of affinity chromatography and hydrophobic chromatography to the purification of serum albumin. In: Curling JM, editor. Methods of plasma protein fractionation. London: Academic Press; 189-200.

More, J. E., Hitchcock, A.G., Price, S., Rott, J., Harvey, M.J., (1989). Dye-protein interactions: developments and applications. In: Vijayalakshimi MA, Bertrand O, editors. London: Elsevier; 265.

Zollinger, H., (1991). Colour chemistry, VCH, Weinheim, New York, Basel, Cambridge, 2nd edition.

Appendices

Appendix 1 Buffer compositions.

SDS-PAGE running buffer (10X)

Components	
Tris-Base	30g
Glycine	144g
SDS	5g
dH_2O	Upto 1L

Western blot transfer buffer (10X)

Components	
Tris-Base	84.4g
Glycine	225.2g
dH_2O	400mL
Methanol	100mL for 1X

Loading dye

Components	**Final Conc.**
Tris-HCl	0.1M
Glycerol	5%
dH_2O	-
SDS	0.10%
Bromophenol	0.01%
β-mercaptoethanol	1%

TBS (10X)

Components	
Tris-Base	6g
NaCl	43g
dH_2O	Upto 500mL

CAB dialysis buffer (10X)

Components	
Tris-Base (pH 7.6)	30.3g
NaCl	58.4g
$CaCl_2$	0.74g
NaN_3 (20%)	50mL
dH_2O	Upto 500mL

Appendix 2 Cell lines origin.

Cell Line	**Origin/ Source**	**Reference**
HT1080	Fibrosarcoma arising adjacent to the acetabulum of a 35 year old Caucasian male.	Rasheed et al., 1974.
HT29	Colorectal adenocarcinoma from a 44-year-old Caucasian female.	J. Natl. Cancer Inst. 59: 221-226, 1977.

Appendix 3 Horse heart myoglobin theoretical digests.

Horse Heart Myoglobin									
Tryptic Digests	**Range**	**Mono MH+**	**Partials**	**Sequence**	**Tryptic Digests**	**Range**	**Mono MH+**	**Partials**	**Sequence**
T1	[1- 16]	1815.90	0	GLSDGEWQQVLNVWGK	T12	[79- 79]	147.11	0	K
T2	[17- 31]	1606.86	0	VEADIAGHGQEVLIR	T13	[80- 96]	1853.96	0	GHHEAELKPLAQSHATK
T3	[32- 42]	1271.66	0	LFTGHPETLEK	T14	[97- 98]	284.17	0	HK
T4	[43- 45]	409.21	0	FDK	T15	[99-102]	470.33	0	IPIK
T5	[46- 47]	294.18	0	FK	T16	[103-118]	1885.02	0	YLEFISDAIIHVLHSK
T6	[48- 50]	397.26	0	HLK	T17	[119-133]	1502.67	0	HPGDFGADAQGAMTK
T7	[51- 56]	708.32	0	TEAEMK	T18	[134-139]	748.44	0	ALELFR
T8	[57- 62]	662.34	0	ASEDLK	T19	[140-145]	631.34	0	NDIAAK
T9	[63- 63]	147.11	0	K	T20	[146-147]	310.18	0	YK
T10	[64- 77]	1378.84	0	HGTVVLTALGGILK	T21	[148-153]	650.31	0	ELGFQG
T11	[78- 78]	147.11	0	K					

Appendix 4 MMP theoretical digests.

MMP-1									
Tryptic Digests	Range	Mono MH+	Partial	Sequence	Tryptic Digests	Range	Mono MH+	Partial	Sequence
T1	[1- 36]	4122.141	0	MHSFPPLLLL.....QEQDVDLVQK	T28	[292-298]	857.423	0	GEVMFFK
T2	[37- 40]	552.303	0	YLEK	T29	[299-300]	290.146	0	DR
T3	[41- 45]	700.366	0	YYNLK	T30	[301-304]	616.291	0	FYMR
T4	[46- 49]	461.21	0	NDGR	T31	[305-337]	3873.88	0	TNPFYPEVEL.....LEAAYEFADR
T5	[50- 53]	503.282	0	QVEK	T32	[338-341]	518.257	0	DEVR
T6	[54- 54]	175.119	0	R	T33	[342-344]	441.25	0	FFK
T7	[55- 55]	175.119	0	R	T34	[345-347]	318.177	0	GNK
T8	[56- 63]	829.441	0	NSGPWEK	T35	[348-362]	1759.891	0	YWAVQGQNVLHGYPK
T9	[64- 65]	260.197	0	LK	T36	[363-372]	1188.568	0	DIYSSFGFPR
T10	[66- 74]	1127.555	0	QMQEFFGLK	T37	[373-375]	347.229	0	TVK
T11	[75- 85]	1158.636	0	VTGKPDAETLK	T38	[376-388]	1384.67	0	HIDAALSEENTGK
T12	[86- 88]	377.222	0	VMK	T39	[389-396]	989.509	0	TYFFVANK
T13	[89- 91]	400.23	0	QPR	T40	[397-399]	524.262	0	YWR
T14	[92-108]	1801.89	0	CGVPDVAQFVLTEGNPR	T41	[400-404]	717.309	0	YDEYK
T15	[109-117]	1233.601	0	WEQTHLTYR	T42	[405-405]	175.119	0	R
T16	[118-127]	1217.616	0	IENYTPDLPR	T43	[406-413]	894.403	0	SMDPGYPK
T17	[128-136]	997.495	0	ADVDHAIEK	T44	[414-425]	1322.667	0	MIAHDFPGIGHK
T18	[137-151]	1752.932	0	AFQLWSNVTPLTFTK	T45	[426-432]	809.423	0	VDAVFMK
T19	[152-165]	1551.784	0	VSEGQADIMISFVR	T46	[433-443]	1393.632	0	DGFFYFFHGTR
T20	[166-169]	484.226	0	GDHR	T47	[444-446]	438.235	0	QYK
T21	[170-202]	3393.479	0	DNSPFDGPGG.....GDAHFDEDER	T48	[447-450]	506.261	0	FDPK
T22	[203-208]	837.4	0	WTNNFR	T49	[451-452]	248.16	0	TK
T23	[209-214]	831.411	0	EYNLHR	T50	[453-453]	175.119	0	R
T24	[215-262]	5089.464	0	VAAHELGHSL.....IDGIQAIYGR	T51	[454-459]	715.471	0	ILTLQK
T25	[263-276]	1490.796	0	SQNPVQPIGPQTPK	T52	[460-467]	997.431	0	ANSWFNCR
T26	[277-281]	523.218	0	ACDSK	T53	[468-469]	261.156	0	KN
T27	[282-291]	1150.647	0	LTFDAITTIR					

MMP-2									
Tryptic Digests	Range	Mono MH+	Partial	Sequence	Tryptic Digests	Range	Mono MH+	Partial	Sequence
T1	[1- 7]	821.40	0	MEALMAR	T35	[328-328]	147.11	0	K
T2	[8- 15]	784.47	0	GALTGPLR	T36	[329-359]	3228.45	0	YGFCPETAMS…..VFPFTFLGNK
T3	[16- 36]	2062.16	0	ALCLLGCLLSHAAAAPSPIIK	T37	[360-368]	973.40	0	YESCTSAGR
T4	[37- 44]	830.44	0	FPGDVAPK	T38	[369-372]	406.19	0	SDGK
T5	[45- 47]	363.19	0	TDK	T39	[373-385]	1561.61	0	MWCATTANYDDDR
T6	[48- 62]	1745.86	0	ELAVQYLNTFYGCPK	T40	[386-386]	147.11	0	K
T7	[63- 71]	1052.54	0	ESCNLFVLK	T41	[387-429]	4756.21	0	WGFCPDQGYSL…..LMAPIYTYTK
T8	[72- 75]	476.27	0	DTLK	T42	[430-432]	436.23	0	NFR
T9	[76- 76]	147.11	0	K	T43	[433-439]	818.43	0	LSQDDIK
T10	[77- 79]	406.21	0	MQK	T44	[440-470]	3139.59	0	GIQELYGASP…..LGPVTPEICK
T11	[80- 98]	2183.04	0	FFGLPQTGDLDQNTIETMR	T45	[471-482]	1374.74	0	QDIVFDGIAQIR
T12	[99-101]	400.27	0	KPR	T46	[483-489]	887.47	0	GEIFFFK
T13	[102-115]	1613.72	0	CGNPDVANYNFFPR	T47	[490-491]	290.15	0	DR
T14	[116-118]	372.26	0	KPK	T48	[492-495]	621.35	0	FIWR
T15	[119-121]	448.22	0	WDK	T49	[496-500]	573.34	0	TVTPR
T16	[122-127]	794.42	0	NQITYR	T50	[501-519]	2168.15	0	DKPMGPLLVATFWPELPEK
T17	[128-146]	2108.02	0	IIGYTPDLDPETVDDAFAR	T51	[520-531]	1391.67	0	IDAVYEAPQEEK
T18	[147-158]	1418.74	0	AFQVWSDVTPLR	T52	[532-550]	2224.07	0	AVFFAGNEYWIYSASTLER
T19	[159-161]	409.22	0	FSR	T53	[551-567]	1838.02	0	GYPKPLTSLGLPPDVQR
T20	[162-175]	1587.76	0	IHDGEADIMINFGR	T54	[568-576]	1037.51	0	VDAAFNWSK
T21	[176-187]	1407.60	0	WEHGDGYPFDGK	T55	[577-578]	261.16	0	NK
T22	[188-222]	3638.72	0	DGLLAHAFAP…..WTLGEGQVVR	T56	[579-579]	147.11	0	K
T23	[223-224]	246.18	0	VK	T57	[580-587]	914.46	0	TYIFAGDK
T24	[225-234]	1119.44	0	YGNADGEYCK	T58	[588-590]	508.27	0	FWR
T25	[235-242]	969.52	0	FPFLFNGK	T59	[591-595]	652.33	0	YNEVK
T26	[243-252]	1145.45	0	EYNSCTDTGR	T60	[596-596]	147.11	0	K
T27	[253-267]	1797.78	0	SDGFLWCSTTYNFEK	T61	[597-597]	147.11	0	K
T28	[268-270]	319.16	0	DGK	T62	[598-604]	791.38	0	MDPGFPK
T29	[271-292]	2357.02	0	YGFCPHEALFTMGGNAEGQPCK	T63	[605-633]	3146.56	0	LIADAWNAIPD…..GGHSYFFK
T30	[293-296]	566.31	0	FPFR	T64	[634-639]	714.38	0	GAYYLK
T31	[297-310]	1551.64	0	FQGTSYDSCTTEGR	T65	[640-646]	831.46	0	LENQSLK
T32	[311-315]	611.28	0	TDGYR	T66	[647-649]	333.21	0	SVK
T33	[316-325]	1245.48	0	WCGTTEDYDR	T67	[650-654]	551.32	0	FGSIK
T34	[326-327]	262.14	0	DK	T68	[655-660]	680.27	0	SDWLGC

MMP-3									
Tryptic Digest	Range	Mono MH+	Partial	Sequence	Tryptic Digest	Range	Mono MH+	Partial	Sequence
T1	[1- 2]	278.153	0	MK	T29	[249-250]	322.187	0	FR
T2	[3- 25]	2358.292	0	SLPILLLLCV.....SAYPLDGAAR	T30	[251-303]	5511.679	0	LSQDDINGIQ.....LSFDAVSTLR
T3	[26- 36]	1221.578	0	GEDTSMNLVQK	T31	[304-310]	819.497	0	GEILIFK
T4	[37- 45]	1220.583	0	YLENYYDLK	T32	[311-312]	290.146	0	DR
T5	[46- 46]	147.113	0	K	T33	[313-316]	645.326	0	HFWR
T6	[47- 49]	361.208	0	DVK	T34	[317-317]	147.113	0	K
T7	[50- 53]	549.314	0	QFVR	T35	[318-320]	375.235	0	SLR
T8	[54- 54]	175.119	0	R	T36	[321-321]	147.113	0	K
T9	[55- 55]	147.113	0	K	T37	[322-349]	3072.556	0	LEPELHLISS.....VDAAYEVTSK
T10	[56- 62]	701.383	0	DSGPVVK	T38	[350-356]	881.513	0	DLVFIFK
T11	[63- 63]	147.113	0	K	T39	[357-364]	991.511	0	GNQFWAIR
T12	[64- 65]	288.203	0	IR	T40	[365-369]	574.294	0	GNEVR
T13	[66- 69]	535.254	0	EMQK	T41	[370-374]	563.294	0	AGYPR
T14	[70- 78]	963.551	0	FLGLEVTGK	T42	[375-386]	1294.727	0	GIHTLGFPPTVR
T15	[79- 88]	1178.572	0	LDSDTLEVMR	T43	[387-387]	147.113	0	K
T16	[89- 91]	400.267	0	KPR	T44	[388-395]	832.441	0	IDAAISDK
T17	[92-101]	1086.515	0	CGVPDVGHFR	T45	[396-397]	276.155	0	EK
T18	[102-108]	759.44	0	TFPGIPK	T46	[398-399]	261.156	0	NK
T19	[109-110]	361.198	0	WR	T47	[400-407]	1048.499	0	TYFFVEDK
T20	[111-111]	147.113	0	K	T48	[408-410]	524.262	0	YWR
T21	[112-117]	790.421	0	THLTYR	T49	[411-414]	538.251	0	FDEK
T22	[118-127]	1159.636	0	IVNYTPDLPK	T50	[415-415]	175.119	0	R
T23	[128-136]	933.452	0	DAVDSAVEK	T51	[416-424]	1006.466	0	NSMEPGFPK
T24	[137-139]	331.234	0	ALK	T52	[425-436]	1319.648	0	QIAEDFPGIDSK
T25	[140-151]	1463.753	0	VWEEVTPLTFSR	T53	[437-463]	3152.456	0	IDAVFEEFGF.....SQLEFDPNAK
T26	[152-166]	1713.852	0	LYEGEADIMISFAVR	T54	[464-464]	147.113	0	K
T27	[167-205]	4256.865	0	EHGDFYPFDG.....HFDDDEQWTK	T55	[465-470]	698.42	0	VTHTLK
T28	[206-248]	4727.356	0	DTTGTNLFLVA.....LYHSLTDLTR	T56	[471-477]	823.34	0	SNSWLNC

MMP-7									
Tryptic Digests	Range	Mono MH+	Partial	Sequence	Tryptic Digests	Range	Mono MH+	Partial	Sequence
T1	[1- 2]	306.159	0	MR	T15	[128-131]	446.297	0	LVSK
T2	[3- 40]	4085.08	0	LTVLCAVCLL.....QWEQAQDYLK	T16	[132-138]	819.418	0	ALNMWGK
T3	[41- 41]	175.119	0	R	T17	[139-145]	911.51	0	EIPLHFR
T4	[42- 50]	1165.541	0	FYLYDSETK	T18	[146-146]	147.113	0	K
T5	[51- 58]	846.432	0	NANSLEAK	T19	[147-160]	1535.804	0	VVWGTADIMIGFAR
T6	[59- 60]	260.197	0	LK	T20	[161-197]	3755.638	0	GAHGDSYPFD.....GDAHFDEDER
T7	[61- 64]	535.254	0	EMQK	T21	[198-245]	5154.342	0	WTDGSSLGIN.....YGNGDPQNFK
T8	[65- 77]	1452.767	0	FFGLPITGMLNSR	T22	[246-252]	818.425	0	LSQDDIK
T9	[78- 86]	1113.645	0	VIEIMQKPR	T23	[253-256]	445.277	0	GIQK
T10	[87-103]	1822.868	0	CGVPDVAEYSLFPNSPK	T24	[257-260]	480.282	0	LYGK
T11	[104-107]	521.272	0	WTSK	T25	[261-261]	175.119	0	R
T12	[108-112]	637.367	0	VVTYR	T26	[262-265]	463.226	0	SNSR
T13	[113-118]	738.414	0	IVSYTR	T27	[266-267]	275.208	0	KK
T14	[119-127]	1065.569	0	DLPHITVDR					

MMP-8									
Tryptic Digests	Range	Mono MH+	Partial	Sequence	Tryptic Digests	Range	Mono MH+	Partial	Sequence
T1	[1- 5]	625.338	0	MFSLK	T23	[243-292]	5334.6	0	ETSNYSLPQD.....LTFDAITTLR
T2	[6- 19]	1622.004	0	TLPFLLLLHVQISK	T24	[293-299]	853.482	0	GEILFFK
T3	[20- 26]	735.404	0	AFPVSSK	T25	[300-301]	290.146	0	DR
T4	[27- 28]	276.155	0	EK	T26	[302-305]	671.33	0	YFWR
T5	[29- 31]	362.203	0	NTK	T27	[306-306]	175.119	0	R
T6	[32- 39]	995.504	0	TVQDYLEK	T28	[307-312]	778.432	0	HPQLQR
T7	[40- 52]	1631.781	0	FYQLPSNQYQSTR	T29	[313-338]	3046.466	0	VEMNFISLFW.....IQAAYEDFDR
T8	[53- 53]	147.113	0	K	T30	[339-345]	895.529	0	DLIFLFK
T9	[54- 62]	973.531	0	NGTNVIVEK	T31	[346-363]	2073.008	0	GNQYWALSGYDILQGYPK
T10	[63- 64]	260.197	0	LK	T32	[364-384]	2320.124	0	DISNYGFPSSVQAIDAAVFYR
T11	[65- 68]	563.261	0	EMQR	T33	[385-386]	234.145	0	SK
T12	[69- 87]	2171.051	0	FFGLNVTGKPNEETLDMMK	T34	[387-397]	1522.711	0	TYFFVNDQFWR
T13	[88- 90]	400.267	0	KPR	T35	[398-402]	695.311	0	YDNQR
T14	[91-107]	1676.777	0	CGVPDSGGFMLTPGNPK	T36	[403-411]	1096.513	0	QFMEPGYPK
T15	[108-110]	490.241	0	WER	T37	[412-423]	1192.621	0	SISGAFPGIESK
T16	[111-116]	767.405	0	TNLTYR	T38	[424-441]	2147.046	0	VDAVFQQEHFFHVFSGPR
T17	[117-118]	288.203	0	IR	T39	[442-451]	1259.642	0	YYAFDLIAQR
T18	[119-131]	1535.734	0	NYTPQLSEAEVER	T40	[452-454]	375.235	0	VTR
T19	[132-134]	331.234	0	AIK	T41	[455-457]	345.224	0	VAR
T20	[135-150]	1851.964	0	DAFELWSVASPLIFTR	T42	[458-460]	318.177	0	GNK
T21	[151-165]	1724.86	0	ISQGEADINIAFYQR	T43	[461-465]	691.334	0	WLNCR
T22	[166-242]	8211.751	0	DHGDNSPFDG.....ALMYPNYAFR	T44	[466-467]	239.103	0	YG

MMP-9									
Tryptic Digests	Range	Mono MH+	Partial	Sequence	Tryptic Digests	Range	Mono MH+	Partial	Sequence
T1	[1- 22]	2429.33	0	MSLWQPLVLVLL.....VLGCCFAAPR	T35	[384-384]	147.11	0	K
T2	[23- 24]	303.18	0	QR	T36	[385-424]	4512.10	0	WGFCPDQGYSL.....PEALMYPMYR
T3	[25- 36]	1345.75	0	QSTLVLFPGDLR	T37	[425-433]	1025.54	0	FTEGPPLHK
T4	[37- 42]	719.37	0	TNLTDR	T38	[434-440]	788.39	0	DDVNGIR
T5	[43- 51]	1184.60	0	QLAEEYLYR	T39	[441-535]	9679.82	0	HLYGPRPEPE.....EIGNQLYLFK
T6	[52- 56]	659.32	0	YGYTR	T40	[536-538]	319.16	0	DGK
T7	[57- 61]	605.31	0	VAEMR	T41	[539-541]	524.26	0	YWR
T8	[62- 65]	420.21	0	GESK	T42	[542-546]	595.28	0	FSEGR
T9	[66- 76]	1152.74	0	SLGPALLLLQK	T43	[547-559]	1385.75	0	GSRPQGPFLIADK
T10	[77- 92]	1701.89	0	QLSLPETGELDSATLK	T44	[560-565]	739.43	0	WPALPR
T11	[93- 95]	377.20	0	AMR	T45	[566-566]	147.11	0	K
T12	[96- 98]	373.22	0	TPR	T46	[567-574]	994.48	0	LDSVFEER
T13	[99-106]	816.40	0	CGVPDLGR	T47	[575-577]	347.23	0	LSK
T14	[107-115]	1084.53	0	FQTFEGDLK	T48	[578-578]	147.11	0	K
T15	[116-134]	2509.18	0	WHHHNITYWIQNYSEDLPR	T49	[579-585]	873.46	0	LFFFSGR
T16	[135-143]	977.51	0	AVIDDAFAR	T50	[586-599]	1532.82	0	QVWVYTGASVLGPR
T17	[144-158]	1680.91	0	AFALWSAVTPLTFTR	T51	[600-600]	175.12	0	R
T18	[159-162]	524.28	0	VYSR	T52	[601-603]	375.22	0	LDK
T19	[163-184]	2350.10	0	DADIVIQFGV.....HGDGYPFDGK	T53	[604-618]	1440.82	0	LGLGADVAQVTGALR
T20	[185-214]	3175.51	0	DGLLAHAFPP.....DDDELWSLGK	T54	[619-621]	319.17	0	SGR
T21	[215-221]	727.45	0	GVVVPTR	T55	[622-623]	204.13	0	GK
T22	[222-239]	1955.89	0	FGNADGAACHFPFIFEGR	T56	[624-630]	823.45	0	MLLFSGR
T23	[240-249]	1060.44	0	SYSACTTDGR	T57	[631-631]	175.12	0	R
T24	[250-267]	2016.82	0	SDGLPWCSTTANYDTDDR	T58	[632-634]	474.28	0	LWR
T25	[268-275]	942.41	0	FGFCPSER	T59	[635-638]	508.28	0	FDVK
T26	[276-307]	3515.56	0	LYTQDGNADG.....SYSACTTDGR	T60	[639-645]	816.40	0	AQMVDPR
T27	[308-312]	597.26	0	SDGYR	T61	[646-652]	763.36	0	SASEVDR
T28	[313-322]	1200.51	0	WCATTANYDR	T62	[653-668]	1921.93	0	MFPGVPLDTHDVFQYR
T29	[323-324]	262.14	0	DK	T63	[669-670]	276.16	0	EK
T30	[325-332]	940.47	0	LFGFCPTR	T64	[671-677]	902.38	0	AYFCQDR
T31	[333-356]	2448.16	0	ADSTVMGG.....CVFPFTFLGK	T65	[678-681]	671.33	0	FYWR
T32	[357-366]	1132.46	0	EYSTCTSEGR	T66	[682-685]	448.25	0	VSSR
T33	[367-370]	404.19	0	GDGR	T67	[686-707]	2528.15	0	SELNQVDQVGYVT....YDILQCPED
T34	[371-383]	1487.65	0	LWCATTSNFDSDK					

MMP-10									
Tryptic Digests	Range	Mono MH+	Partial	Sequence	Tryptic Digests	Range	Mono MH+	Partial	Sequence
T1	[1- 25]	2648.38	0	MMHLAFLVLL.....SAYPLSGAAK	T26	[250-277]	2952.48	0	LSQDDVNGIQ.....STEEPLVPTK
T2	[26- 31]	721.30	0	EEDSNK	T27	[278-288]	1089.52	0	SVPSGSEMPAK
T3	[32- 40]	1107.57	0	DLAQQYLEK	T28	[289-302]	1508.74	0	CDPALSFDAISTLR
T4	[41- 46]	829.41	0	YYNLEK	T29	[303-309]	903.46	0	GEYLFFK
T5	[47- 49]	361.21	0	DVK	T30	[310-311]	290.15	0	DR
T6	[50- 52]	450.25	0	QFR	T31	[312-315]	671.33	0	YFWR
T7	[53- 53]	175.12	0	R	T32	[316-316]	175.12	0	R
T8	[54- 54]	147.11	0	K	T33	[317-348]	3759.79	0	SHWNPEPEFH.....LDAAYEVNSR
T9	[55- 61]	788.45	0	DSNLMK	T34	[349-355]	869.48	0	DTVFIFK
T10	[62- 62]	147.11	0	K	T35	[356-363]	992.50	0	GNEFWAIR
T11	[63- 68]	704.38	0	IQGMQK	T36	[364-373]	1090.53	0	GNEVQAGYPR
T12	[69- 77]	963.55	0	FLGLEVTGK	T37	[374-385]	1308.74	0	GIHTLGFPPTIR
T13	[78- 87]	1192.59	0	LDTDTLEVMR	T38	[386-386]	147.11	0	K
T14	[88- 90]	400.27	0	KPR	T39	[387-394]	818.43	0	IDAAVSDK
T15	[91-107]	1761.81	0	CGVPDVGHFSSFPGMPK	T40	[395-396]	276.16	0	EK
T16	[108-109]	361.20	0	WR	T41	[397-397]	147.11	0	K
T17	[110-110]	147.11	0	K	T42	[398-398]	147.11	0	K
T18	[111-116]	790.42	0	THLTYR	T43	[399-406]	962.46	0	TYFFAADK
T19	[117-126]	1187.64	0	IVNYTPDLPR	T44	[407-409]	524.26	0	YWR
T20	[127-135]	947.47	0	DAVDSAIEK	T45	[410-423]	1671.71	0	FDENSQSMEQGFPR
T21	[136-138]	331.23	0	ALK	T46	[424-435]	1300.68	0	LIADDFPGVEPK
T22	[139-150]	1463.75	0	VWEEVTPLTFSR	T47	[436-462]	3093.44	0	VDAVLQAFGF.....SQFEFDPNAR
T23	[151-165]	1685.85	0	LYEGEADIMISFAVK	T48	[463-469]	841.50	0	MVTHILK
T24	[166-201]	3959.72	0	EHGDFYSFDG.....GDIHFDDDEK	T49	[470-476]	846.36	0	SNSWLHC
T25	[202-249]	5369.60	0	WTEDASGTNL.....NSFTELAQFR					

MMP-13									
Tryptic Digests	Range	Mono MH+	Partial	Sequence	Tryptic Digests	Range	Mono MH+	Partial	Sequence
T1	[1- 18]	2086.051	0	MHPGVLAAFLFLSWTHCR	T25	[280-283]	460.24	0	TPDK
T2	[19- 41]	2503.147	0	ALPLPSGGDE.....SEEDLQFAER	T26	[284-297]	1490.752	0	CDPSLSLDAITSLR
T3	[42- 44]	451.266	0	YLR	T27	[298-304]	825.418	0	GETMIFK
T4	[45- 57]	1476.785	0	SYYHPTNLAGILK	T28	[305-306]	290.146	0	DR
T5	[58- 67]	1095.474	0	ENAASSMTER	T29	[307-310]	655.335	0	FFWR
T6	[68- 69]	288.203	0	LR	T30	[311-324]	1638.885	0	LHPQQVDAELFLTK
T7	[70- 82]	1472.709	0	EMQSFFGLEVTGK	T31	[325-333]	1145.574	0	SFWPELPNR
T8	[83- 92]	1163.561	0	LDDNTLDVMK	T32	[334-350]	2044.029	0	IDAAYEHPSHDLIFIFR
T9	[93- 95]	400.267	0	KPR	T33	[351-352]	232.14	0	GR
T10	[96-109]	1551.726	0	CGVPDVGEYNVFPR	T34	[353-353]	147.113	0	K
T11	[110-112]	361.245	0	TLK	T35	[354-368]	1785.885	0	FWALNGYDILEGYPK
T12	[113-115]	420.224	0	WSK	T36	[369-369]	147.113	0	K
T13	[116-121]	797.397	0	MNLTYR	T37	[370-377]	856.514	0	ISELGLPK
T14	[122-136]	1762.832	0	IVNYTPDMTHSEVEK	T38	[378-380]	375.224	0	EVK
T15	[137-139]	365.218	0	AFK	T39	[381-381]	147.113	0	K
T16	[140-140]	147.113	0	K	T40	[382-393]	1274.638	0	ISAAVHFEDTGK
T17	[141-143]	365.218	0	AFK	T41	[394-404]	1320.706	0	TLLFSGNQVWR
T18	[144-155]	1434.738	0	VWSDVTPLNFTR	T42	[405-414]	1251.531	0	YDDTNHIMDK
T19	[156-170]	1629.867	0	LHDGIADIMISFGIK	T43	[415-418]	550.262	0	DYPR
T20	[171-212]	4537.954	0	EHGDFYPFDG.....DDETWTSSSK	T44	[419-430]	1332.668	0	LIEEDFPGIGDK
T21	[213-234]	2412.21	0	GYNLFLVAAHEFGHSLGLDHSK	T45	[431-437]	823.42	0	VDAVYEK
T22	[235-249]	1673.824	0	DPGALMFPIYTYTGK	T46	[438-458]	2615.235	0	NGYIYFFNGPIQFEYSIWSNR
T23	[250-276]	2971.341	0	SHFMLPDDDV.....GPGDEDPNPK	T47	[459-461]	387.271	0	IVR
T24	[277-279]	381.224	0	HPK	T48	[462-471]	1133.548	0	VMPANSILWC

MMP-14									
Tryptic Digests	Range	Mono MH+	Partial	Sequence	Tryptic Digests	Range	Mono MH+	Partial	Sequence
T1	[1- 9]	1008.54	0	MSPAPRPPR	T34	[344-345]	274.19	0	VR
T2	[10- 51]	4434.31	0	CLLLPLLTLG.....YGYLPPGDLR	T35	[346-362]	2052.94	0	NNQVMDGYPMPIGQFWR
T3	[52- 56]	642.33	0	THTQR	T36	[363-374]	1291.66	0	GLPASINTAYER
T4	[57- 70]	1402.74	0	SPQSLSAAIAAMQK	T37	[375-375]	147.11	0	K
T5	[71- 79]	1012.55	0	FYGLQVTGK	T38	[376-378]	319.16	0	DGK
T6	[80- 86]	751.33	0	ADADTMK	T39	[379-383]	687.39	0	FVFFK
T7	[87- 89]	377.20	0	AMR	T40	[384-386]	319.16	0	GDK
T8	[90- 92]	428.27	0	RPR	T41	[387-401]	1774.84	0	HWVFDEASLEPGYPK
T9	[93- 98]	618.29	0	CGVPDK	T42	[402-404]	397.26	0	HIK
T10	[99-104]	664.37	0	FGAEIK	T43	[405-408]	474.27	0	ELGR
T11	[105-108]	459.27	0	ANVR	T44	[409-414]	630.35	0	GLPTDK
T12	[109-109]	175.12	0	R	T45	[415-426]	1362.69	0	IDAALFWMPNGK
T13	[110-110]	147.11	0	K	T46	[427-431]	733.37	0	TYFFR
T14	[111-111]	175.12	0	R	T47	[432-434]	318.18	0	GNK
T15	[112-118]	792.46	0	YAIQGLK	T48	[435-437]	501.25	0	YYR
T16	[119-134]	2021.95	0	WQHNEITFCIQNYTPK	T49	[438-443]	807.40	0	FNEELR
T17	[135-145]	1271.63	0	VGEYATYEAIR	T50	[444-451]	908.44	0	AVDSEYPK
T18	[146-146]	147.11	0	K	T51	[452-454]	374.24	0	NIK
T19	[147-149]	393.22	0	AFR	T52	[455-464]	1169.60	0	VWEGIPESPR
T20	[150-158]	1058.56	0	VWESATPLR	T53	[465-479]	1777.78	0	GSFMGSDEVFTYFYK
T21	[159-160]	322.19	0	FR	T54	[480-482]	318.18	0	GNK
T22	[161-168]	1010.53	0	EVPYAYIR	T55	[483-485]	496.26	0	YWK
T23	[169-173]	599.28	0	EGHEK	T56	[486-490]	650.33	0	FNNQK
T24	[174-224]	5528.50	0	QADIMIFFAE.....FDSAEPWTVR	T57	[491-492]	260.20	0	LK
T25	[225-276]	5854.71	0	NEDLNGNDI.....ENFVLPDDDR	T58	[493-499]	789.41	0	VEPGYPK
T26	[277-277]	175.12	0	R	T59	[500-503]	446.27	0	SALR
T27	[278-292]	1581.79	0	GIQQLYGGESGFPTK	T60	[504-563]	6255.23	0	DWMGCPSGGR.....AVGLAVFFFR
T28	[293-298]	725.38	0	MPPQPR	T61	[564-564]	175.12	0	R
T29	[299-310]	1312.72	0	TTSRPSVPDKPK	T62	[565-569]	567.30	0	HGTPR
T30	[311-330]	2198.00	0	NPTYGPNICDGNFDTVAMLR	T63	[570-570]	175.12	0	R
T31	[331-337]	857.42	0	GEMFVFK	T64	[571-576]	795.42	0	LLYCQR
T32	[338-339]	304.16	0	ER	T65	[577-582]	674.41	0	SLLDKV
T33	[340-343]	694.35	0	WFWR					

Appendix 5 Experimental *m/z* of rhMMPs including signature peptides.

MMP-1	MMP-2	MMP-3	MMP-7	MMP-8	MMP-9	MMP-10	MMP-13	MMP-14
m/z	m/z	m/z	m/z	m/z	m/z	m/z	m/z	m/z
830.55	843.38	707.21	1065.46	714.28	714.26	733.15	717.20	715.32
836.53	1158.47	817.75	1105.47	733.19	733.16	875.31	719.20	817.79
873.51	1184.57	862.37	1113.47	735.18	735.17	897.34	795.34	824.98
879.50	1201.46	886.43	1129.45	748.29	741.33	942.32	1045.52	841.61
915.48	1223.47	905.37	1156.47	791.29	750.46	988.37	1085.48	860.94
954.49	1223.48	924.28	1165.35	804.36	823.33	992.34	1087.47	878.91
958.44	1266.47	926.28	1175.38	847.41	824.29	997.37	1089.54	880.91
960.54	1295.59	961.40	1177.37	942.36	867.30	1009.36	1129.49	890.87
1072.48	1401.47	991.41	1180.40	1007.42	873.33	1022.34	1131.49	892.86
1115.45	1403.53	1005.39	1208.35	1045.55	959.27	1041.41	1133.56	894.89
1127.51	1418.57	1006.37	1227.27	1047.39	977.36	1085.41	1145.42	911.37
1132.69	1461.56	1049.40	1229.31	1096.38	997.35	1090.36	1173.51	1010.37
1176.78	1587.54	1068.27	1290.29	1105.45	999.29	1129.44	1175.51	1032.35
1213.38	1603.51	1090.51	1321.42	1111.40	1001.41	1133.51	1177.58	1034.36
1216.46	1608.45	1093.42	1364.41	1124.47	1041.41	1135.41	1207.32	1053.37
1220.70	1651.44	1101.50	1452.51	1126.43	1044.42	1160.35	1217.52	1058.39
1232.41	1653.48	1126.39	1468.49	1129.51	1061.19	1173.46	1219.52	1083.89
1259.42	1670.51	1133.50	1577.53	1133.59	1065.34	1174.41	1221.60	1101.86
1264.71	1673.49	1137.44	1601.48	1135.40	1085.41	1177.53	1261.54	1103.85
1275.38	1728.47	1143.42	1609.51	1154.40	1089.52	1217.45	1263.54	1243.48
1308.72	1732.39	1178.43	1620.52	1162.54	1129.46	1221.55	1265.62	1271.42
1352.72	1837.76	1181.46	1634.53	1167.44	1133.54	1251.50	1305.56	1287.50
1396.71	1880.76	1185.52	1639.49	1174.43	1152.55	1261.49	1307.56	1303.43
1440.70	1901.64	1186.42	1765.42	1177.61	1166.45	1265.55	1309.64	1313.49
1484.71	2107.71	1188.30	1791.40	1183.41	1167.36	1298.38	1320.51	1320.45
1572.70	2114.78	1190.29	1862.50	1188.36	1173.48	1308.51	1349.58	1325.42
1682.28	2146.70	1205.33	1879.53	1217.50	1177.56	1313.41	1351.58	1331.52
1792.29	2150.66	1207.33	1941.44	1221.63	1184.40	1349.53	1353.65	1335.47
1798.64	2154.63	1225.48	1943.44	1238.38	1214.46	1351.53	1357.50	1342.43
1835.25	2178.64	1237.57	2383.50	1252.51	1216.39	1353.61	1363.51	1356.49
1840.24	2182.72	1267.23	2630.74	1261.57	1217.48	1358.43	1382.42	1375.41
1857.26	2223.75	1269.40	2704.63	1263.58	1221.58	1359.46	1393.59	1377.38
1897.21	3017.91	1294.58	2738.83	1265.65	1227.39	1370.43	1395.59	1399.49
1900.22	3309.91	1310.58	2748.16	1295.51	1246.30	1372.43	1397.67	1402.51
		1313.52	2772.33	1305.59	1261.51	1393.54	1437.61	1419.55
		1315.54	2786.83	1309.66	1265.60	1397.62	1439.61	1424.49
		1317.59	2793.01	1314.43	1305.53	1437.55	1441.69	1432.54
		1337.58	2802.80	1316.42	1309.61	1441.63	1457.66	1463.57
		1356.50	2815.24	1349.61	1322.43	1467.45	1476.57	1765.47
		1358.50	2829.82	1353.68	1328.49	1481.56	1481.63	2383.55
		1399.50	2843.82	1389.61	1345.51	1484.52	1483.63	2410.78
		1401.54	2848.73	1393.63	1353.63	1525.59	1485.70	2497.79
		1418.40		1395.62	1388.52	1565.48	1525.64	2625.83
		1420.40		1397.71	1391.53	1569.61	1527.64	2706.77
		1445.58		1426.47	1393.56	1595.51	1529.72	2953.95
		1463.59		1437.65	1397.65	1613.64	1538.48	2975.93
		1489.59		1439.64	1437.58	1617.63	1569.66	2985.92
		1492.57		1441.73	1440.58	1638.55	1571.66	2996.93
		1553.56		1467.54	1481.59	1657.63	1573.74	
		1596.55		1468.54	1485.66	1671.41	1591.47	

MMP-1	MMP-2	MMP-3	MMP-7	MMP-8	MMP-9	MMP-10	MMP-13	MMP-14
m/z	m/z	m/z	m/z	m/z	m/z	m/z	m/z	m/z
		1615.46		1481.67	1532.55	1701.65	1608.49	
		1691.61		1485.75	1569.61	1819.62	1613.68	
		1713.64		1522.51	1611.41	1842.62	1615.68	
		1734.61		1525.69	1619.46	1885.61	1617.76	
		1753.52		1529.76	1672.44	1898.51	1638.62	
		1755.53		1535.53	1680.61	2063.64	1651.49	
		1775.75		1565.50	1701.60	2120.62	1657.70	
		1815.42		1569.71	1794.59	2136.74	1659.71	
		1838.67		1573.79	1798.62	2142.68	1661.78	
		2064.74		1578.54	1837.56	2176.56	1670.40	
		2073.80		1612.46	1856.49	2179.68	1672.41	
		2107.75		1613.73	1858.50	2192.59	1701.71	
		2122.84		1617.81	1921.57	2198.69	1705.79	
		2165.84		1657.75	1938.57	2200.75	1741.62	
		2184.75		1661.83	1952.77	2235.58	1745.74	
				1701.77	1983.47	2249.59	1749.81	
				1705.85	1997.99	2254.50	1789.75	
				1724.63	2012.54	2498.81	1793.82	
				1737.61	2055.53	2596.81	1833.77	
				1745.79	2069.76	2635.84	1837.84	
				1749.87	2074.45	2704.70	1988.67	
				1767.63	2077.46	2871.88	1997.68	
				1780.62	2091.25	2899.37	2011.51	
				1786.54	2105.78	2913.94	2043.69	
				1804.68	2148.77	2931.97	2073.41	
				1828.67	2167.68	2956.33	2136.72	
				1890.68	2169.69	2962.96	2174.54	
				1926.70	2178.67	2970.94	2416.29	
				1974.70	2464.16	2975.85	2431.70	
				2017.70	2478.67	3032.85	2437.94	
				2072.73	2540.58	3092.88	2460.10	
				2103.79	2646.59	3119.84	2474.70	
				2134.64	2665.76	3247.92	2488.70	
				2136.66	2720.81	3526.09	2493.61	
				2146.76	2920.81	3749.21	2495.62	
				2156.74	3013.83	3759.14	2552.81	
				2187.71	3025.70		2555.50	
				2204.76	3039.20		2557.52	
				2208.67	3053.69		2559.03	
				2210.68	3108.98		2568.80	
				2266.66	3115.59		2575.89	
				2270.59	3123.78		2584.78	
				2272.58	3152.17		2594.75	
				2309.82	3166.78		2600.92	
				2319.81	3174.93		2637.76	
				2402.88	3185.68		2657.68	
				2822.98	3674.97		2885.94	
				3033.93			2986.82	
				3233.18			3049.73	
				3320.20			3131.86	

Appendix 6 Mass peaks of Brij-35.

Brij-35 (0.05%)	Brij-35 (0.05%)
m/z	m/z
745.14	1425.45
781.25	1441.42
789.15	1469.47
825.25	1485.44
833.16	1513.49
869.26	1529.46
877.17	1557.50
913.28	1573.48
921.18	1601.52
941.30	1617.50
957.29	1645.53
965.19	1661.52
985.30	1689.55
1001.29	1705.54
1009.20	1749.56
1029.31	1793.56
1045.30	1837.59
1053.21	2241.60
1073.33	2285.61
1089.31	2329.62
1097.22	2373.64
1117.34	2417.65
1133.32	2461.67
1141.24	2505.68
1161.35	2549.69
1177.33	2593.70
1185.25	2637.72
1205.36	2681.73
1221.34	2725.75
1229.27	2769.76
1249.38	2813.78
1265.35	2857.79
1293.39	2901.81
1309.37	2945.82
1337.41	2989.84
1353.39	3033.85
1381.43	3077.87
1397.40	

Appendix 7 FCS LC-MS/MS results.

FCS (Repeat 1)											
Protein	Accession	Score	MW [kDa]	SC [%]	# Pept.	Protein	Accession	Score	MW [kDa]	SC [%]	# Pept.
Abhydrolase domain-containing protein 12B OS=Homo sapiens GN=ABHD12B PE=2 SV=1	AB12B_HUMAN	38.78	40.75	1.66	1.00	Inter-alpha-trypsin inhibitor heavy chain H3 OS=Bos taurus GN=ITIH3 PE=1 SV=2	ITIH3_BOVIN	65.65	99.49	2.13	2.00
Alpha-1-acid glycoprotein OS=Bos taurus GN=ORM1 PE=2 SV=1	A1AG_BOVIN	131.13	23.17	10.40	2.00	Inter-alpha-trypsin inhibitor heavy chain H4 OS=Bos taurus GN=ITIH4 PE=2 SV=1	ITIH4_BOVIN	89.95	101.45	3.93	5.00
Alpha-1-antiproteinase OS=Bos taurus GN=SERPINA1 PE=1 SV=1	A1AT_BOVIN	300.15	46.07	13.70	5.00	Kininogen-1 OS=Bos taurus GN=KNG1 PE=1 SV=1	KNG1_BOVIN	53.93	68.85	6.92	6.00
Alpha-1B-glycoprotein OS=Bos taurus GN=A1BG PE=1 SV=1	A1BG_BOVIN	343.67	53.52	19.28	7.00	Nuclear pore complex protein Nup155 OS=Homo sapiens GN=NUP155 PE=1 SV=1	NU155_HUMAN	36.31	155.10	1.01	3.00
Alpha-2-antiplasmin OS=Bos taurus GN=SERPINF2 PE=1 SV=2	A2AP_BOVIN	51.48	54.68	2.24	1.00	Pigment epithelium-derived factor OS=Bos taurus GN=SERPINF1 PE=1 SV=1	PEDF_BOVIN	121.95	46.20	8.65	2.00
Alpha-2-HS-glycoprotein OS=Bos taurus GN=AHSG PE=1 SV=2	FETUA_BOVIN	556.81	38.39	37.60	11.00	Protein AMBP OS=Bos taurus GN=AMBP PE=1 SV=2	AMBP_BOVIN	36.79	39.21	6.53	2.00
Alpha-2-macroglobulin OS=Bos taurus GN=A2M PE=1 SV=2	A2MG_BOVIN	675.01	167.47	15.96	17.00	Putative beta-actin-like protein 3 OS=Homo sapiens GN=POTEKP PE=5 SV=1	ACTBM_HUMAN	58.79	41.99	3.47	1.00
Alpha-fetoprotein OS=Bos taurus GN=AFP PE=2 SV=1	FETA_BOVIN	143.41	68.54	6.89	4.00	Serotransferrin OS=Bos taurus GN=TF PE=2 SV=1	TRFE_BOVIN	578.26	77.70	21.16	14.00
Antithrombin-III OS=Bos taurus GN=SERPINC1 PE=1 SV=2	ANT3_BOVIN	71.60	52.31	4.52	2.00	Serotransferrin OS=Sus scrofa GN=TF PE=1 SV=2	TRFE_PIG	68.79	76.92	6.18	3.00
Apolipoprotein A-I OS=Bos taurus GN=APOA1 PE=1 SV=3	APOA1_BOVIN	185.48	30.26	26.04	8.00	Serpin A3-1 OS=Bos taurus GN=SERPINA3-1 PE=1 SV=3	SPA31_BOVIN	255.56	46.21	12.41	4.00
Beta-2-glycoprotein 1 OS=Bos taurus GN=APOH PE=1 SV=4	APOH_BOVIN	65.02	38.23	8.12	2.00	Serpin A3-5 OS=Bos taurus GN=SERPINA3-5 PE=3 SV=1	SPA35_BOVIN	101.54	46.37	7.30	3.00
Complement C3 OS=Bos taurus GN=C3 PE=1 SV=2	CO3_BOVIN	138.20	187.14	4.70	6.00	Serpin A3-7 OS=Bos taurus GN=SERPINA3-7 PE=3 SV=1	SPA37_BOVIN	121.07	46.91	6.71	2.00
Fetuin-B OS=Bos taurus GN=FETUB PE=2 SV=1	FETUB_BOVIN	71.79	42.64	5.17	2.00	Serum albumin OS=Bos taurus GN=ALB PE=1 SV=4	ALBU_BOVIN	1675.17	69.25	52.06	38.00
Fibronectin OS=Bos taurus GN=FN1 PE=1 SV=4	FINC_BOVIN	64.26	271.98	0.89	1.00	Serum albumin OS=Mesocricetus auratus GN=ALB PE=1 SV=1	ALBU_MESAU	104.49	68.18	8.22	7.00
Hemoglobin fetal subunit beta OS=Bos taurus PE=1 SV=1	HBBF_BOVIN	74.98	15.85	38.62	6.00	Serum albumin OS=Oryctolagus cuniculus GN=ALB PE=2 SV=2	ALBU_RABIT	124.79	68.87	5.76	3.00
Hemoglobin subunit alpha-I/II OS=Bison bonasus PE=1 SV=2	HBA_BISBO	122.87	15.13	10.56	1.00	Serum albumin OS=Rattus norvegicus GN=Alb PE=1 SV=2	ALBU_RAT	127.31	68.69	5.10	2.00
Hemopexin OS=Bos taurus GN=HPX PE=2 SV=1	HEMO_BOVIN	147.02	52.18	11.98	5.00	Transthyretin OS=Bos taurus GN=TTR PE=1 SV=1	TTHY_BOVIN	164.20	15.72	15.65	1.00
Inter-alpha-trypsin inhibitor heavy chain H1 OS=Bos taurus GN=ITIH1 PE=2 SV=1	ITIH1_BOVIN	130.78	101.17	2.65	1.00	Vitamin D-binding protein OS=Bos taurus GN=GC PE=2 SV=1	VTDB_BOVIN	182.47	53.31	6.96	2.00
Inter-alpha-trypsin inhibitor heavy chain H2 OS=Homo sapiens GN=ITIH2 PE=1 SV=2	ITIH2_HUMAN	90.88	106.40	3.49	3.00	Vitronectin OS=Homo sapiens GN=VTN PE=1 SV=1	VTNC_HUMAN	101.67	54.27	3.14	1.00

Appendix 8 BSA peptide sequences.

FCS (Repeat 1)						
Protein	Serum Albumin, Mascot Score = 1675.17, No.Of Peptides = 38					
	Miss	**Sequence**	**Variable Modifications**	**Miss**	**Sequence**	**Variable Modifications**
Peptides	0	DLGEEHFK		0	DAFLGSFLYEYSR	
	0	QTALVELLK		0	DAFLGSFLYEYSR	
	0	QNCDQFEK	Carbamidomethyl (C)	0	LKPDPNTLCDEFK	Carbamidomethyl (C)
	0	QNCDQFEK	Carbamidomethyl (C)	1	KVPQVSTPTLVEVSR	
	0	SHCIAEVEK	Carbamidomethyl (C)	1	QEPERNECFLSHK	Carbamidomethyl (C)
	0	CCTESLVNR	2 Carbamidomethyl (C)	1	QEPERNECFLSHK	Carbamidomethyl (C)
	0	LVNELTEFAK		1	DAFLGSFLYEYSRR	
	1	FKDLGEEHFK		0	MPCTEDYLSLILNR	Carbamidomethyl (C); Oxidation (M)
	0	HPEYAVSVLLR		0	ECCHGDLLECADDR	3 Carbamidomethyl (C)
	0	HLVDEPQNLIK		0	RPCFSALTPDETYVPK	Carbamidomethyl (C)
	0	SLHTLFGDELCK	Carbamidomethyl (C)	0	HPYFYAPELLYYANK	
	1	RHPEYAVSVLLR		0	HPYFYAPELLYYANK	
	1	RHPEYAVSVLLR		1	NECFLSHKDDSPDLPK	Carbamidomethyl (C)
	1	RHPEYAVSVLLR		0	LFTFHADICTLPDTEK	Carbamidomethyl (C)
	0	YICDNQDTISSK	Carbamidomethyl (C)	1	CCAADDKEACFAVEGPK	3 Carbamidomethyl (C)
	0	LGEYGFQNALIVR		1	CCAADDKEACFAVEGPK	3 Carbamidomethyl (C)
	0	EYEATLEECCAK	2 Carbamidomethyl (C)	1	DAIPENLPPLTADFAEDKDVCK	Carbamidomethyl (C)
	0	VPQVSTPTLVEVSR		2	QEPERNECFLSHKDDSPDLPK	Carbamidomethyl (C)
	0	DDPHACYSTVFDK	Carbamidomethyl (C)	2	SHCIAEVEKDAIPENLPPLTADFAEDKDVCK	2 Carbamidomethyl (C)

FCS (Repeat 2)						
Protein	Serum Albumin, Mascot Score = 1633, No.Of Peptides = 30					
Peptides	**Miss**	**Sequence**	**Variable Modifications**	**Miss**	**Sequence**	**Variable Modifications**
	0	AEFVEVTK		0	DDPHACYSTVFDK	Carbamidomethyl (C)
	1	ALKAWSVAR		1	KVPQVSTPTLVEVSR	
	0	EACFAVEGPK	Carbamidomethyl (C)	1	QEPERNECFLSHK	Carbamidomethyl (C)
	0	LVNELTEFAK		1	DAFLGSFLYEYSRR	
	1	FKDLGEEHFK		0	MPCTEDYLSLILNR	Carbamidomethyl (C)
	0	HPEYAVSVLLR		0	MPCTEDYLSLILNR	Carbamidomethyl (C); Oxidation (M)
	0	HLVDEPQNLIK		0	ECCHGDLLECADDR	3 Carbamidomethyl (C)
	1	RHPEYAVSVLLR		0	RPCFSALTPDETYVPK	Carbamidomethyl (C)
	1	RHPEYAVSVLLR		0	HPYFYAPELLYYANK	
	1	RHPEYAVSVLLR		1	NECFLSHKDDSPDLPK	Carbamidomethyl (C)
	1	RHPEYAVSVLLR		0	LFTFHADICTLPDTEK	Carbamidomethyl (C)
	0	YICDNQDTISSK	Carbamidomethyl (C)	1	CCAADDKEACFAVEGPK	3 Carbamidomethyl (C)
	0	LGEYGFQNALIVR		1	DAIPENLPPLTADFAEDKDVCK	Carbamidomethyl (C)
	0	EYEATLEECCAK	2 Carbamidomethyl (C)	2	QEPERNECFLSHKDDSPDLPK	Carbamidomethyl (C)
	0	VPQVSTPTLVEVSR		2	SHCIAEVEKDAIPENLPPLTADFAEDKDVCK	2 Carbamidomethyl (C)

Appendix 9 LC-MS/MS (HT1080 SFCS E2a).

HT1080 SFCS 2M Eluate a														
Protein							Matched Peptides							
Protein Name	Accession	Score	MW [kDa]	pI	SC [%]	RMS [ppm]	# Pept.	MH+ (calc) [Da]	Δ m [Da]	Ions Sc.	Rank	Miss	Sequence	Variable Modifications
Annexin A2	ANXA2_HUMAN	54.95	38.58	8.54	15.34	16.53	6	1036.54	0.03	20.45	1	1	DLYDAGVKR	
								1111.55	0.01	47.77	1	0	QDIAFAYQR	
								1164.64	0.01	5.27	2	2	DLYDAGVKRK	
								1244.62	0.02	25.55	1	0	TNQELQEINR	
								1667.82	0.04	18.49	1	1	SNAQRQDIAFAYQR	
								2064.98	0.02	39.40	1	1	RAEDGSVIDYELIDQDAR	
Fructose-bisphosphate aldolase A	ALDOA_HUMAN	63.84	39.40	9.18	22.80	9.26	7	1342.71	0.01	50.07	1	0	ADDGRPFPQVIK	
								1488.80	0.02	8.10	3	1	GILAADESTGSIAKR	
								1646.81	0.01	42.24	1	1	LQSIGTENTEENRR	
								1802.91	0.02	14.44	1	2	RLQSIGTENTEENRR	
								1847.94	0.02	14.53	1	1	FSHEEIAMATVTALRR	Oxidation (M)
								2272.14	0.00	20.34	1	0	GVVPLAGTNGETTTQGLDGLSER	
								2614.33	0.00	26.94	1	1	VDKGVVPLAGTNGETTTQGLDGLSER	
Heterogeneous nuclear ribonucleoprotein A1	ROA1_HUMAN	84.48	38.82	9.66	12.10	12.41	5	1437.74	0.01	9.19	2	0	EDSQRPGAHLTVK	
								1699.76	0.04	12.04	1	0	GFAFVTFDDHDSVDK	
								1879.97	0.02	28.63	1	1	IFVGGIKEDTEEHHLR	
								2008.06	0.02	47.43	1	2	KIFVGGIKEDTEEHHLR	
								2008.06	0.02	57.75	1	2	KIFVGGIKEDTEEHHLR	
Heterogeneous nuclear ribonucleoproteins A2/B1	ROA2_HUMAN	84.48	37.41	9.34	9.63	7.51	5	1798.92	0.00	13.17	1	0	LFIGGLSFETTEESLR	
								1879.97	0.02	28.63	1	1	LFVGGIKEDTEEHHLR	
								1927.02	0.02	19.55	1	1	KLFIGGLSFETTEESLR	
								2008.06	0.02	47.43	1	2	KLFVGGIKEDTEEHHLR	
								2008.06	0.02	57.75	1	2	KLFVGGIKEDTEEHHLR	
Histone H2B type 1-C/E/F/G/I	H2B1C_HUMAN	29.28	13.81	10.75	10.40	18.11	1	1605.89	0.03	29.28	1	2	KESYSVYVYKVLK	
Inter-alpha-trypsin inhibitor heavy chain H2 precursor	ITIH2_HUMAN	52.04	106.37	6.41	1.27	4.32	2	1337.72	0.01	52.68	1	0	FYNQVSTPLLR	
								1465.82	0.00	24.86	1	1	KFYNQVSTPLLR	
Lamin-A/C (70 kDa lamin)	LMNA_HUMAN	53.54	74.09471	6.60	3.92	16.29941725	2	1363.62	0.03	11.56	1	0	AQNTWGCGNSLR	Carbamidomethyl (C)
								1605.81	0.01	53.54	1	1	VAVEEVDEEGKFVR	
Malate dehydrogenase, mitochondrial precursor	MDHM_HUMAN	40.30	35.51	9.82	21.89	24.30	5	1338.72	0.00	40.30	1	0	GCDVVVIPAGVPR	Carbamidomethyl (C)
								1370.77	0.01	14.06	1	0	TIIPLISQCTPK	Carbamidomethyl (C)
								1470.70	0.02	19.39	1	0	AGAGSATLSMAYAGAR	Oxidation (M)
								1560.80	0.02	21.86	1	0	VDFPQDQLTALTGR	
								2143.17	-0.11	6.10	2	1	HGVYNPNKIFGVTTLDIVR	
Metalloproteinase inhibitor 1 precursor (TIMP-1)	TIMP1_HUMAN	40.92	23.15555	9.78	11.11	13.38	2	1233.62	0.02	34.95	1	0	GFQALGDAADIR	
								1346.65	0.02	32.97	1	0	EPGLCTWQSLR	Carbamidomethyl (C)
Phosphoglycerate mutase 1	PGAM1_HUMAN	41.82	28.79	6.82	4.33	17.44	1	1312.60	0.02	41.82	1	0	HGESAWNLENR	
Protein disulfide-isomerase A3 precursor	PDIA3_HUMAN	52.42	56.74675	5.95	16.63	14.839048	7	877.49	0.01	10.42	1	0	LNFAVASR	
								1188.54	0.02	14.84	1	0	FVMQEEFSR	Oxidation (M)
								1515.76	-0.01	26.27	1	1	FLQDYFDGNLKR	
								1652.77	0.03	29.39	1	1	IFRDGEEAGAYDGPR	
								1664.76	0.02	26.02	1	0	MDATANDVPSPYEVR	
								1680.75	0.02	43.49	1	0	MDATANDVPSPYEVR	Oxidation (M)
								2703.40	-0.05	12.33	1	1	KTFSHELSDFGLESTAGEIPVVAIR	
Serum albumin precursor	ALBU_HUMAN	72.8	69.32149	5.88	3.61	20.21607119	2	927.49	0.02	30.16	1	0	YLYEIAR	
								1639.94	0.04	66.64	1	1	KVPQVSTPTLVEVSR	
Splicing factor, arginine/serine-rich 1	SFRS1_HUMAN	43.03	27.73	10.83	5.65	18.96	1	1564.74	0.03	43.03	1	0	GGPPFAFVEFEDPR	

Appendix 10 Publication.

Contents lists available at ScienceDirect

Journal of Pharmacological and Toxicological Methods

journal homepage: www.elsevier.com/locate/jpharmtox

Use of matrix-assisted laser desorption/ionisation mass spectrometry in cancer research

Hannah Bateson, Saira Saleem, Paul M. Loadman, Chris W. Sutton *

Institute of Cancer Therapeutics, University of Bradford, Trumbling Hill Street, Bradford BD7 1DP, United Kingdom

ARTICLE INFO

Article history:
Received 12 January 2011
Accepted 6 April 2011
Available online xxxx

Keywords:
MALDI
Mass spectrometry
Proteomics
Cancer
Biomarker

ABSTRACT

Cancer significantly affects millions of people worldwide. It is possible to use proteomic techniques to aid in detection, monitoring of treatment and progression, as well as gaining an increased understanding of cancer. Matrix-assisted laser desorption/ionisation (MALDI) mass spectrometry can be utilised to detect the presence of proteins and peptide s within various samples from the body, including blood, biological fluids and tumour tissue. This review aims to introduce MALDI mass spectrometry and discuss a range of applications in the field of cancer research, from quantitative to qualitative methods. Also described is MALDI imaging mass spectrometry which differs from typical sample preparation methods, as analytes are ionised directly from the tissue. Finally, presented is a brief summary of the status of biomarker discovery using blood/serum and biological fluids samples, and the implications in the clinic.

Contents

1. Introduction . . . 0
2. Proteomics . . . 0
2.1. Protein profiling techniques . . . 0
2.2. Bottom-up versus top-down . . . 0
3. MALDI-TOF and cancer biomarker discovery . . . 0
3.1. Quantitative mass spectrometry approaches . . . 0
3.2. MALDI imaging mass spectrometry . . . 0
3.3. Blood and serum biomarker research . . . 0
3.4. Proximal fluid biomarker research . . . 0
4. Conclusions and future directions . . . 0
Acknowledgements . . . 0
References . . . 0